

1995

WETTING AND DRYING IN TWO-DIMENSIONAL TIDAL NUMERICAL MODELS

STRIPLING, STUART

<http://hdl.handle.net/10026.1/1139>

<http://dx.doi.org/10.24382/4660>

University of Plymouth

All content in PEARL is protected by copyright law. Author manuscripts are made available in accordance with publisher policies. Please cite only the published version using the details provided on the item record or document. In the absence of an open licence (e.g. Creative Commons), permissions for further reuse of content should be sought from the publisher or author.

store

WETTING AND DRYING IN TWO-DIMENSIONAL
TIDAL NUMERICAL MODELS

STUART STRIPLING

Ph.D.

1995



1

REFERENCE ONLY

LIBRARY STORE

This book is to be returned on
or before the date stamped below

STORE

25 JUN 2003

REFERENCE ONLY

UNIVERSITY OF PLYMOUTH

PLYMOUTH LIBRARY

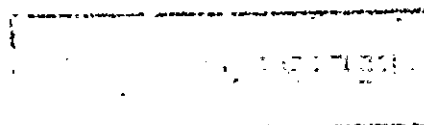
Tel: (01752) 232323

This book is subject to recall if required by another reader

Books may be renewed by phone

CHARGES WILL BE MADE FOR OVERDUE BOOKS

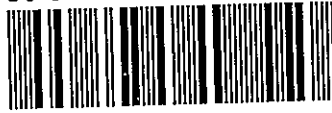
This copy of the thesis has been supplied on condition that anyone who consults it is understood to recognize that its copyright rests with the author and that no quotation from the thesis and no information derived from it may be published without the author's prior written consent.



LIBRARY STORE

REFERENCE ONLY

90 0265689 7



UNIVERSITY OF PLYMOUTH	
Item No.	900 2656897
Date	17 APR 1996 S
Class No.	551.470807 24 STR
Contl. No.	X703269118
LIBRARY SERVICES	

LIBRARY STORE

WETTING AND DRYING IN TWO-DIMENSIONAL

TIDAL NUMERICAL MODELS

STUART STRIPLING

A thesis submitted to the University of Plymouth
in partial fulfilment for the degree of

DOCTOR OF PHILOSOPHY

Institute of Marine Studies
Faculty of Science

Collaborating Institute: Proudman Oceanographic Laboratory

September 1995

CONTENTS

Chapter/Section	Title	Page Number
	List of Tables	v
	List of Figures	vi
	List of Plates	ix
	Acknowledgements	x
	Authors Declaration	xi
	Abstract	xii
	Introduction	xiii
1	A LITERARY REVIEW	1
1.1	Introduction	1
1.2	State-of-the-Art Modelling	2
1.3	Early Work on Wetting and Drying (Reid & Bodine)	3
1.4	The Approach of the Civil Engineer	4
1.4.1	Leendertse's Models	5
1.4.2	Leendertse & Gritton	6
1.4.3	Falconer's Models	9
1.4.4	Owen's Model	11
1.4.5	Other Models	12
1.5	The Approach of the Oceanographer	13
1.5.1	Flather & Heaps	13
1.5.2	Flather & Hubbert	14

CONTENTS (continued)

Chapter/Section	Title	Page Number
2	FORMATION OF A STUDY TOOL	16
2.1	The Hydrodynamic Equations in Two Dimensions	17
2.2	Solution of the Hydrodynamic Equations	20
2.2.1	The Method of Characteristics	20
2.2.2	The Harmonic Method	21
2.2.3	Finite Elements	21
2.2.4	Finite Differences	23
2.2.5	Non-linearity	26
2.2.6	The Courant Number	26
2.3	Choice of Discretization in Time	27
2.3.1	Implicit	27
2.3.2	Semi-Implicit	28
2.3.3	Explicit	29
2.4	Instability	30
2.5	A Numerical Model of an Idealized Portion of Shelf Sea	31
2.5.1	Setting Up the Model	31
2.5.2	Tidal Input to a Theoretical Model	32
2.5.3	Boundary Conditions	34
2.5.4	Bathymetric Design	36
2.5.5	Introducing a Moving Land/Sea Boundary	38
2.5.5.1	Addition of a Drying Algorithm	38
2.5.6	Horizontal Eddy Diffusion	40
2.5.7	Coriolis Acceleration	41
2.6	Data Output	41
2.6.1	Representation of Output Data	42

CONTENTS (continued)

Chapter/Section	Title	Page Number
3	EXISTING DRYING ALGORITHMS	44
3.1	Leendertse & Gritton	44
3.2	Falconer & Owens	48
3.3	Flather & Heaps	51
3.4	Flather & Hubbert	52
3.5	Comparison of Results	58
3.5.1	Leendertse's (1970) Drying Algorithm	58
3.5.2	Owens' (1984) Drying Algorithm	62
3.5.3	Flather & Heaps (1975) Drying Algorithm	67
3.5.4	Rate of Rise of Flooding Cells	71
4	THE NEW DRYING ALGORITHM	73
4.1	The Richardson Grid	73
4.2	Difficulties in Wetting and Drying	75
4.2.1	Cells Which Dry too Slowly	75
4.2.2	Cells Which Wet too Slowly	78
4.3	The Method of Sloping Facets	81
4.3.1	Introducing Areal Factors	82
4.4	Comparison With Other Drying Methods	92
4.5	A Rogue Situation	92
5	'THE WASH' - FIELD MEASUREMENTS	95
5.1	The Wash	95
5.2	The Study Area	99

CONTENTS (continued)

Chapter/Section	Title	Page Number
5.3	Aims of the Field Work	102
5.4	Methods of Measurement	102
5.5	Period of Observation	104
6	'THE WASH' - A NUMERICAL MODEL	106
6.1	Model Design	107
6.1.1	Bathymetric Data File	107
6.1.2	Masking File	109
6.1.3	Model Area	109
6.1.4	Open Boundary Conditions	112
6.1.5	Model Time-Step	118
6.2	Results	118
6.2.1	Station 6	126
6.2.2	Further Survey Stations	128
6.2.3	Bed Friction	129
7	SUMMARY AND CONCLUSIONS	130
	REFERENCES	133
	APPENDICES	

LIST OF TABLES

Table Number	Title	Page Number
1	To show the difference between the rate of rise in a wetting cell and the environmental rate of rise	72
2	Summary of survey programme	105
3	Data provided by P.O.L. for production of boundary conditions	113

LIST OF FIGURES

Figure Number	Title	Page Number
1.1	Diagrammatic representation of the cross-section of a cell	7
2.1	A finite element grid showing a wide density of cells	22
2.2	Richardson grid used in the model showing grid numbering and labelling	24
2.3	Surface plan of model area showing amplitude and phase differences	35
2.4	Gaussian shoal bathymetry used to test algorithms	39
3.1	Diagram to show depth related variables used to evaluate the volume of a cell	46
3.2	Diagram to show cross-sections used for determining the moving boundary	47
3.3	Diagram showing the location of elevation points used to establish the elevation at a stream point	50
3.4	Diagram showing the positions in space of the variables which define the moving boundary	53
3.5	To show high frequency oscillations for two different experimental runs	57
3.6	Elevation and easterly velocity component of a test cell with elevation of an adjacent cell	59
3.7	Elevation and accelerations due to both gravity and friction of a test cell with the elevation of an adjacent cell	60
3.8	Initial Wetting Period	61

LIST OF FIGURES (continued)

Figure Number	Title	Page Number
3.9	Elevation and easterly velocity component of a test cell with elevation of a test cell	64
3.10	Elevation and accelerations due to both gravity and friction of a test cell with the elevation of an adjacent cell	65
3.11	Initial Wetting Period	66
3.12	Elevation and easterly velocity component of a test cell with elevation of an adjacent cell	68
3.13	Elevation and accelerations due to both gravity and friction of a test cell with the elevation of an adjacent cell	69
3.14	Initial Wetting Period	70
4.1	Definition of a cell in the Richardson grid for the purposes of wetting and drying	74
4.2	A dry cell, b, about to become wet through cell s	79
4.3	A stepped bathymetry	83
4.4	An example of an isometric projection	84
4.5	The stepped bathymetry from fig. 4.3 shown as sloping facets	85
4.6	Elevation and easterly velocity component of a test cell with the elevation of an adjacent cell	89
4.7	Elevation in a cell with accelerations due to both gravity and friction	90
4.8	Initial Wetting Period	91
4.9	A pyramidal cell	94
5.1	Location map of the Wash, U.K.	96

LIST OF FIGURES (continued)

Figure Number	Title	Page Number
5.2	Aerial photograph of the Wash showing survey line	98
5.3	Location of hydrological survey stations, Frieston Shore, 1993	100
6.1	Isometric projection of the Wash	110
6.2	2NM model of the Wash	111
6.3	Continental Shelf model: CS3 (P.O.L.)	115
6.4	M ₂ co-tidal chart of the Wash, U.K.	116
6.5	Obtaining boundary values from the co-tidal chart for station 6, 22/06/93	117
6.6	A portion of 0.4NM/2NM model area showing positions of survey stations and the coastline	119
6.7	Comparison of measured and predicted elevations for Station 6	120
6.8	Comparison of measured and predicted stream rate and set for Station 6	121
6.9	Comparison of measured and predicted elevations for Station 4	122
6.10	Comparison of measured and predicted elevations for Station 1	123
6.11	Comparison of measured and predicted elevations for Station 5	124
6.12	Comparison of measured elevation and stream rate with predicted elevation and stream rate for Station 3	125

LIST OF PLATES

Plate Number	Title	Page Number
1	Seawards from station 6	101
2	Current meter rig	101
3	Valeport multi-channel pulse-meter	103
4	Near high water showing benefit of bow and stern anchors	103

ACKNOWLEDGEMENTS

I would like to sincerely thank Dr. K.J. George for his tremendous undying assistance and enthusiasm for this thesis.

Thanks also to Prof. P.P.G. Dyke for keeping me going, to SERC for providing me with most of the funding for this research and to the Governor of H.M.P. Frieston, North Sea Camp, for allowing us access to the beach.

Thanks to Xiankun and Adrian for their help at the Wash, and to HR Wallingford for the use of their resources in completing this thesis.

Most of all I have to thank my wife for her matter-of-factness where I am concerned, for her love and her friendship through all of this...

AUTHOR'S DECLARATION

At no time during the registration for the degree of Doctor of Philosophy has the author been registered for any other university award.

This study was financed with the aid of a studentship from the Science and Engineering Research Council, and carried out in collaboration with the Proudman Oceanographic Laboratory.

Publications:

George K.J. & Stripling S. (1995) 'Improving the simulation of wetting and drying in a two-dimensional tidal numerical model', Applied Mathematical Modelling.

Stripling S., Dyer K.R. and Huntley D.A. (1994) 'A review of transport models in the marine environment', Commercial report confidential to Westlakes Research Institute and BNFL, Sellafield.

Signed Stuart Stripling.....
Date 15th February 1996.....

WETTING AND DRYING IN TWO-DIMENSIONAL TIDAL NUMERICAL MODELS

STUART STRIPLING

ABSTRACT

The purpose of this research is to adapt and improve existing two-dimensional numerical tidal models so that they can cope with regions where the tide falls and rises to uncover and cover inter-tidal banks without incurring numerical shocks which may be caused by the discretization of time and space.

This thesis presents a review of current practices in the numerical modelling of flooding and drying banks in two dimensions. A two-dimensional depth-averaged numerical model has been written and is presented. It is used as a tool with which to investigate various existing algorithms which represent the physical process of the wetting and drying of intertidal zones.

An alternative method with which to represent the moving boundary has been developed. This method is free from disturbances usually caused by the implementation of a moving boundary in such a numerical scheme.

A 2NM numerical model of the Wash, U.K., is run to provide hind-cast tidal data pertaining to a particular site and period. A field programme is established to provide validation data for the model.

Finally, conclusions from the programme of research are drawn.

INTRODUCTION

When an area of coast becomes exposed as the tide falls, and covered as the tide rises, we can term this phenomenon the drying and wetting of an inter-tidal zone. The representation of this physical process in a numerical model can create disturbances in the solution. These disturbances are essentially the result of an attempt to incorporate, in numerical terms, a boundary which moves in a discrete manner.

Due to the nature of the frictional term in the hydrodynamic equations of motion, a mathematical singularity occurs at zero water depth resulting in the numerically calculated velocity value potentially increasing to infinity. It is therefore essential that this singularity is avoided and an alternative method to represent this very shallow water phenomenon be found, either in the way that the frictional force is represented (i.e. to modify the physics expressed by Newton's Second Law) or by some other physical or numerical means.

Algorithms for drying and wetting used in existing numerical models, whether they be solved implicitly, semi-implicitly or explicitly, appear to have been developed with the elimination of instability as their primary aim rather than the faithful representation of the physical processes in very shallow water (Leendertse, 1970; Flather & Heaps, 1975; Owens, 1984; Falconer, 1985; Cheng *et al.*, 1993). Other workers, Davies (1986), Backhaus (1983), have developed and used three-dimensional models for the analysis of effects such as bottom stress,

wind stress and convective circulations. However, three-dimensional models are very costly to run, and there is much pressure these days to develop two-dimensional models that have a general ability to function even in very shallow seas.

Stripling *et al.* (1994) have established that the incorporation of a moving land/sea boundary is one which commercial companies have spent considerable time addressing. Many companies are now satisfied that their representation of the physical processes involved is adequate; but they also indicate that it could be improved upon if they had sufficient time and inclination for the problem to be addressed further.

Two-dimensional models developed by George at the University of Plymouth over the last nine years incorporate a drying algorithm, but are unsatisfactory and require improvement. In order to attain this improvement, existing drying algorithms have been analyzed using a working two-dimensional model of an idealized sea basin based on those of George & Evans (1991) and Prandle (Proudman Oceanographic Laboratory's General Purpose Model). These algorithms have been critically examined to establish precisely what happens to certain terms in the hydrodynamic equations as the water depth tends to zero. On the basis of this examination, the algorithms have been improved upon and incorporated in the model of an idealized sea basin, leading to the design of a model of a real sea area, The Wash (on the east coast of the U.K.), which has been validated by reference to field measurements taken by the Author, together with Mr. X. Ke¹ and Mr. A. Flavell¹

It is on the strength of these findings that an improved representation of flooding and drying in two-dimensional numerical tidal models has been developed and presented in this thesis.

¹Department of Oceanography, University of Southampton.

Chapter 1 provides the reader with a literary review, together with a descriptive view of the modelling of wetting and drying banks.

Chapter 2 describes the development of a two-dimensional depth-averaged numerical model which is used as a tool for investigating existing drying algorithms.

Chapter 3 introduces the reader to a numerical description of the problems encountered when it is necessary to incorporate a moving land/sea boundary. This chapter also gives results from experiments with existing drying algorithms using the numerical model described in Chapter 2 as an experimental basis.

Chapter 4 gives specific detail about the development of a new drying algorithm using the method of sloping facets, and offers results showing that the technique is an improvement upon those methods investigated in Chapter 3.

Chapter 5 introduces a field programme which was set up to provide a database for the validation of a model of a real sea area.

Chapter 6 defines a model of the Wash, U.K. and presents results which are compared to the field observations as described in Chapter 5.

Finally, a summary is presented and conclusions are drawn from the programme of research.

CHAPTER 1

A LITERARY REVIEW

1.1 Introduction

The numerical modelling of tidal propagation in shelf seas was not possible until the late 1960s when computers became large enough to carry out the vast numbers of calculations necessary to execute even a coarse-mesh two-dimensional representation. A classic example of such a model was that by Heaps (1969) in which the tidal propagation of the North-West European Shelf was modelled using finite differences (see Chapter 2, section 2.2.4) applied to a mesh of 20' in latitude by 30' in longitude and containing some 2400 cells. This model was adequate in most places for examining the vertical tide, which varies but slowly in space.

Two-dimensional models are based on the depth integrated equations of motion and continuity (see Chapter 2) and as such, provide results in the form of vertical tidal elevations and depth-averaged stream velocities. The results are generally good for the vertical tide in sea areas which are well-mixed. Difficulties, however, arise in areas which become dry as the tide falls and become wet as it rises again.

1.2 State-of-the-Art in Modelling Flooding and Drying Banks

In order to place in a wider perspective the problem of representing the flooding and drying of intertidal flats in a numerical tidal model, attention may be drawn to the weaknesses inherent in some commercially available two-dimensional numerical models.

In a review of state-of-the-art marine transport models, Stripling *et al.* (1994) have assessed the ability of currently available commercial models to predict the fate and dispersion of pollutants in the marine environment. These models are highly modular, in that separate modules are required for the prediction of tidal propagation, sediment transport, pollutant transport, the effect of wind-waves, and the chemistry involved with differing pollutants. To ensure that predictions of the fate and dispersion of pollutants are as accurate as possible, it is first essential to establish a tidal model that represents the tidal physics accurately.

Stripling *et al.* (1994) showed that the current level of technical expertise and presentation was generally excellent. It also indicated areas of development in which knowledge of processes is scant, with the outcome that one can not have full confidence in all of the results obtained.

It is beyond the scope of this thesis and would contravene contractual obligations to provide specific details of the companies reviewed and their modelling procedures. It is possible, however, to draw attention to a particular area of weakness, and therefore potential development, while maintaining complete company anonymity.

The research for the above report has shown that commercial companies have spent considerable time addressing the incorporation of a moving land/sea boundary. One company has found that the introduction of a moving land/sea boundary can have a severely detrimental

effect on tidal solutions both in close proximity and at a distance from intertidal regions. Another company has had to omit wetting and drying processes completely from one of their models, with the operator having to decide on whether the intertidal regions are to be modelled as permanently wet or permanently dry. This is evidently unrealistic.

1.3 Early Work on Wetting and Drying (Reid & Bodine)

As early as the 1960s, it was well recognized that there were numerical problems associated with the accurate representation of the tide through the solution of the depth-averaged hydrodynamic equations. For instance, the advection terms, which are non-linear, were often ignored for the purpose of ease of calculation (Reid & Bodine, 1968). More important in the numerical representation of the drying and subsequent flooding of inter-tidal flats is the mathematical singularity in the frictional term as the water depth approaches zero. Other workers, e.g. Sielecki & Wurtele (1970), evaded this problem by ignoring the friction term completely.

The earliest attempt to attack the problem of this singularity was that by Reid & Bodine (1968), who, although they were not able fully to represent the non-linear terms, tried to treat the singularity numerically. This early scheme involved the application of weir theory to two-dimensional flow in the sea. The conditions necessary for the expected flooding or drying of a grid square are given by Evans (1987) and are quite thorough. Contrary to almost all subsequent work (Leendertse & Gritton, 1971; Flather & Heaps, 1975; Falconer, 1983, 1984 & 1985; Owens, 1984; Stelling *et al.*, 1986; Falconer & Owens, 1987; Flather & Hubbert, 1989) the use of weir theory avoided the incorporation of a critical depth to prevent the

singularity occurring in the frictional term. A predetermined depth was still necessary, however, to indicate that a cell had dried and to induce the setting of the stream velocities to zero. A cell was deemed to dry when the stream velocities fell below a preset value (0.02 ms^{-1}). This scheme was highly artificial, since the natural sea-bed does not consist of cells bounded by barriers which create weir-like flow. However, for Reid and Bodine's study this representation was adequate.

Reid and Bodine (1968) were severely restricted by the processing power of their computer since they had to run their numerical scheme on a GE225 computer which possessed only an 8K memory. In the subsequent few years, computer power increased considerably and more complex numerical techniques could be utilized.

1.4 The Approach of the Civil Engineer

Since shelf-sea modelling became a reality, the need to represent the movement of the land/sea boundary has been one addressed by oceanographers and civil engineers alike.

Essentially, a civil engineer is very practical in his approach to the construction and use of a numerical model to represent the tide. Large sums of money are available to him in his quest to solve a problem; he may have to make decisions that could affect large areas of land and water, and possibly the lives of many people in the vicinity of a proposed project. However, the need to abide by strict time-limits, under the dictum that 'time is money', may lead to an engineer 'cutting corners' at appropriate moments in his appraisal of a situation. For instance, he may decide that it is more important to maintain stability in a numerical scheme than to worry about how he maintains that stability. Thus, accuracy in areas such as

a moving land/sea boundary may not be of prime concern to a civil engineer.

Civil engineers generally have no need to develop numerical models on the oceanic or shelf-sea scale. In fact, a civil engineer is largely concerned with smaller scale modelling such as that pertaining to estuaries, harbours or small bays. His models typically have a mesh-size of tens of metres. This is usually adequate for his contractual obligations where localized conditions are of direct importance.

1.4.1 Leendertse's models

Leendertse (1970) developed a water quality model for well-mixed estuaries and coastal seas. The computational procedures were tested on models of Jamaica Bay, Long Island, New York - a shallow bay containing many tidal flats. This appears to be the first thorough approach to the problem of modelling flow over tidal banks which flood and dry.

The work of Leendertse (1970) was primarily concerned with introducing to his peers, and the public, a quantitative method of assessing the impact of urbanization on the environment, in particular 'the study of technical alternatives in the management of fluid waste discharges in well-mixed estuaries and coastal seas', a subject which is still very much of public concern and is still being addressed by governmental and private sector bodies.

Leendertse's study involved a testing of computational procedure on models of Jamaica Bay, Long Island, New York. A grid size of 500ft (150m) was used. However, a larger grid size of 833.3ft (250m) was used for a series of experiments in which stability was studied. This model was not of the moving land/sea boundary type and, in fact, the land/sea boundary was fixed by the minimum depth being set at 3ft below mean sea-level, highlighting the problems

encountered coping with a moving land/sea boundary as the grid size increases.

In 1970, Leendertse made his first attempt to cope with a moving boundary. As he states, the principle may be simple, but the computational procedures are very complex. His simple principle was that if a cross-section (see figure 1.1, where the water level is shown by ζ , and the cross-sections are shaded) for any particular point decreased to less than a preset value, then that point should be removed from the computational field, the preset value being positive and close to zero. Since finite difference techniques rely upon variables changing gradually in time and space, discrete changes such as those experienced when the land/sea boundary moves, impart discontinuities into the solution. Leendertse overcame this initially by making the check for the location of the new boundary at intervals larger than the time-step, allowing the disturbance generated time to decay before the next check for the boundary location. These disturbances were suppressed by enlarging the bottom friction values artificially as the water became very shallow.

When the water level rose again, grid points were returned to the computational field if an average of the water depths at any of the surrounding grid points which were wet resulted in cross-sections which were greater than the preset value. Thus the average water level all the way around the 'dry' point had to rise above the level left in that cell before the point was considered wet again.

1.4.2 Leendertse & Gritton

In Leendertse & Gritton's report of 1971, the procedure of Leendertse (1970) was modified to include further drying checks and an important alteration to the process of the 'wetting'

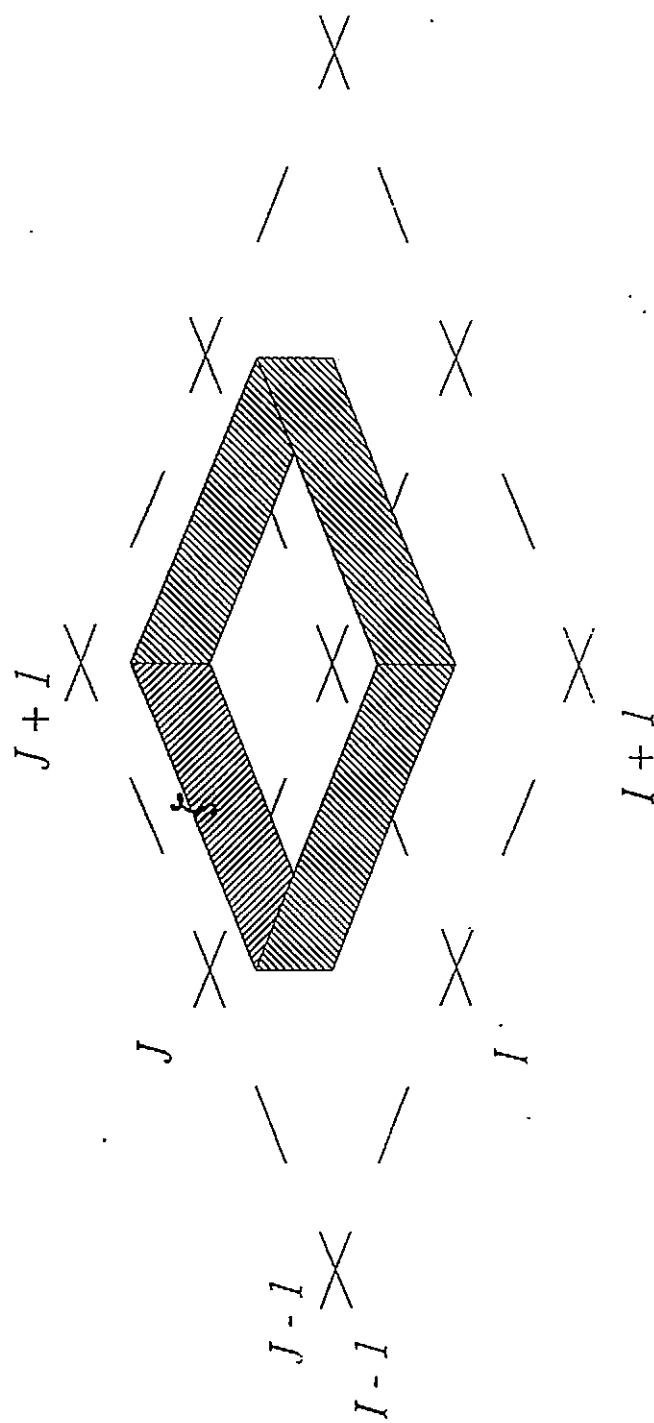


Figure 1.1: Diagrammatic representation of the cross-sections of a cell

of a cell. One of the new additions to the drying check was carried out at every time-step at the time horizon for the calculation of the tidal stream components. This states that, 'if at a particular grid point, the new computed value of the water level has decreased so that a negative volume is obtained, then that grid point is taken out of the computation'. This meant that if the tidal elevation fell below the depth specified at the elevation-point of the grid cell, then the cell was deemed dry. Then, before proceeding to the solution in the next row or column, the velocities and water levels were recalculated for the previous row or column with the point now taken as dry, as well as a recalculation of the row or the column (depending on which direction the calculation is in at the time) on which the recently dried out cell lay. When a cell dried, it was assumed to hold a thin layer of water over it. The depth of this water was set at the previous time-step before a negative volume was obtained.

Another additional check carried out every time-step after the flow calculations was to evaluate all four cross-sections associated with each of the four adjacent grid points. If any of these were negative, the point was noted.

Physically, a negative cross-sectional area is meaningless, but since these cross-sections are concerned with mass-transport, it simply means that transport is worked out as being in the opposite direction to which it should be.

At the end of the calculation of all the velocity components, the grid points marked as having a negative cross-section adjacent to them had all velocity components leading to that point set to zero. A thin layer of water was left over the cell in this case as well.

Leendertse and Gritton found that these two additions had very little effect in adding discontinuities to the tidal solution. This was because a large proportion of cells dried

through the initial check for drying, while only a few would dry as a result of negative volumes or cross-sections, because the preset value was always greater than zero, thus removing a cell before the volume or cross-section had a chance to become negative.

In addition to the initial process for the wetting of a cell *i.e.* the average surrounding wet point depths had to be above the depth of the water left in the dry cell, a dry grid point could become wet only if all of the adjacent transport cross-sections were positive as well. That being the case, then the water level was set to that which was over the cell when it was 'dry'.

The paper by Leendertse & Gritton (1971) does not contain any validation data so the accuracy and performance of the technique remains undisclosed. However, Owens (1984) suggests that the use of this technique is restricted in its ability to model on larger scale grids due to the unrealistic amount of water left in a grid square that is deemed to have dried out. It seems probable that the drying technique developed by Leendertse & Gritton (1971) was not introduced as an accurate representation of the natural phenomena but merely to satisfy the numerical requirements (that is, to ensure stability) of the models.

1.4.3 Falconer's models

By far the closest work to that of J. J. Leendertse in the quest to represent a moving land/sea boundary accurately in a numerical model is that of Prof. R.A. Falconer. Falconer began his interest in numerical modelling in the late 1970s, possibly encouraged by the need at that time to study, in detail, tidal flushing characteristics and circulation in harbours and estuaries in order to provide solutions to water-quality problems. Hydraulic engineers had, traditionally, used physical models to predict water movement in estuaries but, by 1980, computing

knowledge had reached a level where numerical models were just beginning to replace physical models in this field. Thus, numerical techniques had to be developed and improved upon by engineers themselves. Falconer was one engineer who developed a keen interest in these numerical methods. He followed Leendertse and consequently he adopted the ADI (alternating direction implicit) numerical scheme as used by Leendertse.

His early models (Falconer, 1980; 1984; 1985) were used to simulate the propagation of the tide within harbours and estuaries.

However, it was not until 1984 that he published details (Falconer, 1984a) on how he had confronted the problem of a moving boundary. Wessex Water Authority had two proposals for modifying the shape of Holes Bay, a creek in Poole Harbour in Dorset. They had asked Falconer to examine the effects of the two proposals on the tidal characteristics of the bay. Essentially, he used Leendertse's (1970) and Leendertse and Gritton's (1971) procedure. Later, Falconer (1984b), he was required to investigate the velocity fields and temperature distributions (very difficult to do using a physical model) that would be produced by the siting of either a 700 or 350MW capacity power station on the perimeter of Poole Harbour. He stated in this paper that a main problem was 'significant changes' which occur in the plan cross-sectional area as large regions of shallow water were dried out and flooded on each tide'. The procedure adopted in simulating this moving boundary was similar to that used by Leendertse (1970) and Leendertse and Gritton (1971) with some modifications, and the same as that used previously by Falconer (1984a). He reported that the drying regions were 'successfully modelled'. However, lack of field calibration data rendered the numerical predictions as merely a guide.

Falconer persisted with his representation of flooding and drying processes for work carried out in Port Talbot Harbour (Falconer, 1985). He used the same procedure as in Falconer (1984b) and reported that 'the mathematical reproduction of the flooding and drying of the shallow water region at the upper end of the harbour appears to be satisfactorily simulated'. In 1986 (although this work was actually conducted in 1984) Falconer published more work on Holes Bay, Poole Harbour. A slight alteration appeared in this paper in that all four cross-sections of a wet cell were checked for water-level as oppose to just the two cross-sections in the direction of the calculation. This was necessary in order to account for modifications he had made to the finite difference equations.

1.4.4 Owens' model

In 1984, Falconer supervised a research student, P. H. Owens, who developed an improved technique for representing the drying and flooding of tidal flats. He addressed the problem encountered when using Leendertse's method that this method cannot cope with large grid sizes. This is because the water elevation can change considerably with each time-step, thus requiring that the preset limit at which the minimum water-level can be is excessively large. Owens (1984) used a one-dimensional basin with a grid size of 1200m - large in hydrographic engineering terms - as a study base for his improved algorithm. He adopted an approach which was designed to reduce the magnitude of each discontinuity occurring. This was different from Leendertse who tried to reduce the number of discontinuities. To achieve this he allowed cross-sections to 'disappear' one at a time as each became negative, but only deemed the cell dry when the last cross-section became negative.

1000

1000

1.4.5 Other models

Leendertse & Gritton's (1971) technique has, in the main, been adopted by many subsequent authors; Xanthopoulos and Koutitas (1976) used their approach to model the propagation of a flood wave over a flat plain, although not strictly modelling inter-tidal flats, this experiment still required the representation of a moving boundary. Yeh and Chou (1979) were also inspired by Leendertse's (1970) approach in their attempt to introduce a moving land/sea boundary in their prediction of storm surge levels. Their paper compares the results of a fixed boundary model to those obtained using a moving boundary model and concluded that the moving boundary model over-predicted surge levels less than the fixed boundary method. It also stated that, for a very steep bed-slope, there was very little difference between the solutions obtained from a fixed boundary and a moving boundary model. Gunn and Yenigün (1985) claimed to have developed a method which provided solutions in 'good agreement' with observations, over the entire extent of the model field. They used a small grid size of 250m, which required a time-step of less than 12s. Using an estimate of the rate of flood and ebb of the tide over an inter-tidal flat of 1ms^{-1} , they concluded that for a grid size of 250m, it would be necessary to check for a moving boundary only every 250s. This meant that approximately every twenty time-steps, the position of the boundary was located. This has similarities to Leendertse's (1970) technique in that any discontinuities caused could decay in the time between checks.

Despite their claim that 'good agreement' was achieved throughout the model area, graphical representations in their paper suggest that differences of up to 30cm could occur between computed and observed values.

Stelling *et al.* (1986) demonstrated some of the effects on tidal solutions of cells which are in close proximity to cells which wet and dry. Sensibly, they have stressed that numerical procedures must be carefully considered before calibration is attempted by adjusting physical properties. Although Stelling *et al.* (1986) appear to have compared three different methods of representing the moving land/sea boundary, the procedures adopted in their entirety are almost equivalent to Leendertse and Gritton's (1971) attempt. Therefore, it cannot really be considered as an analysis of three different methods (as is the case with this research). However, this is a valuable study as it addresses solely and directly the problem of how to represent a moving land/sea boundary.

1.5 The Approach of the Oceanographer

For the oceanographer, all space scales are considered from global scale modelling to models of turbulence. He has interest in a wide range of oceanographic modelling problems, particularly in terms of scale, and therefore his approach to finding a solution to a specific problem will essentially be different to that of a civil engineer. Numerical modellers at the Proudman Oceanographic Laboratory in Birkenhead, e.g. Davies, Flather, Prandle, Proctor, Jones, are actively involved in the development of techniques in modelling.

1.5.1 Flather & Heaps

Flather & Heaps (1975) published a paper entitled 'Tidal Computations for Morecambe Bay'. In this paper a finite difference method for solving the shallow water hydrodynamic equations

was introduced, with different conditions defining whether a grid square had become wet or dry. These included a testing of the local water-depth and an examination of the slope of the free surface between adjacent grid squares. The testing of the local water-depth involved comparing the present water-depth in a grid to a predetermined minimum depth. Within the model this prevented the actual depth from falling below the preset minimum depth, terminating the growth of the frictional dissipation before it became too large and before the water depth became so shallow that the physical laws expressed in the model were no longer applicable. The restriction invoked in the model by the introduction of an examination of the slope of the free surface had the effect of preventing artificial grid-scale oscillations which may occur causing a grid square to alternate between being wet and being dry at each time-step calculation.

The results of this model showed clearly that grid squares near to grid squares that were becoming dry were receiving 'shocks' as the squares dried out. These 'shocks' were seen as discontinuities in the tidal profiles that were reproduced. It is in this sense that Flather & Heaps' (1975) paper is important since it clearly demonstrates the problems associated with the mathematical modelling of flooding and drying banks. Their drying procedure has recently been adapted by Flather & Hubbert (1989) in an attempt to reduce the severity of the 'shocks' induced by the discrete movements of the land/sea boundary.

1.5.2 Flather & Hubbert

Flather & Hubbert's (1989) adaption of Flather & Heaps' (1975) drying procedure was based

2000

2000

2000

2000

upon the principle that if, when a grid square dries out, a shock is imparted through the model, then an attempt should be made to reduce the severity of this shock. Flather & Hubbert (1989) applied their new drying procedure to the same area as Flather & Heaps (1975) but to achieve resolution of subgrid-scale features, they digitized the bathymetry in part of Morecambe Bay at ten times the resolution of their basic model. It was in this part of the Bay that they applied their new experimental procedures. They developed an idea using area and breadth factors. These were factors which could change according to the ratio of the wetted area of a grid square to the total area of the grid square, and the ratios of the breadth over which flow occurred to the total breadth of the grid square.

Flather & Hubbert's results showed that having constant area and breadth factors made little difference to the time series obtained from the experiments they did using solely a two-dimensional scheme, and were apparently considerably noisier. However, the experiments in which the wetted area of a grid square was allowed to vary with time substantially reduced the discontinuities by representing the flooding and drying process 'in a physically more realistic manner'. Unfortunately, the practicalities of digitizing bathymetric data to ten times the basic resolution in order to obtain a variable factor is a severe hindrance in the application of this drying procedure.

CHAPTER 2

FORMATION OF A STUDY TOOL

In order that the flooding and drying of intertidal flats may be studied numerically, it is necessary to formulate a numerical model which must be readily adaptable and of good solid foundation. Drying algorithms tend to be rigorous in character, and therefore the source code of the numerical model must be able to cope adequately with whatever algorithms are incorporated within it. It is through long periods of experimentation that a source code becomes the aid that it is required to be. Many problems are encountered during and after the development stages and must be dealt with accordingly; a model simply cannot work if even small errors are left unaltered.

It is important to realise that the problems associated with the incorporation of a moving land/sea boundary do not exist when the numerical model is three-dimensional, since layers within the vertical coordinate representation can be reduced until none remain. The need for reduced computational costs however, requires that accurate tidal predictions are obtained from the more economic two-dimensional depth integrated non-linear hyperbolic differential hydrodynamic equations. These are considered appropriate when modelling the propagation

of the tide in non-stratified, i.e. well-mixed, water columns.

A two-dimensional numerical model of tidal propagation is based upon the solution of the hydrodynamic equations in two dimensions.

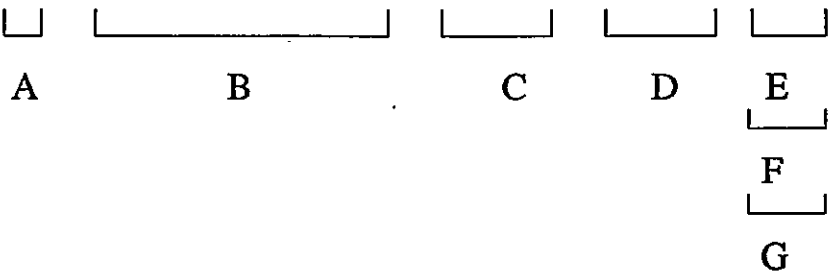
2.1 The Hydrodynamic Equations in Two Dimensions

The hydrodynamic equations are an expression of the physics of tidal propagation in mathematical notation. They are obtained from Newton's Second Law of motion (1687) which states, crudely, that the rate of change of momentum of a particle of constant mass is proportional to the force acting upon it in the direction of that force. The hydrodynamic equations express Newton's Second Law but are more complex than the crude definition stated above since each 'water particle', or unit mass of water, is subject to three forces, three accelerations and in three dimensions. Equations 2.1, 2.2, and 2.3 below show the easterly, northerly, and upwards components of the hydrodynamic equations (e.g. George, 1994):

$$\frac{\partial u}{\partial t} + u \frac{\partial u}{\partial x} + v \frac{\partial u}{\partial y} + w \frac{\partial u}{\partial z} - 2\omega v \sin\phi = -\frac{1}{\rho} \frac{\partial p}{\partial x} - \frac{1}{\rho} \frac{\partial \tau_{xz}}{\partial z} \tag{2.1}$$

$$\frac{\partial v}{\partial t} + u \frac{\partial v}{\partial x} + v \frac{\partial v}{\partial y} + w \frac{\partial v}{\partial z} + 2\omega u \sin\phi = -\frac{1}{\rho} \frac{\partial p}{\partial y} - \frac{1}{\rho} \frac{\partial \tau_{yz}}{\partial z} \tag{2.2}$$

$$\frac{\partial w}{\partial t} + u \frac{\partial w}{\partial x} + v \frac{\partial w}{\partial y} + w \frac{\partial w}{\partial z} + 2\omega u \cos\phi = -\frac{1}{\rho} \frac{\partial p}{\partial z} - g \tag{2.3}$$



where,

A = Temporal accelerations, ms^{-2}

B = Advective accelerations, ms^{-2}

C = Coriolis accelerations, ms^{-2}

D = Pressure forces / unit mass in the easterly, northerly and upward directions, ms^{-2}

E = Frictional force / unit mass in the easterly direction, ms^{-2}

F = Frictional force / unit mass in the northerly direction, ms^{-2}

G = Gravitational force / unit mass, ms^{-2}

These equations are sometimes referred to as the Navier-Stokes² equations.

In the ocean, shallow waters and rivers, the three forces acting on a particle are those of pressure, gravity and friction per unit mass. The three accelerations experienced by a particle are: (i) Coriolis acceleration, which is due to the rotation of the Earth, (ii) the temporal acceleration, *i.e.* the change of a particle's velocity with time, and (iii) the advective acceleration, due to the fact that the particle changes its position in space. Equations 2.1, 2.2, and 2.3 are the equations of motion in three dimensions and express the balance between these accelerations and forces per unit mass.

Large computing power and storage are required to solve these non-linear three-dimensional equations, so two-dimensional versions are often used in preference. Two-dimensional equations of motion are obtained from the three-dimensional equations of motion by integrating them vertically with respect to depth from the bottom to the surface of the water column. When integrated, the unknown velocities u and v in equations 2.1 and 2.2 become U and V where;

$$U = \frac{1}{(\zeta + h)} \int_{-h}^{\zeta} u dz \quad \text{and} \quad V = \frac{1}{(\zeta + h)} \int_{-h}^{\zeta} v dz$$

²Named after L.M.H. Navier (1785-1836) and G.G. Stokes (1819-1903).

Since in a two-dimensional model there is no vertical gradient, $\partial w/\partial z = \partial w/\partial t = \partial w/\partial x = \partial w/\partial y = 0$; equation 2.3 thus reduces to the hydrostatic equation and becomes unnecessary. The water column is now considered as one unit from sea surface to sea bed in that the whole of the water column moves in the same direction and with the same velocity within each cell of the model. After integration, equations 2.1 and 2.2 become equations 2.4 and 2.5 which are a two-dimensional representation of motion in an easterly and a northerly direction respectively;

$$\frac{\partial U}{\partial t} + U \frac{\partial U}{\partial x} + V \frac{\partial U}{\partial y} - 2\omega V \sin \phi = -g \frac{\partial \zeta}{\partial x} - KU \frac{\sqrt{U^2 + V^2}}{(h + \zeta)} + \epsilon \left(\frac{\partial^2 U}{\partial x^2} + \frac{\partial^2 U}{\partial y^2} \right) \quad (2.4)$$

$$\frac{\partial V}{\partial t} + U \frac{\partial V}{\partial x} + V \frac{\partial V}{\partial y} + 2\omega U \sin \phi = -g \frac{\partial \zeta}{\partial y} - KV \frac{\sqrt{U^2 + V^2}}{(h + \zeta)} + \epsilon \left(\frac{\partial^2 V}{\partial x^2} + \frac{\partial^2 V}{\partial y^2} \right) \quad (2.5)$$

where;

U = depth averaged velocity in an easterly direction, ms^{-1} .

V = depth averaged velocity in a northerly direction, ms^{-1} .

ω = period of Earth's rotation, s.

ϕ = latitude, °N.

g = acceleration due to Earth's gravity, ms^{-2} .

ζ = tidal elevation, m.

K = coefficient of drag.

h = bed elevation below a fixed datum, m.

ϵ = eddy viscosity, m^2s^{-1} .

$\partial t \equiv \Delta t$ = time step, s.

$\partial x, \partial y \equiv \Delta x, \Delta y$ = grid spacing in x and y directions, m.

To ensure that no water enters or leaves the system, a two-dimensional representation of continuity of volume, equation 2.6, is required. In this the density of the water is considered uniform with depth, an assumption based on the premise that the water column is well-mixed

and that sea-water is incompressible. The continuity equation is derived from the volume of water entering and leaving a cuboid (see for example; Proudman, 1953):

$$\frac{\partial \zeta}{\partial t} + \frac{\partial}{\partial x} \{ (h + \zeta) U \} + \frac{\partial}{\partial y} \{ (h + \zeta) V \} = 0 \quad (2.6)$$

2.2 Solution of the Hydrodynamic Equations

Several techniques are available for the solution of equations (2.4), (2.5) and (2.6), which form a system of two-dimensional non-linear partial differential equations of the hyperbolic type. These may be the method of characteristics, harmonics, finite elements or finite differences.

2.2.1 The Method of Characteristics

This method relies on the fact that it is a known characteristic of the hydrodynamic equations that they are hyperbolic by nature. Since the characteristics of the equations are known, a solution may be projected forward (in time, perhaps) to where the hyperbolic nature is upheld.

The method of characteristics is often used in the modelling of compression waves or situations when a wavefront is progressing through a non-disturbed medium (Jeffery, 1976). It may also be used in the solution of the hydrodynamic equations (Dronkers, 1964) in estuaries.

Characteristics are designed for calculations where discontinuities are prevalent. This would therefore make them seem ideal for the modelling of flooding and drying regions. In fact,

100

1

2

3

4

5

6

7

8

9

10

11

12

13

14

15

16 - 17

18

19

20

21

however, this is not the case.

In order to solve two-dimensional problems using the method of characteristics, much time is needed to write the machine coding. Once the coding has been written, the solution is very expensive computationally due to the excessive amounts of interpolation needed to maintain a consistent grid pattern.

Whilst the solution may be precise, and the physical attributes of the equations being solved are followed closely, the extraordinarily complex programming and expensive solution process have meant that tidal modellers have abstained from using the method of characteristics for problems of higher order than one-dimension. In addition, when the point spacing is large (as would be required in this research), truncation errors become significant and convergence of the solution is delayed considerably.

2.2.2 The Harmonic Method

This method of solution makes use of the fact that the dependence of tidal motion on time is known, and that the frequencies at which the tidal motion is forced are known very precisely.

At present it is not possible to include intertidal regions in the solution of the hydrodynamic equations using the method of harmonics.

This is an new branch of tidal modelling that has yet to become established, at least in the U.K., however, there is some British interest developing (e.g. George, 1995).

2.2.3 Finite Elements

Figure 2.1 shows an example of a finite element grid. In order for this type of grid to be

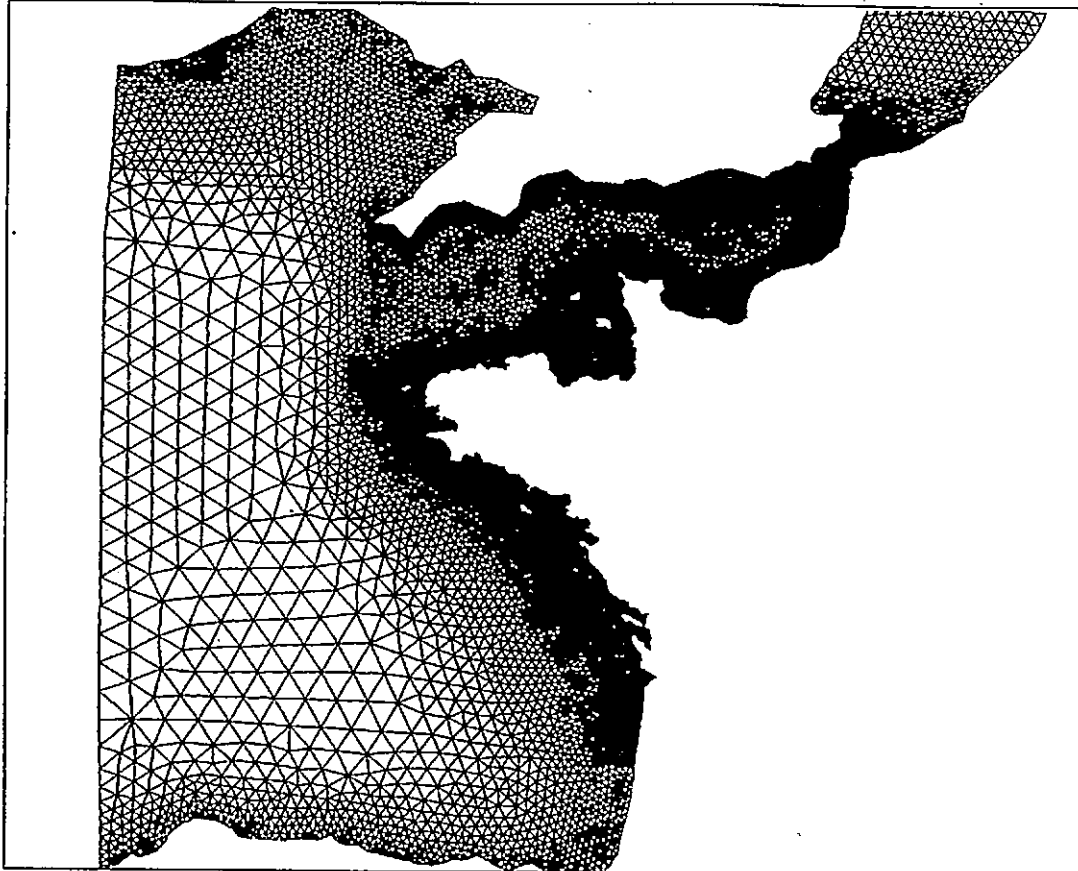


Figure 2.1: A finite element grid showing a wide range of density of cells (HR Wallingford)

established, it is necessary to purchase a standard commercially available finite element grid generator, such as I-DEAS or SIMAIL (Hydraulics Research Ltd., 1993).

The solution of the hydrodynamic equations using a finite element method was, until very recently, computationally expensive. Holz and Witham (1977) present a moving boundary scheme which is analogous to Leendertse (1970) using a fixed-grid finite-element approach. Lynch and Gray (1980) proposed an improved method of incorporating the moving boundary by allowing the boundary of the finite-element grid to deform as the land/sea boundary moved. Recent developments, in the field of finite-elements, have been made (Hervouet, 1991) for use by Electricité de France in the French nuclear industry. The improvements made are dependent upon the use of a vector computer to store the vast numbers of arrays associated with the finite-element scheme. This can decrease the computational time needed by twenty to one hundred times that of a conventional finite-element scheme.

However, finite-element representations are computationally complex and have therefore not been used here.

2.2.4 Finite Differences

It was decided to perform the entire numerical procedure using finite differences on a Richardson grid (Figure 2.2). This grid avoids instabilities by requiring that the unknown terms in equations (2.4), (2.5) and (2.6) are all evaluated at different locations in space.

A finite difference technique involves taking the differences in variables (for instance the U and V stream components) over a finite distance in space, normally a divisor of the grid size, and using these differences to find the unknowns within the equations themselves. For instance, the horizontal eddy diffusion term:

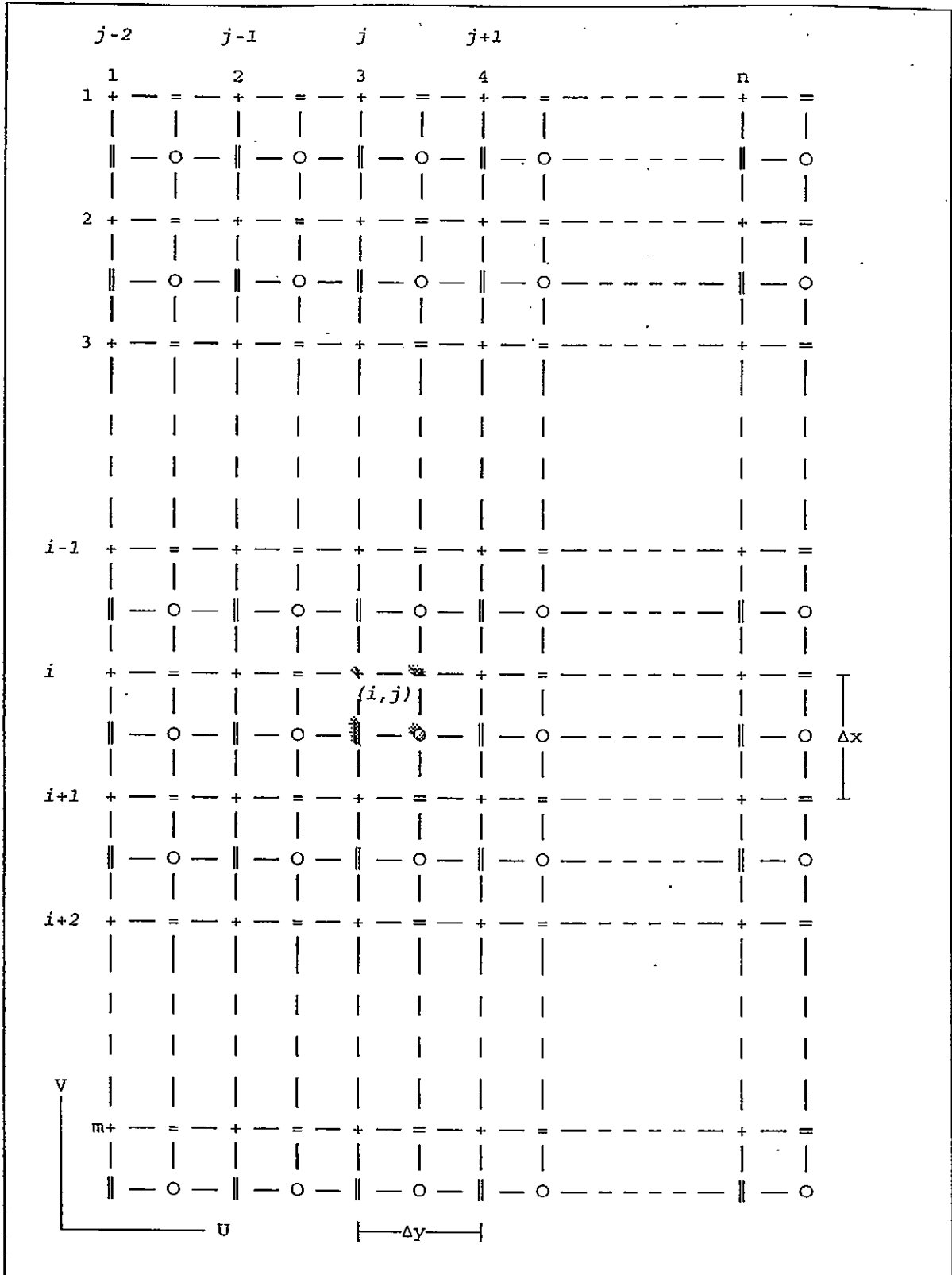


Figure 2.2: Richardson grid used in the model showing grid numbering and labelling ('+': ζ -point, '=': U-point, '||': V-point, 'O': h-point)

$$e \left(\frac{\partial^2 U}{\partial x^2} + \frac{\partial^2 U}{\partial y^2} \right) \quad (2.7)$$

when taken a component at a time expressed as differences:

$$\frac{\partial^2 U}{\partial x^2} = \frac{\left(\frac{\partial U}{\partial x} \right)_{(i,j+1)} - \left(\frac{\partial U}{\partial x} \right)_{(i,j-1)}}{\Delta x} = \frac{\frac{U_{(i,j+1)} - U_{(i,j)}}{\Delta x} - \frac{U_{(i,j)} - U_{(i,j-1)}}{\Delta x}}{\Delta x} \quad (2.8)$$

$$\therefore \frac{\partial^2 U}{\partial x^2} = \frac{1}{(\Delta x)^2} \{ U_{(i,j+1)} + U_{(i,j-1)} - 2U_{(i,j)} \} \quad (2.9)$$

and;

$$\frac{\partial^2 U}{\partial y^2} = \frac{\left(\frac{\partial U}{\partial y} \right)_{(i-1,j)} - \left(\frac{\partial U}{\partial y} \right)_{(i+1,j)}}{\Delta y} = \frac{\frac{U_{(i-1,j)} - U_{(i,j)}}{\Delta y} - \frac{U_{(i,j)} - U_{(i+1,j)}}{\Delta y}}{\Delta y} \quad (2.10)$$

$$\therefore \frac{\partial^2 U}{\partial y^2} = \frac{1}{(\Delta y)^2} \{ U_{(i-1,j)} + U_{(i+1,j)} - 2U_{(i,j)} \} \quad (2.11)$$

would become:

$$H.E.D. = \frac{e}{(\Delta x)^2} \{ U_{(i,j+1)} + U_{(i,j-1)} - 2U_{(i,j)} \} + \frac{e}{(\Delta y)^2} \{ U_{(i-1,j)} + U_{(i+1,j)} - 2U_{(i,j)} \} \quad (2.12)$$

A finite difference form of each and every component within the hydrodynamic equations can then be obtained. These expressions are then incorporated as algorithms in a programming language, such as FORTRAN, and solved for 'the unknowns'.

2.2.5 Non-linearity

The non-linearity of the advection of momentum in the hydrodynamic equations is often ignored for the purpose of ease of calculation (e.g. Reid & Bodine, 1968). The equations solved here, however, are fully non-linear and incorporate all the advective terms.

2.2.6 The Courant Number

To achieve stability in an explicitly solved numerical model, a suitable time-step must be chosen. This time-step is dependent upon the maximum depth of a grid cell in the model area and is calculated using the Courant-Friedrichs-Lowewy criterion expressed in equation 2.27:

$$C = \Delta t \sqrt{g h_{max}} \left\{ \frac{1}{(\Delta x)^2} + \frac{1}{(\Delta y)^2} \right\}^{\frac{1}{2}} \quad (2.27)$$

where,

C = Courant number (< 1 for stability, see section 2.3.3)

Δt = time-step, s

Δy = meridional grid size, m

Δx = zonal grid size, m

h_{max} = maximum depth of the model area, m.

Since the ideal model presented here is of an area small enough for the meridional grid size not to be significantly affected by the change in latitude, and that we try to define the area

as a series of squares, we can assume that $\Delta x \approx \Delta y$. Equation 2.27 then becomes equation 2.28 below.

$$C = \frac{\Delta t \sqrt{2gh_{max}}}{\Delta y} \quad (2.28)$$

As the grid size changes or the maximum depth of the model changes, the time-step will have to be altered accordingly. For instance, in a morphodynamic model where the bathymetry of the sea-bed is constantly changing, if the maximum depth increases significantly then instabilities could be induced. In this case, a restriction must be imposed on the maximum attainable depth in the model or the time-step must be altered to account for the deeper water.

2.3 Choice of Discretization in Time

Once discretization of the hydrodynamic equations has been established in space, it is then necessary to discretize the solution procedure in time. The interval at which time is advanced is known as a time-step.

In order to maintain stability during the solution of the hydrodynamic equations, it is necessary to stagger the process of establishing the unknowns, i.e. ζ , U and V . There are several methods that may be adopted in order to time-stagger the solution procedure.

2.3.1 Implicit

An implicit process is one in which there are several unknowns in each equation. The equations must, therefore, be solved simultaneously at each whole time-step. One method

adopted is that of Gauss elimination and back substitution (e.g. Smith (1978)). This requires the setting up of large sparse matrices, leading to lengthy computations. Owens (1984) gives the appropriate finite difference equations.

Implicit schemes are unconditionally stable in theory, implying that there is no limit to the length of time-step. In practice, however, large time-steps produce inaccurate solutions and therefore an accuracy constraint based on the Courant number and the speed of propagation of the tidal wave is necessary, thus limiting the time-step.

The popular 'Alternating-Direction-Implicit' scheme (ADI scheme) is so-called because of the implicit manner of solution and the fact that all the streams in one direction are evaluated, after which the streams in the remaining direction are evaluated. In areas of intricate geometry, however, this scheme does not work well.

Although time-steps can be large with an implicit manner of solution, thus giving a shorter overall run-time, the complexity of the programming negates straight-forward implementation of various comparative algorithms.

2.3.2 Semi-Implicit

The semi-implicit scheme has been adopted by various authors (e.g Casulli, 1990). This scheme introduces a time-splitting of the advection terms from the rest of the terms. The advective terms are evaluated explicitly at a set time interval, while the rest of the terms are evaluated implicitly at a time interval less than the interval for the advective terms, hence the term semi-implicit. This avoids the complex programming that is required in the solution of the advective terms in an implicit manner, while still allowing large time-steps. This method of solution has not been chosen here.

2.3.3 Explicit

In explicit schemes, there are fewer unknowns than in implicit schemes and the equations can therefore be solved by rearranging. In a central explicit scheme, the time-step is split into two parts. During the first half time-step, the velocities are evaluated from the elevations given in the previous time-step. In the second half-time step, the new velocity values are used to establish the new tidal elevations.

Explicit schemes are conceptually the simplest of all the solution methods and are also the most straight-forward to programme. The method of solution adopted here is wholly explicit in that subsequent solutions of the unknowns are obtained from solutions from a previous time-step. Hence the solution procedure can be known as an 'explicit forward time-stepping finite-difference numerical model'.

In an explicit model, the Courant number must be less than one for the stability criterion (equation 2.28) to be satisfied i.e.

$$1 \geq \frac{\Delta t \sqrt{2gh_{max}}}{\Delta y} \quad (2.29)$$

For the idealized model described in section 2.5, which may have:

$$\Delta x = \Delta y = 5000\text{m},$$

$$h_{max} = 54\text{m},$$

then, to satisfy inequality 2.29:

$$1 \geq \frac{\Delta t \sqrt{2 \times 9.81 \times 54}}{5000}$$

or,

$$\Delta t \leq \frac{5000}{\sqrt{2 \times 9.81 \times 54}} \leq 153.61s \quad (2.30)$$

giving a time-step of less than or equal to 153.61s. In fact, $\Delta t=124.2s$ is a convenient value to choose, it being one three hundred and sixtieth of a tidal cycle. Therefore, one time-step becomes equivalent to one degree of tidal time; thus not only are there 360° in the cycle but also 360 time-steps.

2.4 Instability

Even experienced modellers that have been practising for perhaps ten years or so are still plagued by instabilities within their numerical schemes. It is through the application of differing techniques that 'weak spots', *i.e.* potential sources of instability, in the source code become apparent, be they simply typing errors that have passed unnoticed for a period of time or more serious anomalies (which are generally harder to locate) such as accidentally taking differences over incorrect positions in space or the incorrect labelling of variables involving the misuse of values in subsequent routines.

The above errors may or may not induce instabilities, as there are many possible reasons why instability should occur. Even programming structure may create the necessary conditions. The actual sources of instabilities are extremely awkward to pinpoint, but even so, for every small error that is eradicated during the search for the cause, whether the cause is found immediately or not, the source code contains less potential for instability. The result is that actual source programs become stronger and more robust.

2.5 A Numerical Model of an Idealized Portion of Shelf Sea

A source code written in FORTRAN, called MODKS.FTN77 (see Appendix 1), was developed by the Author to solve the equations of motion (2.4), (2.5) and continuity (2.6) in two dimensions. It is based on models by George & Evans (1991) and by Prandle (Proudman Oceanographic General Purpose Model).

Specification for a numerical model of an idealized portion of shelf sea has been laid down for the comparison and contrasting of methods, principles and algorithms which represent the physical phenomenon of tidal flooding and ebbing. A theoretical bathymetry has been assumed while tidal conditions for the area have been chosen as roughly that of an area of the North Sea off the Humber coast.

It became apparent that a theoretical model design has a great advantage over a model of a real sea area for research purposes in that it is readily adaptable and is not bound by the need to follow rigid guidelines. It is also not restricted by validation processes, since these are not necessary when only internal comparisons are being made. The results from the model are therefore not a guideline for the assessment of its absolute performance in representing a real situation outside of the model environment; instead, the relative performance of algorithms within the model environment become the judgemental factors. This works on the premise that if, say, algorithm 1 gives better results in relation to those obtained from algorithm 2, when all other factors are equivalent, within a theoretical system, then algorithm 1 will also perform better in a representation of a real system.

2.5.1 Setting Up the Model

The model region itself consists of a square divided into 40 x 40 grid cells, each grid cell

having the nominal dimensions 5km × 5km (although different grid sizes can be chosen). A beach was required (see section 2.5.5) in order that the land/sea boundary should move as the tide progressed through its cycles.

2.5.2 Tidal Input to a Theoretical Model

Tidal input to the idealized model was assumed to be sinusoidal and given by:

$$\zeta(t) = A \cos(\omega t - \mathcal{E}) = \alpha \cos \omega t + a \sin \omega t \quad (2.13)$$

where; $\alpha = A \cos \mathcal{E}$, $a = A \sin \mathcal{E}$, \mathcal{E} = phase.

Since the model region is sufficiently small, then the tidal input may be expressed as a Taylor expansion:

$$\alpha = \alpha_0 + x \frac{\partial \alpha}{\partial x} + y \frac{\partial \alpha}{\partial y} \quad (2.14)$$

$$a = a_0 + x \frac{\partial a}{\partial x} + y \frac{\partial a}{\partial y} \quad (2.15)$$

where α_0 and a_0 are the real and imaginary values at the centre of the model, which may be considered as the origin.

Now, if the real and imaginary components from equation 2.13 are differentiated with respect to the x and y (east-west and north-south) directions, we get equations 2.16, 2.17, 2.18 and 2.19:

$$\frac{\partial \alpha}{\partial x} = \frac{\partial}{\partial x} (A \cos \mathcal{E}) = \cos \mathcal{E} \frac{\partial A}{\partial x} - A \sin \mathcal{E} \frac{\partial \mathcal{E}}{\partial x} \quad (2.16)$$

$$\frac{\partial \alpha}{\partial y} = \frac{\partial}{\partial y} (A \sin \mathcal{E}) = \sin \mathcal{E} \frac{\partial A}{\partial y} + A \cos \mathcal{E} \frac{\partial \mathcal{E}}{\partial y} \quad (2.17)$$

$$\frac{\partial a}{\partial x} = \frac{\partial}{\partial x} (A \sin \mathcal{E}) = \sin \mathcal{E} \frac{\partial A}{\partial x} + A \cos \mathcal{E} \frac{\partial \mathcal{E}}{\partial x} \quad (2.18)$$

$$\frac{\partial a}{\partial y} = \frac{\partial}{\partial y} (A \cos \mathcal{E}) = \cos \mathcal{E} \frac{\partial A}{\partial y} - A \sin \mathcal{E} \frac{\partial \mathcal{E}}{\partial y} \quad (2.19)$$

The model area was taken to be a square of side 200km, aligned north-south, with $A_0 = 2\text{m}$ and $\mathcal{E}_0 = 180^\circ$, these particular values being close to values from P.O.L.s' Tidal Atlas Of The British Isles for an area of the North Sea off the Humber coast for species M_2 . There were several reasons for this particular choice. The first was that the maximum depth of the theoretical model was close to that of the sea-bed off the Humber coast. Secondly, this region had an area of similar size to that of the theoretical model which had almost straight co-phase lines for the M_2 tide, with the range varying (approximately) only zonally, and the phase only meridionally, thus allowing simplification of the calculation of the tidal input.

If we assume that, in the theoretical model, the range varies only meridionally, and the phase varies only zonally then, with $\mathcal{E} = 180^\circ$, equation 2.16 becomes equation 2.20, and 2.17 becomes 2.21. Since there is no zonal variation of A , 2.18 becomes 2.22. Equation 2.19 becomes 2.23;

$$\frac{\partial \alpha}{\partial x} = -\frac{\partial A}{\partial x} = 0 \quad (2.20)$$

$$\frac{\partial \alpha}{\partial y} = -A \frac{\partial \mathcal{E}}{\partial y} = -2 \times 0.005 = 10 \text{ mm/km} \quad (2.21)$$

$$\frac{\partial a}{\partial x} = 0 \quad (2.22)$$

$$\frac{\partial a}{\partial y} = -\frac{\partial A}{\partial y} = 10mm/km \quad (2.23)$$

However, when the phase is at 180° , the imaginary component of the tidal elevation is equal to zero. Therefore, the change in tidal elevation is represented by Equation (2.21). This value is based on the assumption that the figure 0.005rad/km is equivalent to $0.3^\circ/\text{km}$, the phase difference obtained from the Tidal Atlas Of The British Isles.

2.5.3 Boundary Conditions

When starting off the numerical model, there is deemed to be no tide anywhere *i.e.* $\zeta = U = V = 0$ everywhere. A tidal regime has to be specified at the sea boundaries in order that a tide may propagate throughout the model area. For a 'wind-up' period, the amplitude of the tide on the boundaries is gradually and linearly increased, which ensures that momentum within the model builds up gradually.

Since there are no restrictions caused by validation procedures, any tide may be chosen for any theoretical basin whether large volumes of water are required to move or smaller volumes. The only restriction is that of maintaining stability. In short, a tidal regime can be chosen to suit whichever phenomenon is being studied. However, it is perhaps better practice to attempt as close a match as possible to real conditions. Figure 2.3 shows a surface plan of the model area including the phase difference along the north and south boundaries and the amplitude differences along the east and west boundaries, there being no phase difference

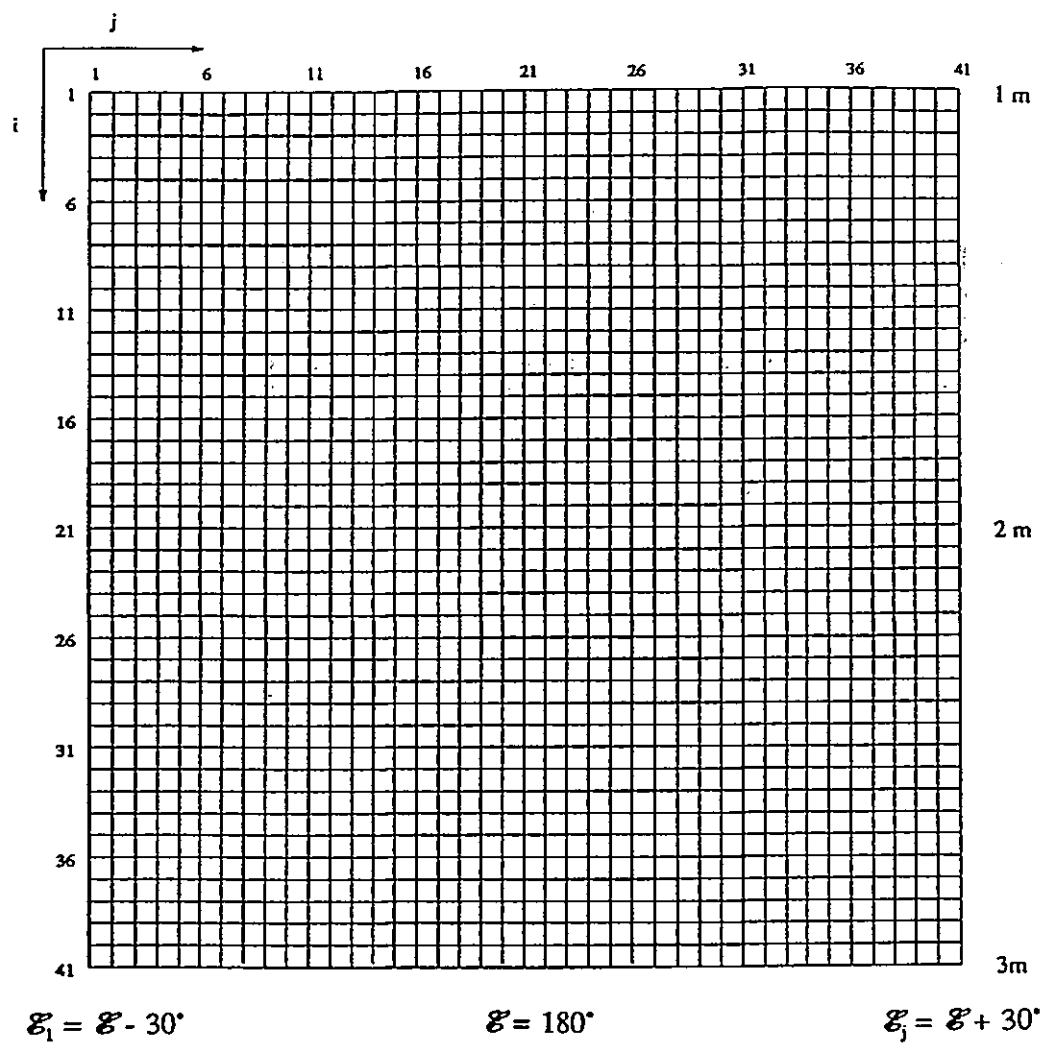


Figure 2.3: Surface plan of model area showing amplitude and phase differences

from north to south and no amplitude difference from east to west.

2.5.4 Bathymetric Design

The process of developing a numerical model from scratch involves the correction of many mistakes and much experimentation. Many of the methods used during the development of a model tend to cope only with the temporary requirements at any given stage in its development. Steps which carry out specific functions are added and subtracted throughout the course of the procedure as different problems and new ideas arise.

One fine example of such a process comes about from the need to establish a bathymetry over which the tide can propagate. Before any flooding and drying of intertidal flats can be incorporated, *i.e.* the introduction of a moving land/sea boundary, the source code must perform in a stable manner throughout a run.

In order that stability could be established, the model was first tested using a completely flat sea-bed with each cell having a depth of 50m, thus avoiding the numerical need of coping with a moving boundary. This gave the sea basin the appearance of a large box. However, instabilities frequently arose leading to an addressing of the problem of defining the bathymetry in a theoretical manner whilst retaining a measure of closeness to the real world.

A short analysis can demonstrate the theory involved when a flat sea-bed is used as the bathymetric specification in an idealized model:

If equation 2.6 is expanded to show the various terms:

$$\frac{\partial \zeta}{\partial t} = -U \left(\frac{\partial \zeta}{\partial x} + \frac{\partial h}{\partial x} \right) - (\zeta + h) \frac{\partial U}{\partial x} - V \left(\frac{\partial \zeta}{\partial y} + \frac{\partial h}{\partial y} \right) - (\zeta + h) \frac{\partial V}{\partial y} \quad (2.24)$$

and if spatial derivatives of ζ and h are separated equation 2.24 becomes equation 2.25:

$$\frac{\partial \zeta}{\partial t} = - \left(U \frac{\partial \zeta}{\partial x} + V \frac{\partial \zeta}{\partial y} \right) - \left(U \frac{\partial h}{\partial x} + V \frac{\partial h}{\partial y} \right) - (\zeta + h) \left(\frac{\partial U}{\partial x} + \frac{\partial V}{\partial y} \right) \quad (2.25)$$

then typical sizes of the terms from equation 2.25 in a shelf sea might be:

	INSHORE	OFFSHORE
U, V	1 ms ⁻¹	1 ms ⁻¹
ζ+h	10 m	100 m
∂ζ/∂x, ∂ζ/∂y	10 mmkm ⁻¹ = 10 ⁻⁵	10 mmkm ⁻¹ = 10 ⁻⁵
∂h/∂x, ∂h/∂y	10 mkm ⁻¹ = 10 ⁻²	1 mkm ⁻¹ = 10 ⁻³
∂U/∂x, ∂V/∂y	1 ms ⁻¹ km ⁻¹ = 10 ⁻³ s ⁻¹	1 ms ⁻¹ 10km ⁻¹ = 10 ⁻⁴ s ⁻¹
giving:		
$-\left(U \frac{\partial \zeta}{\partial x} + V \frac{\partial \zeta}{\partial y} \right)$	10 ⁻⁵ ms ⁻¹	10 ⁻⁵ ms ⁻¹
$-\left(U \frac{\partial h}{\partial x} + V \frac{\partial h}{\partial y} \right)$	10 ⁻² ms ⁻¹	10 ⁻³ ms ⁻¹
$-(\zeta + h) \left(\frac{\partial U}{\partial x} + \frac{\partial V}{\partial y} \right)$	10 ⁻² ms ⁻¹	10 ⁻² ms ⁻¹
$\frac{\partial \zeta}{\partial t}$	<10 ⁻³ ms ⁻¹	<10 ⁻³ ms ⁻¹

If the terms in the equation of continuity of mass, equation 2.6, are scaled (see above), the analysis shows that under normal circumstances, the spatial variation of depth below M.S.L. is typically 2 dex greater than the spatial variation of the tidal elevation. *i.e.* $\partial h/\partial x \approx \partial h/\partial y \gg \partial \zeta/\partial x \approx \partial \zeta/\partial y$. In the case of the flat bottomed idealized model however, $\partial h/\partial x = \partial h/\partial y = 0$ which leads to equation 2.6 being dominated by the terms containing $\partial \zeta/\partial x$ and $\partial \zeta/\partial y$ whereas in normal circumstances these terms are negligible. This appeared to provoke instability and so a random variation in sea-bed depth was imposed.

2.5.5 Introducing a Moving Land/Sea Boundary

Once the model had remained stable for several tidal cycles it became necessary to introduce a moving land/sea boundary. This was achieved by adding a Gaussian expression, equation 2.26, as a loop to MODKS.FTN77, producing a Gaussian shoal. This gave a representation of an island in the middle of a basin with coastline all the way around on which the land/sea boundary would move.

$$h_{(i,j)} = -50 \times (1 - e^{(-R^2/100)}) - 4 \quad (2.26)$$

where, $R^2 = (i-21)^2 + (j-21)^2$, i and j being the model coordinates.

However, before the bathymetry was altered to introduce a 'sudden' moving boundary, the top of the Gaussian shoal was set at a depth of 4m below mean sea-level for five tidal cycles, accounting for the 4 at the end of equation 2.26. At this point the shoal was set to slowly rise to mean sea level, exposing the shoal as the tide fell to ensure drying. The shoal would then stay at mean sea level for a further six tidal cycles, when the model reached a steady state. When confidence had increased in the programming, the shoal was input as an island that did not rise and was set with the 'peak' at mean sea-level. This became the 'test ground' for three existing drying algorithms. Figure 2.4 shows a three-dimensional view of the Gaussian bathymetry.

2.5.5.1 Addition of a Drying Algorithm

Now that a moving boundary had been introduced, it became necessary to include a drying algorithm. Since the Author was most familiar with that of Flather & Heaps' (1975) method,

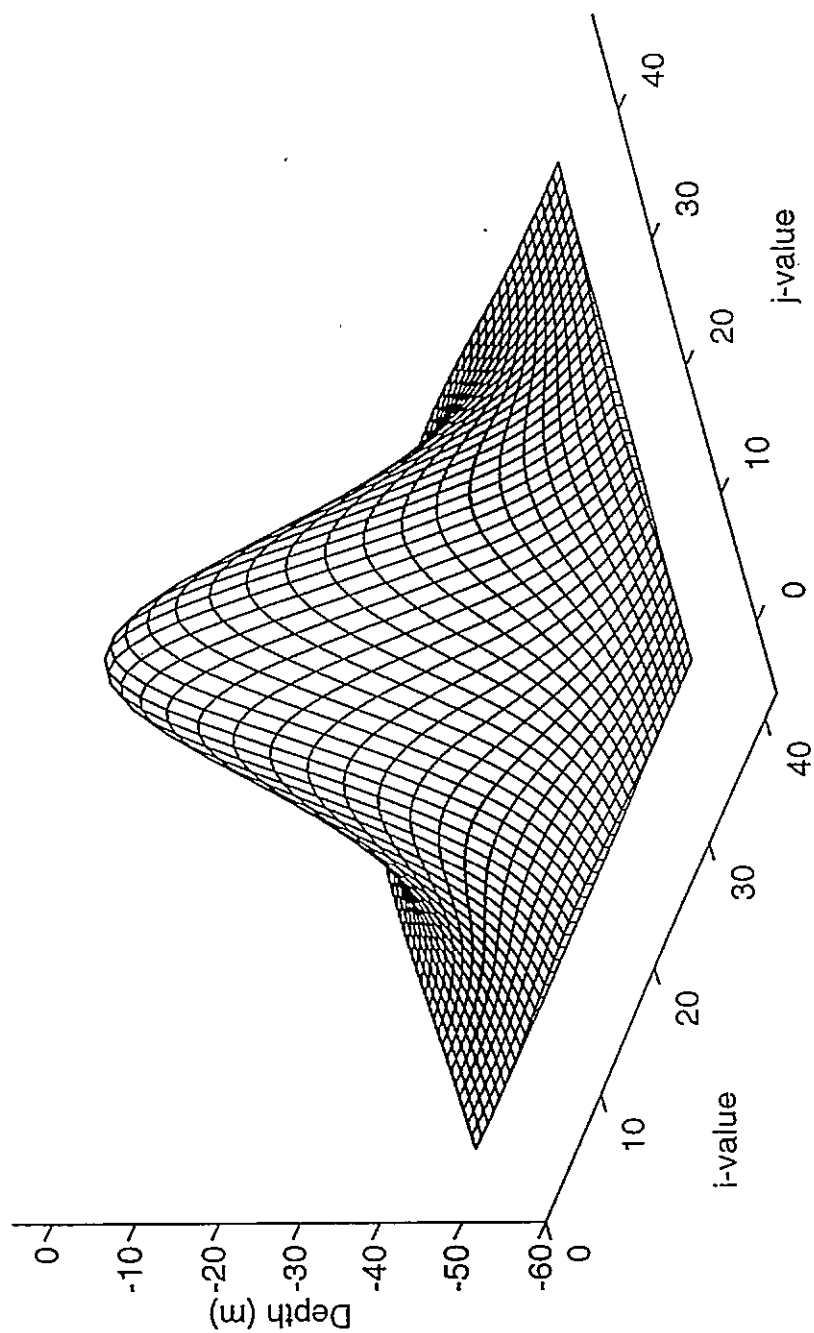


Figure 2.4: Gaussian shoal bathymetry used to test algorithms

it being the one adopted by Dr. George at the University of Plymouth after his initial work incorporating Reid and Bodine's (1968) algorithm, this became the first drying algorithm incorporated into the source code (see Chapter 3). The strength and stability of the numerical scheme was built solidly around this algorithm before the incorporation of any other was considered.

2.5.6 Horizontal Eddy Diffusion

Horizontal eddy diffusion can be quite a perceptual nightmare, it being a rather indefinable quantity. However, possibly the best way to understand the actual functioning of this phenomenon is to picture a swimming pool with a wave machine working. At certain points in the swimming pool, waves will meet and peak, possibly resulting in clapotis (a splash or a spout of water into the air). In modelling terms, this may be considered as a precursor to instability. Although in Public Baths this may be a desirable effect, in a numerical model it is most undesirable. But, supposing the above effect were to be prevented, given that all energy input must remain at the same frequencies, then the most assured method would be to restrict the movement of the water. This could be achieved by covering the surface with a material that has just the correct properties to prevent the splashing from occurring - or a heavier material that could even begin to suppress the formation of waves. This is the behaviour of the horizontal eddy diffusion term. A particularly high value makes the sea system behave as though it has a material spread over the surface that has a strong damping effect. A lower value may be considered to have a lesser damping effect. Obviously, it is not desirable to achieve stability simply by applying a greater and greater eddy diffusion value as this would provide misleading results through over-restriction of water movement.

Ideally, eddy diffusion should be as light as possible in order that the water column has as much freedom of movement as possible.

In MODKS.FTN77, horizontal eddy diffusion was made depth-dependent, increasing with increase in depth. Once stability was achieved with a flat-bottomed sea-bed, a sensitivity analysis was conducted to establish a minimum value of the horizontal eddy diffusion required to ensure stability. This turned out to be ten times the depth.

2.5.7 Coriolis Acceleration

The Coriolis acceleration has been included in the model since the scale of the water-body considered here makes it significant. The spinning of the Earth has an effect on accelerating particles, of any size, and deflects the path of the particle to the right in the Northern Hemisphere. Calculation of the 'Coriolis effect' can be simplified in numerical tidal models for small sea areas, over which the latitude changes only slightly, by adopting the '*f-plane approximation*' (e.g. Gill, 1982) which allows $2\omega\sin\phi$ to remain constant over the small change in latitude. For models which cover large sea areas, however, it is apparent that this component would vary significantly over the large change in latitude and therefore must be included as a varying quantity (e.g. George, 1993).

2.6 Data Output

Output files consisted of consecutive or periodic values of all possible variables within the hydrodynamic equations.

A subroutine was written into MODKS.FTN77 to produce an interim output over a 'window' of the model area which would provide a time-sequenced view of an area specifically chosen

1. 1. 1.

2. 2. 2.

3. 3. 3.

4. 4. 4.

5. 5. 5.

6. 6. 6.

7. 7. 7.

8. 8. 8.

9. 9. 9.

to observe the progression of the tidal elevation and current component values. This was of particular value in locating the cause/source of an instability as it developed.

Other components of the hydrodynamic equations were logged throughout a cycle so as to provide time-series which would show how each component varied for a particular cell and its surrounding cells. This provided the basis for a qualitative analysis of the effects of a drying and wetting cell on its surrounding cells and the physical processes occurring within the chosen cell.

2.6.1 Representation of Output Data

Graphical illustration of output data was achieved through software written by the Author in FORTRAN using calls to graphics subroutines in the GINO-F package. This software provided graphical representation of up to five of the time-series obtained, and can be seen in Appendix 2. This proved to be invaluable for the initial qualitative assessment of different drying algorithm performances since the effects of discontinuities and errors in programming could be observed. It was an aim to produce smooth tidal curves, so, for instance, it could be assumed that the more effective the drying algorithm used, the smoother the tidal curves should appear.

Abnormally long or short drying periods could also be spotted by comparison of the tidal curve obtained to a basic tidal curve for a specific point. A basic tidal curve, in this case, was one obtained analytically assuming that there was no shoal present. This provided an approximation of the time when the tidal height should, ignoring shallow water distortion, pass the sea-bed elevation of a dry cell, thus indicating that it should become wet at around that time.

Tidal stream information can also be represented as 'arrows', showing their direction and magnitude (set and rate). Commercially available software, such as MATLAB®, allows the production of 'arrow' pictures from the large data matrices output from MODKS.FTN77 without the need to write extensive plotting software.

CHAPTER 3

EXISTING 'DRYING' ALGORITHMS

Since there have been numerous attempts at the incorporation of a moving land/sea boundary in two-dimensional numerical tidal models, the Author has chosen to analyze the underlying principles of the apparent two differing approaches to the solution of the problem.

In this chapter, the minutiae of the existing wetting and drying algorithms are critically examined. In addition, subsequent improvements to each traditional method have been analyzed.

3.1 Leendertse & Gritton

Leendertse & Gritton (1971) adopted a method whereby three tests were applied at each grid point, in order to locate grid cells which were becoming dry, and to remove them from the computational field, thereby inducing a moving land/sea boundary. Firstly, a volumetric flow was calculated through the walls of each grid square and if this cross-sectional flow became negative (that is, in the opposite sense to which it should be) then the grid square was assumed to have become dry and removed from the computation whilst the current values

were set to zero. Or, with the volume given by (see figure 3.1):

$$VOL_{i,j}^t = [\zeta_{i,j}^t + \frac{1}{4}(h_{v_1} + h_{v_2} + h_{u_1} + h_{u_2})] \cdot \Delta s^2$$

where s = grid spacing, if $VOL_{i,j}^t$ was negative, then the grid square was assumed dry and

the water depth set to the value at the previous computation, $\zeta_{i,j}^{t-\frac{1}{2}}$. In addition, the previous

row or column of calculations were then recalculated with the grid square taken as being dry.

Secondly, the depths of each of the four cross-sections (see figure 1.1) surrounding each grid square were calculated at the end of each half time step, i.e. $H_{c_1}^t, H_{c_2}^t, H_{c_3}^t, H_{c_4}^t$ (see figure

3.2) where;

$$H_{c_1}^t = h_{v_1} + \frac{1}{2}(\zeta_{i,j}^t + \zeta_{i-1,j}^t)$$

Again, if the results were numerically negative, the grid square was deemed to have become dry.

The third and most rigorous test of whether a grid square had dried or not was that if any of the four cross-sections decreased to less than a critical value, then that grid point was removed from the computation and the water level was set at its last value and maintained at that level until the grid square flooded. The critical value, ζ_{cr} , was determined by the depths of the surrounding grid squares such that:

$$\zeta_{cr_{i,j}} = h_{pr} - h_{\min_{i,j}}$$

where h_{pr} is a height preset above the highest surrounding mean depth value and $h_{\min_{i,j}}$ is

the minimum value of $h_{v_1}, h_{v_2}, h_{u_1}$ and h_{u_2} .

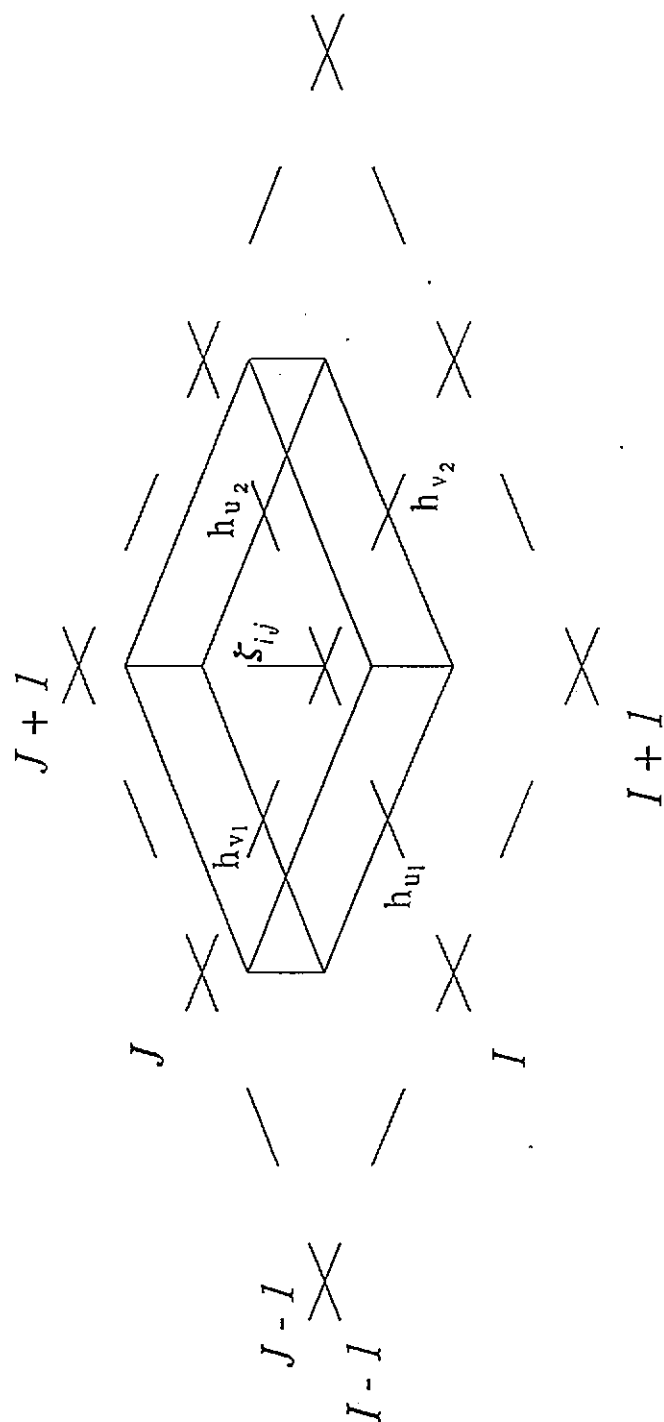


Figure 3.1: Diagram to show depth related variables used to evaluate the volume of a cell

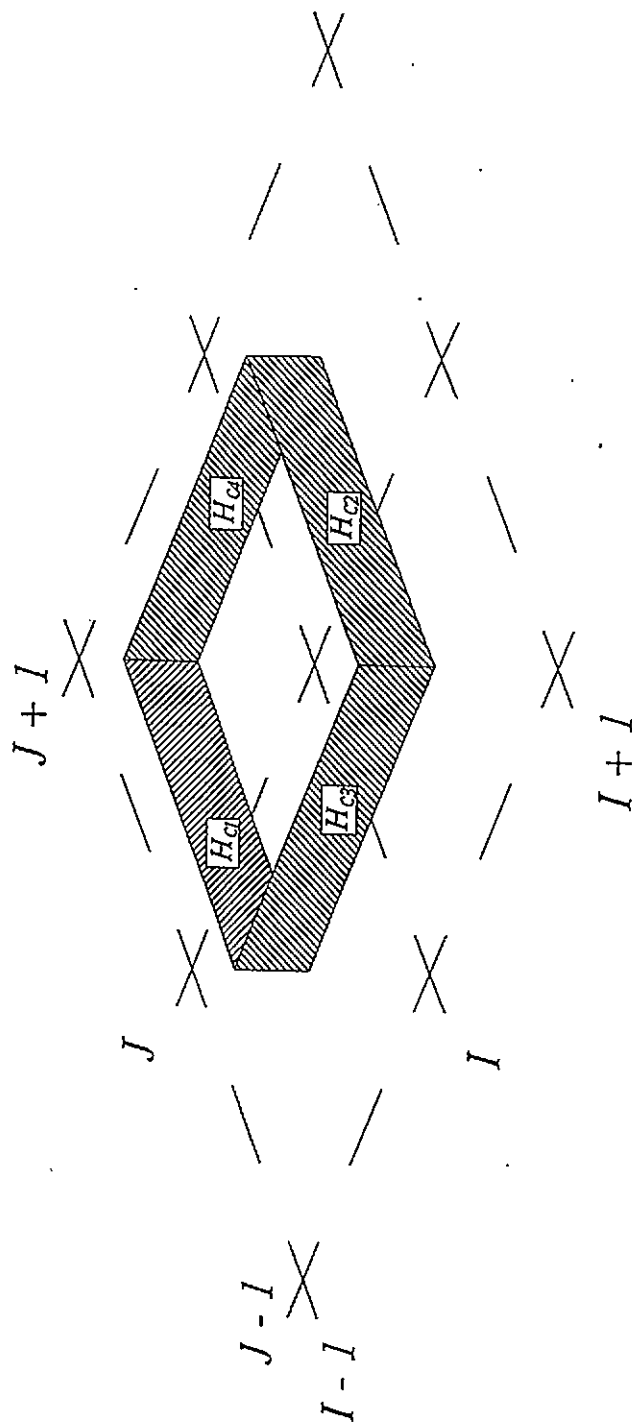


Figure 3.2: Diagram to show cross-sections used for determining the moving boundary

Leendertse and Gritton (1971) found that discrete changes in the land boundary as grid squares began to dry out, and also to flood, created numerical disturbances. To overcome this they allowed computational time for the disturbances to decay by making this third and final test, since it was by this test that most grid squares became dry, at intervals greater than the time-step.

The test for flooding was whether or not the average water depth of the surrounding grid squares was greater than the depth of water left in the grid square by the drying procedure:

$$\zeta_{i,j}^{t-\frac{1}{2}} < \frac{1}{4}(h_{v_1} + h_{v_2} + h_{u_1} + h_{u_2})$$

Again, transport cross-sections were computed with a positive cross-section resulting in the flooding of that square. This check was also carried out at intervals greater than the time-step to allow the computational noise generated by the moving boundary time to decay.

This method has been incorporated in the study tool described in Chapter 2.

3.2 Falconer & Owens

In 1984 Falconer applied his technique to a comparison of the hydraulic features and flushing characteristics of Holes Bay in Dorset, to test two proposed new outlines of the bay. In this bay, large areas of marshland are dried out and flooded throughout the tidal cycle, creating a moving land boundary. Falconer (1984, 1986) overcame the associated problems using Leendertse & Gritton's (1971) drying technique with two basic differences. Firstly, the first two checks were combined and carried out at a different time in the tidal solution and only two cross-sections in the direction of the calculation were considered rather than all four cross-sections for each grid square. However, in the 1986 paper all four cross-sections were

considered in the finite difference equations. Secondly, an average water elevation was used in calculating each cross-section rather than a particular elevation in a wet grid square (see figure 3.3):

$$H_{c_1}^t = h_{v_1} + \frac{1}{4}(\zeta_{i-1,j-1}^t + \zeta_{i-1,j+1}^t + \zeta_{i,j-1}^t + \zeta_{i,j+1}^t)$$

Falconer reported that although this increased the computational cost, it improved the accuracy of the scheme, with the possibility of numerical instabilities being generated reduced.

However, Falconer discovered that when this procedure was applied to a model of the Humber Estuary, unstable solutions were produced despite the claim that implicit solutions are unconditionally stable. In order to refine the procedure, a method was developed which would allow for large grid size and time-step models (Owens, 1984; Falconer & Owens, 1987). An analysis of the method was made using an idealized basin. This illustrated the discontinuities produced by the sudden setting to zero of streams in grid squares which still retained significant volumes of water. Owens (1984) redefined the way that the volume element of a grid square was evaluated:

$$VOL_{i,j}^t = (\zeta_{i,j}^t + h_{\max_{i,j}}) \cdot \Delta S^2$$

where, $h_{\max_{i,j}}$ = maximum value of h_{v_1} , h_{v_2} , h_{u_1} and h_{u_2} .

This assumed that the bed within a grid square was level with the value of the lowest surrounding mean depth. Falconer & Owens (1987) modified the method by introducing two new tests. The first was to check each cross-section at the end of every half time-step, if a cross-section was found to be negative then it was equated to zero along with the perpendicular velocity component. Therefore, if the deepest cross-section of a grid square

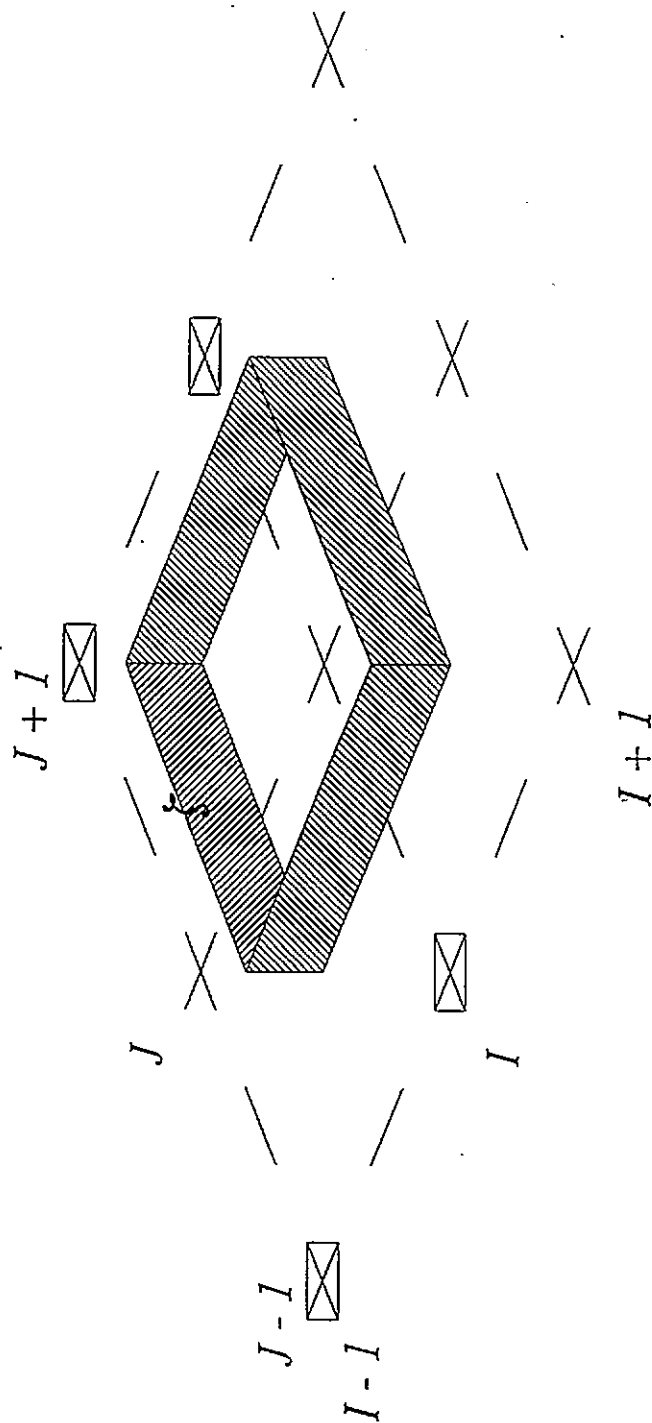


Figure 3.3: Diagram showing the location of elevation points used to establish the elevation at a stream point

became negative then the stream velocities across all four cross-sections were zero and the grid square had become dry. This had the effect of smoothing the reduction of velocity components to zero by removing the grid squares from the calculation in a more evenly spaced manner during the solution of the hydrodynamic equations. Also, the test for a dry square becoming wet was carried out at every time-step rather than every few time-steps (Leendertse 1970; Leendertse & Gritton 1971; Falconer 1984, 1985, 1986). The second test involved setting a critical level at a predetermined depth above the lowest surrounding depth. This defined a minimum cross-sectional area through which water could flow when a grid square flooded again. With this method however, the predetermined depth is most effective when set at different levels depending on the tidal range. For instance, Falconer found the best results for the tidal range in his study of the Humber Estuary were obtained using a predetermined depth of 0.2m.

This method has been incorporated in the study tool described in Chapter 2.

3.3 Flather & Heaps

Independently of the work initiated by Leendertse (1970), Flather and Heaps (1975) proposed a new finite difference method for tidal computations in shallow water.

The test-bed for the development of their new techniques was Morecambe Bay. This was considered to be suitable due to the large areas of sandbanks exposed at low tide. Their approach was less complex than that of Leendertse and Gritton (1971). The specific detail of whether or not a cell had become wet or dry was:

If (i) $H_{i,j}^{t+\Delta t} > 0$ and $H_{i,j+1}^{t+\Delta t} > 0$ so that $H_{u,i,j}^{t+\Delta t} > 0$,

or (ii) $H_{i,j}^{t+\Delta t} > 0$ and $H_{i,j+1}^{t+\Delta t} \leq 0$ and $H_{u,i,j}^{t+\Delta t} > 0$ and $\zeta_{i,j}^{t+\Delta t} - \zeta_{i,j+1}^{t+\Delta t} > \varepsilon$,

or (iii) $H_{i,j}^{t+\Delta t} \leq 0$ and $H_{i,j+1}^{t+\Delta t} > 0$ and $H_{u,i,j}^{t+\Delta t} > 0$ and $\zeta_{i,j+1}^{t+\Delta t} - \zeta_{i,j}^{t+\Delta t} > \varepsilon$,

where H_u is the total water depth at the east-west velocity point and ε is a critical elevation difference, then there was still considered to be flow through the grid square (see figure 3.4 for a description of the variables involved).

As with other drying procedures, if a grid square was deemed to have become dry, then the streams were set to zero; if it had become wet, then new values of the tidal streams were calculated from the solution of the equations of motion.

Flather and Heaps' 1975 paper presents time series which show the distortion of the tide as it propagates through shallow water as well as discontinuities induced by the presence of cells which wet and dry.

This method has been tested using the study tool described in Chapter 2.

3.4 Flather & Hubbert

Flather and Hubbert (1989) presented a refined version of Flather and Heaps' (1975) drying technique.

This refined method was developed through the comparison of various schemes. In their first scheme the depth was defined at the centre of each coarse grid square but in the high resolution area the depth was taken to be:

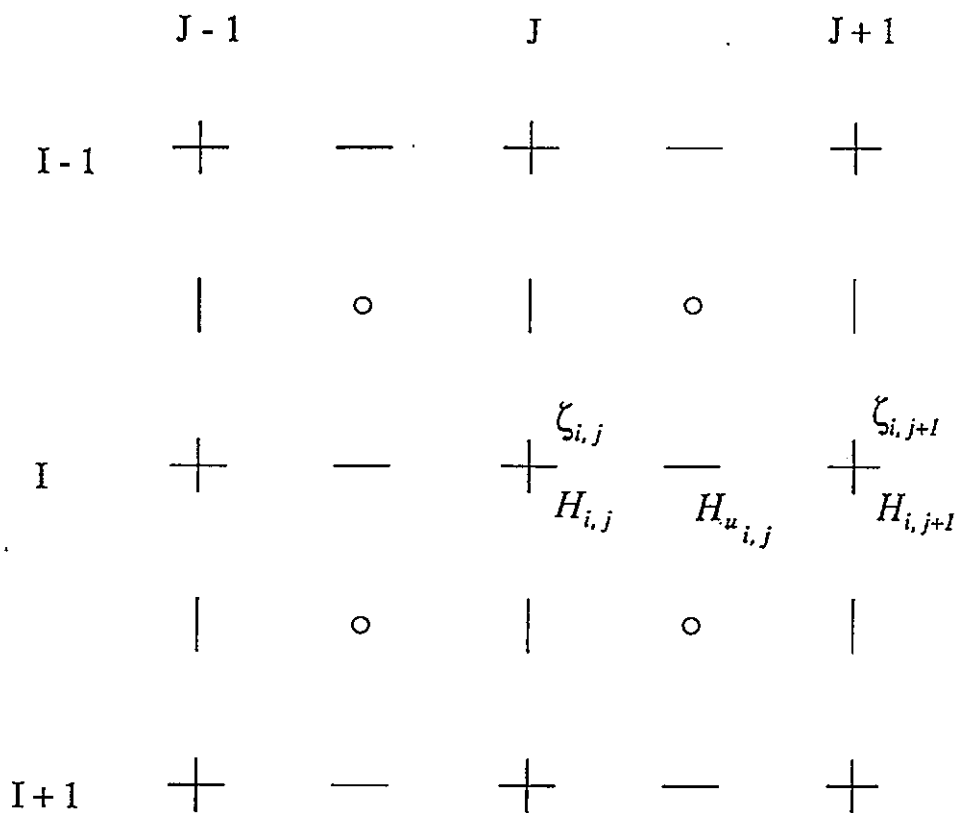


Figure 3.4: Diagram showing the positions in space of the variables which define the moving boundary

$$h = \frac{1}{N} \cdot \sum (h_j | h_j > h_{land}) \quad \text{if } 50 \leq N \leq 100$$

$$h = h_{land} \quad \text{if } 0 \leq N < 50$$

where N is the number of high resolution grid points within a grid square which are not permanent land points. This provided a mean depth of the 'wet' part of a grid square. It also 'smoothed out' a deep channel, so Flather & Hubbert artificially increased the depth along a route corresponding to the topographical position of the channel thus artificially creating a deep water channel. This made the channel unrealistically wide, so Flather & Hubbert decided to represent the deep channel in a one-dimensional format by modifying the two-dimensional scheme in this area. By including additional factors, in terms of area and breadth constants, Flather & Hubbert were able to make the one-dimensional and two-dimensional representations of the equation of continuity equivalent. To achieve this, the continuity equation, equation 2.6, was re-written thus:

$$A \frac{\partial \zeta}{\partial t} + \frac{\partial}{\partial x} \{ (h + \zeta) B U \} + \frac{\partial}{\partial y} \{ (h + \zeta) C V \} = 0 \quad (3.1)$$

If $A = B = C = 1$, then equation (3.1) is identical to equation (2.6). Written in finite-differences, equation (3.1) becomes equation (3.2):

$$A(\zeta_{i,j}^{t+\Delta t} - \zeta_{i,j}^t) + \Delta t \left(\frac{H_{u,i,j}^t B_{i,j} U_{i,j}^t - H_{u,i,j-1}^t B_{i,j-1} U_{i,j-1}^t}{\Delta x} \right) + \Delta t \left(\frac{H_{v,i-1,j}^t C_{i-1,j} V_{i-1,j}^t - H_{v,i,j}^t C_{i,j} V_{i,j}^t}{\Delta y} \right) = 0 \quad (3.2)$$

where;

A	=	area factor
	=	wetted area of grid box/total area of grid box
B	=	breadth factor for <i>U</i> -point of cell
	=	breadth factor over which flow occurs/total breadth of cell
C	=	breadth factor for <i>V</i> -point of cell
H_u	=	total water depth at <i>U</i> -point
H_v	=	total water depth at <i>V</i> -point

Thus, for example, if there is no north-south flow (i.e. $V = 0$) then with arbitrary values of the area and breadth factors, the two-dimensional equation approximates a one-dimensional flow in the east-west direction.

Changing from one-dimensional to two-dimensional flow as the banks of the channel is breached is represented by an appropriate drying procedure which either sets V to zero if the surrounding banks are dry or computes its value from the momentum equation.

The drying test used was that by Flather & Heaps (1975) (see section 3.3), where the tests were carried out after each U and V calculation to determine whether the associated grid point was 'wet' or 'dry'.

A final scheme allowed the area and breadth factors to be included but used as variables so that they could change as the water level changed. This allowed the water level in a cell to decrease progressively until the cell dried completely, thus reducing the shock that a sudden change from a cell being entirely 'wet' to entirely 'dry' induces in the system.

This was attained by combining the breadth factors with the total water depths at the stream points of a cell. This meant replacing BH_u and CH_v in equation (3.2) with the redefined factors B' and C' . These now represent the transport across the cross-sectional area of each side of the cell. The new areal and cross-sectional factors were established from the high

resolution bathymetry and defined at fixed surface elevation levels every 0.1m in the range -3.5m to 3.5m. If the surface water level was between any of the 0.1m increments, the values of A' , B' and C' were calculated by linear interpolation.

With the variable areal and cross-sectional factors, equation (3.2) now becomes equation (3.3) expressed in finite-differences:

$$A(\zeta_{i,j}^{\Delta t+t} - \zeta_{i,j}^t) + \Delta t \left(\frac{B'_{i,j} U_{i,j}^t - B'_{i,j-1} U_{i,j-1}^t}{\Delta x} \right) + \Delta t \left(\frac{C'_{i-1,j} V_{i-1,j}^t - C'_{i,j} V_{i,j}^t}{\Delta y} \right) = 0 \quad (3.3)$$

Publication of results for this method show that there are still considerable anomalies present in the solution. Figure 3.5 shows the wetting part of the tidal cycle for the same cell under two different experimental conditions. It can be seen that there is a considerable measure of disturbance caused by the wetting of this cell. The result of a cell wetting on nearby cells has not been published. In addition, R.A. Flather has indicated, through personal communication, that although the present level of moving land/sea boundary computations at P.O.L. is quite refined, the results are still unsatisfactory. It is a problem, however, that he considers would require too much time for further development.

Due to the impracticalities of digitizing the bathymetry to obtain an area of high resolution and the significant increase in computational costs (particularly high when large areas wet and dry), the Author has not tested this numerical scheme.

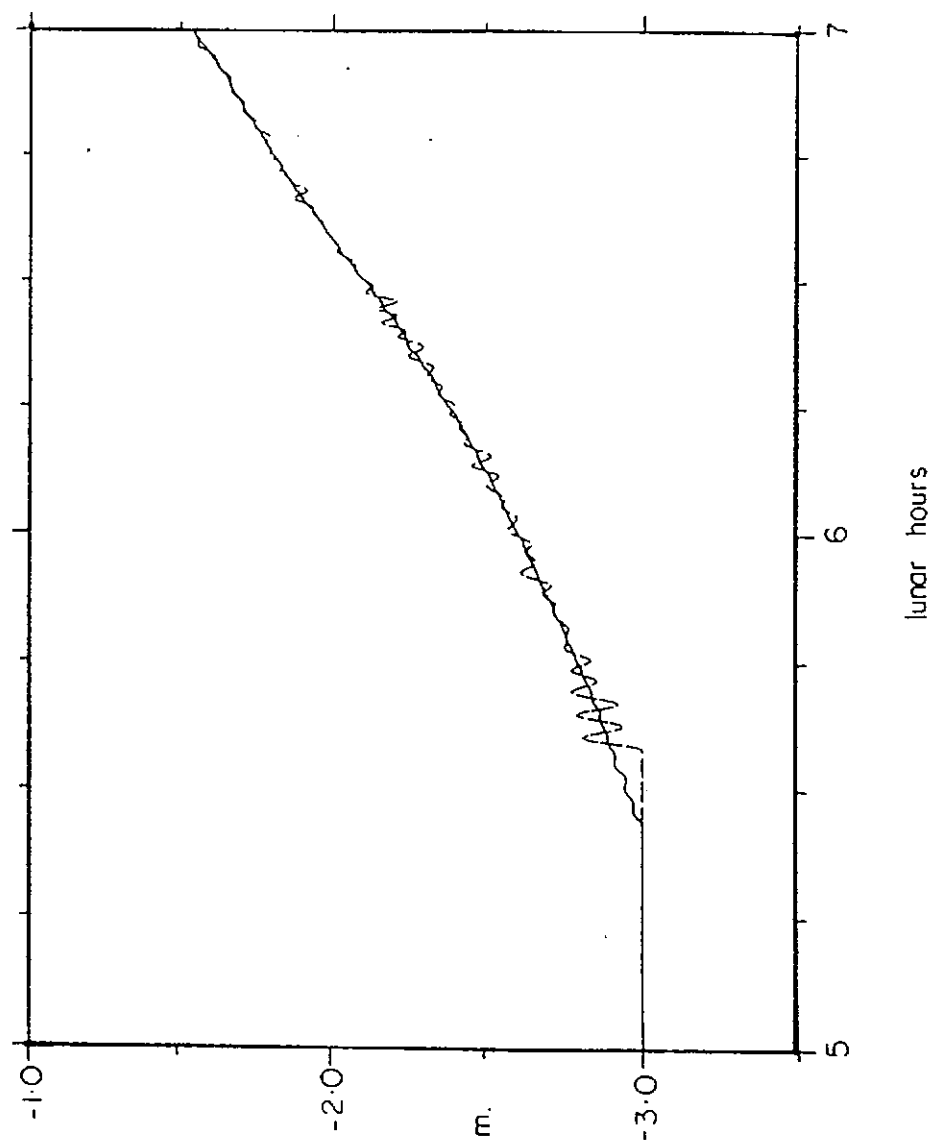


Figure 3.5: To show high frequency oscillations for two different experimental runs (after Flather & Hubbert, 1989)

3.5 Comparison of Results

The results obtained from MODKS.FTN77 have been presented in graphical format, showing time series of; the elevation of a cell chosen to be a test cell, the elevation of a cell adjacent to the test cell in order to demonstrate the effect that nearby cells can have on each other, and various components from the hydrodynamic equations in two dimensions which pertain specifically to the test cell already mentioned.

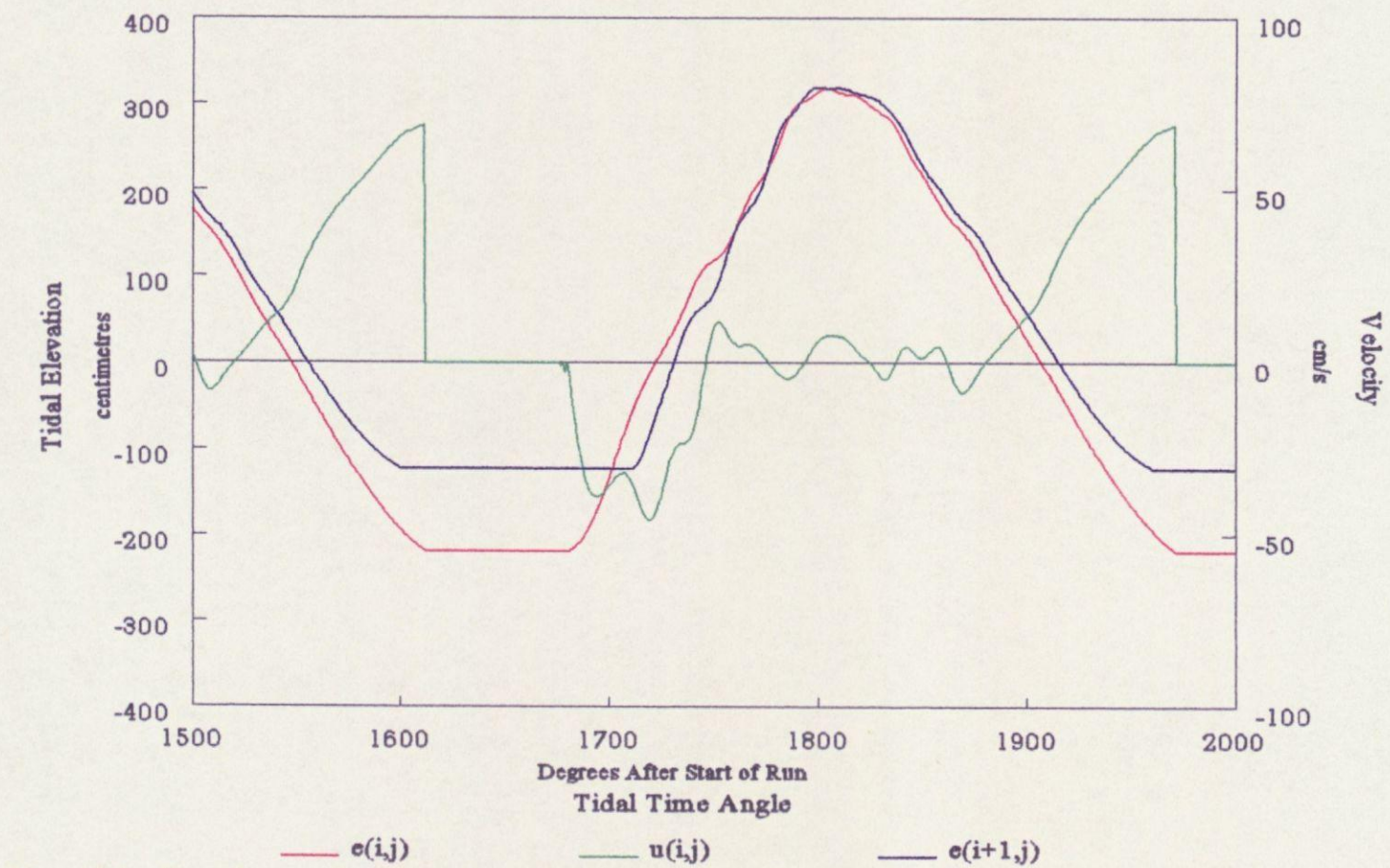
3.5.1 Leendertse's (1970) Drying Algorithm

Figure 3.6 shows two tidal elevation profiles and the easterly component of the depth-averaged velocity. Qualitative analysis shows that there are quite powerful 'shocks' introduced into the system, causing the elevation profiles to kink quite considerably at , for example, about 1750°. These kinks are caused by a nearby cell becoming wet; slowing the rate of rise in the already wet cells as the momentum balance adjusts to the sudden appearance of a large area of sea. This slowing of the rate of rise becomes too exaggerated and the rate of rise is then accelerated, which is also too severe and eventually another decrease in the rate of rise occurs. This time, however, the rate of decrease in the rate of rise is less severe than the initial decrease, indicating the damping of an oscillatory process which is trying to attain equilibrium.

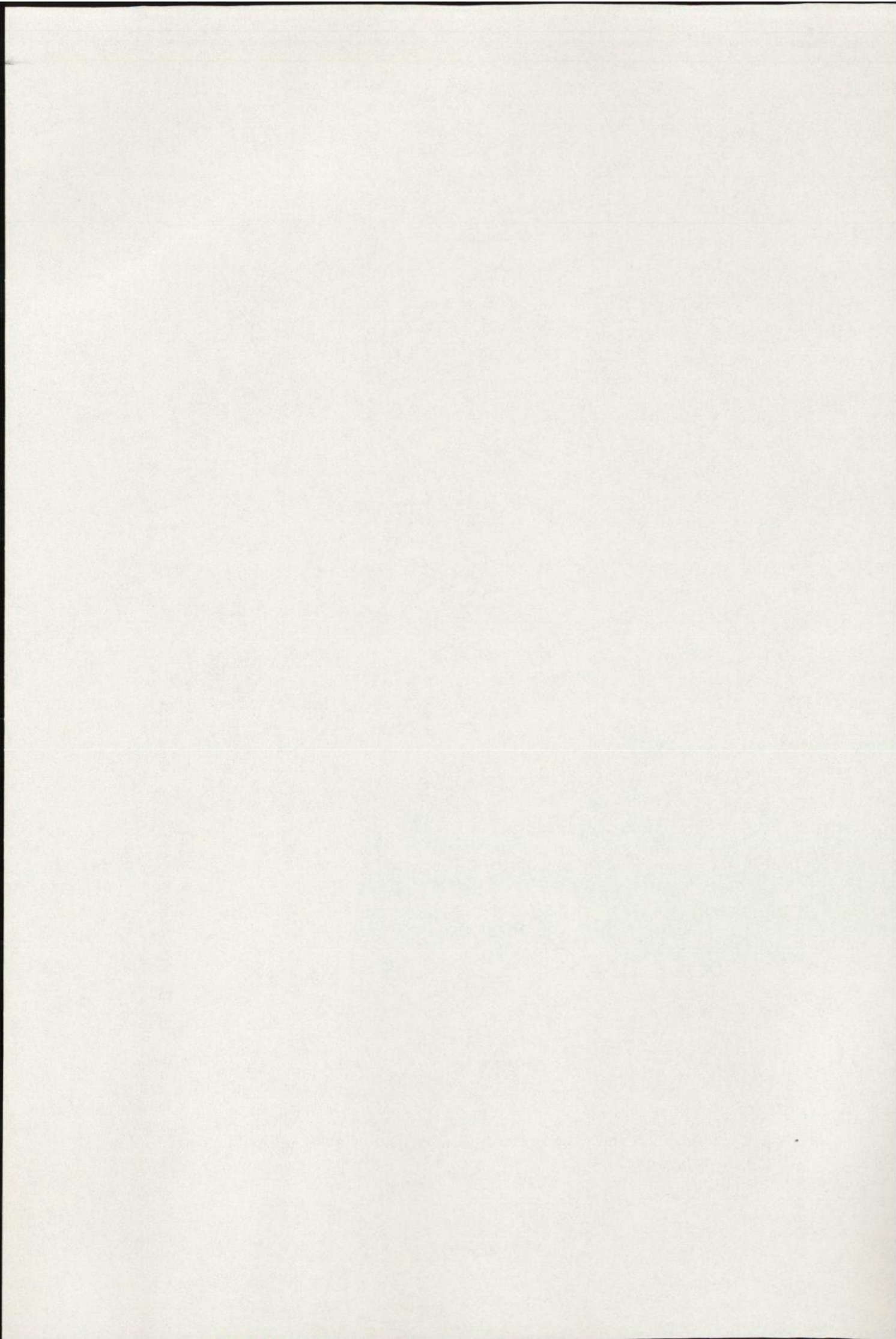
The effects of this disruption in the elevation profiles can be seen until just after high water when equilibrium is attained for a short while.

The velocity profile shown in figure 3.6 is the u-component of the depth averaged velocity (*mutatis mutandis*, the v-component behaves similarly). It can be clearly seen in figure 3.6 that there is uncertainty in the wetting process of this particular algorithm as the velocity

Figure 3.6:
Elevation and easterly velocity component of a test cell with elevation of an adjacent cell



Note: Using Leendertse's (1970) Drying Algorithm
Test Cell: (18,21)



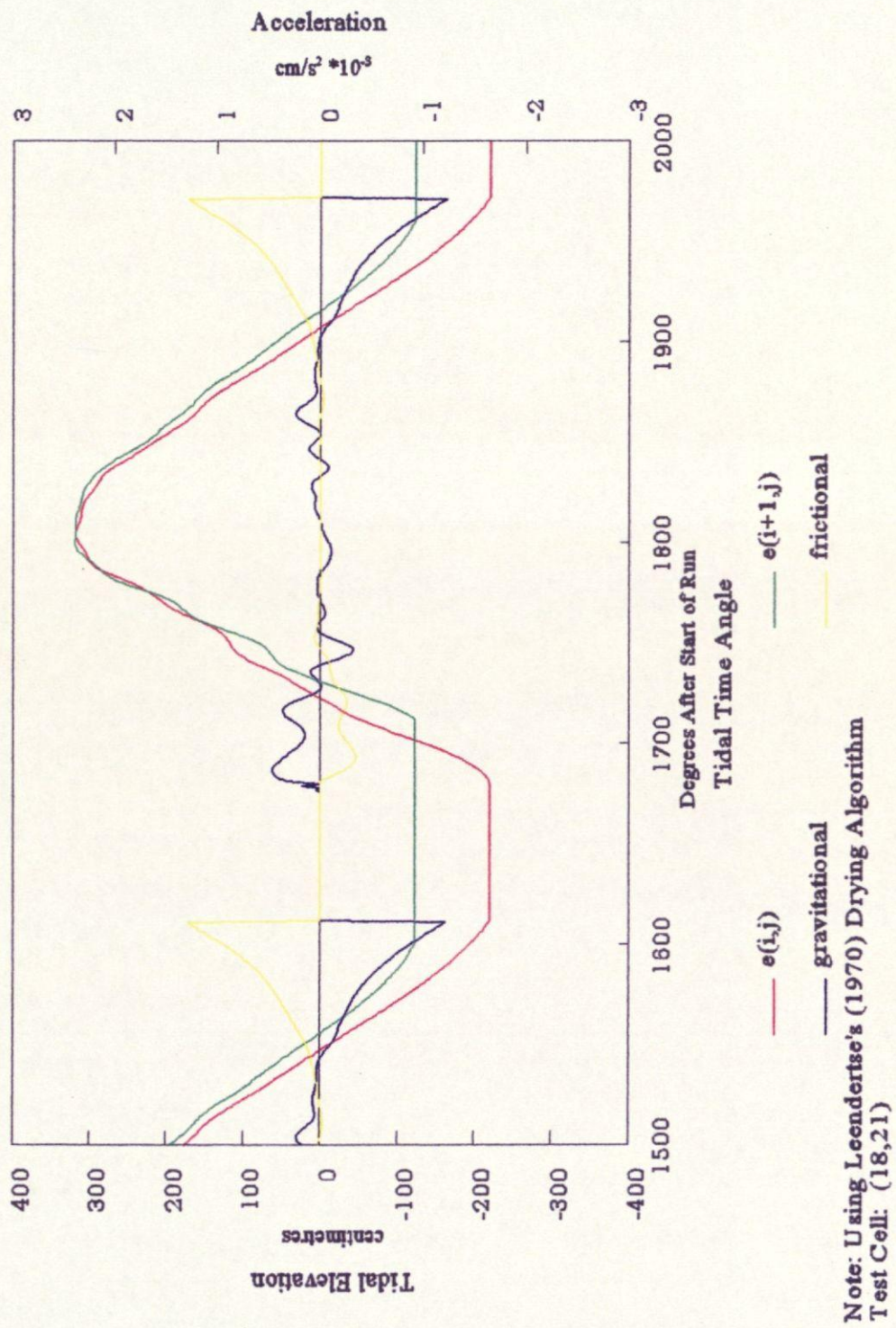


Figure 3.7: Elevation and accelerations due to both gravity and friction of a test cell with the elevation of an adjacent cell

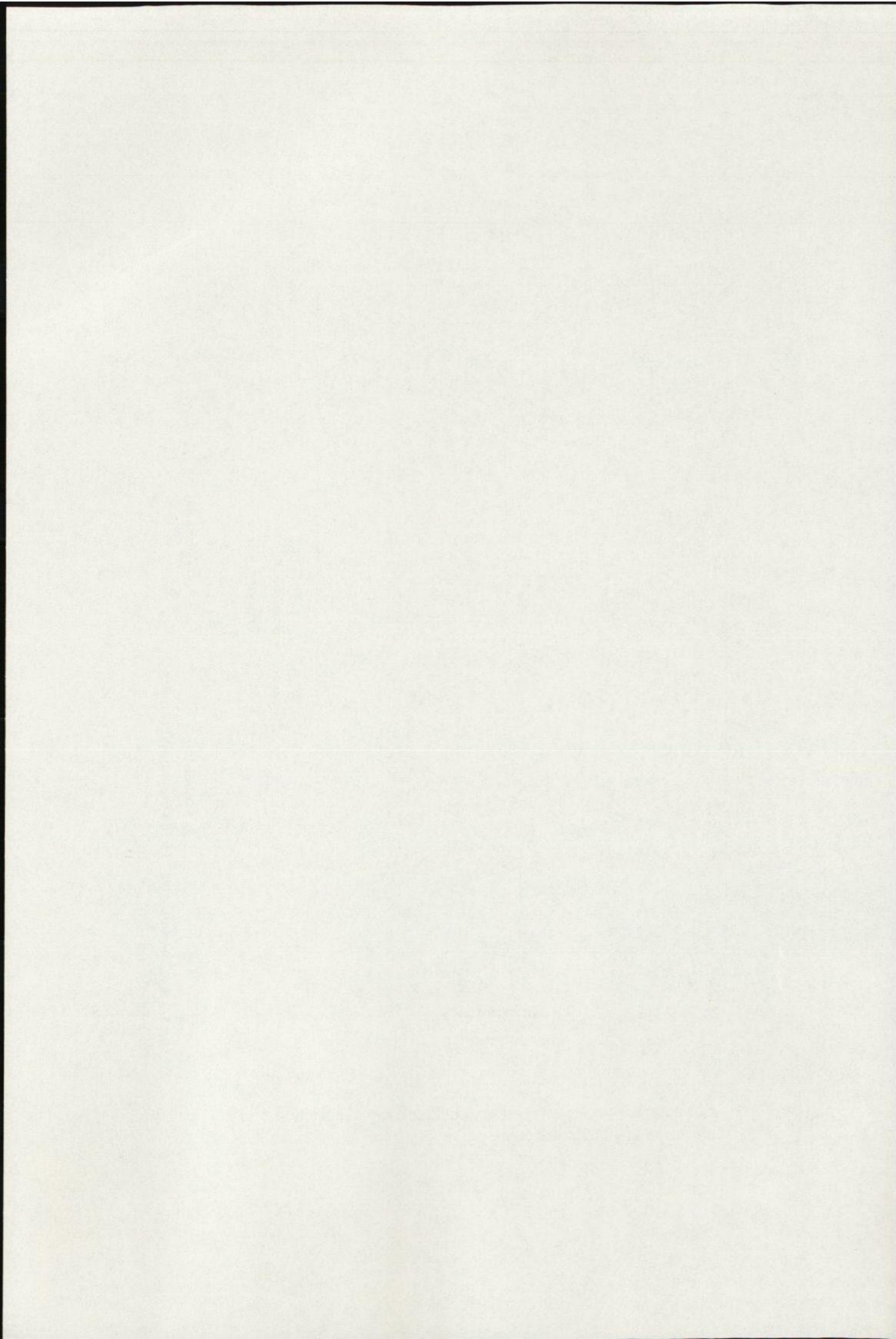
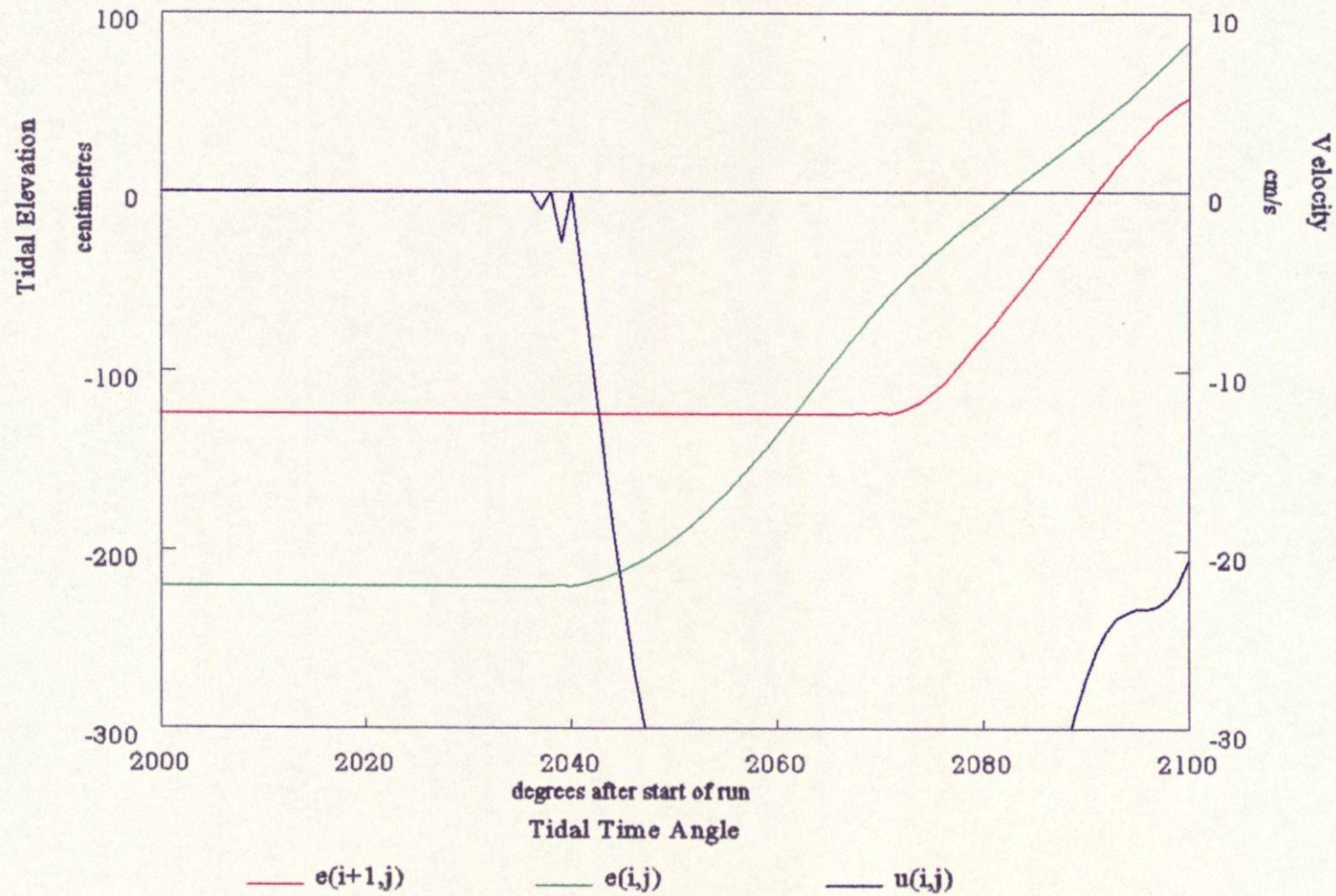
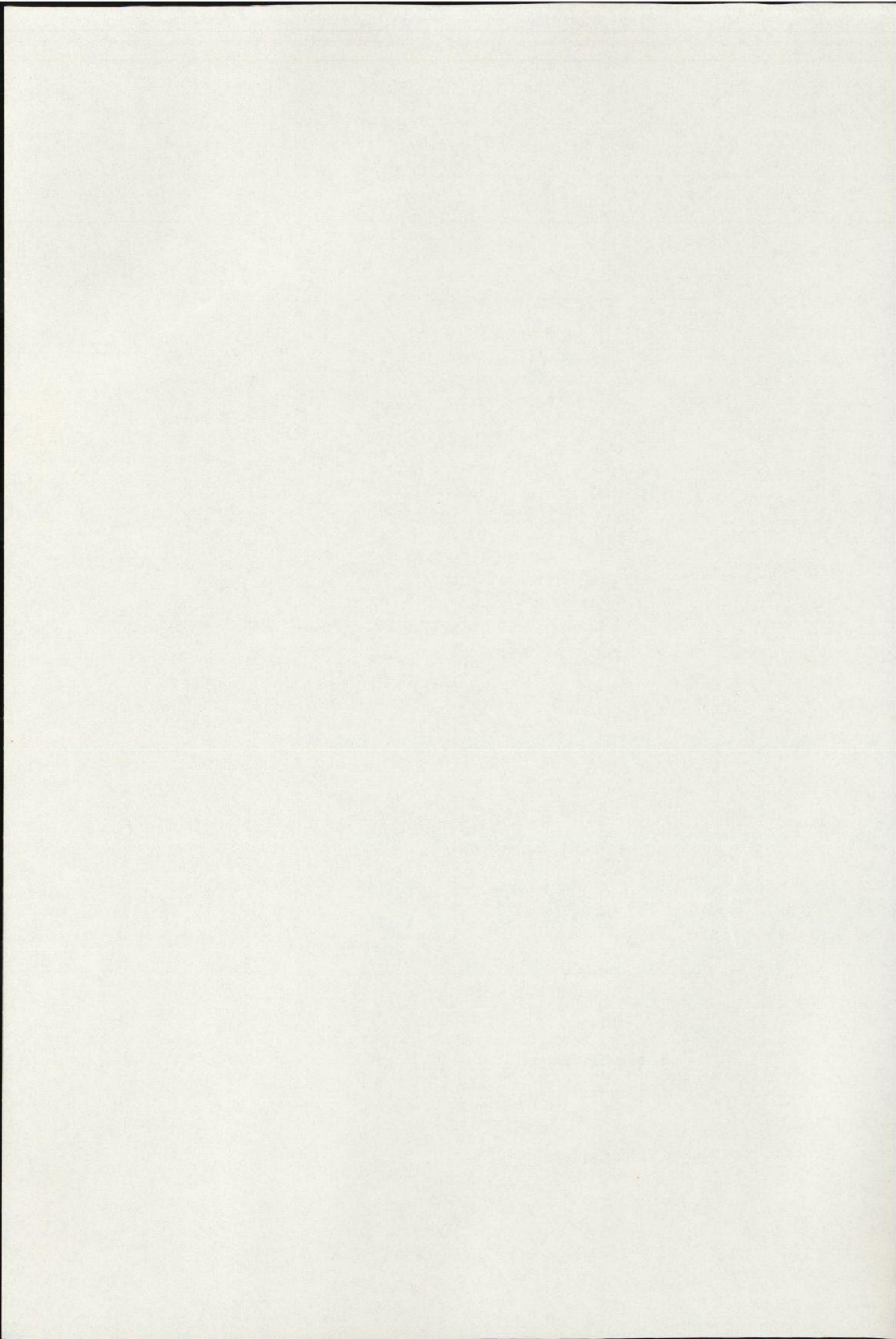


Figure 3.8: Initial wetting period



Note: Using Leendertse (1970) Algorithm
Test Cell: (18,21)



alternates between a real value and zero for several time-steps after the initial wetting.

This is also reflected in the profiles of the gravitational and frictional terms (in the easterly direction only) shown with the tidal elevations in figure 3.7 at around 1680°.

Figure 3.7 also shows that the gravitational and frictional terms tend to balance each other out as the water becomes shallow.

The drying process appears to operate satisfactorily, however, one must bear in mind that once a cell has been 'switched off', it takes no further part in the computational process until it becomes wet again. The actual effects of a cell drying on its surroundings are therefore far less pronounced than those disturbances caused by a cell becoming wet and its subsequent behaviour.

The initial wetting period can be seen in more detail in figure 3.8. This figure demonstrates the alarming effect that the wetting of a cell using Leendertse's (1970) method can have. We can see here that there is a pronounced disparity between the rates of rise of the two adjacent cells and the effect that this has on the shape of the profile after the initial wetting. This figure also enlarges the disturbance in the velocity field. This disturbance shows the uncertainty of wetting in this method.

3.5.2 Owens' (1984) Drying Algorithm

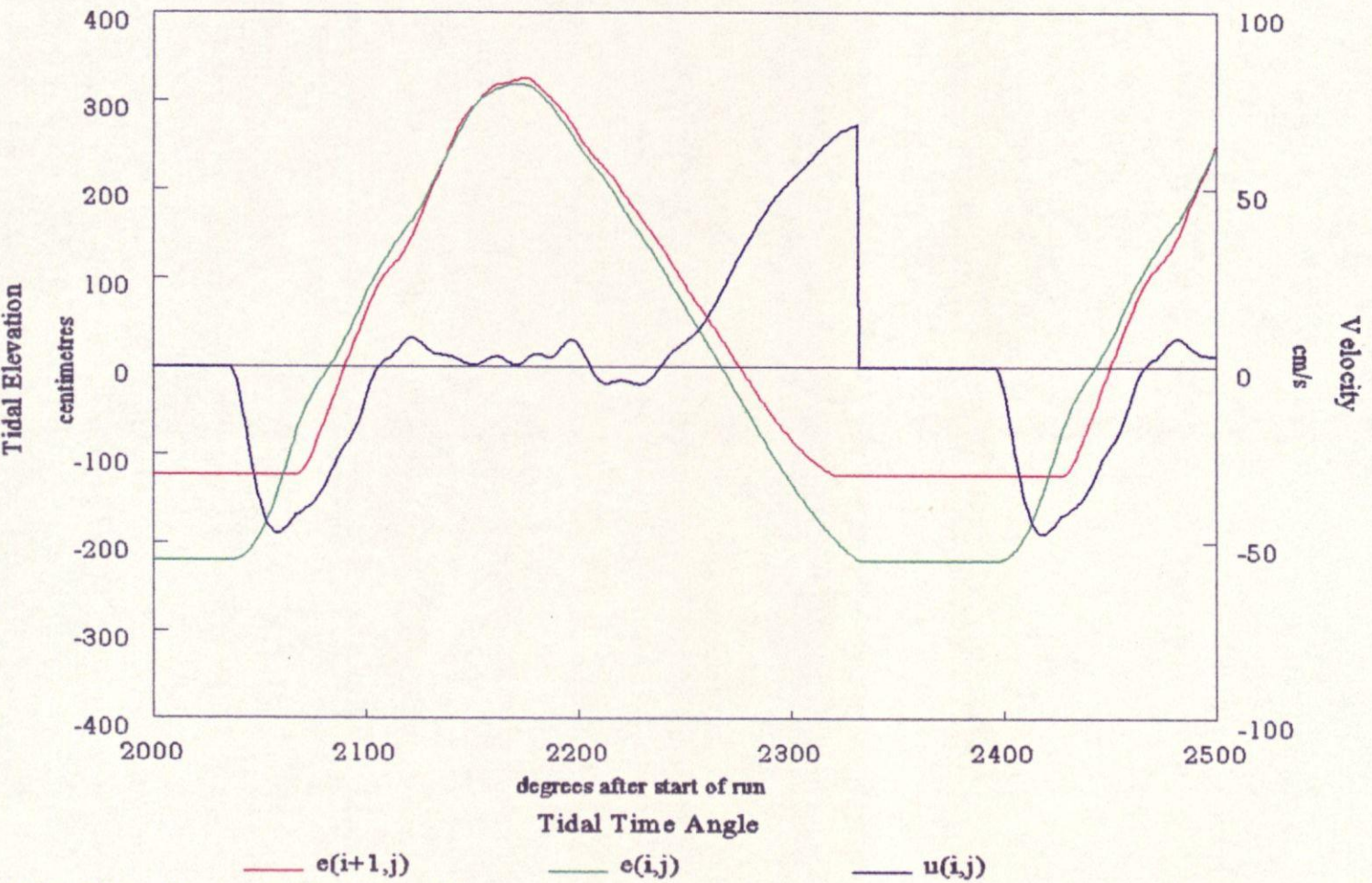
Time series that were produced with the incorporation of Owens' (1984) drying algorithm can be seen in figures 3.9 and 3.10. The elevation profiles show distinct short period and longer period oscillations about a smooth profile. In order that an equilibrium state is obtained, the model has to be run for a longer period of time than is necessary for the other algorithms used.

There are ripples apparent in the solution shortly after high water at about 2200°. At this time, there are no nearby cells which are becoming wet or dry. It seems plausible that these small anomalies in the profile may be caused by energy balance problems, possibly created by the symmetry of the Gaussian bathymetry. The purely mathematical nature of this shape may have repercussions in the solution, but it is also likely that an island of this shape may have the ability to create shorter period trapped internal waves which propagate around the island. The shorter period oscillations seen in the elevation profiles may well be crude attempts of the model to represent this phenomenon. This explanation is unlikely to be the case though, since the resolution of the model is probably insufficiently fine to represent this type of feature.

Alternatively, a more likely explanation for these short period oscillations may be that they are, in fact, an indication of trains of energy advecting around the model, perhaps with some form of total (or partial) internal reflection from the boundaries, with their source being a shock induced by the moving of the land-sea boundary. If this is the case then the conservation of momentum seems to be adhered to quite rigorously in the model.

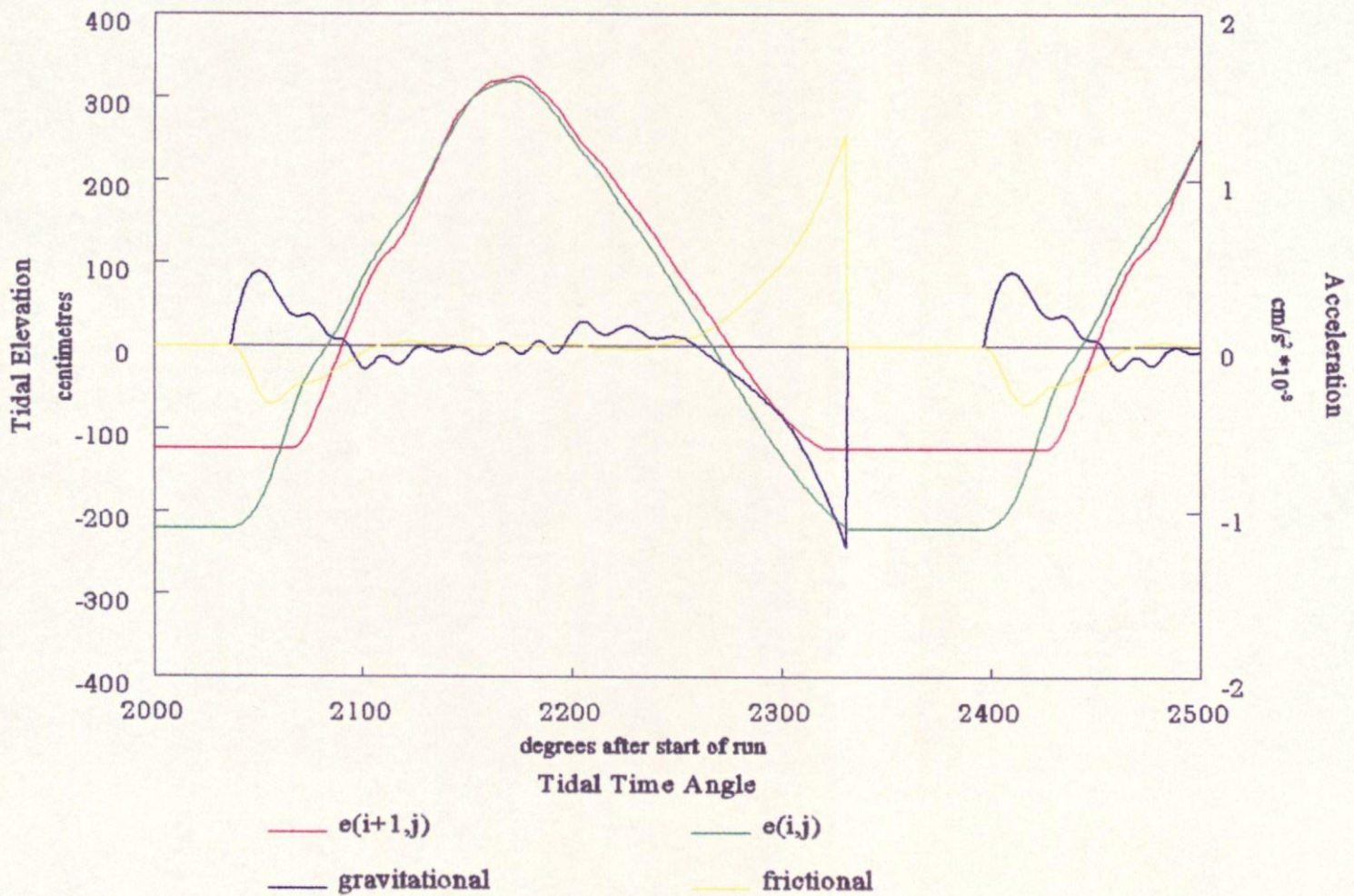
The short period oscillations are also apparent in the velocity profile shown in figure 3.5. As with Leendertse's (1970) method, there are quite large discontinuities apparent caused by the wetting of nearby cells. These discontinuities cause the rise of the tide to be modelled as a tendency towards a smooth curve rather than a smooth curve. In other words, the profile is attempting to become smooth with the apparent effect of the discontinuities being dampened towards high water.

The drying of the cells appear to be quite well represented, with only a slightly marked decrease in the rate of fall of the tide in the shallowest cell as it approaches dryness at around 2320°.



— $e(i+1,j)$ — $e(i,j)$ — $u(i,j)$
 Note: Using Owens (1984) Algorithm
 Test Cell: (18,21)

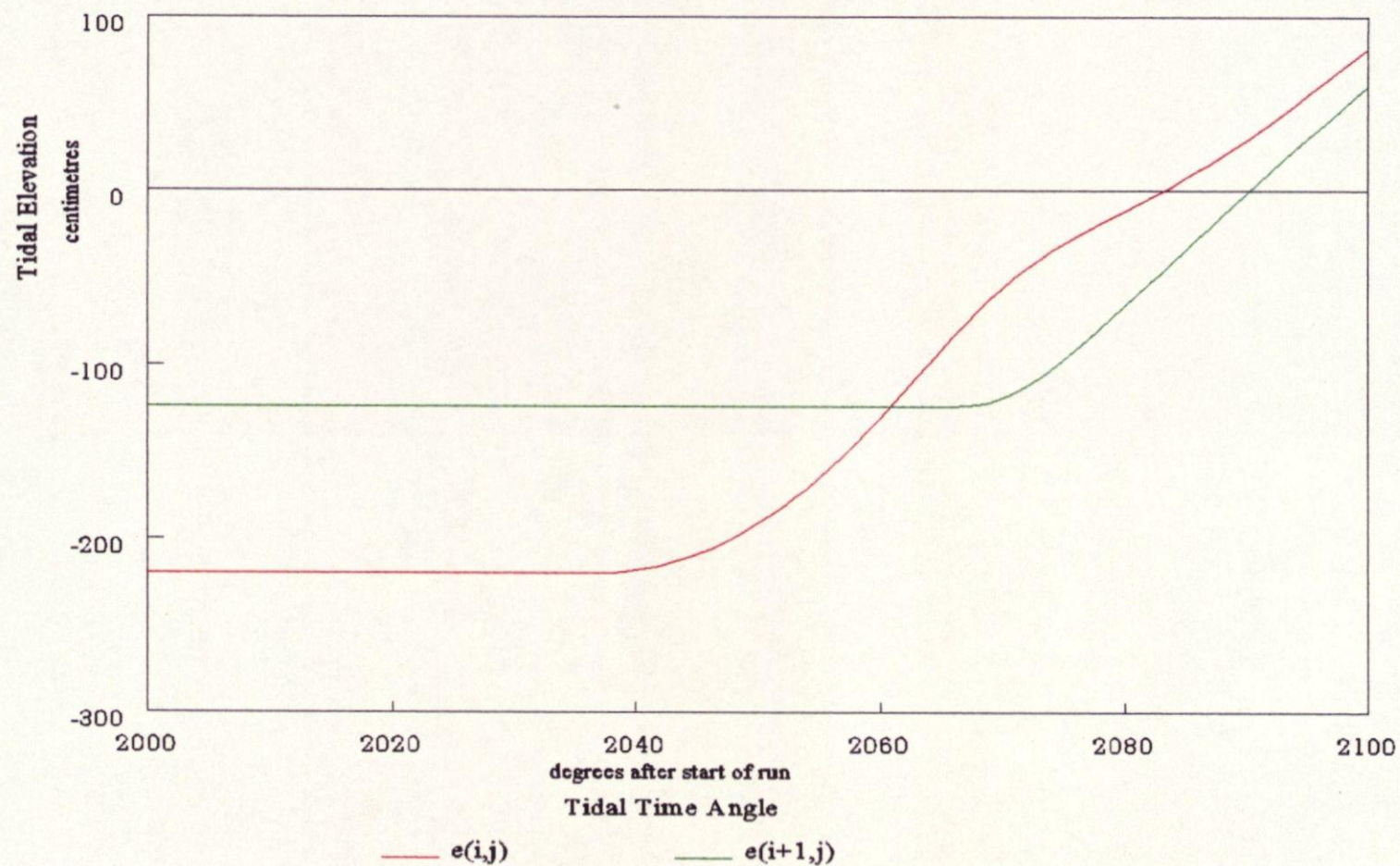
Figure 3.9: Elevation and easterly velocity component of a test cell with elevation of an adjacent cell



Note: Using Owens (1984) Algorithm
Test Cell: (18,21)

Figure 3.10: Elevation and accelerations due to both gravity and friction of a test cell with the elevation of an adjacent cell

Figure 3.1.1: Initial wetting period



Note: Using Owens (1984) Algorithm

The initial wetting period can be seen much more clearly in figure 3.11. Again, we can see the differences in the rise rates of an already wet cell and a cell which has just become wet, along with the subsequent oscillation caused by the attempt of the momentum balance to gain a hold.

The gravitational and frictional terms again show a balance as the water depth decreases.

3.5.3 Flather & Heaps (1975) Drying Algorithm

Time series obtained through the implementation of Flather & Heaps (1975) drying algorithm can be seen in figures 3.12 to 3.14. Figure 3.12 shows some elevation profiles of adjacent cells together with the easterly velocity component. The elevation profiles can be seen to be suffering from a similar effect previously described, where there are long frequency oscillations in the profiles caused by the unrealistic wetting rates.

The velocity profile in figure 3.12 also demonstrates this effect. From about 2090° to 2130° there are some quite severe falls in the strength of the predicted tidal stream, which would not occur in nature. These anomalies are a reflection of the momentum balance trying to gain equilibrium between the two different water levels in the adjacent cells. In contrast, the rate of the tidal stream during the falling tide is free from such numerical disturbances.

There are more examples of this phenomenon in figure 3.13. This figure shows the balance between the slope term (gravitational) and the friction term. The slope term is as it says, in that it is dependent on the surface slope between adjacent cells. During the period on the rising tide where there is a discrepancy between the rates of rise of the tide in nearby cells, *i.e.* the slope between them is uncertain, the slope term demonstrates dramatic oscillations which appear to dampen by high water. The frictional acceleration is very small when the

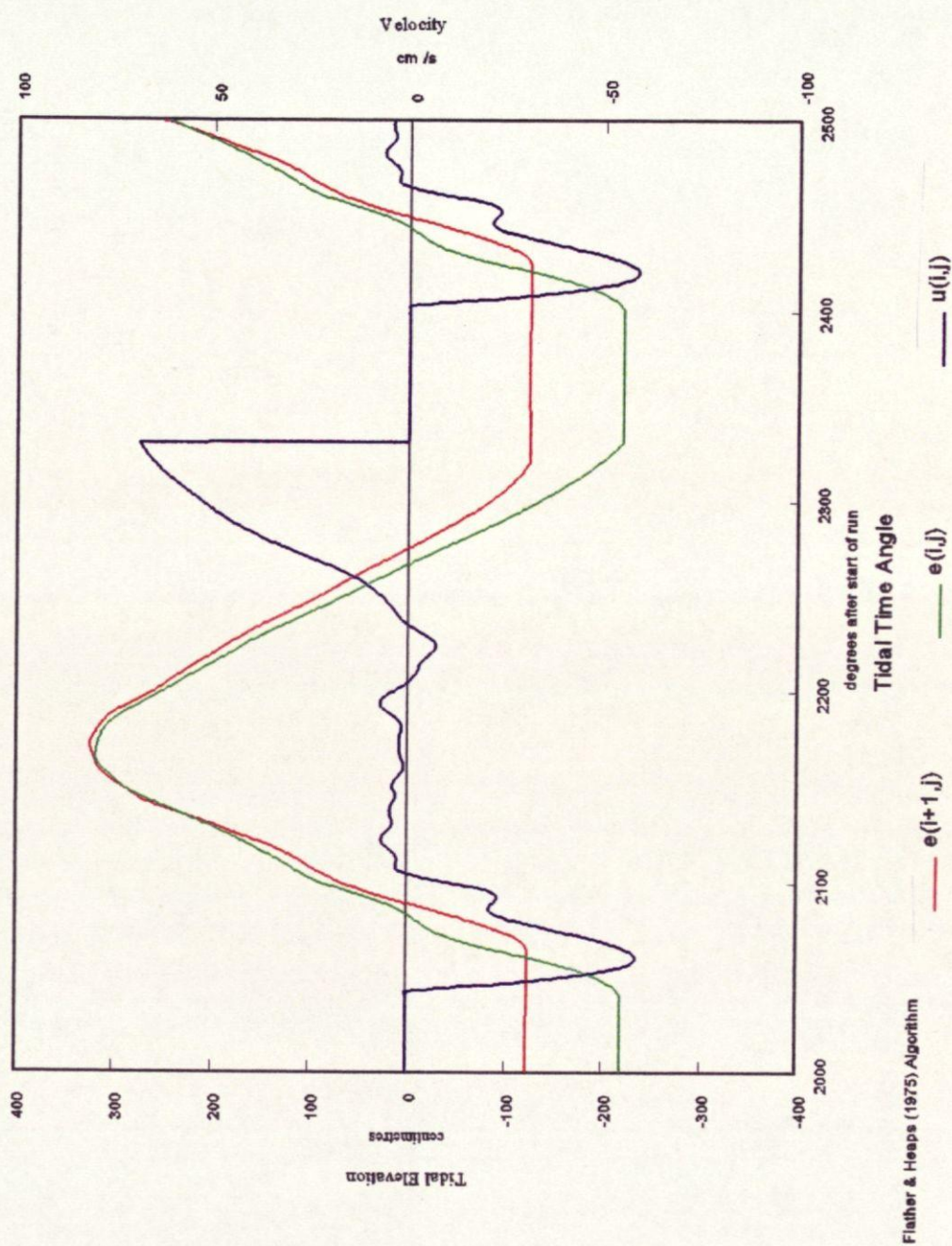
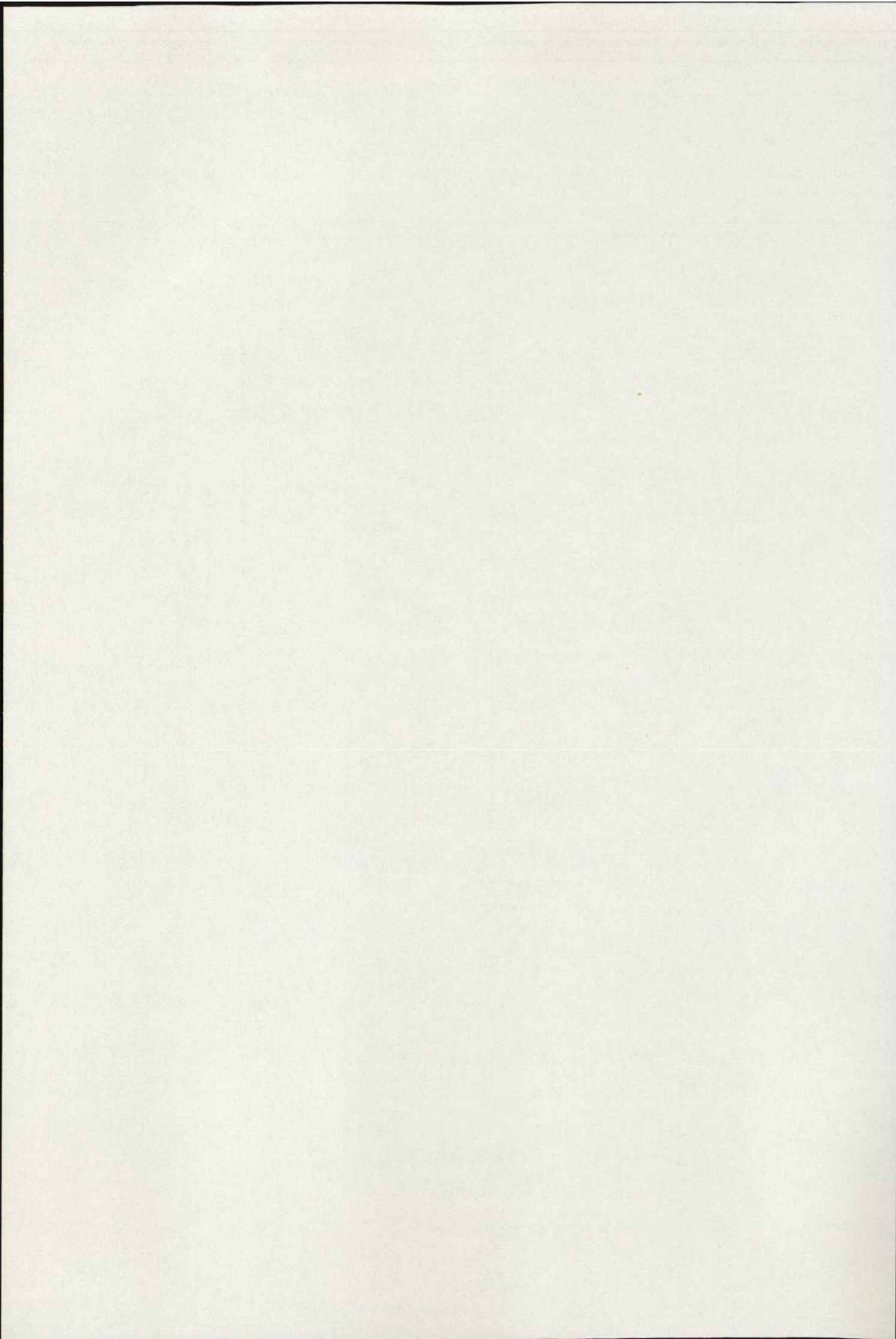


Figure 3.12: Elevation and easterly velocity component of a test cell with elevation of an adjacent cell



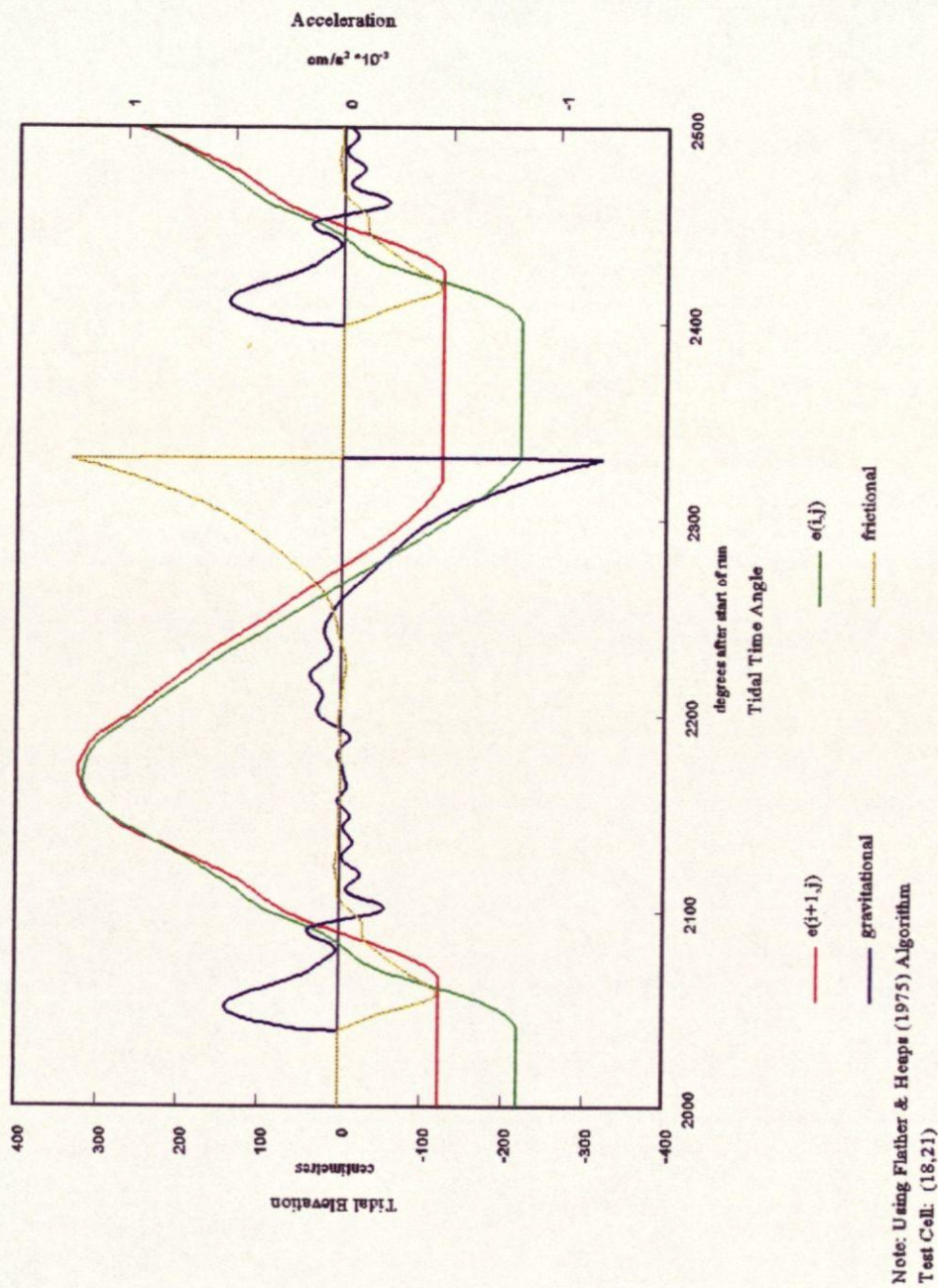
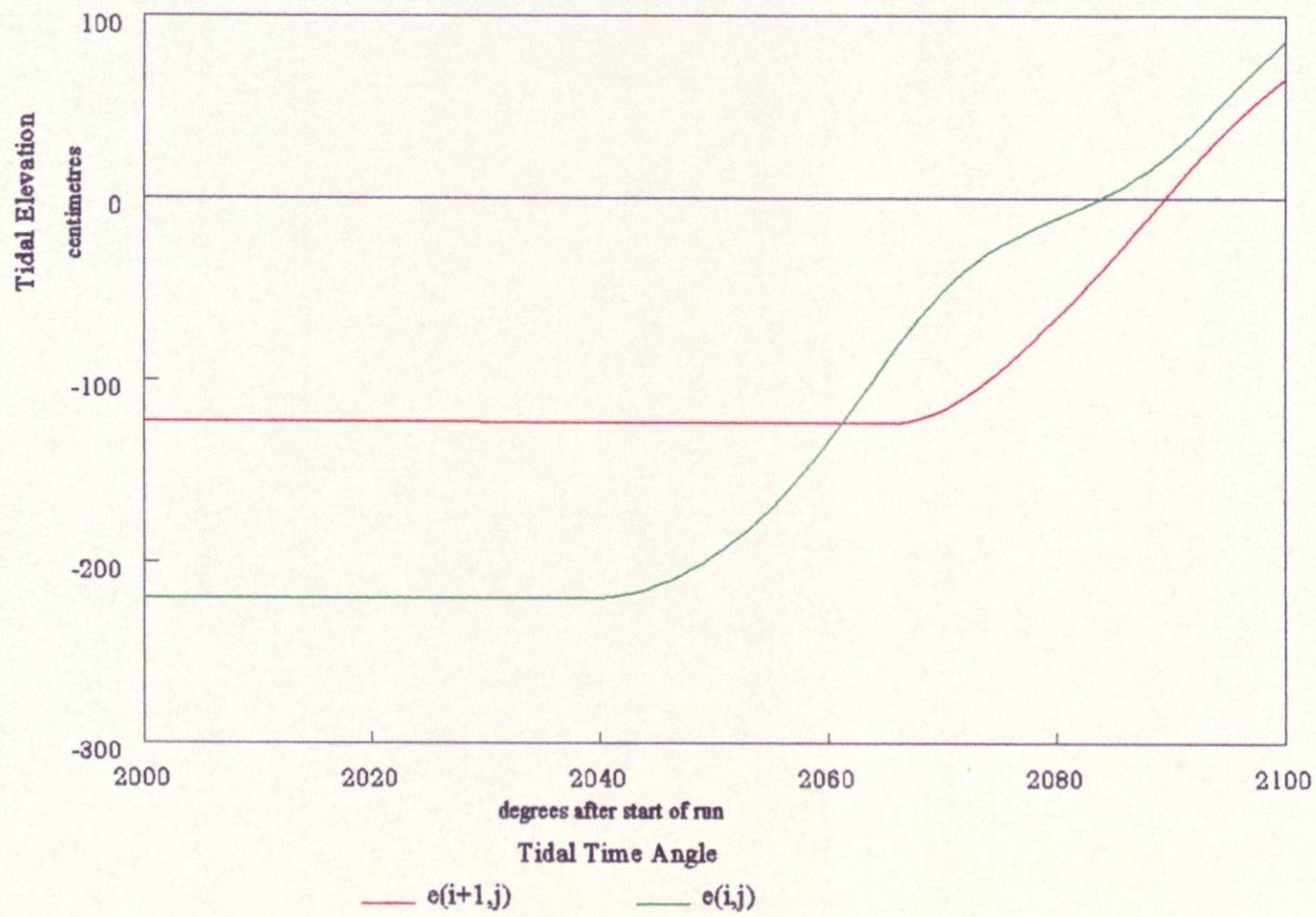


Figure 3.13: Elevation and accelerations due to both gravity and friction of a test cell with the elevation of an adjacent cell

Figure 3.14: Initial wetting period



Note: Using Flather & Heaps (1974) Algorithm
Test Cell: (18,21)

water is deeper, and the relative effect of the uncertainty in rates of rise is therefore not as marked in the profile of the frictional acceleration. When the water is shallower, however, the frictional and gravitational terms tend to balance each other.

Figure 3.14 shows an enlargement of the initial wetting period for the method presented by Flather & Heaps (1975). In this figure we can just make out that at about 2030° , cell $e(1+1,j)$ dries completely after having become slightly wetted about 50° of tidal time earlier. This is purely a numerical artefact. We can also see the wide differential between the rates of rise of the adjacent cells at the point of cell $e(i+1,j)$ becoming wet.

3.5.4 Rate of Rise of Flooding Cells

Table 1 shows quantitatively the difference between the rates of rise of the tide between the test cell and a nearby cell (as shown in figures 3.6 to 3.14) the instant that the test cell becomes wet. The nearby cell may be considered to be representative of the environmental tidal conditions as it is already completely wet. As can be seen, there is an order of magnitude difference in the rise rates between the test cell as it becomes wet and the environmental rate of rise of the tide in the nearby wet cell. Ideally, the rates of rise of the tide in the wetting cell and its environment should be almost identical. Included in the table is information on the improved algorithm as presented in Chapter 4.

Chapter 4 discusses the problems demonstrated by the above drying algorithms, together with explanations of the causes.

Drying Algorithm	Environmental Rate of Rise of Tide, ms⁻¹	Rate of Rise of Tide in Wetting Cell, ms⁻¹
Leendertse (1970)	$5.11 \cdot 10^{-4}$	$4.11 \cdot 10^{-5}$
Flather & Heaps (1975)	$5.65 \cdot 10^{-4}$	$9.66 \cdot 10^{-5}$
Owens (1984)	$5.75 \cdot 10^{-4}$	$5.79 \cdot 10^{-5}$
George & Stripling (1994)	$4.35 \cdot 10^{-4}$	$3.91 \cdot 10^{-4}$

Table 1: To show the difference between the rate of rise of tide in a wetting cell and the environmental rate of rise

CHAPTER 4

THE NEW DRYING ALGORITHM

As has been shown in Chapter 1, much work has been done in attempts to eradicate the inherent errors which occur when representing the moving land/sea boundary during solution of the hydrodynamic equations in two dimensions. A method has been developed whereby the moving boundary can be modelled with a minimum of numerical disturbance while computational time allowed for the calculations has not been significantly increased.

This improvement in moving boundary representation is applicable to finite difference methods in particular and, although the physical representation has been modified, the relevant physical laws expressed by Newton have remained unaltered.

4.1 The Richardson Grid

For the purposes of wetting and drying, a cell in the Richardson grid (figure 2.2) is defined as being centred about the elevation point (figure 4.1), rather than consisting of an elevation point, two stream points, and a depth point (as shown in figure 2.2). Such a cell is deemed to be bordered by four 'gates' leading to the four adjacent cells. This provides a

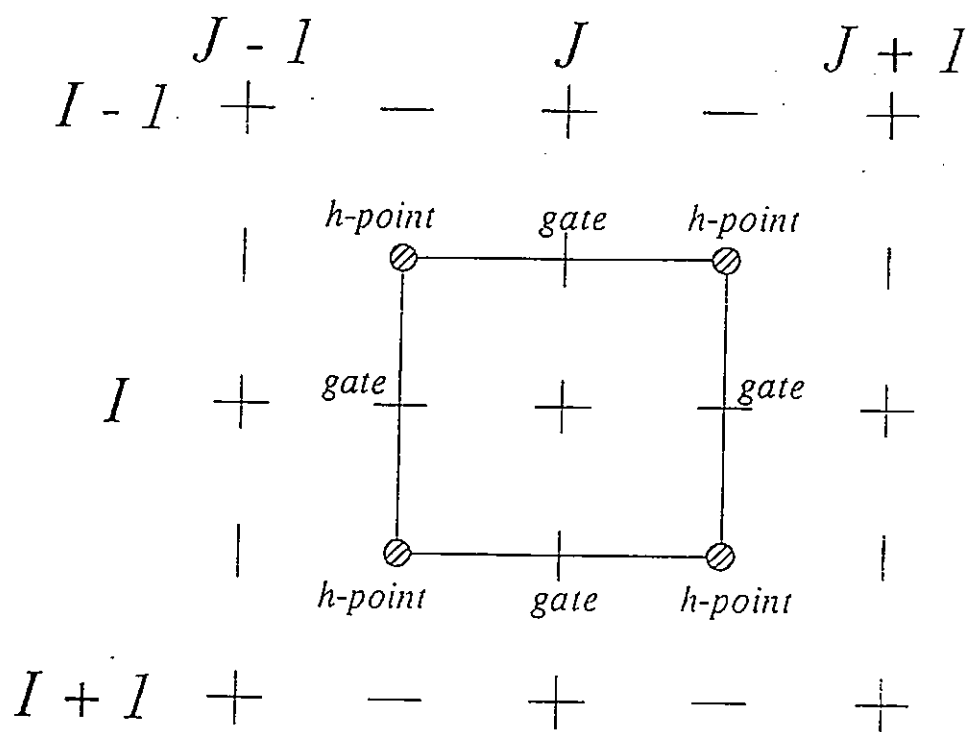


Figure 4.1: Definition of a cell in the Richardson grid for the purposes of wetting and drying

computational grid with an elevation point at the centre, four stream points at each side and four depth points, one at each of the vertices of the cell.

Typically, cells are deemed dry if the water elevation at the elevation point is less than the elevation of the sea bed at the elevation point and wet if the water elevation is above the elevation of the sea bed at this point. Gates are switched on and off according to techniques already discussed in Chapter 3.

Since the depth of the cell as defined in figure 2.2 is specified not at the ' ζ -point' but at the ' h -point', then the depth of the sea bed (referenced to a fixed datum) at the ' ζ -point' of a potential drying cell, defined as in figure 4.1, must be evaluated from the depths at the surrounding ' h -points'.

4.2 Difficulties in Wetting and Drying

4.2.1 Cells Which Dry too Slowly

Early test runs of the existing algorithms analyzed showed that cells which were drying had a layer of water left in them which amounted to a few decimetres. This water was gradually draining out of the grid square but not fast enough to keep up with the decrease in water level in the surrounding wet grid squares. This represented a state whereby a 'dry' grid square was 'high but not dry'. For this water to keep up with the surrounding environmental fall rate, the remaining water had to leave the drying grid square at grossly exaggerated speeds of up to 20 ms^{-1} , thus affecting the streams in nearby wet grid squares through the continuity equation.

In order to avoid having grid squares which do not dry fast enough, the real depth of water is replaced by a computational depth if it drops below a critical depth, H_c . The usual reason

given for the necessity of a 'critical depth' is to avoid the frictional term becoming too large and inducing instability. It is, however, possible for the critical depth to be very small (e.g. 0.01m) before instability due to this cause arises. It is therefore suggested that the introduction of a critical depth will be more effective in preventing the slow drainage of drying grid squares than in preventing instabilities occurring. It is true, however, that some value of a critical depth is needed to prevent a singularity occurring in the friction term.

The value required to prevent grid squares suffering from slow drainage can be estimated from theory. This theory begins with the assumption that in very shallow water, the motion is dominated by friction and gravity. This can be shown by scaling. The equations of motion therefore may be reduced to:

$$-g \frac{\partial \zeta}{\partial x} - \frac{KU\sqrt{U^2 + V^2}}{\zeta + h} \approx 0$$

$$-g \frac{\partial \zeta}{\partial y} - \frac{KV\sqrt{U^2 + V^2}}{\zeta + h} \approx 0$$

If we consider a cell with only one adjacent wet cell, (cell *b*, figure 4.2) then the equations may be reduced to one dimension:

$$-g \frac{\partial \zeta}{\partial r} - \frac{KR|R|}{\zeta + h} \approx 0$$

where R = rate of stream.

Ignoring signs, and putting $S = \partial \zeta / \partial r$ = slope of the water surface, we have:

$$gSH \approx KR^2 \quad (4.1)$$

where $H = \zeta + h$.

If we consider a cell of side 'r'; the rate of discharge of water from it, Q, is given by:

$$Q = RHr$$

and also by:

$$Q = \phi r^2$$

where ϕ is the rate of fall.

Equating these two expressions gives:

$$\phi = \frac{RH}{r} \quad (4.2)$$

Substitution of 4.1 in 4.2 gives:

$$\phi = \frac{H}{r} \sqrt{\frac{gSH}{K}} = \frac{1}{r} \sqrt{\frac{gS}{K}} H^{3/2} \quad (4.3)$$

In order for cells not to be subjected to slow drainage, the rate of fall as given by very shallow water theory in equation 4.3 must be the same as that experienced in the adjacent deeper cell due to the general (environmental) rate of fall of the tide. Rearranging equation 4.3 gives:

$$H = \left(\frac{Kr^2\phi^2}{gS} \right)^{1/3} \quad (4.4)$$

where S is taken to be the environmental rate of fall.

Typical values of these parameters in the idealized model may be:

$$\begin{aligned} \phi &= 3 \times 10^{-4} \text{ ms}^{-1}, & S &= 10 \text{ mm/km} = 1 \times 10^{-5}, & r &= 5000 \text{ m}, \\ g &= 10 \text{ ms}^{-1} \text{ and} & K &= 0.0025 \text{ giving:} \end{aligned}$$

$$H_c = \left\{ \frac{0.0025 (5000 \times 3 \times 10^{-4})^2}{10 \times 1 \times 10^{-5}} \right\} = 3.8 \text{ m}$$

This is surprisingly deep, and since equation 4.1 is less likely to hold at such a depth, it must

be regarded as an estimate only. It would appear that operating the idealized model with a critical depth of 3.8m would eliminate the difficulties associated with drying and wetting.

As this is clearly not an option, an alternative must be sought.

4.2.2 Cells Which Wet too Slowly

As a dry cell begins to wet, the environmental rate of rise of the tide is larger than the rate of rise that can be withstood by the wetting cell while retaining sensible flooding velocities. To show this, consider a cell which is beach and is about to flood (figure 4.2):

The wet cell, cell s , has a head of water waiting to wet the dry cell, cell ' b '. In this instance, cell b is totally dry. Now, consider what will happen on the first wetting time-step:

The cross sectional area = $(\zeta_s - \zeta_b)r$,

where; ζ_s = elevation in cell s ,

ζ_b = elevation in cell b ,

r = length of side of cell.

Therefore, the volume of water entering cell b on the first wetting time-step is given by:

$$Vol = (\zeta_s - \zeta_b)rU\Delta t$$

This volume of water is instantly distributed over the whole area of cell b (r^2). Therefore, the depth of water, D , in cell b immediately after the first wetting time-step is given by:

$$D = \frac{(\zeta_s - \zeta_b)U\Delta t}{r}$$

which gives a rate of rise of tide in cell b , R_b , of:

$$R_b = \frac{(\zeta_s - \zeta_b)U}{r} \quad (4.5)$$

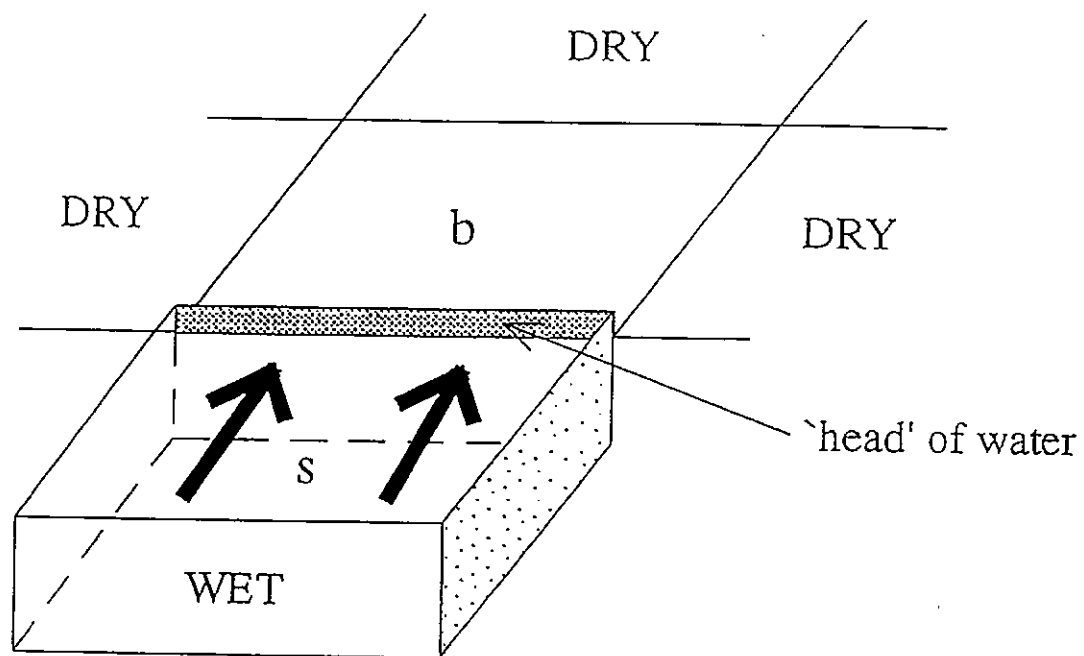


Figure 4.2: A dry cell, b, about to become wet through cell s

For a 10m tidal range, the rate of rise of tide in cell s , $R_s \approx 0.7 \times 10^{-3} \text{ms}^{-1}$. With a time-step of 124.2s, the difference in sea-surface elevations between the wet and the wetting cell is given by:

$$\zeta_s - \zeta_b = R_s \Delta t = 0.7 \times 10^{-3} \times 124.2 = 0.09 \text{m}$$

With the rate of rise of the tide in the wetting cell given by equation 4.5, assuming a remarkably fast flow rate of 2ms^{-1} ;

$$R_b = \left(\frac{0.09 \times 2.00}{5000} \right) = 3.6 \times 10^{-5} \text{ms}^{-1}$$

Thus there is a large difference in the rate of rise of the tide in the wet cell and the wetting cell.

For a model which has a much smaller grid size, e.g. a fine-scale model of The Wash:

$$r = 740 \text{m}, \quad \Delta t = 62.1 \text{s}.$$

$$\text{Here, } \zeta_s - \zeta_b = 0.7 \times 10^{-3} \times 62.1 = 0.043 \text{m}$$

Again, assuming a reasonably fast flow of 2ms^{-1} :

$$R_b = \left(\frac{0.043 \times 2.000}{740} \right) = 1.2 \times 10^{-4} \text{ms}^{-1}$$

This shows that even for a finite difference grid of a considerably smaller size, the problem of wetting too slowly is still significant.

We can determine at what rate the water needs to enter the wetting cell for there to be no difference in the rate of rise of the tide therein, i.e. $R_s = R_b$:

$$R_b = \left(\frac{(\zeta_s - \zeta_b) U}{r} \right) = \frac{R_s \Delta t U}{r}$$

Therefore, for $R_s = R_b$:

$$\frac{\Delta t U}{r} = 1 \quad \text{or;} \quad U = \frac{r}{\Delta t}$$

For $r = 5000\text{m}$ and $\Delta t = 124.2\text{s}$:

$$U = \frac{5000.0}{124.2} = 40.3 \text{ms}^{-1}$$

Clearly, this is unrealistic.

Eventually, the differences in rates of rise of tide between wetting and wet grid squares will be overcome as the pressure difference induces 'normal' flow.

There are several ways of solving this problem. These are either artificially to slow down the rate at which the tidal wave rises (the 'Canute method'), or to increase the rate of rise in the flooding cell whilst retaining a sensible flow rate.

As the first option would represent an unnatural phenomenon, it can not really be considered. The second approach involves the addition of 'layers' of water in the flooding cell at discrete intervals to keep the sea-surface elevation in equilibrium with the seaward rise in elevation. However, the addition of small volumes of water in such a process again introduces discontinuities in the solution of the Navier-Stokes equations.

4.3 The Method of Sloping Facets

An alternative solution to the introduction of a critical depth is to allow the cell in question, defined by the Richardson grid, to remain operational for as long as possible without disobeying the physical laws.

Traditionally, in the use of finite difference methods, the bathymetry of the sea bed is schematized through the representation of each grid square as having a constant depth over its entire area. When the depth of each grid square is defined in this manner, the sea bed loses its gently sloping nature and becomes artificially represented by a series of steps or plateaux. Thus, computationally, grid squares appear to have vertical walls leading to adjacent grid squares (figure 4.3).

It may be noted here that when the bathymetry of a sea area is shown graphically as a three-dimensional image (e.g. figure 4.4), what is being seen is not what is being used computationally. However, it does seem to be a closer representation of nature than a series of plateaux joined together at vertical walls.

A method has been developed whereby the bathymetry is approximated by a series of 'sloping facets' (figure 4.5). As with the stepped sea-bed representation, these facets are also centred on the ' ζ -point'.

This creates a situation where each gate can allow water to flow through it even when the water level has dropped below the bed elevation at the ' ζ -point'. In fact, water may flow in or out of a cell when as little as 1% of the sloping facet has water in it. Obviously, this will be in the deepest corner of the cell.

4.3.1 Introducing Areal Factors

The idea of areal factors is not a new one. Flather and Hubbert (1989) have also applied a method of areal factors. However, their technique remained rigid to the finite difference scheme and consequently only considered a higher resolution of grid squares within a coarser scale grid square.

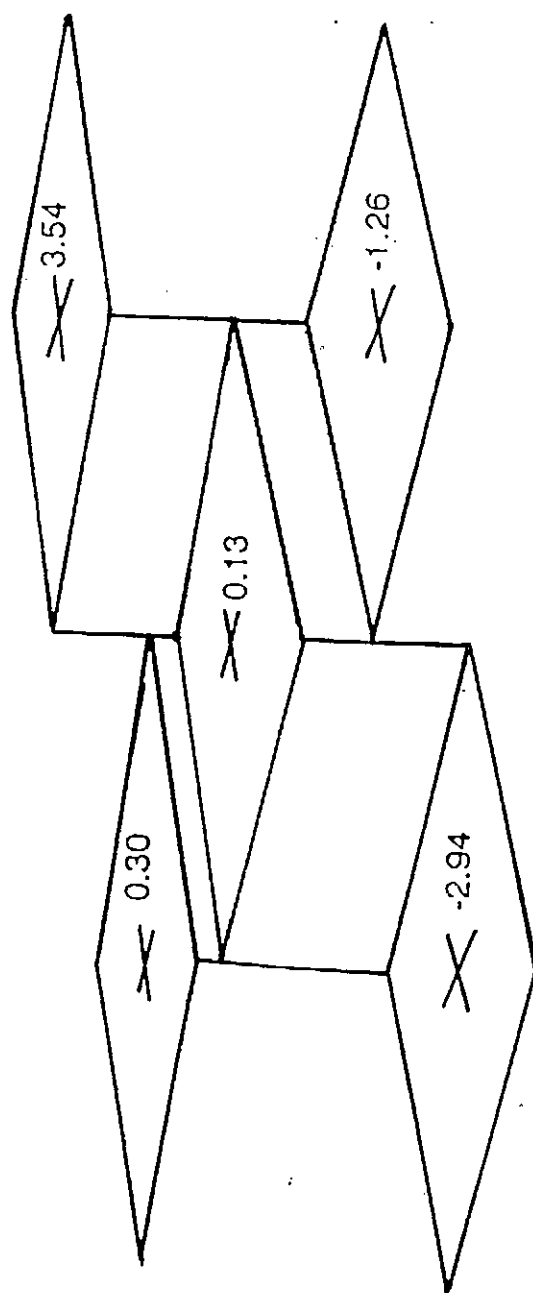


Figure 4.3: A stepped bathymetry

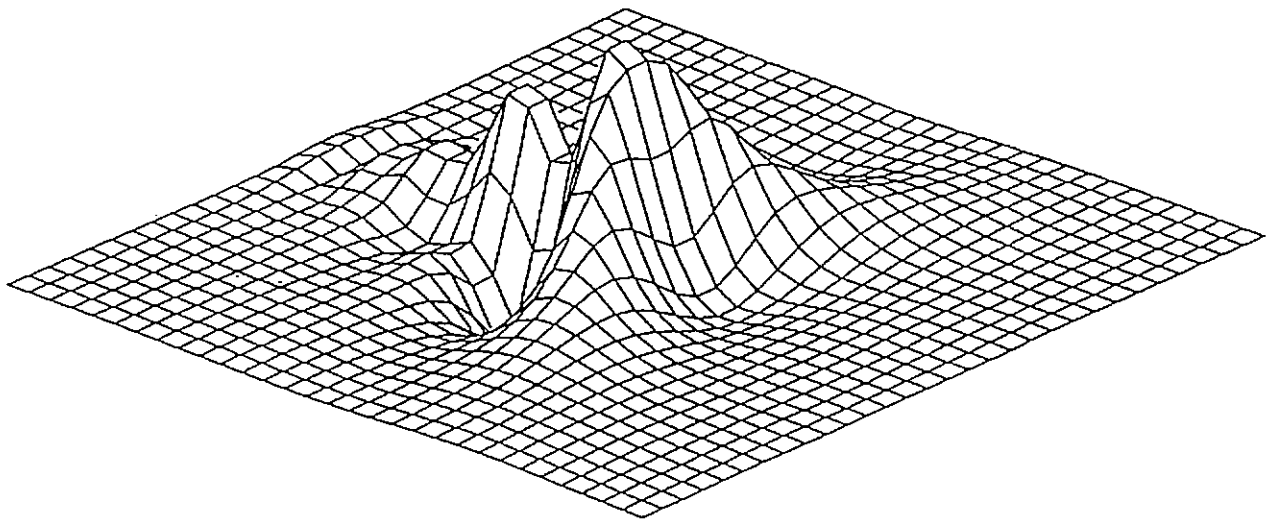


Figure 4.4: An example of an isometric projection (HR Wallingford)

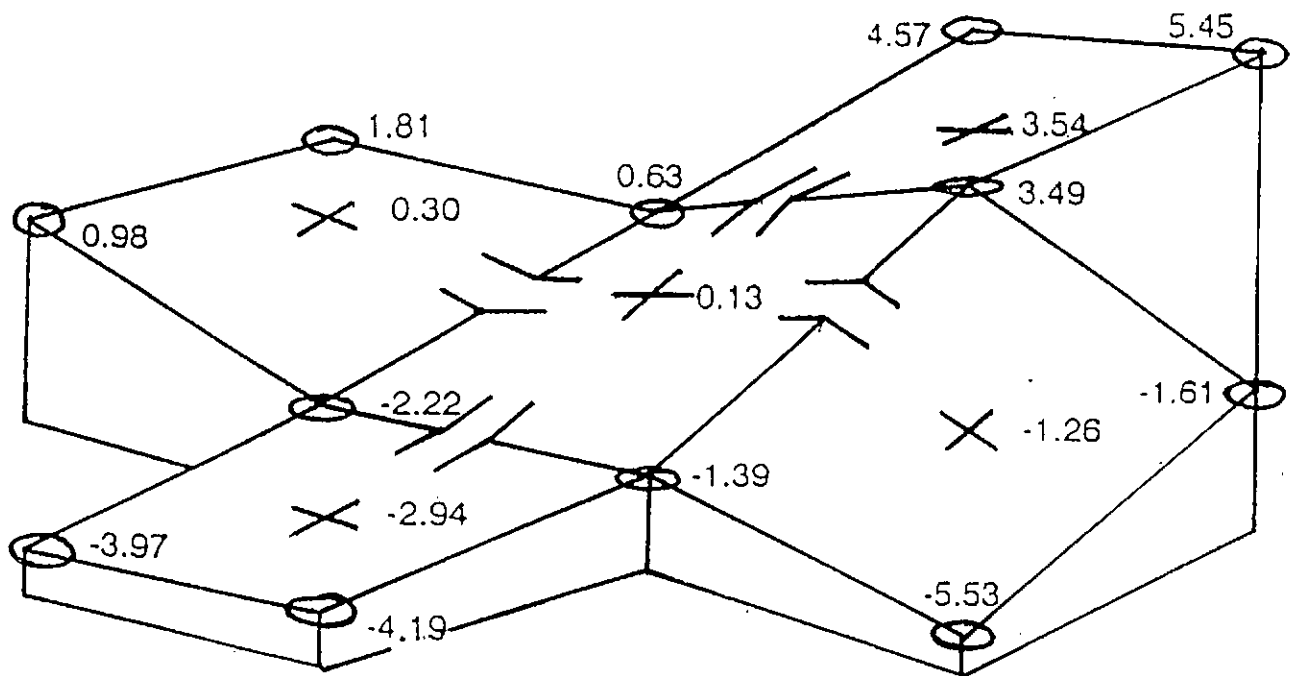


Figure 4.5: The stepped bathymetry from fig. 4.3 shown as sloping facets

Through the improved application of areal factors, there is absolutely no need for extra bathymetric digitization and higher computational costs. It works by the areal factor being defined as a triangular portion of the whole grid square. Consequently, a cell may gradually become wet or dry by the change of area of a triangle or two triangles, depending on the orientation of the slope and the water level within that sloping cell.

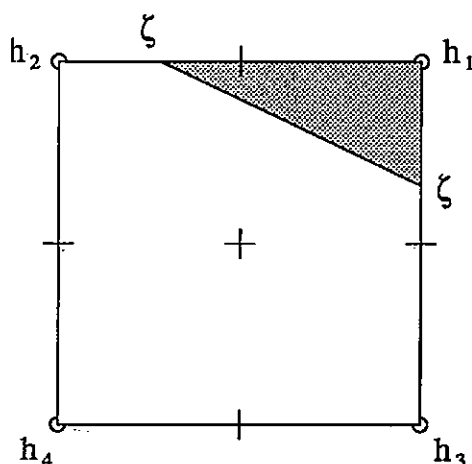
There are five cases possible, each requiring a different method of evaluating the areal factor. Let the heights above a fixed datum of the sea bed at the corners of a cell defined on the Richardson grid be h_1 , h_2 , h_3 and h_4 , where $h_1 < h_2 < h_3 < h_4$ (h measured positive above a fixed datum). Let ζ be the elevation of the sea surface within the cell:

Case 1

$$\zeta < h_1 \quad \text{Areal Factor} = 0 \quad (\text{i.e. cell is completely dry})$$

Case 2

$$h_1 < \zeta < h_2 \quad \text{Areal Factor} = \text{shaded area} = \frac{1}{2} \left(\frac{\zeta - h_1}{h_2 - h_1} \right) \left(\frac{\zeta - h_1}{h_3 - h_1} \right)$$

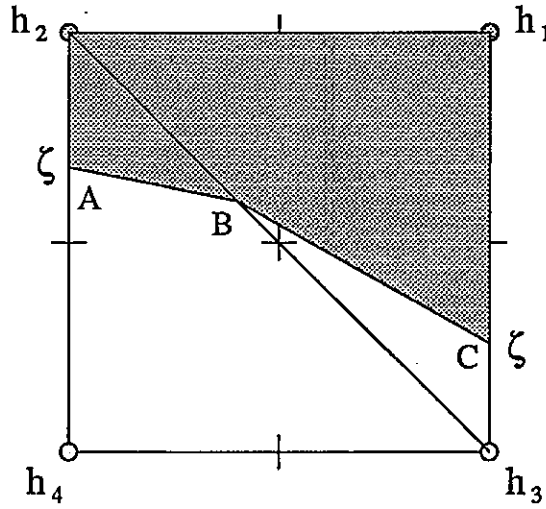


Case 3

$$h_2 < \zeta < h_3$$

The areal factor is established using a local coordinate system and Heron's formula is used to find the areas of the triangles whose vertices are indicated below.

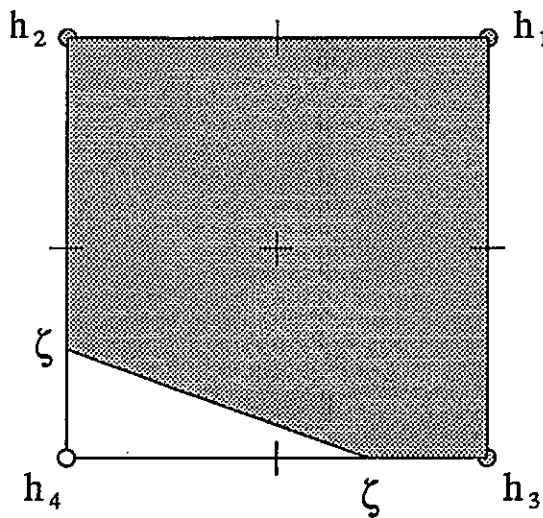
$$\text{Areal factor} = (\text{area}\triangle h_1 h_2 h_3 - \text{area}\triangle B C h_3) + \text{area}\triangle h_2 A B$$



Case 4

$$h_3 < \zeta < h_4$$

$$\text{Areal factor} = \text{shaded area} = 1 - \frac{1}{2} \left(\frac{h_4 - \zeta}{h_4 - h_3} \right) \left(\frac{h_4 - \zeta}{h_4 - h_2} \right)$$

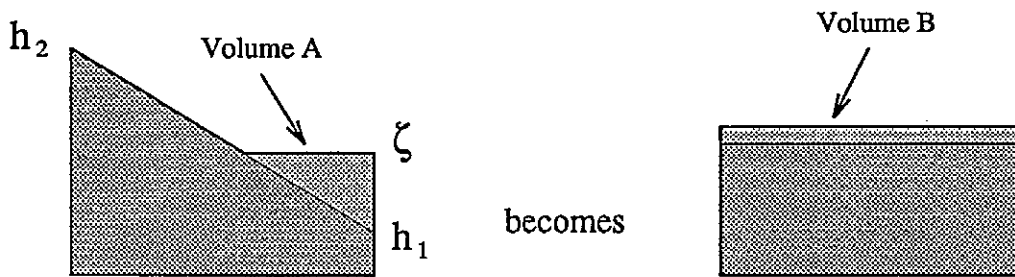


Case 5

$$h_4 < \zeta$$

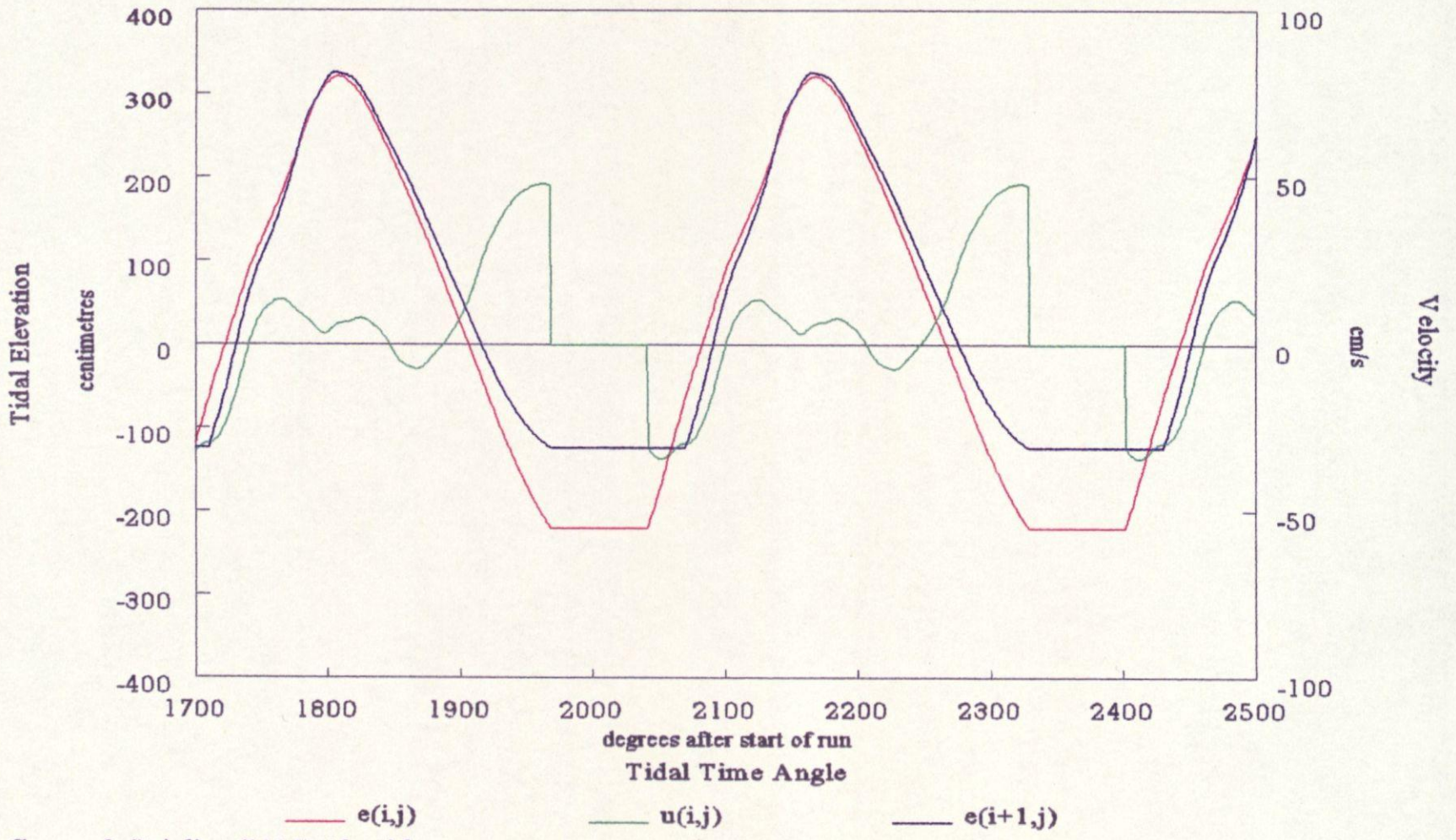
$$\text{Areal factor} = 1$$

In order that the cell is computationally active, even when the tidal elevation is below the depth at the elevation point of the cell, a breadth factor is applied. This factor has the effect of redistributing the volume of water in a partially wet sloping cell along the whole edge of a computational cell which has horizontal edges, causing the stream point along the edge to be considered wet. Thus, volume A is equal to volume B below:



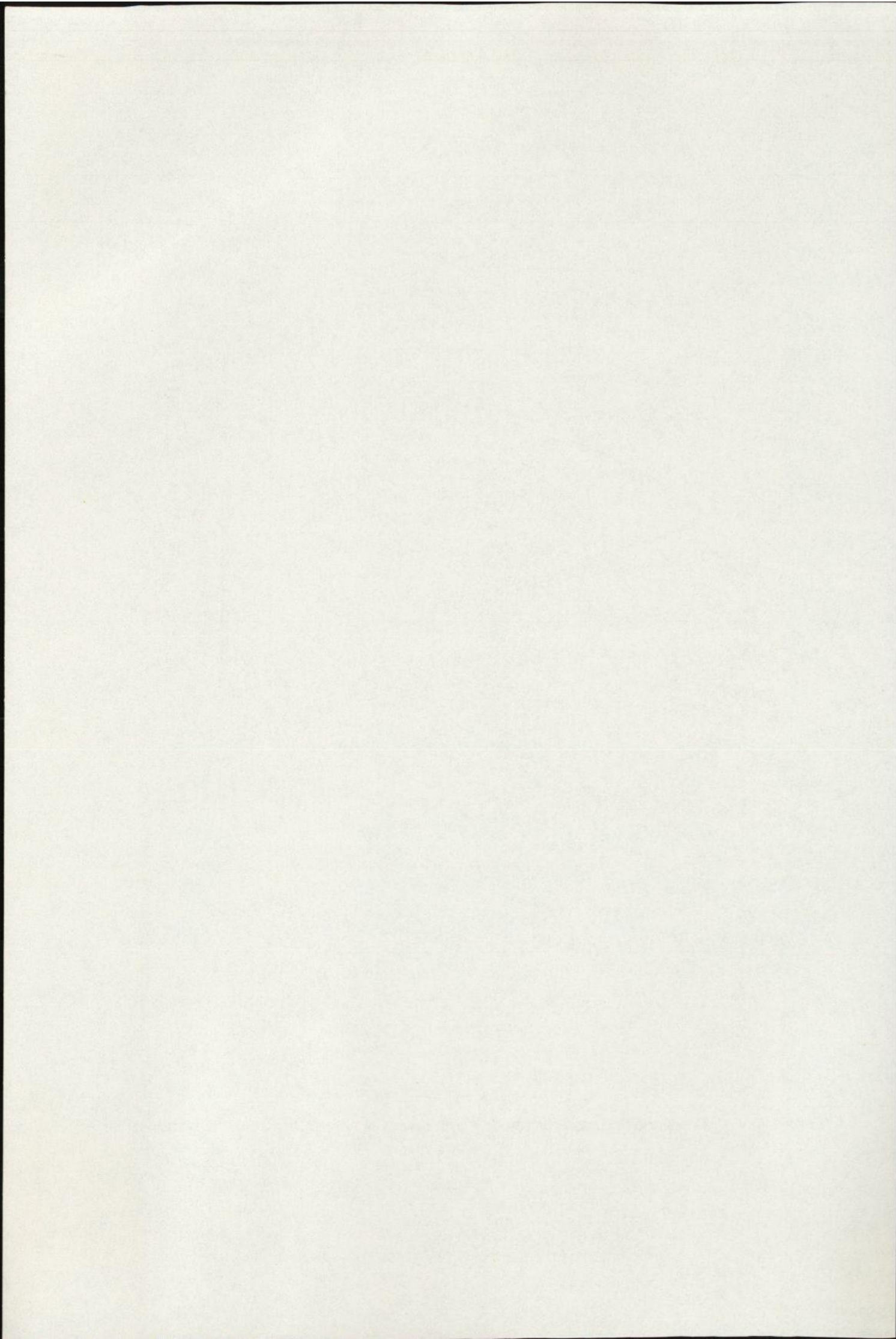
There are three possibilities which may arise here, firstly, if $\zeta < h_1$ then the breadth factor is zero, secondly, if $\zeta > h_2$ then the breadth factor is one. In the third case, when $h_1 < \zeta < h_2$, the breadth factor is given by:

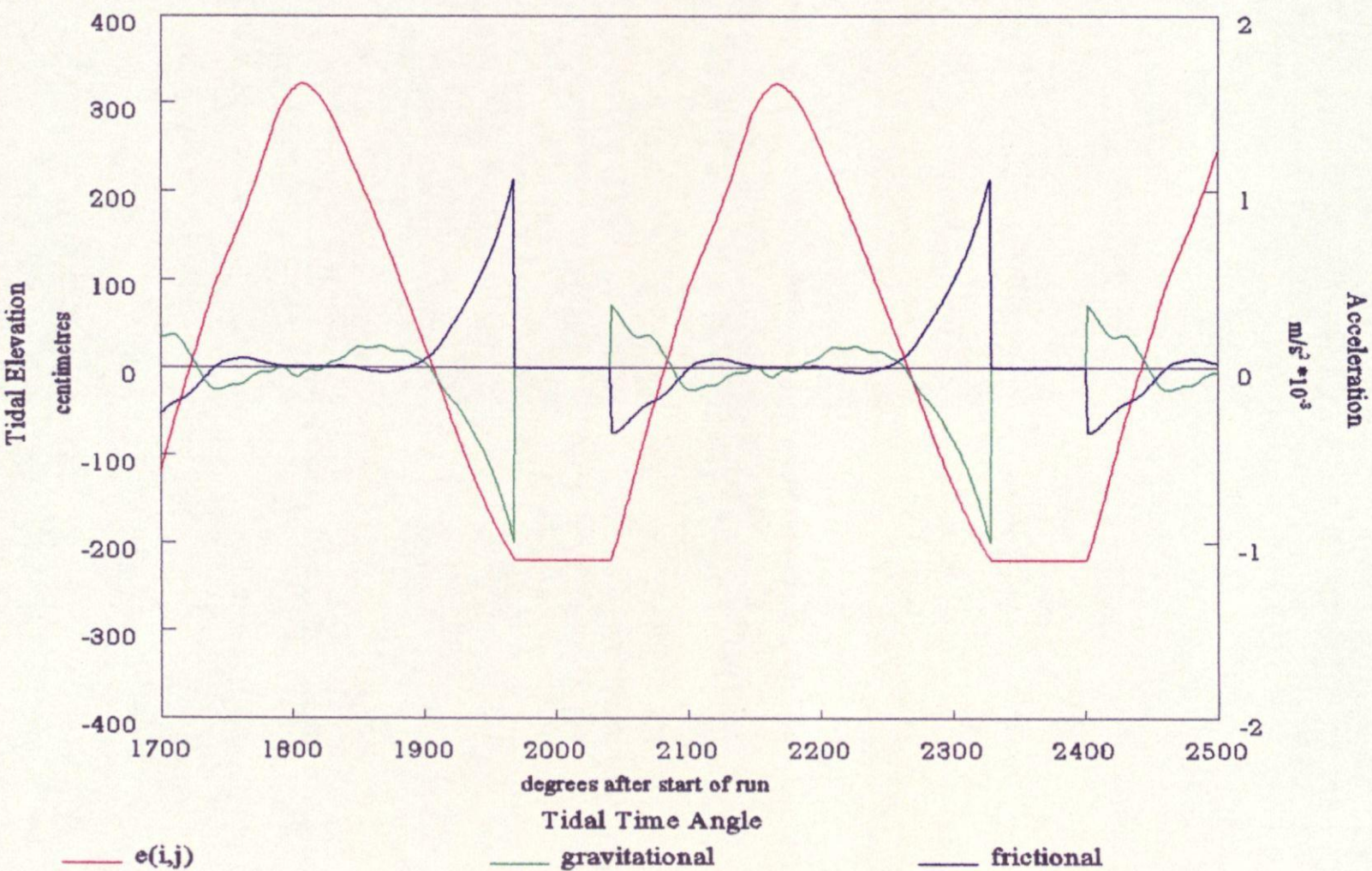
$$\text{breadth factor} = \frac{\zeta - h_1}{h_2 - h_1}$$



George & Stripling (1994) Algorithm
Test Cell: (18,21)

Figure 4.6: Elevation and easterly velocity component of a test cell with the elevation of an adjacent cell





George & Stripling (1994) Algorithm

Figure 4.7: Elevation in a cell with accelerations due to both gravity and friction

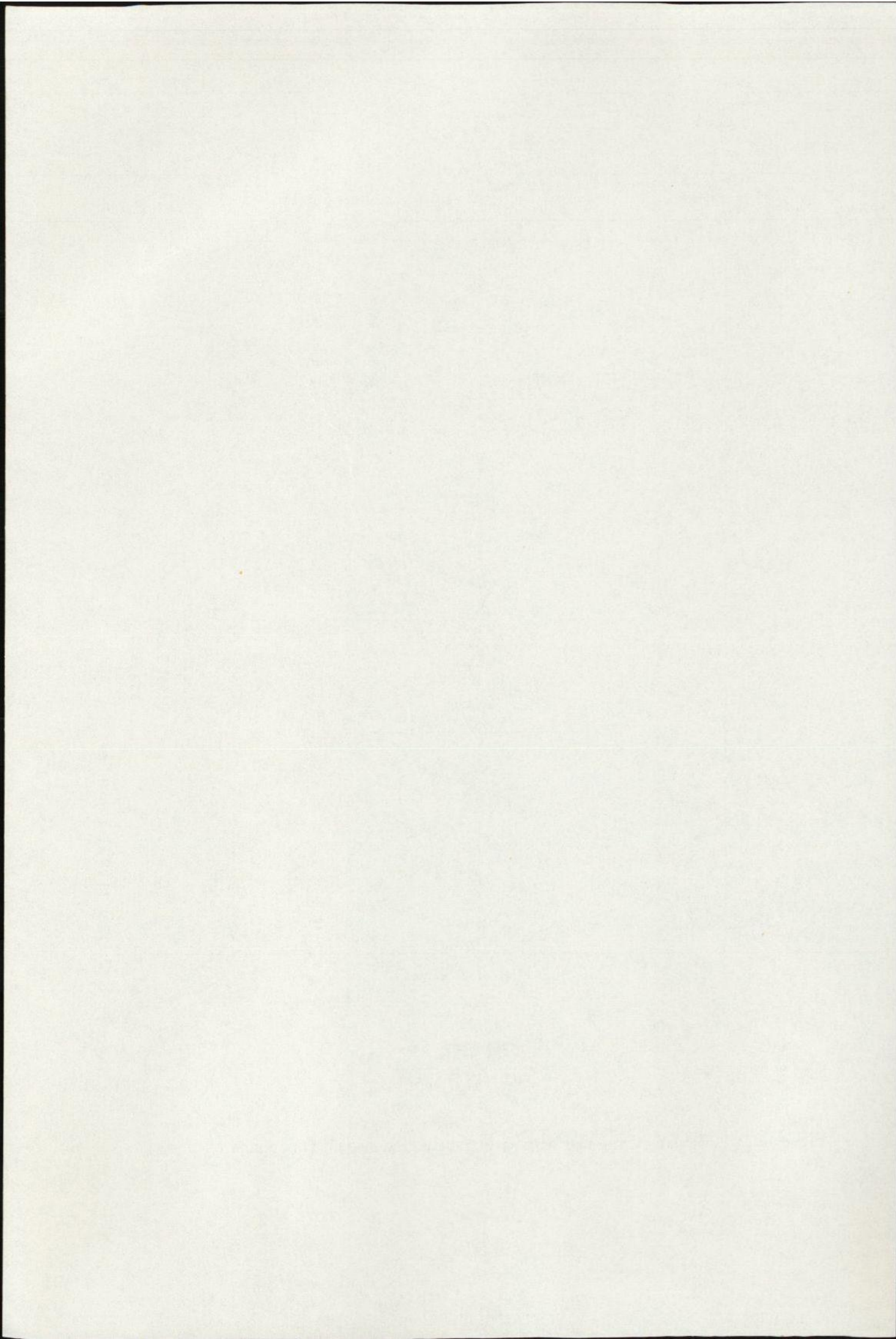
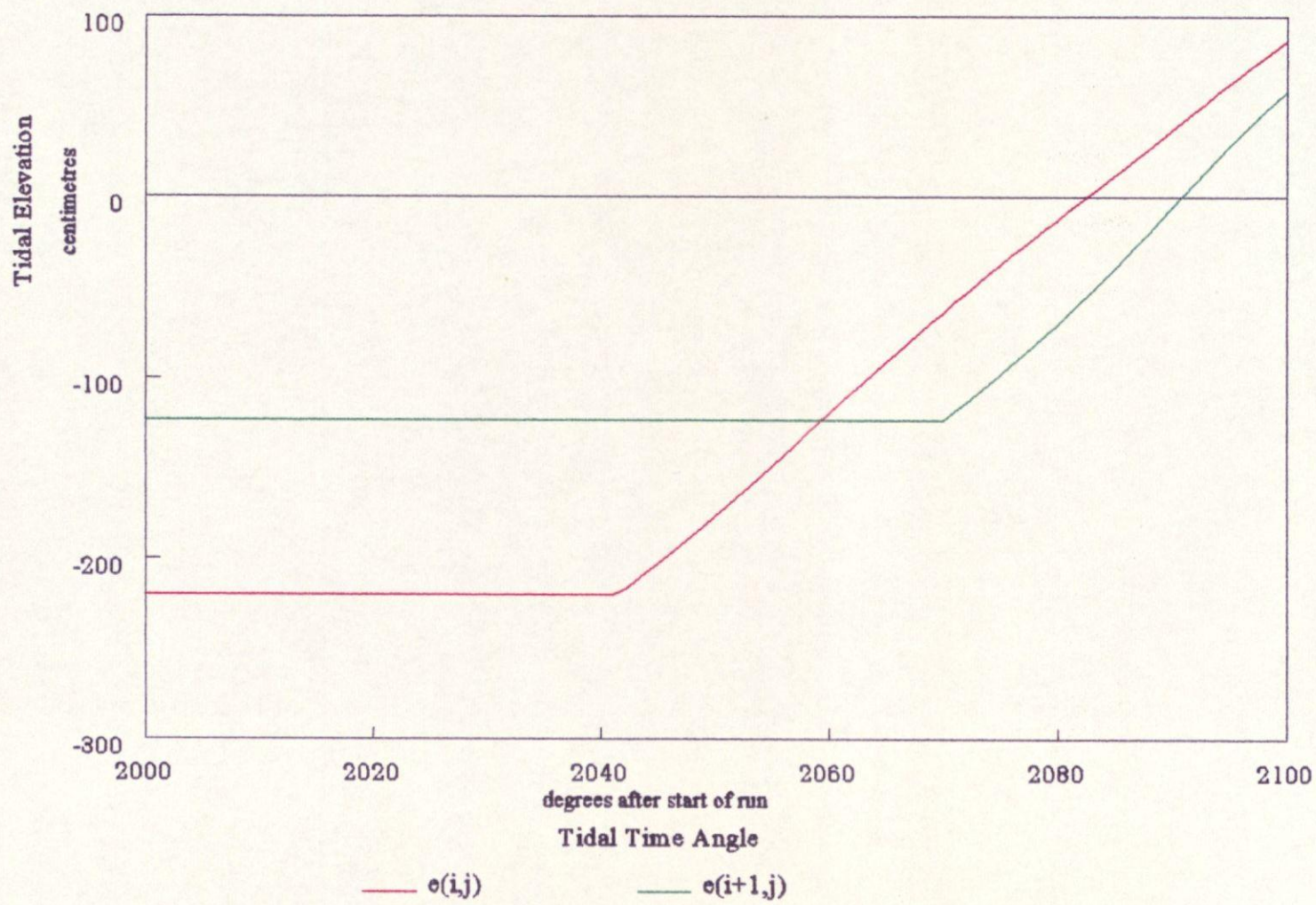


Figure 4.8: Initial wetting period



Note: Using George & Stripling (1994) Algorithm

4.4 Comparison With Other Drying Methods

The idealized model has been used as a tool to compare the method of sloping facets with the algorithms tested in Chapter 3.

The results can be seen in Figures 4.6, 4.7 and 4.8. This comparison shows a marked improvement on the existing algorithms, with numerical shocks caused by the wetting of a nearby cell having been completely eliminated using the new method of sloping facets. The velocity profile (figure 4.6) shows little or no adverse effects due to surrounding cells. The initial uncertainty of whether or not a cell has become wet or not as demonstrated in figure 3.8 (Leendertse ;1970) does not apply with this method.

The oscillations in the gravitational profile that were so prevalent in figures 3.7, 3.10 and 3.13 during the rise of the tide have been almost completely eliminated, see figure 4.7.

The initial wetting period shown in detail in figure 4.8 illustrates how the rate of rise of the tide in the cell and its environment are almost identical, even at the precise moment of wetting. Indeed, as table 1 shows (p. 72), the rate of rise of tide in the wetting cell at the instant it becomes wet is almost identical to the environmental rate of rise that is represented by the rate of rise of the tide in a fully wetted adjacent cell. This appears to have eradicated the associated resultant oscillations in the solution entirely.

4.5 A Rogue Situation

During the course of experimentation, a situation was found in which the method of sloping facets ceased to work. As has been previously stated, on a finite difference grid the depths of the sea-bed are specified at the h -points, however, the Richardson grid requires that a cell is centred on a ζ -point. This leads to the necessity of having to establish the depth of the sea-

bed at the ζ -point by averaging the depths specified at the four surrounding h -points.

It was thought that if the depths of the sea-bed were initially specified at the ζ -point, as well as at the h -points, then the extra computational time which arises from the process of averaging would be avoided. This is readily achieved when the model is idealized and the extra depths merely need to be calculated with a simple algorithm. However, this led to a 'pyramidal' cell (figure 4.9) appearing at the peak of the Gaussian shoal. In this instance, the method of sloping facets does not work.

In reality though, this situation would not arise as depths are extracted from charts and other sources, not created through short algorithms. Even so, the author recommends that if this method is to be implemented anywhere that the tradition of specifying the depths of the sea-bed at the h -points should continue.

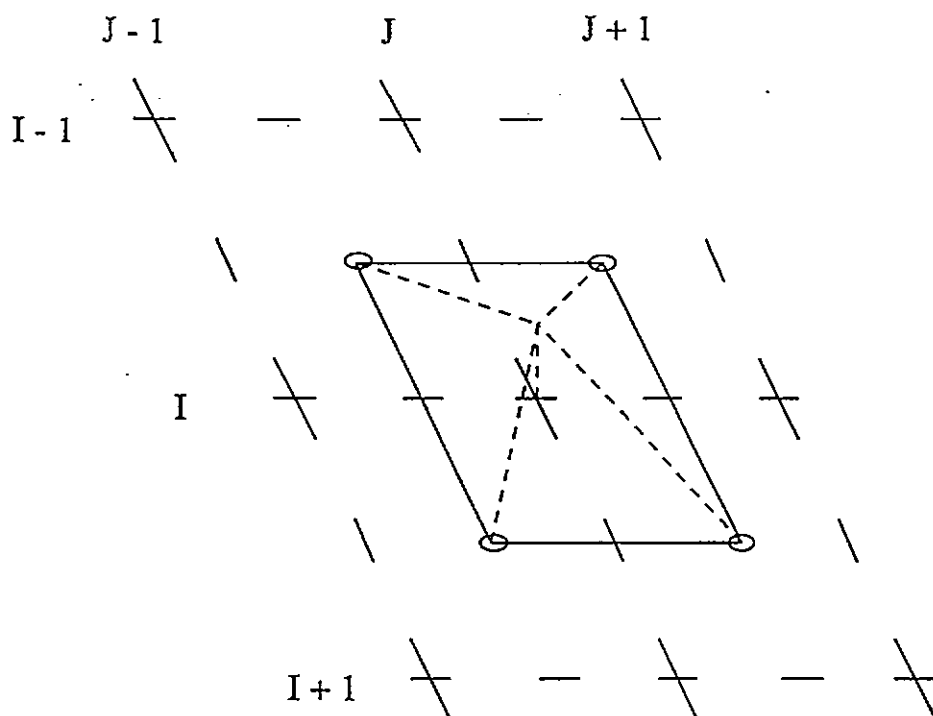


Figure 4.9: A pyramidal cell

CHAPTER 5

'THE WASH' - FIELD MEASUREMENTS

As a final test in determining the performance of the new drying algorithm it is necessary to apply the technique in a real situation. It was decided that a suitable test-bed for the algorithm would be The Wash, East Anglia.

5.1 The Wash

The Wash is a large embayment on the east coast of England, latitude $53^{\circ}00'N$, longitude $00^{\circ}20'E$ (figure 5.1). It faces approximately northeast and is about 20km wide by 30km in length. At the entrance to the embayment there are deep channels (e.g. the Lynn Deep) with maximum depths of about 40m. Over most of the area, however, depths are generally less than 10m. Mean tidal ranges are 6.5m during spring tides and 3.5m during neap tides.

Before land reclamation began, the Wash was a much larger area of sea and marsh (e.g. Harris, 1953). During the 17th century, a Dutch engineer called Vermuyden (1567 - 1641) initiated a remarkable feat of engineering which involved the draining of large parts of marshland surrounding the Wash, and its reclamation from the sea. This area is known as the Fennes. Since this reclamation began, extensive deposits of sediment have formed broad

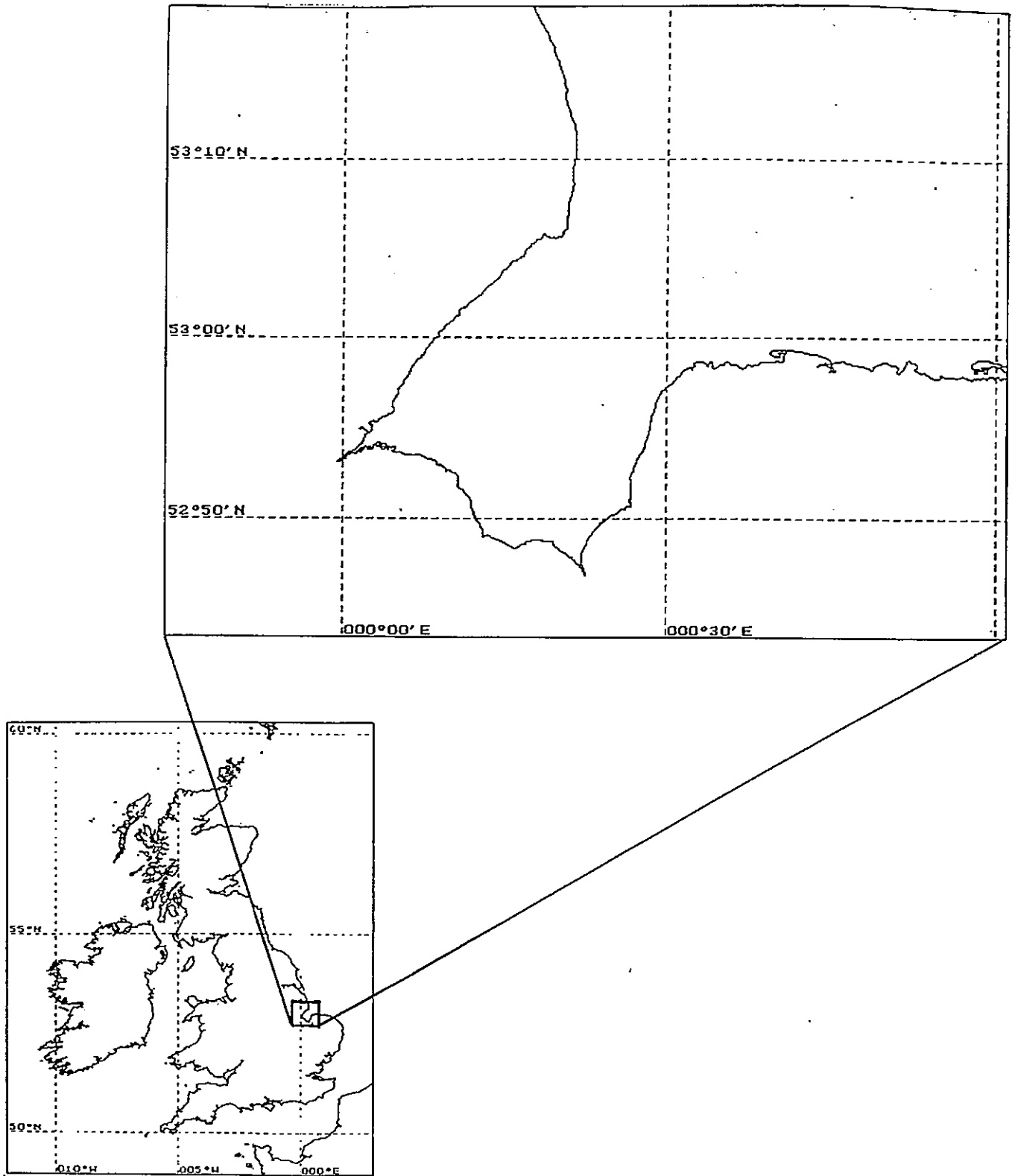


Figure 5.1: Location map of the Wash, U.K.

bands of intertidal regions along the northern and western regions of the Wash. Offshore, there are also large intertidal banks. Figure 5.2 shows an aerial photograph of the Wash. The sandbanks can be clearly seen, as well as the possible presence of large amounts of suspended sediment. It is probable that the majority of the silt in the Wash stems from the erosion of parts of the coast north up to the Humber estuary.

There are three main rivers draining in to the Wash; the Welland, Nene and Ouse. These drain a large portion of central eastern England (1.3×10^6 hectares (= 13000km²), (Evans and Collins (1975)) between the Trent drainage basin to the north and the Thames to the south. Shipping channels for the inland ports of Spalding, Wisbech and Kings Lynn on these rivers can be seen in figure 5.2. There are substantial difficulties in keeping these channels open to shipping due to the vast quantities of sediment that are deposited in them. Retaining walls have had to be constructed to maintain the buoyed shipping lanes at constant positions. Regular dredging helps to keep them open.

Further inland, long sections of these rivers are raised high above the surrounding land (some surrounding areas can be more than 3m below mean sea level) and it is often possible to walk alongside the river bank and be below the level of the river bed. This gives some idea of the effect of land reclamation in the Fenland area.

Due to the fact that the majority of the surrounding countryside is very close to the mean springs high water level, the Wash is surrounded by a man-made sea-wall. Large sections of this sea-wall were built by convicts in the 1940s and 1950s. Apparently, very few returned for another go. Landward of the sea-wall runs a dyke system which holds any water which has seeped through during periods of high water. Periodically, automatic and manual pumping stations return the water to the sea.



Figure 5.2: Aerial photograph of the Wash showing survey line

5.2 The Study Area

A visit to the Wash was made in January 1992. This was intended as a reconnaissance exercise to assess a likely situation for measurement. After observing possible positions, a meeting with the harbourmaster at the port of Kings Lynn was arranged. The author was informed that during the previous year several people had drowned on the mudflats and advice was given that a survey should only be attempted by a minimum of two people, with distress packs, lifejackets and V.H.F. radio. In addition, an inflatable boat with a powerful engine, if not two, would be required.

It was therefore apparent that to set up a survey programme would require extensive planning and considerable funding. Fortunately, it came to the Author's attention that the Department of Oceanography at the University of Southampton had an ongoing programme of field measurements in the Wash, under the direction of Professor M.B. Collins. It was arranged that the Author would accompany their research team during the next period of field work. A week of field measurements were conducted by the Author in association with two of Professor M.B. Collins' research students (Mr. X. Ke and Mr. A. Flavell). This period of observation included the measurement of suspended sediment concentrations, water depth and current velocity detail for six different sites during nine tidal cycles.

The observations were taken along line 'AB' shown in figure 5.2 on the Frieston Shore. Access to the site was made through H.M.P Frieston (North Sea Camp) with the permission of the prison Governor (this particular site provided an undisturbed working environment. It also provided access to the shore by road and was situated away from the R.A.F bombing range).

Figure 5.3 shows a cross sectional representation of Frieston shore along the survey line.

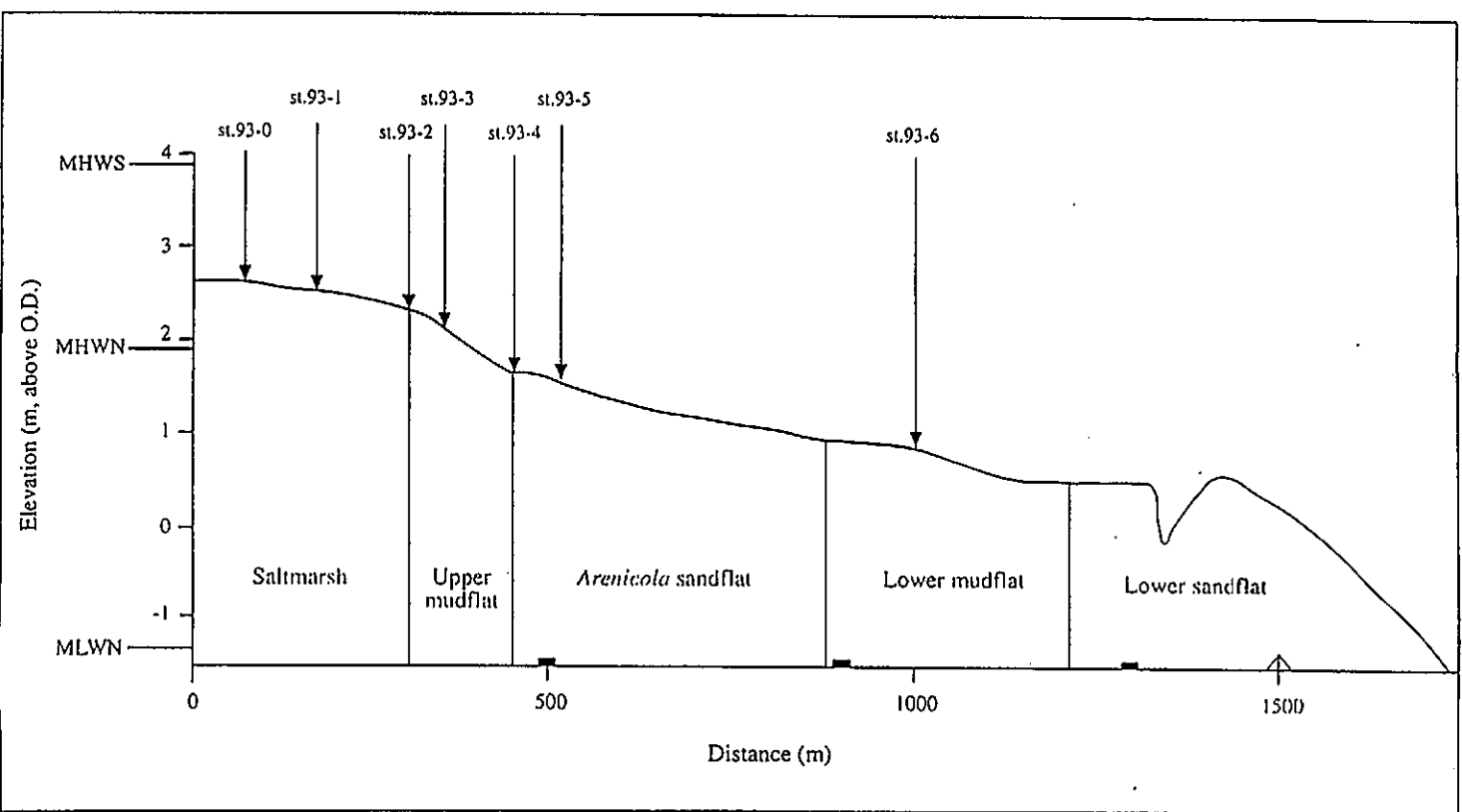


Figure 5.3: Locations of hydrological survey stations, Friesion Shore, 1993 (courtesy of Mt. X. Ke)



Plate 1: Seawards from station 6

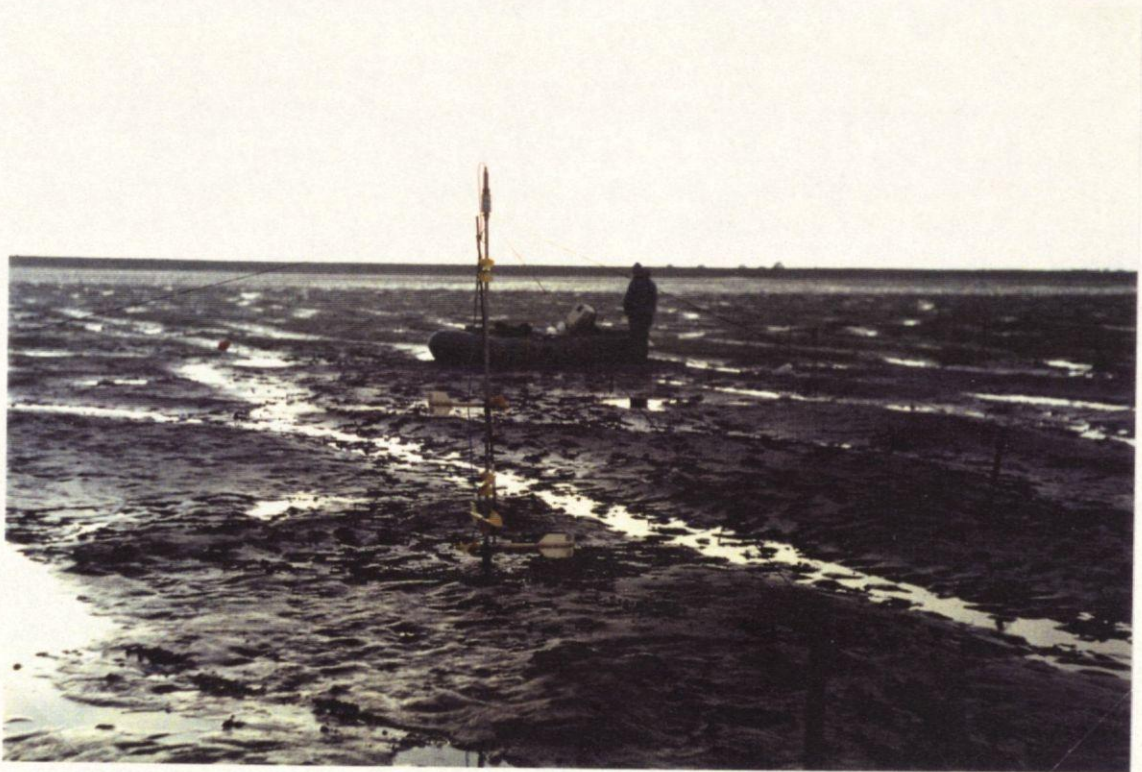


Plate 2: Current meter rig

It also shows the positions of the six survey stations, and their approximate elevations relative to Ordnance Datum Newlyn. Plate 1 shows the expanse of inter-tidal flat from station 6, seaward.

5.3 Aims of the Field Work

Since the critical times during the tidal cycle, with respect to the accurate representation of flooding and drying, are the periods of wetting and immediately after, and the short period approaching drying, *i.e.* when the water is extremely shallow, it was required that detailed measurements should be taken during these times. These measurements would then be used for validation purposes in a hind-casting model of the Wash.

5.4 Methods of Measurement

At present, there are no methods known to the Author which allow the measurement of tidal currents in extremely shallow water to any great accuracy, even the electromagnetic method can give spurious results in extremely shallow water. Therefore, the existing method of determining currents from the rotation of impellers was used and eventually adapted (see the tilting method below).

Two Braystoke direct-reading current meter rigs (see plate 2) were employed at each station of the survey site. The five impellers on each rig were set at optimum heights in order to obtain velocity readings throughout the water column. These current meters were connected to a Valeport multi-channel pulse counter (see plate 3) by thirty metres of cable.

During the initial wetting period and the period shortly before drying, the smaller of the two rigs, mounted with microimpellers (1.5cm in diameter), was held by hand and tilted so that

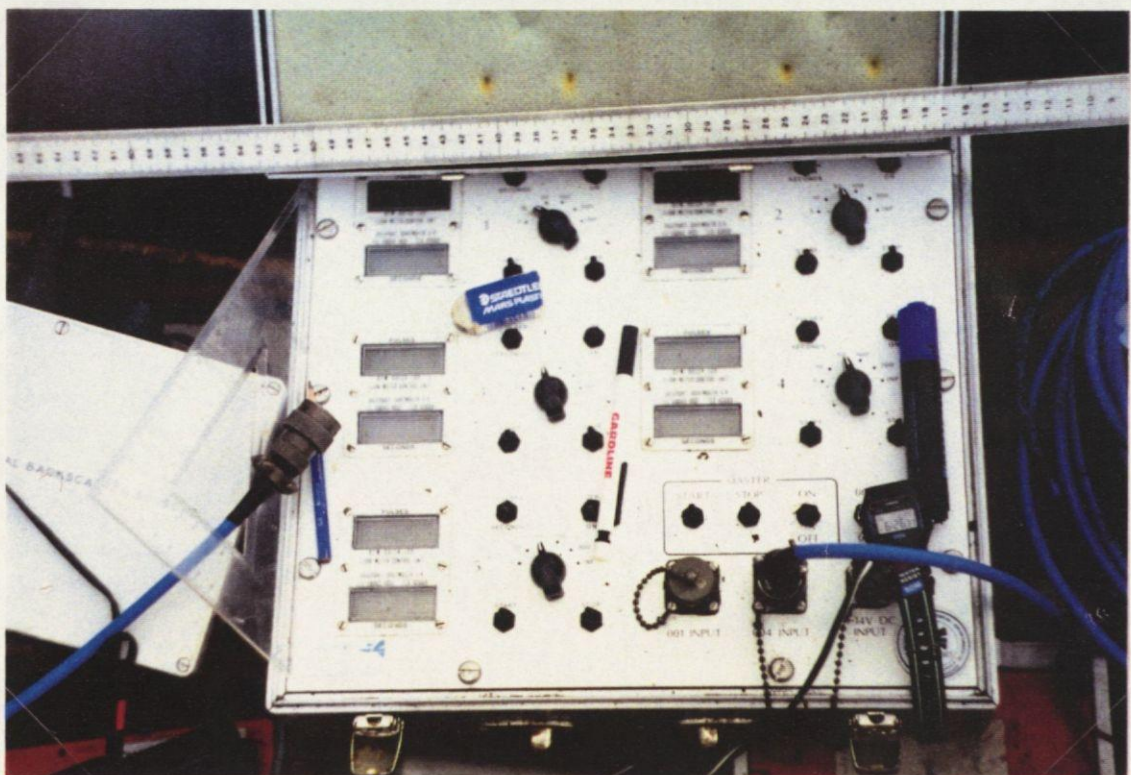
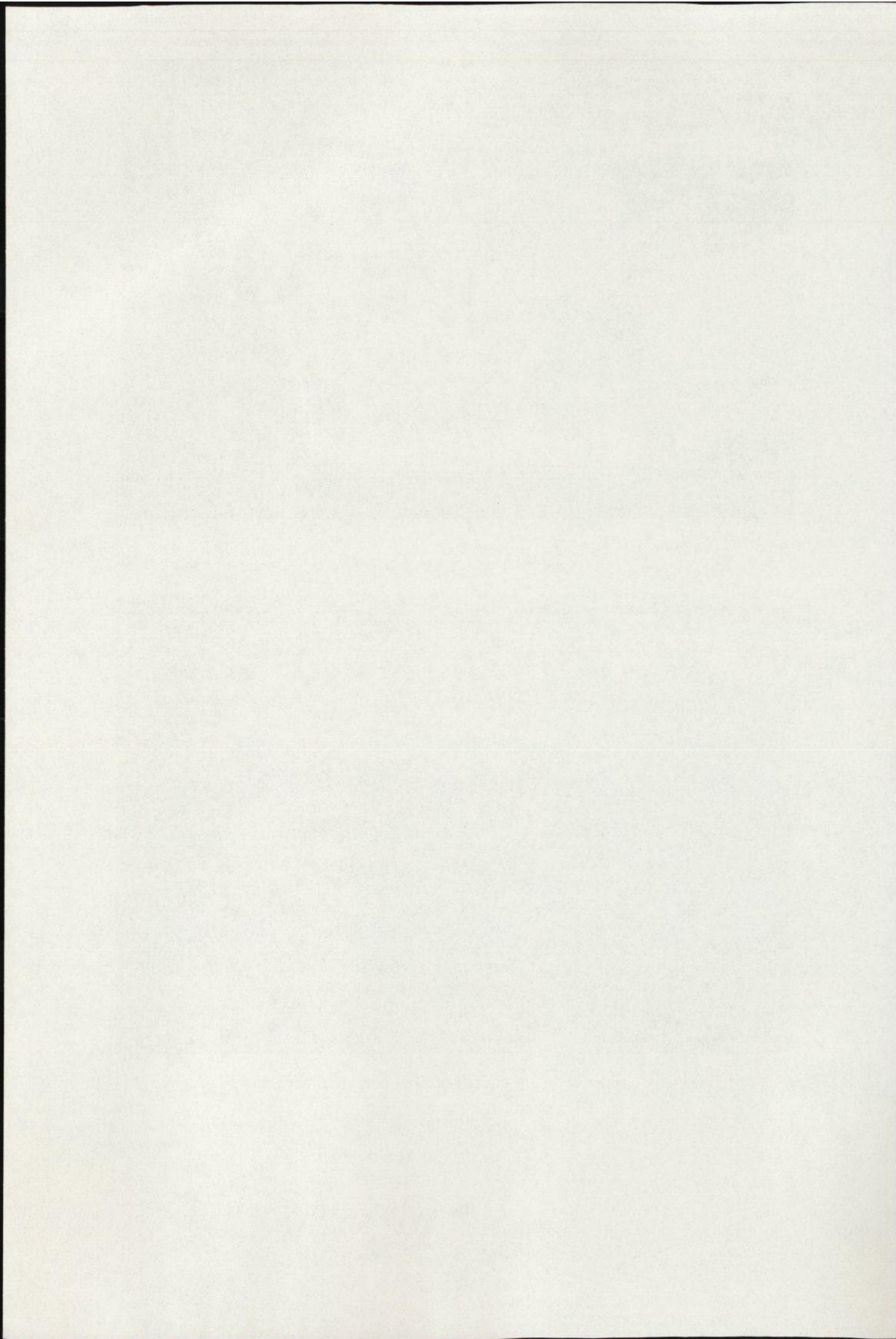


Plate3: Valeport multi-channel pulse-meter



Plate 4: Near high water showing benefit of bow and stern anchors



the lower impellers could be positioned as close to the sea-bed as possible. The reliability of this method is not known as there was a tendency for small sediment particles to jam the impeller and prevent rotation. If this occurred, the rig was removed from the water, freed, and returned as quickly as possible. Generally, though, measurements were continuous.

During periods when the water was extremely shallow, readings were taken every thirty seconds if possible, however, once the water depth had reached about 0.2m, readings were taken at greater intervals.

The inflatable boat was anchored fore-and-aft at some distance from the deployment site in order that it remained in a fixed position away from the current meter rigs. Thus avoiding over-riding the rigs at high water (see plate 4). Anchor lines were lengthened and shortened as the tide rose and fell, thus preventing the anchors dragging or keeping the slack out of them. Measurements could not be taken throughout consecutive tidal cycles as alternate tides were required to float the boat so that it could be towed to the next station.

Out of the nine tidal cycles measured, five provided thorough time series measurements in extremely shallow water. This was due to the differing requirements of the survey team and the rota system adopted to allow periods of rest. The Author was therefore not present on every tide measured and time series obtained during his absence were not entirely of the required detail.

5.5 Period of Observation

The survey took place from the 19th June 1993 to the 24th June 1993. This was during spring tides, so that the maximum amount of water was entering and leaving the Wash.

The weather during this period was exceptionally calm, leading to the almost complete

absence of wind waves. Only on one occasion was there rough weather of any kind. This turned out to be extremely valuable as interference by wind/wave induced currents with the tidal signal was kept to an absolute minimum.

Table 2 shows a summary of the survey programme, including a brief description of the sea-state and weather conditions.

Date	Time (BST)	Station	H.W. (m)	Survey Contents	Environmental Conditions
				(H,R,S,SPM,WS)	
19/06/93	03:45-07:15	93-5	6.7	H,R,SPM	Breeze, high cloud, sunny, waves ↓20cm.
19/06/93	16:15-19:15	93-4	6.7	H,R,S,SPM	Light breeze, sunny, calm sea.
20/06/93	04:30-07:45	93-3	6.9	H,R,SPM,WS	W/NW breeze, clear sky, waves ↓5cm.
20/06/93	17:20-19:50	93-2	7.0	H,R,SPM,WS	NW breeze, high cloud, no waves.
21/06/93	05:15-08:00	93-1	7.0	H,R,SPM,WS	Fine, calm sea.
21/06/93	17:25-21:25	93-5	7.0	H,R,SPM,WS	SE breeze, bright, calm sea.
22/06/93	17:45-23:00	93-6	7.1	H,R,S,SPM,WS	SE breeze, drizzle, wind increasing, waves ↑50cm, choppy.
23/06/93	19:00-22:45	93-3	7.1	H,R,S,SPM,WS	Light breeze, overcast, slight swell.
24/06/93	07:25-11:00	93-0	7.4	H,R,SPM,WS	Calm, no breeze, no waves.

Where; H = Water Depth, R = Current Rate, S = Current Set, SPM = Suspended Particulate Matter, WS = Water Sample.

Table 2: Summary of Survey Programme.

Appendix 3 shows the entire data set of field measurements.

CHAPTER 6

'THE WASH' - A NUMERICAL MODEL

Typically, model development has proceeded by comparing new model output with earlier test results, as presented in Chapter 3, or by studying the sensitivity of model results to changes in model input parameters (e.g. section 2.5.6). Whilst refinements in modelling and parameterization are intuitively sensible extensions to existing procedures and are expected to result in better predictions, there is, generally, disappointingly little direct evidence from field observations that this is the case. Field researchers, struggling with limited resources and frequently attempting to identify particular processes from amongst the complexity of other processes which occur in nature, have generally not used models to inform and assist with the planning of field work, with the result that many of their results are not directly relevant to model testing. The result of these two separate approaches is too often modellers who are uncritical of their model results and see no need for field testing, and field researchers who distrust models because of their experience of the real environment.

It is quite apparent that in order for model predictions to become more accurate and field workers to begin to accept the valuable contribution of numerical modelling to the understanding of natural phenomena, that the two must be drawn closer together. However, due to the lack of resources available for modellers to carry out their own field measurements and the field researchers reluctance to place trust in modelling techniques, further

understanding of marine processes is unnecessarily hindered.

It is to further this end that the Author has carried out a programme of field observations with which to validate a numerical model; to show that it is possible for field work and numerical modelling to combine together to achieve greater understanding.

6.1 Model Design

There are several differences between the layout of an idealized model and a model of a real area. Whereas in an idealized model it is possible to avoid time-consuming construction of hydrographic data-files, in a model of a real area it is necessary to spend considerable time creating the required input files.

Two models have been designed here; a coarse grid model (2NM) and a fine grid model (0.4NM). Due to processing restrictions, only the coarse grid model has been run, with the intention of obtaining adequate computational power to run the finer grid (0.4NM) model in the future

6.1.1 Bathymetric Data File

Whereas for the idealized models the bathymetry could be specified using simple loops within the source code, when a model of a real sea area is desired, the shape of the sea-bed must be arrived at in a more complicated and time-consuming manner.

In order to provide a bathymetric data-file for a numerical model, two steps must be taken; firstly to gather the necessary data and secondly to interpolate these raw data in order to be represented on the structured grid. Data can be obtained by digitizing bathymetric charts, taking bathymetry from a larger scale model which covers the same region, and using

available measurements. Care must be taken when using data from several different sources to ensure that differing reference points for the measurement of depth values are accounted for.

The quality of certain data may be suspect depending on how they were obtained or how recent they are. This may cause problems when it comes to interpolation of bathymetric data as good quality data may easily become contaminated by the presence of poorer quality data. The combination of such data should be carefully considered before the decision is made to include or discard any material.

The best bathymetry is not always obtained by assigning specific depth measurements to the exact geographical position in the model area. Because two-dimensional numerical models calculate averaged stream velocities and water depths, it follows that averaged bathymetric features are more important than bathymetric features at discrete positions.

It is possible for a bathymetric file to be constructed in one of two ways. One method may be termed the 'gridding method', the other the 'sounding method' (George, 1993).

The gridding method requires that the average depth of a grid square be obtained directly from a grid drawn on the chart and a method of proportion assigned to account for any soundings and isobaths that may be present in the superimposed grid square (see George (1993) for specific detail on averaging methods).

The sounding method requires that depth soundings and their locations in space be compiled in a file and interpolation methods be used to establish a schematization of the sea-bed bathymetry over the model area. This has the advantage that one database can be used for many different models over a region which has had its depths digitized. However, isobaths, which provide much needed information in regions of sparse soundings, are difficult to incorporate in the interpolation process, whereas the gridding method readily allows isobaths

to be taken into consideration during the method of averaging. Due to the fact that the soundings found on an Admiralty Chart are referred to chart datum while tidal elevations in numerical models are computed relative to mean sea level, it is necessary to adjust each depth value taken from the chart in order that they should also be relative to mean sea level.

Since this numerical model of the Wash is 'study specific', *i.e.* it is not deliberately intended to be part of a larger database, the gridding method has been used to create a bathymetric database. Admiralty Charts N^o's 108 and 1200 have been used to provide the bathymetric information. The bathymetric file for the 0.4NM model may be seen in Appendix 4, while figure 6.1 shows an isometric presentation produced from this data set. The bathymetric input for the 2NM model was obtained by averaging the bathymetry in 5x5 squares of cells from the 0.4NM model, which correspond to the same area as one cell from the 2NM model.

6.1.2 Masking File

For the model of the Wash the precise locations of land and sea are defined by a masking file (see George, 1993). This has a similar format to that of the bathymetric file and can be superimposed on the bathymetric file to produce a graphical image of the area being modelled. This is invaluable during the development of such files as areas of inconsistency between bathymetric and masking files can be readily observed and altered.

6.1.3 Model Area

Figure 6.2 is a graphical representation of the whole of the 2NM model of the Wash. This figure shows the masking file and bathymetry (in decimetres) superimposed, as suggested above. In addition, the coastline and the open sea boundary of the model can be seen.

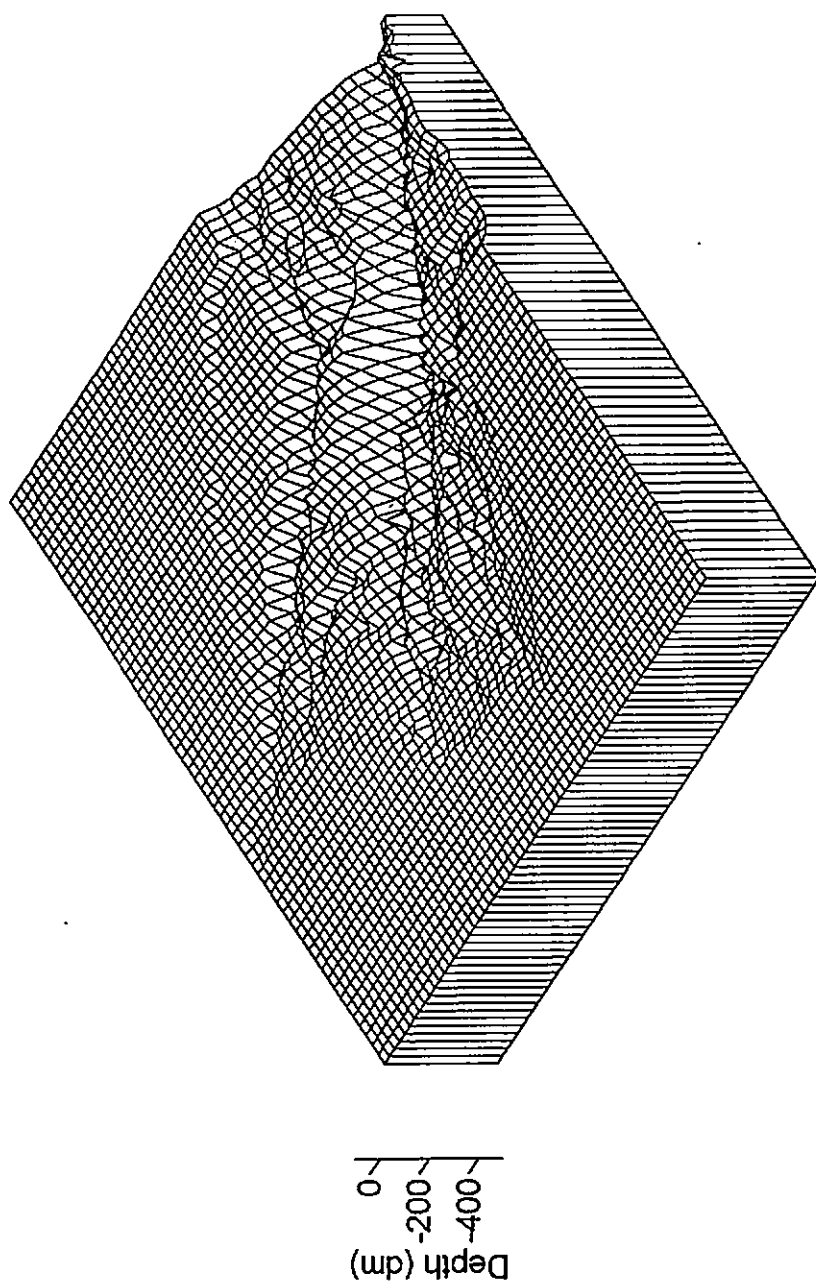
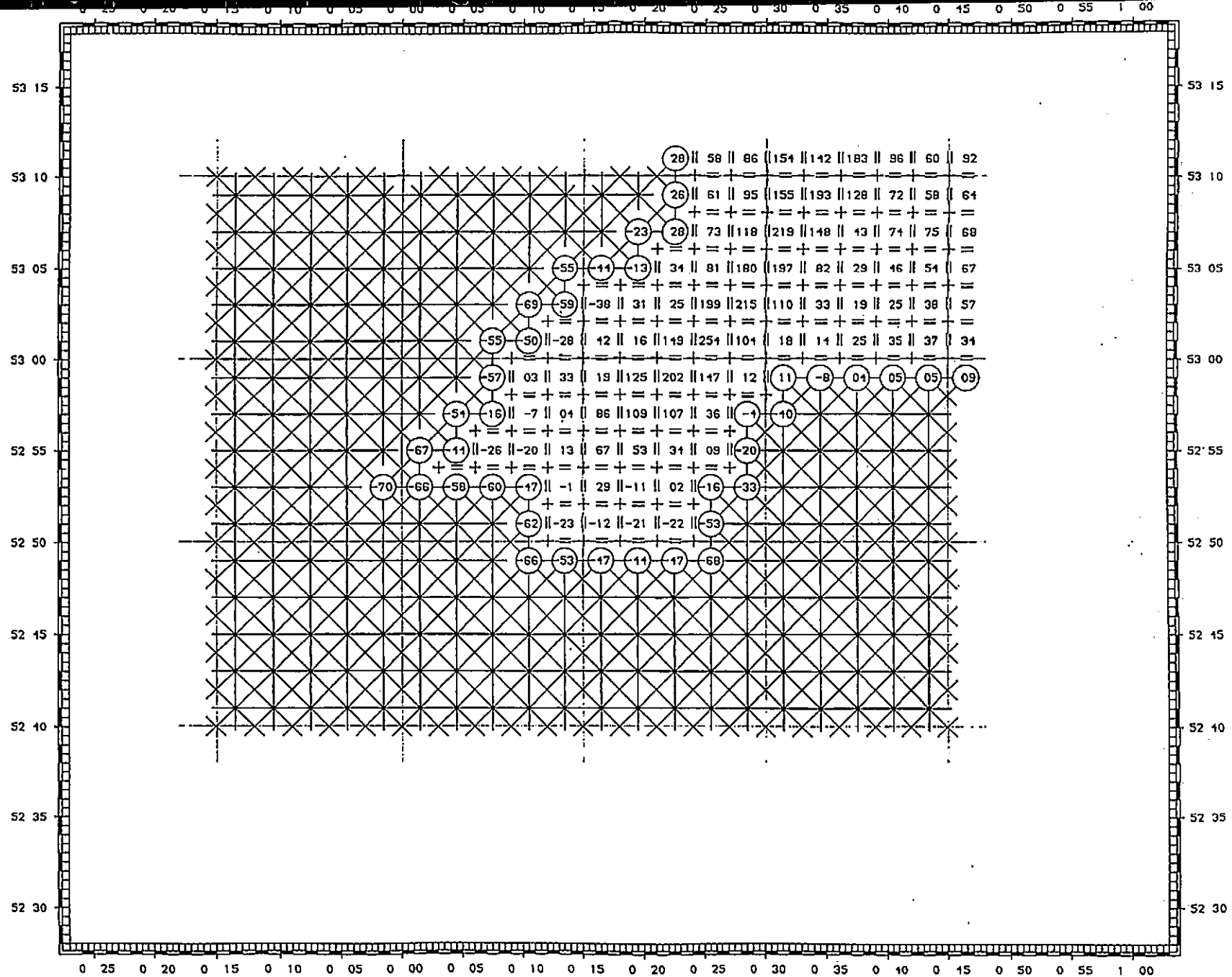


Figure 6.1: Isometric projection of the Wash

Figure 6.2: 2NM model of the Wash



6.1.4 Open Boundary Conditions

Tidal input for the idealized model has been described in Chapter 2, section 2.5.2. This is inapplicable to the model of the Wash, and therefore boundary conditions must be defined in some other manner.

There are five basic forms of boundary conditions, which may be applied in different situations, in different combinations. These are water levels, tidal velocities, water fluxes, Riemann (weakly reflective) boundaries, or gravitational effects. The exact form of the boundaries depends on the phenomena being studied. The form should, ideally, be chosen to give the best driving force to the modelled phenomena. For instance, models of water in an estuary should be driven by the specification of water levels at the entrance to the estuary. Fluxes, stream velocities, and Riemann boundaries can equally be applied in order to obtain the same internal solution. However, since velocities and fluxes are only weakly connected to water levels, then in the estuarine case used as an example above, the control over the final solution would be less than if the tidal input were in the form of water levels.

If there is more than one open boundary, different forms of boundary conditions should be applied at each boundary. For instance, at the open ends of a straight channel, the application of velocities at both boundaries would lead to continuity problems if the fluxes were not compatible. In this instance, it would probably be best to specify at one end water levels and at the other end velocities. To model a large basin (of the order of kilometres), the prescription of water level forcing at the boundaries is generally adequate.

In practice, the availability of certain types of boundary condition data determines the selection of type made. Most open sea models can be driven only by water level input at the boundaries since these may well be the only quantities known at the sea boundaries.

Table 3: Data provided by P.O.L. for production of boundary conditions

M2	AMPLITUDE (CM)		- ELEVATION			
	0.0000	0.0000	0.0000	228.9792	219.2066	207.4745
	0.0000	0.0000	252.1376	239.5120	226.2165	213.0491
	0.0000	270.6418	262.7488	254.8744	0.0000	0.0000
	0.0000	0.0000	269.3411	266.4209	0.0000	0.0000
	0.0000	0.0000	0.0000	0.0000	0.0000	0.0000

M2	PHASE (DEGS)		- ELEVATION			
	0.0000	0.0000	0.0000	168.0250	168.6870	170.1100
	0.0000	0.0000	180.9720	178.1630	175.3540	174.4910
	0.0000	189.2860	187.8050	187.3220	0.0000	0.0000
	0.0000	0.0000	190.4240	190.8710	0.0000	0.0000
	0.0000	0.0000	0.0000	0.0000	0.0000	0.0000

When water level boundaries are applied on their own it is the gradient of the sea-surface level which drives the system and therefore care must be taken with the data as small errors in these values can be compensated within the model only by large responses of the internal forces of the model. This could, for instance, induce higher velocities in order to compensate for the exaggerated pressure gradients on the boundary. The influence of this kind of error is not restricted to the area of data error determined by grid sizes, but by the physical area of influence according to the error in water level specification.

In order to minimize the effects of possible errors in boundary specifications, it is normal practice to specify the boundaries as far away geographically as possible from the area of interest.

The information needed to provide boundary conditions for the model of the Wash has been obtained from a larger scale model (POL Continental Shelf model: CS3), figure 6.3. These data can be seen in table 3, where the values of elevation and phase pertaining to the M_2 tidal constituent are given in the form of a grid which provides coverage of the area of the Wash model. Table 3 can be considered as a crude co-tidal chart. From the values provided by POL, a detailed co-tidal chart was constructed (figure 6.4). The crosses on figure 6.4 represent the positions of the data points provided by P.O.L.. From this chart, the phase and amplitude of the M_2 tidal constituent were extracted at each ζ -point on the 0.4NM model boundary (see figure 6.5). The boundary values pertaining to the coarser 2NM model were taken at every fifth point from the 0.4NM model boundary.

In addition to the M_2 constituent, the amplitude and phase of the S_2 and N_2 constituents were also used as input. These were extracted from co-tidal charts published by Howarth (1990) and are based on observation rather than on the results of modelling. Appendix 5 shows the boundary values.

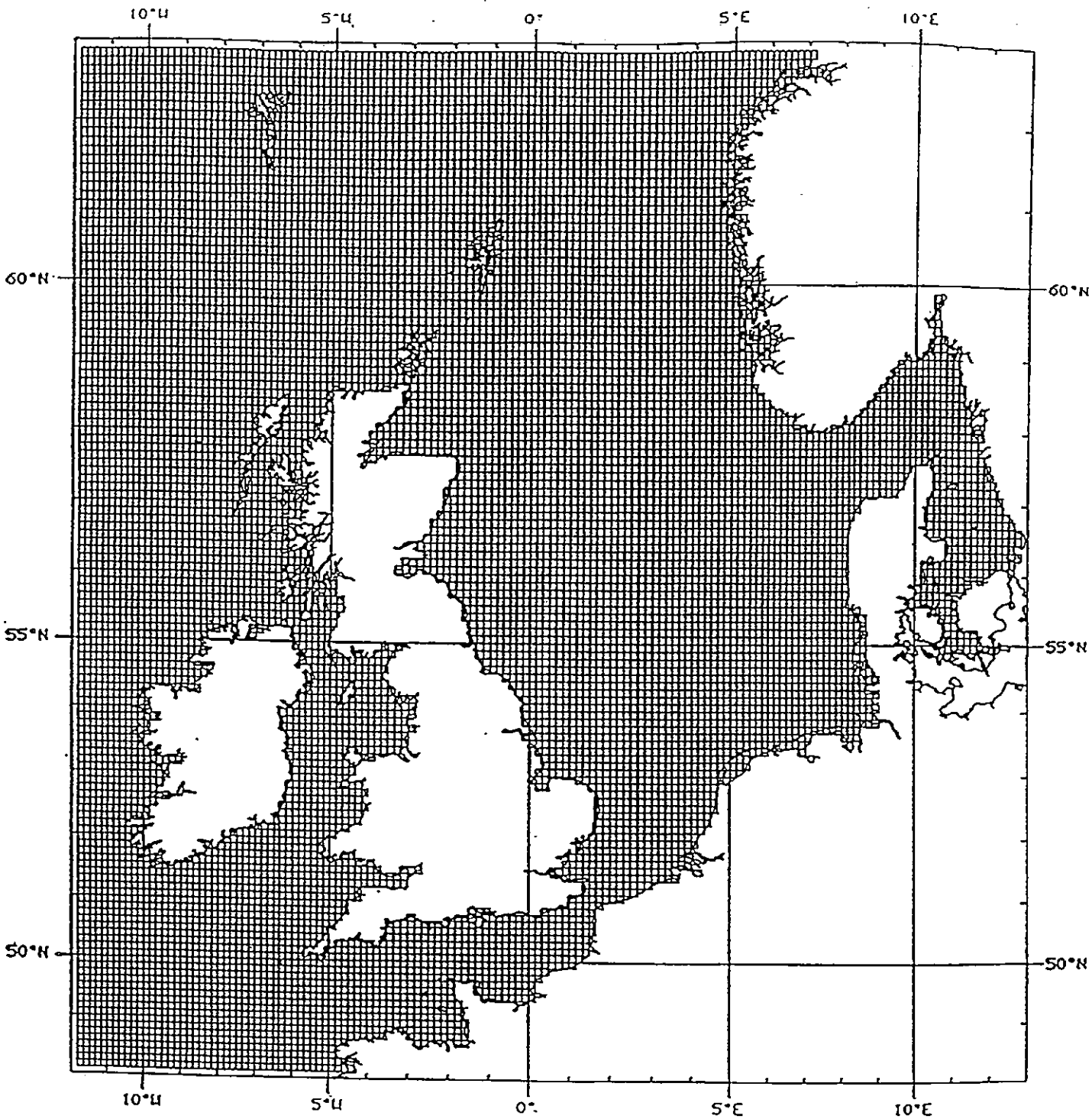


Figure 6.3: Continental Shelf model: CS3 (P.O.L.)

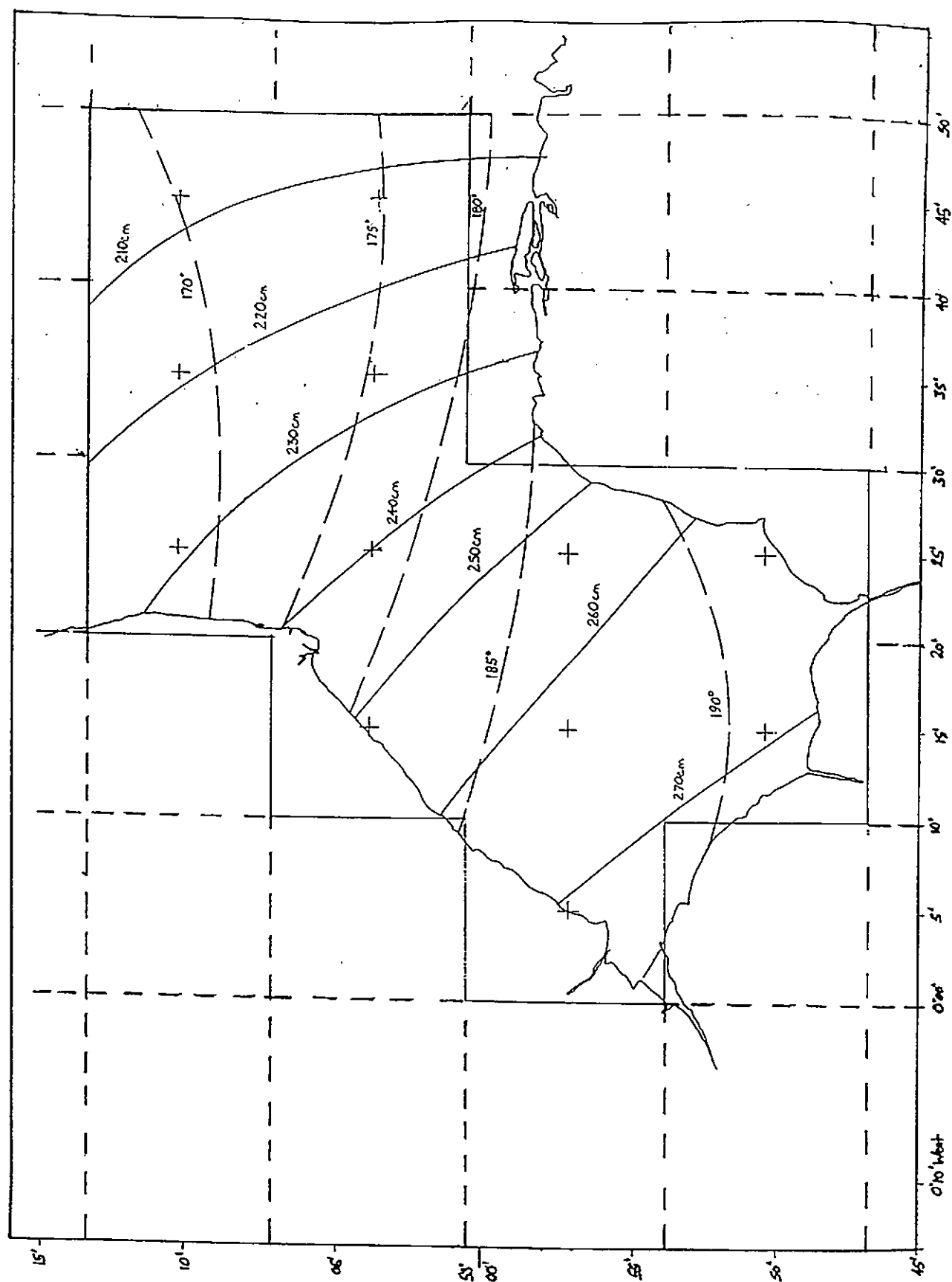


Figure 6.4: M₂ co-tidal chart of the Wash, U.K.

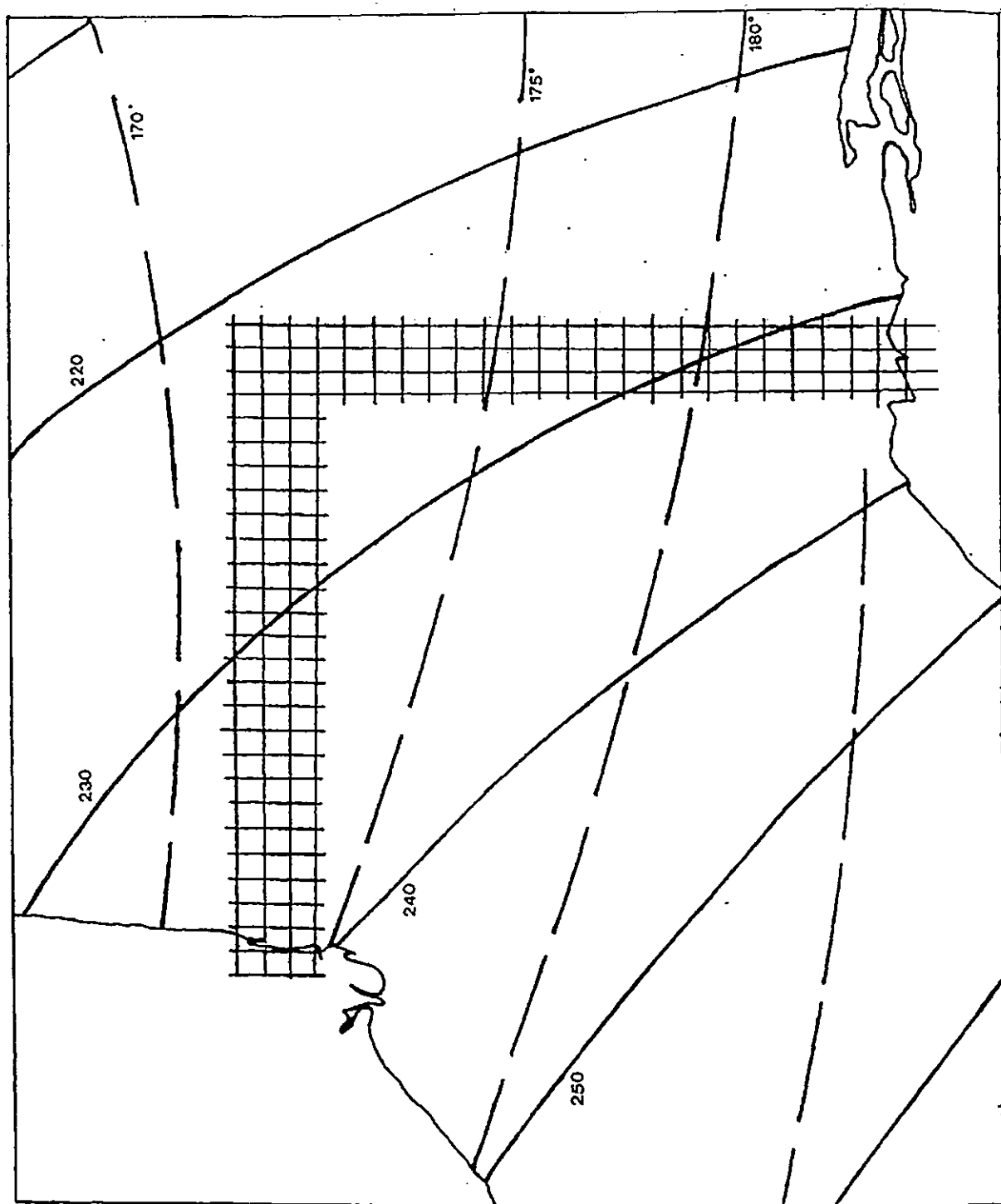


Figure 6.5: Obtaining boundary values from the co-tidal chart

6.1.5 Model Time-Step

By rearranging the inequality equation 2.29, the time-step for the 2NM model of the Wash can be evaluated from:

$$\Delta t \leq \frac{3700}{\sqrt{2 \times 9.81 \times 40}} \leq 132.1s$$

Since one three hundred and sixtieth of the tidal cycle is 124.2s, and it fulfils the stability requirement above, it has been chosen as the time-step for the model of the Wash.

6.2 Results

In this comparison exercise, results output from a cell in the 2NM model are compared to the measurements taken along the transect 52° 57' 17''N, 00° 06' 33''E to 52° 57' 34''N, 00° 05' 40''E. The time, date and the tidal conditions of the model output correspond to the field measurements. The exact position in space of the nearest model point, however, is 52° 56' 00''N, 00° 06' 00''E; over a mile away from the field survey transect (see figure 6.6).

Results from the 2NM model of the Wash can be seen in Appendix 6. Particular sets of results are also reproduced here in figures 6.7 to 6.12. These sets have been chosen due to the completeness of the corresponding field data sets.

Elevations of the survey stations were taken from figure 5.3, and converted to mean sea level. Meteorological and environmental effects (such as river discharge) on the tide cannot, at present, be represented in the model, and therefore, perturbations in the tide caused by wind set-up/set-down, wave/current interaction, or freshwater influences are deemed to be inherent errors of the model, and will be dealt with no further in the discussion of the results, although it is recognized that there is some contribution in the measurements from these phenomena.

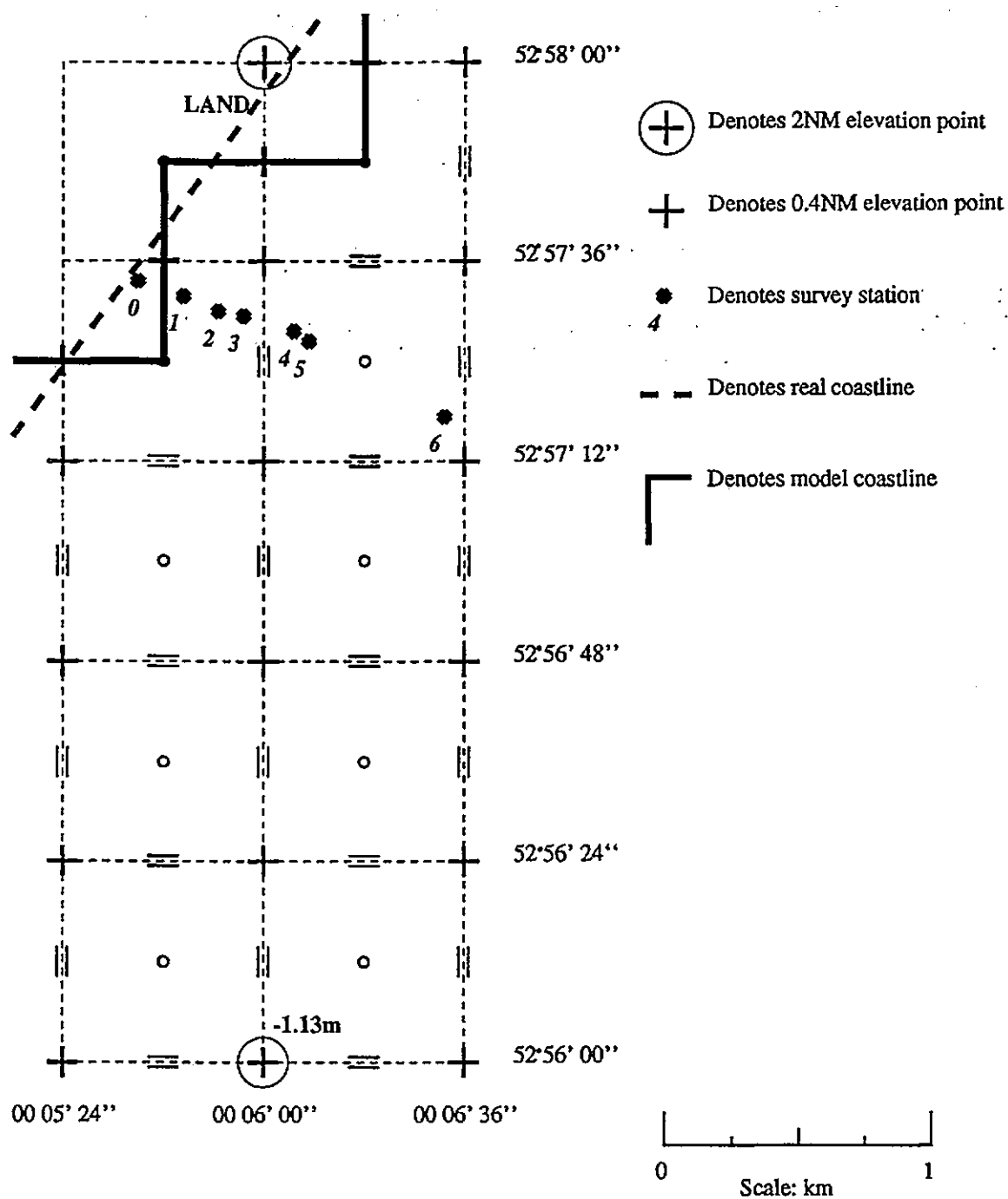
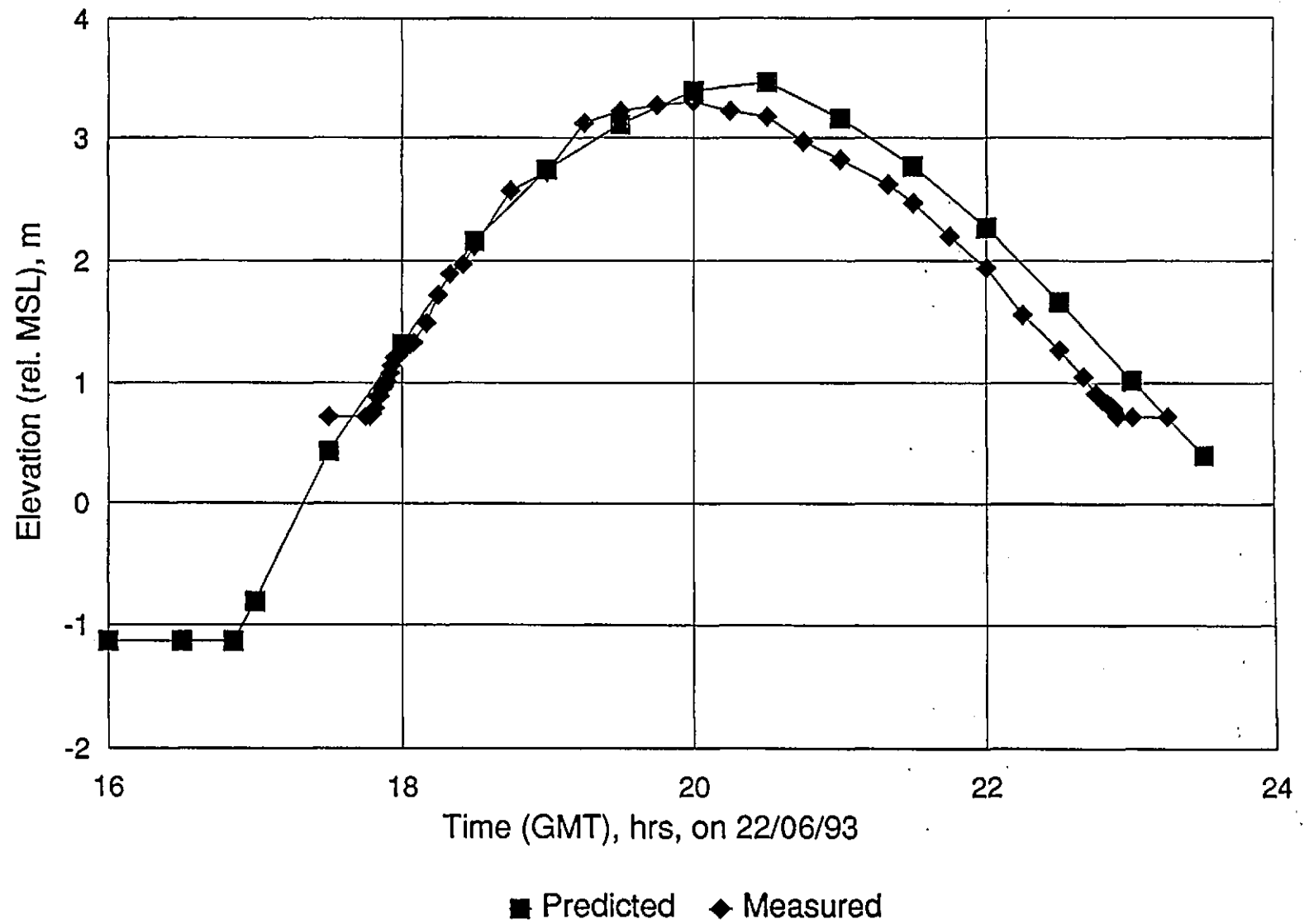


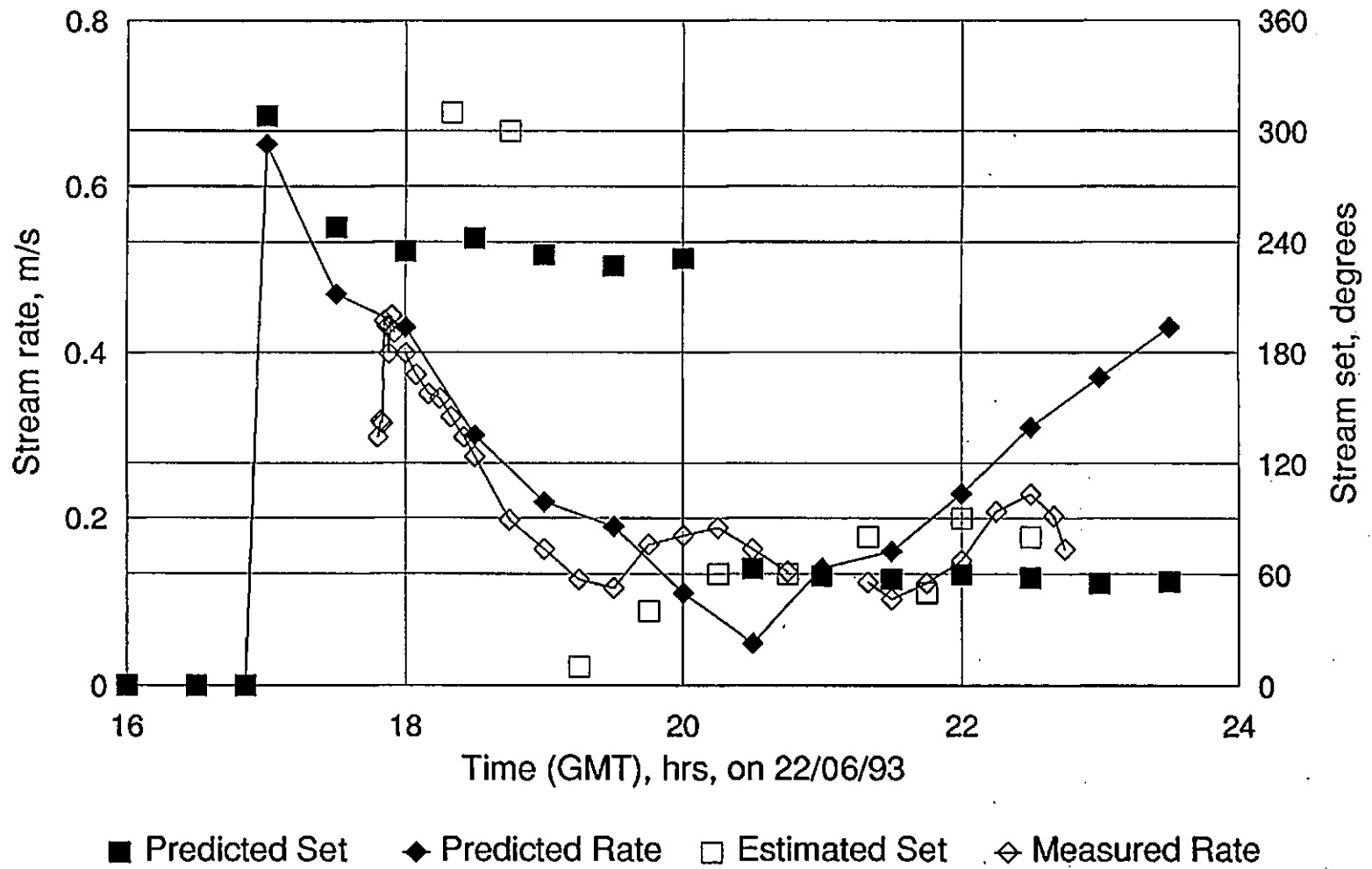
Figure 6.6: A portion of 0.4NM/2NM model area showing positions of survey stations and the coastline



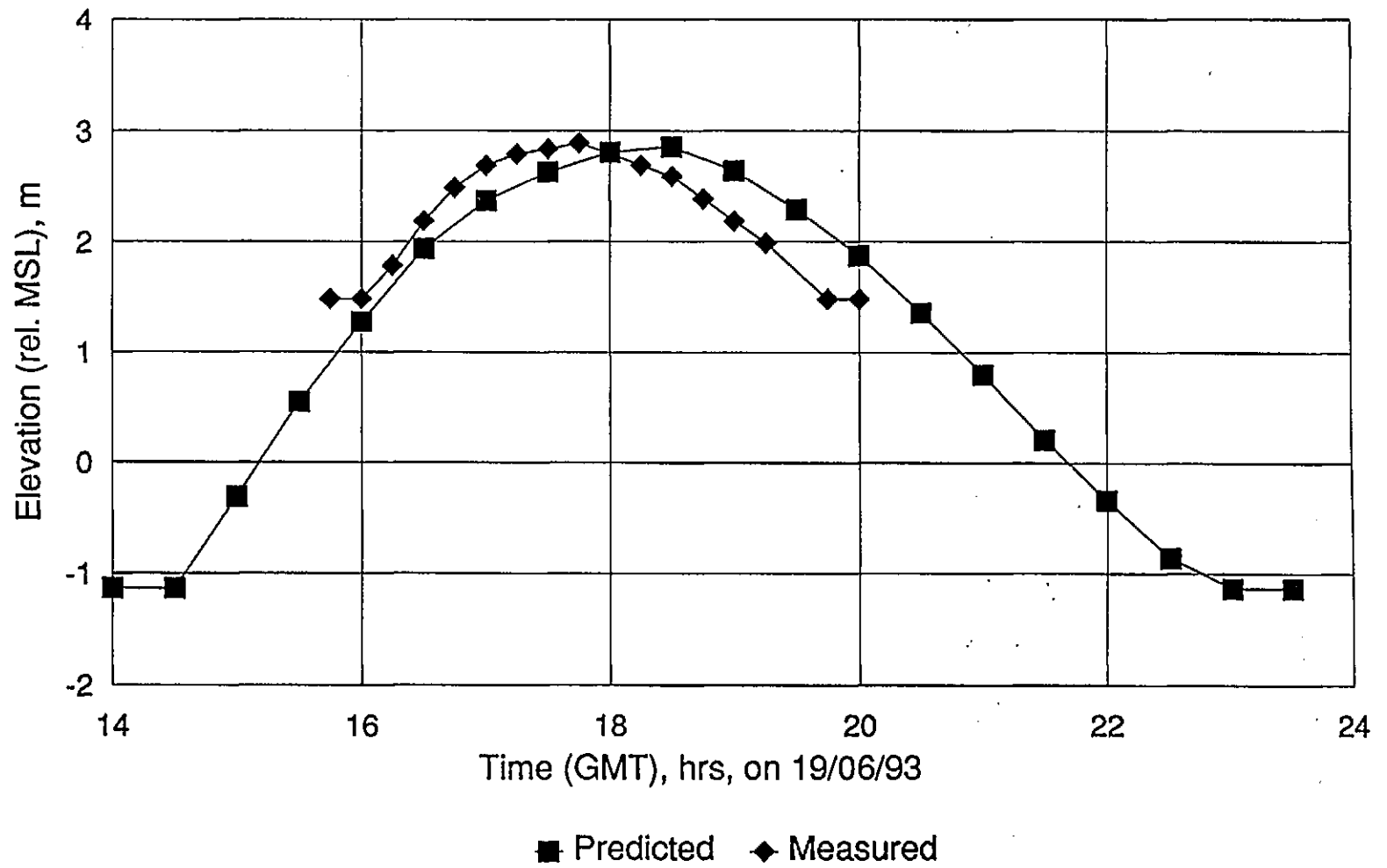
Note: The predicted data are from a point 52 56' 00"N, 00 06' 00"E, while the measured data are from a point 52 57' 17"N, 00 06' 33"E.

Figure 6.7: Comparison of measured and predicted elevations for Station 6

Figure 6.8: Comparison of measured and predicted stream rate and set for Station 6

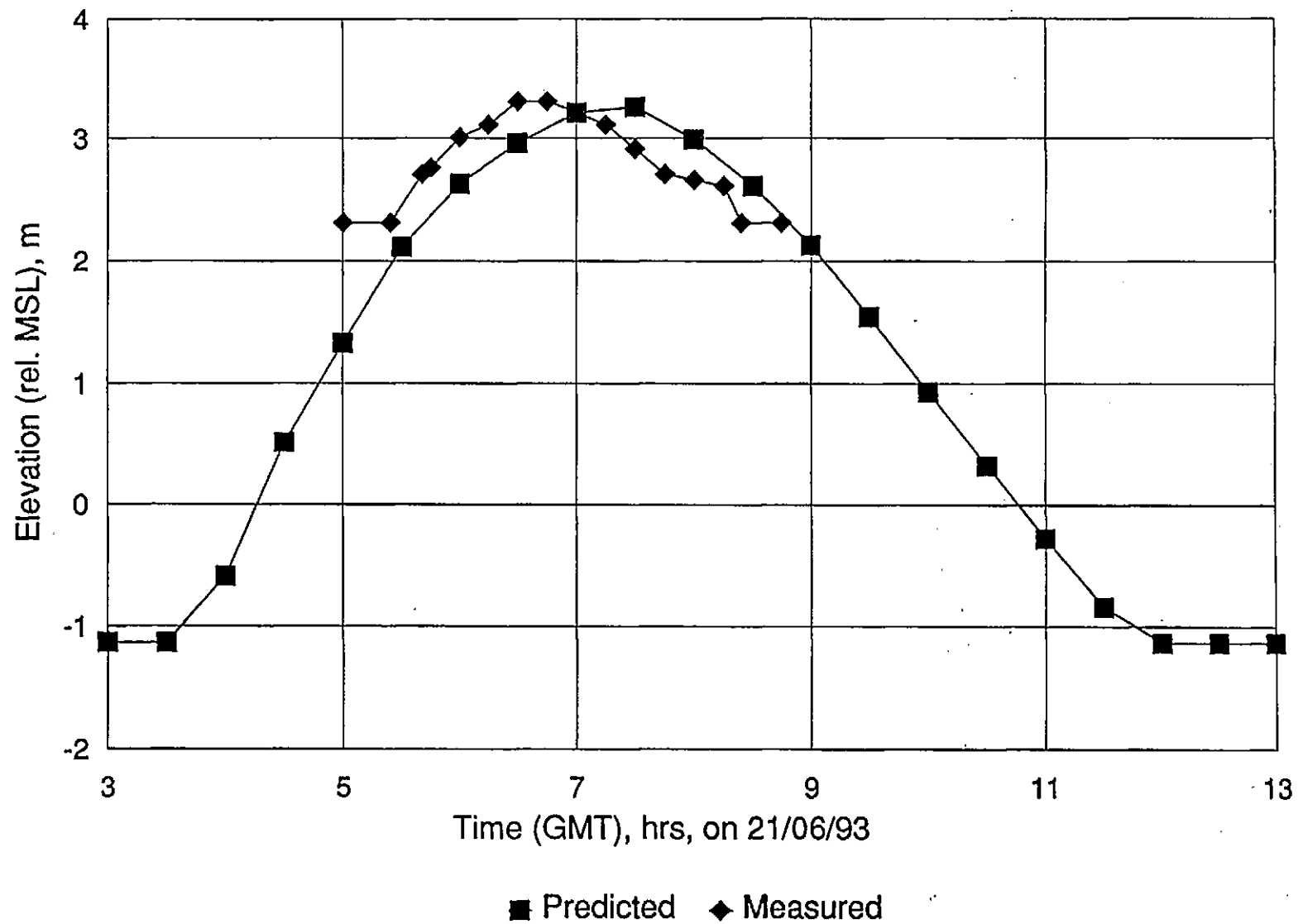


Note: The predicted data are from a point 52 56' 00"N, 00 06' 00"E, while the measured data are from a point 52 57' 17"N, 00 06' 33"E.



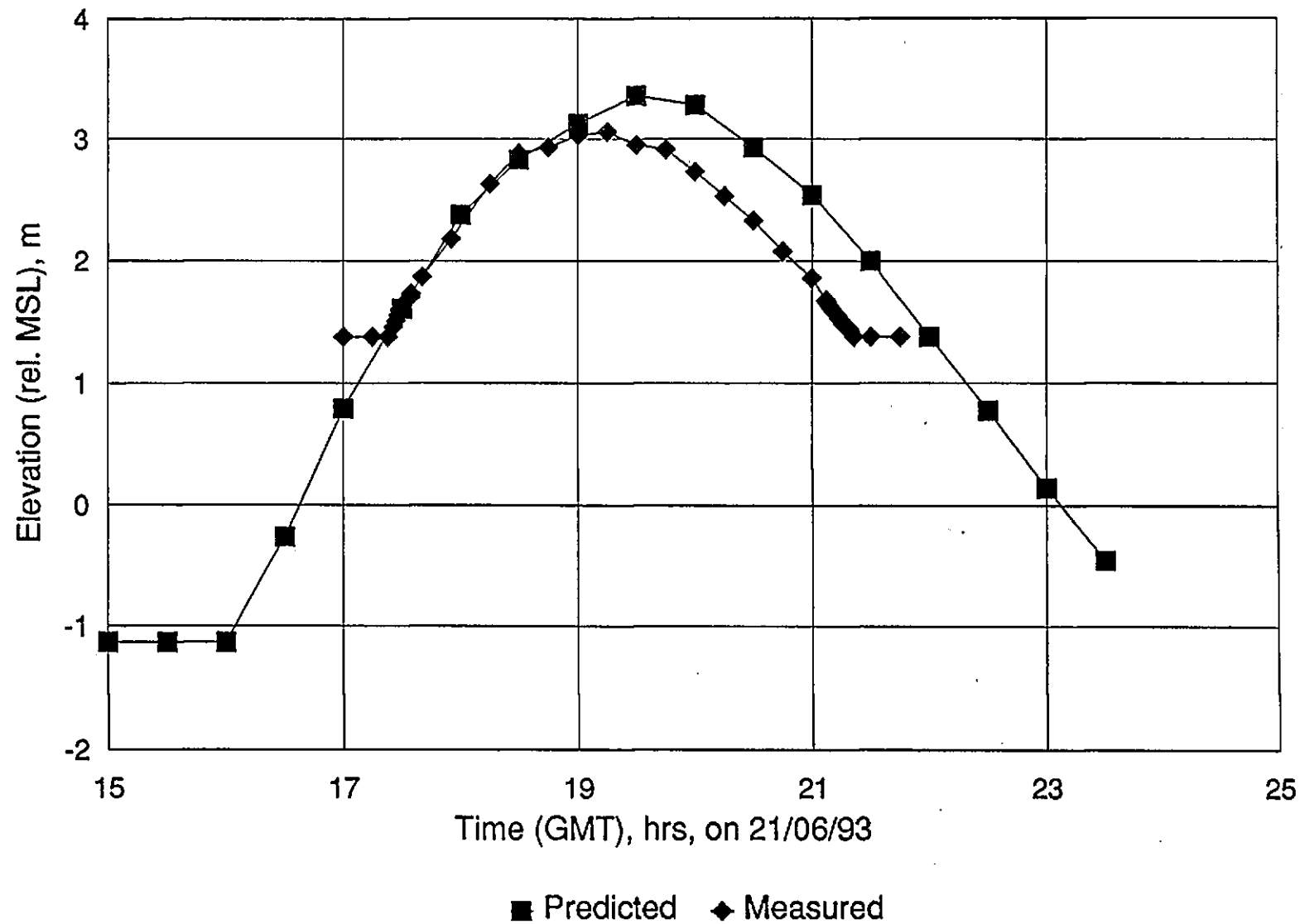
Note: The predicted data are from a point 52 56' 00"N, 00 06' 00"E, while the measured data are from a point 52 57' 26"N, 00 06' 05"E.

Figure 6.9: Comparison of measured and predicted elevations for Station 4

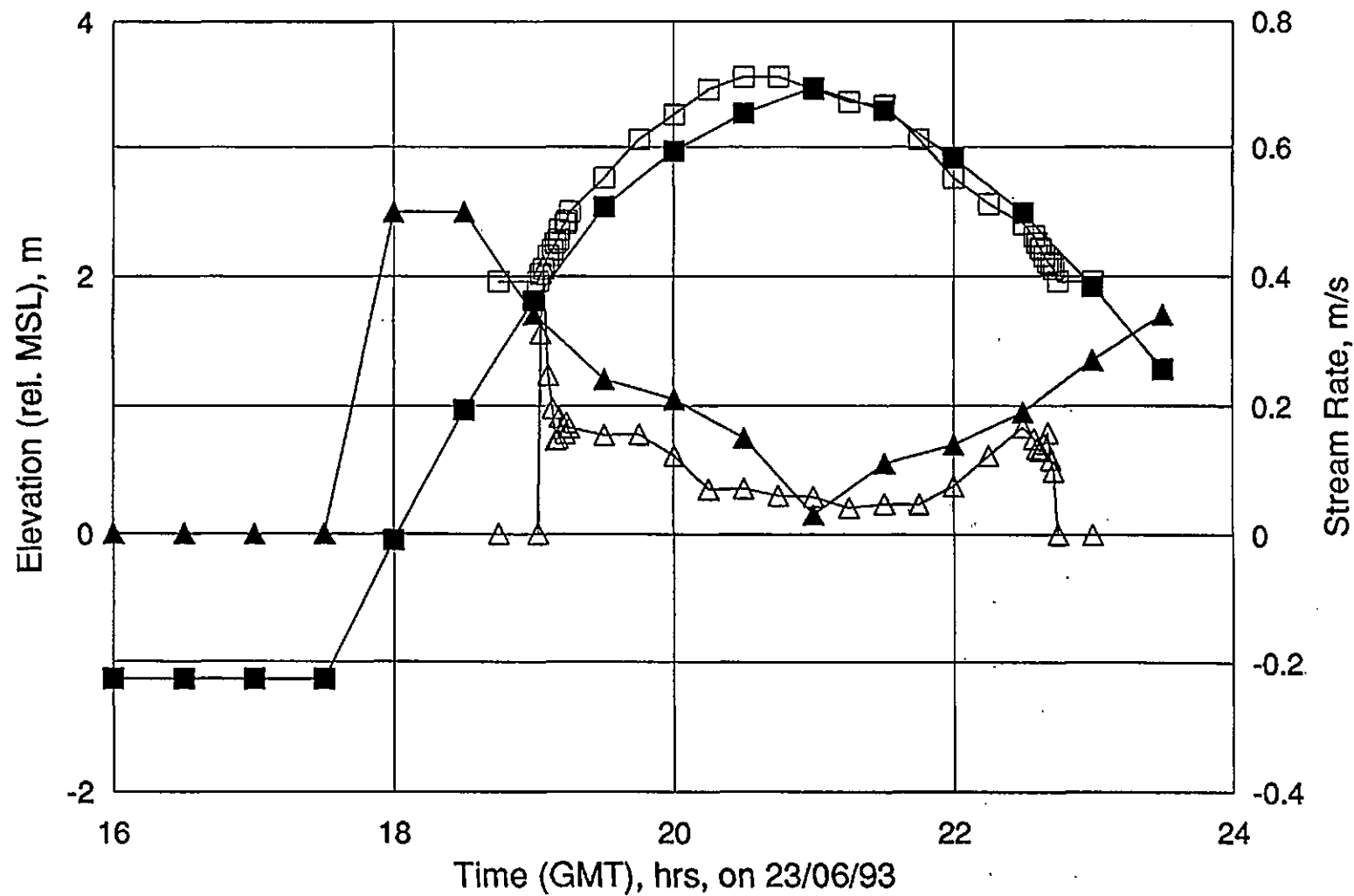


Note: The predicted data are from a point 52 56' 00"N, 00 06' 00"E, while the measured data are from a point 52 57' 32"N, 00 05' 46"E.

Figure 6.11: Comparison of measured and predicted elevations for Station 5



Note: The predicted data are from a point 52 56' 00"N, 00 06' 00"E, while the measured data are from a point 52 57' 25"N, 00 06' 08"E.



■ Elevation, pred. □ Elevation, meas. ▲ Rate, predicted △ Rate, measured

Note: The predicted data are from a point 52 56' 00"N, 00 06' 00"E, while the measured data are from a point 52 57' 29"N, 00 05' 57"E.

Figure 6.12: Comparison of measured elevation and stream rate with predicted elevation and stream rate for Station 3

6.2.1 Station 6

The nearest survey station to the model output point was Station 6 at $52^{\circ} 57' 17''\text{N}$, $00^{\circ} 06' 33''\text{E}$. Figure 6.7 shows the measured elevation profile and the elevation profile at the nearest 2NM model point. The model cell wets suddenly and smoothly, with no sign of spurious oscillations. The field measurements, too, show a sudden wetting. Unfortunately, measurements on this particular survey were hampered by waves and poor light. As a result, there are apparent oscillations in the measured profile.

Good agreement is shown in the general shape of the tidal curves, with the model reproducing the faster rate of rise of the tide than the rate of fall of the tide demonstrated by the field measurements. However, there is an obvious discrepancy between the two curves; the time series from the model cell implies that the survey station became wet approximately half an hour after it actually did.

The time of high water being predicted half an hour late is likely to be partly due to the inaccurate representation of bed friction, which may have allowed too much water to propagate inshore, thus delaying the time of high water. It may also be a feature of the coarseness of the model or perhaps due to the difference in bed-levels as explained below.

In the field, water-levels could be determined relative to the level of the sea-bed, but absolute water-levels were difficult to determine, because the survey stations were well over a kilometre from the nearest bench-mark. Predicted tide heights were determined for the secondary port of Tabs Head (close to Frieston and less than 2km from the survey stations) using the simplified harmonic method (N.P. 159A). Comparisons of the estimated absolute levels with these predictions suggested that the former were up to 1m in error. In the light of this discrepancy, the bed-levels were each raised by 0.8m to produce the curves shown in

figures 6.7 to 6.12.

The remaining discrepancy in the actual value of high water could be due to several other points. One is the inadequate specification of boundary input data. For the three tidal components which were used, errors could be $\pm 0.1\text{m}$ in total, while an estimate of the effects of all the other harmonics which were not used (there were no quarter diurnal or species 0 input) could be $\pm 0.3\text{m}$. Another, the inadequate representation of bed friction (see section 6.2.3), may be responsible for an error of $\pm 0.2\text{m}$.

Figure 6.7 shows the tidal stream and set predictions with the tidal stream measurements and estimates of the actual stream set. It is difficult to assess the validity of comparisons between the measured and predicted values of these two variables in this instance, since stream measurements close to the shore are affected by currents from short period wave action and local topographic features. Longshore currents may also contribute to the signal, particularly close to the surf zone. This station, however, was too far seaward of the surf zone for longshore currents to cause too much of a problem, although the effect of possible resultant rip currents is not known. Perhaps the most problematic cause of variance is the topography and characteristics of the bed, which may vary considerably, even on a scale of metres. The fact that the model cells are $3700 \times 3700\text{m}$ indicates that local features will not be delineated by the model.

In spite of all the potential for inaccurate predictions, figure 6.8 shows that the time series produced are very good when compared to the measurements. With regards to the stream rate, the initial peak velocity predicted by the model is $\sim 30\%$ higher than the initial peak velocity that was measured. Apart from errors in measurement, this is probably due to the larger volume of water being propagated inshore by the model than the measurements indicate (as shown by the higher predicted level at high tide). The model had to cope with this 'extra'

volume of water through continuity, thus moving more water in the same amount of time, resulting in a higher flux. In addition, it must be remembered that the model output point is over a mile away from the survey station.

The shape of the stream rate profile is very encouraging, however, with peak velocities predicted on wetting and on drying, by both the model and the measurements, with lower velocities predicted at around slack water. The velocities on drying are predicted to be smaller than the velocities on wetting, which agrees with the measurements, obviously due to the vast mass of water seaward 'holding back' the receding water-line. The character of the flood stream rate is predicted very well in that it shows a sudden rise to a peak velocity from dry as the point becomes wet. Following this, the model predicted a steady decrease in the velocity magnitude at a rate close to that shown by the measurements. The stream set is shown to be reasonably well reproduced; however, the measurements cannot be relied upon as they were estimates of the direction of movement, since no apparatus was deployed on site for the purpose of measuring this attribute.

6.2.2 Further Survey Stations

Figure 6.9 to 6.12 show the elevations measured at four other stations along the transect that yielded comprehensive data sets and were sea points according to the model. Again, the rates of wetting and drying are predicted well; however, the times and heights of high water are consistently poorly reproduced. The retardation of the time of high-water is more than likely due to two factors. The first is minimal, and is due to the predictions being made at such a distance from the survey transect. The main factor is probably the representation of bed friction in this, or any, numerical model where discretization in space is necessary.

178
178

178
178

178
178

6.2.3 Bed Friction

The fact that an area of sea is separated into discrete cells, which themselves may cover a substantial area of sea, leads to the necessity of making assumptions or generalisations. One generalisation made here is that the roughness of the sea bed was considered to be constant over the whole area of the numerical model, *i.e.* the drag coefficient applied was not variable. In fact, no attempt was made here to tune the model through the drag coefficient.

When tuning a tidal numerical model, adjusting the drag coefficient parameter is a good place to begin, since friction is of paramount importance in tidal propagation (Svendsen & Jonsson, 1980), especially in shallow water as shown, for instance, in figure 3.7. The Author decided here though, that simply to change the drag coefficient to another number in order to obtain a closer fit to the measurements was inappropriate.

The concept of having a drag coefficient (or bed roughness) that is variable over the entire model area is not a new concept (e.g. Wallace, 1994). Varying the bed roughness is possible, at present, only from cell to cell, or area to area. When we are dealing with large cells, such as those in the 2NM model of the Wash presented here, the bed roughness can alter considerably from one part of the cell to another, so varying the bed roughness from cell to cell solves only part of the problem. This is based on the presumption that the bed roughness over the entire area (or at least the area of interest) of the model is known. In addition, bed roughness is certainly not linear with horizontal distance or depth, but dependent upon bed-forms and material, so discrete measurements or calculations are again only of limited value and very costly. The expense is further increased when we consider that, even if such detailed measurements were to become available to modellers, they would be site specific, and consequently, applicable only to the area where the measurements were taken.

CHAPTER 7

SUMMARY AND CONCLUSIONS

SUMMARY

Three existing drying algorithms were incorporated into a numerical scheme and analyzed. Their performance was found to be unsatisfactory so a new algorithm was developed. The results have shown an improvement upon general modelling techniques in wetting and drying models.

A week of field work was conducted alongside the numerical development. This has proved that provided there are sufficient research funds, it is possible for numerics and real life observations to work in unison towards a common end.

Field measurement techniques were adapted to provide the best measurements possible of the initial wetting and the late drying periods on a tidal flat in the Wash, U.K.. A 2NM numerical tidal model of the Wash was designed and validated by these field measurements. On the whole, the model performed very well, with the biggest problems being; precisely where the measurements were output from (*i.e.* the model output point was over a mile from the survey transect), the lack of a detailed survey of the bed levels at the survey stations, and the uncertainty in the representation of bed friction in large cells.

CONCLUSIONS

1/ With regards to wetting and drying in tidal numerical models, there is one problem which appears to cause more disruption of the solutions than any other. This is the fact that cells are not able to wet quickly enough when the tidal elevation surrounding them has risen sufficiently. For cells which are large, e.g. 5km, the current methods for wetting a cell require that a 25km² area of sea are required to suddenly and instantaneously become wholly wet and active within the numerical scheme. There is simply not the volume of water available for this to happen, neither can water physically travel fast enough to reach the opposite computational edge of the cell.

2/ Disturbances which are generated by unnaturally imposed requirements (e.g. the sudden wetting of a cell) have a considerable effect on cell dynamics and surrounding solutions. If a cell is required to wet suddenly, there will naturally be an imbalance in the conservation of momentum equation.

3/ A new numerical technique has been devised which allows a cell to wet and dry gradually. In principle this is a very straightforward idea. However, the computational process can be quite complex. This method, the 'method of sloping facets', was used to eliminate discontinuities inherent in a 'large cell' wetting and drying process as the tide rises and falls. The testing of this method has proved that sloping facets provide solutions which are not adversely affected by the wetting and drying of cells. It was concluded that the models incorporating this new technique resembled nature in that discontinuities related to cell size inherent with discretization demonstrated in previous work were removed.

4/ It is suggested that a finer scale model of the Wash be run in order to resolve the field observation profile better, thus providing model output at a position in space closer to where

these field measurements have been taken. It may also be interesting to compare output from coarse and fine models of the same area.

5/ An area of further work which would require considerable attention is to attempt to find a more realistic manner of expressing the effect of frictional drag on the water column, and for the new knowledge to be integrated into numerical models. This suggests that it will be necessary for field workers to work more closely with numerical modellers, in order to combine their experience and understanding.

6/ There has been some light shed in this thesis on the relationship between frictional and gravitational accelerations in very shallow water, *i.e.* that they balance each other. This has interesting connotations, as the resulting hydrodynamic equations become, in this case, ordinary differential equations which can be solved through an iterative process, with no need for time-stepping in the solution technique. This suggests that, potentially, hydrodynamic approximations for cases tens of years into the future could be found very quickly. This would naturally be tempered though, perhaps when applied to a practical situation such as the need for long-term morphodynamic modelling, in which the speed of computation would be dependant upon the time-step required to maintain stability of the morphodynamic scheme. Nonetheless, it could be a valuable area for future research.

REFERENCES

- Backhaus J.O. (1983) A semi-implicit scheme for the shallow water equations for the application of shelf sea modelling. *Continental Shelf Research*, 2, 243-245.
- Casulli V. (1990) Semi-implicit finite difference methods for the two-dimensional shallow water equations, *Journal of Computational Physics*, 86, pp56-74.
- Cheng R.T. and Casulli V. (1992) 'Tidal residual, intertidal mudflat (TRIM) model using a semi-implicit Eulerian-Lagrangian method', *U.S. Geol. Surv. Open File Rep.*, 96-62
- Davies A.M. (1986) Numerical modelling of marine systems. *Numerical Modelling Application to Marine Systems*, ed. J. Noye, Published by North Holland.
- Davies A.M. (1991) Modelling currents in highly sheared surface and bed boundary layers. *Continental Shelf Research*, December.
- Dronkers J.J. (1964) *Tidal Computations in Rivers and Coastal Waters*. Published by North Holland, Amsterdam.
- Evans E.M. (1987) 'Tidal stream energy', Unpublished Ph.D. thesis, Plymouth Polytechnic.
- Evans J.J. & Pugh D.T. (1982) Analysing clipped sea-level records for harmonic tidal constituents. *International Hydrographic Review*, Monaco, LIX (2), July.
- Evans G. and Collins M.B. (1975) 'The transportation and deposition of suspended sediment over the intertidal flats of the Wash', in: 'Hails J. and Carr A. (1975) *Nearshore Sediment Dynamics and Sedimentation*, John Wiley & Sons, pp. 273-306, Ch. 11.
- Falconer R.A. (1980) Numerical modeling of tidal circulation in harbors. *J. of the Waterway, Port, Coastal & Ocean Division, Proc. of the Am. Soc. of Civ. Engrs.*, Vol. 106, No. WW1

Feb..

Falconer R.A. (1984a) A mathematical model study of the flushing characteristics of a shallow tidal bay. *Proc. Instn. Civ. Engrs.*, Part 2, 77, Sept. pp 311-332.

Falconer R.A. (1984b) Temperature Distributions in Tidal Flow Field. *J. of Environmental Engineering*, Vol.110, No. 6, Dec..

Falconer R.A. (1985) Residual Currents in Port Talbot Harbour: a mathematical model study. *Proc. Instn. Civ. Engrs.*, Part 2, 79, Mar., 33-55.

Falconer R.A. (1986) Water quality simulation study of a natural harbor. *Port, Coastal, and Ocean Engineering Div. Am. Soc. Civ. Engrs.*, Vol 112, Jan. No.1, 15-34.

Falconer R.A. & Owens P.H. (1987) Numerical simulation of flooding and drying in a depth-averaged tidal flow model. *Proc. Instn. Civ. Engrs.*, Part 2, 83, Mar., 161-180.

Flather R.A. & Heaps N.S. (1975) Tidal Computations for Morecambe Bay. *Geophys. J. R. Astr. Soc.* 42, 489-517.

Flather R.A. & Hubbert K.P. (1989) Tide and Surge Models for Shallow Water - Morecambe Bay Revisited. *Modeling Marine Systems*, CRC Publications, ed. A. M. Davies (1991).

George K.J. (1993) 'Hydrographic data bases for tidal numerical models', *International Hydrographic Review*, LXX(2), September 1993.

George K.J. (1994) *Tides for Marine Studies*. Institute of Marine Studies, University of Plymouth

George (1995) 'A split-mesh harmonic tidal numerical model using finite differences', submitted to *Journal of Marine Systems*

10

11

George K.J. & Evans E.M. (1991) Using tidal stream data to fine-tune a 2-D tidal numerical model. *Tidal Hydrodynamics*, Chapter 12. Ed. B.B. Parker, J. Wiley & Sons Inc..

George K.J. and Stripling S. (1995) 'Improving the simulation of drying and wetting in a two-dimensional tidal numerical model', *Applied Mathematical Modelling*, Vol 19 pp. 2-6.

Gill A.E. (1982) *Atmosphere-Ocean Dynamics*, Academic Press.

Gunn D.J. and Yenigün O. (1985) 'Modelling of tidal motion in shoaling waters: The estuary of Milford Haven', *Estuarine, Coastal and Shelf Science*. 21, pp. 337-356

Heaps N.S. (1969) 'A two-dimensional numerical sea model', *Phil. Trans. R. Soc. Lond.* A265, 93-137.

Hervouet J.-M. (1991) 'TELEMAC, a fully vectorized finite element software for shallow water equations', *EDF-LNH*, Report No. E4303R.

Howarth M.J. (1990) 'Atlas of tidal elevations and currents around the British Isles' H.M.S.O., London.

HR Wallingford (1993) TELEMAC-2D - Background Information. October.

HR Wallingford (1993) 'PISCES A morphodynamic Coastal Area Model, First Annual Report'. Report No. SR 337.

Jeffery A. (1976) *Research Notes in Mathematics*, 5: *Quasilinear hyperbolic systems and waves*. Publ. Pitman Ltd.

Leendertse J.J. (1970) A water quality simulation model for well-mixed estuaries and coastal seas, The Rand Corporation, Santa Monica.

Leendertse J.J. & Gritton E.C. (1971) A water quality simulation model for well-mixed estuaries and coastal seas, VOL 2, Computation Procedures, The New York City Rand Institute.

Lynch D.R. and Gray W.G. (1980) 'Finite element simulation of flow in deforming regions', *Journal of Computational Physics*, 36, pp. 135-153.

McDowell D.M. & O'Connor B.A. (1977) *Hydraulic Behaviour of Estuaries*. Macmillan, London

Owens P.H. (1984) Numerical modelling of two-dimensional flows in coastal waters. *MSc thesis*, Univ. of Birmingham. Unpublished.

Proudman J. (1953) *Dynamical Oceanography*. London.

Reid R.O. & Bodine B.R. (1968) Numerical model for storm surges in Galveston Bay. *Proc. of the Am. Soc. of Civ. Engrs. J. of the Waterways and Harbours Div.* February.

Sielecki A. & Wurtele M.G. (1970) The numerical integration of the non-linear shallow water equations with sloping boundaries. *Journal of Computational Physics*, 6, 219-236.

Smith G.D. (1978) 'Numerical Solution of Partial Differential Equations: Finite Difference Methods', Oxford University Press, 2nd Edition.

Stelling G.S., Wiersma A.K. & Willemse J.B.T.M. (1986) Practical aspects of accurate tidal computations. *J. of Hydraulic Engineering*, Vol. 112, No. 9, September.

Stripling S., Dyer K.R. & Huntley D.A. (1994) A review of Transport models in the Marine Environment. For Westlakes Research Institute, Cumbria. Confidential

Svendsen I.A., & Jonsson I.G. (1980) Hydrodynamics of coastal regions. Published by Den Private Ingeniørfond Technical University of Denmark.

Wallace H.M. (1994) 'COSMOS-2D (Ver. 2.3): Nearshore sediment transport Model, Description of Model Structure and Input' HR Wallingford Report No. IT388 (issue B).

Xanthopoulos Th. and Koutitas Ch. (1976) 'Numerical simulation of a two-dimensional flood wave propagation due to dam failure', *J. Hydraulic Research*, 14(4), pp. 321-331.

Yeh G.-T. and Chou F.-K. (1979) 'Moving boundary numerical surge model', *J. of the Waterway, Port, Coastal and Ocean Division, Proc. A.S.C.E.*, Vol. 105, No. WW3, pp. 247-263.

APPENDIX 1

LIST OF TERMS USED IN MODK.FTN77

(upper case \equiv lower case for all terms)

- A - Amplitude of tide, m
- CD - Stability constraint on the water depth value
- CDRAG - Coefficient of drag
- CORX - Zonal Coriolis component, ms^{-2}
- CORY - Meridional Coriolis component, ms^{-2}
- CV - Stability constraint on the velocity magnitude
- DA - Change in amplitude
- DDX - Slope of water over distance ∂x
- DDY - Slope of water over distance ∂y
- DE - Depth of water at U-point east of test-cell
- DEDT - Change of tidal elevation with time, $\partial \zeta / \partial t$
- DEPTHX - Water depth at U-point
- DEPTY - Water depth at V-point
- DN - Total water depth at V-point north of test cell
- DP - Change in tidal phase
- DS - Total water depth at V-point south of test cell
- DT - Time step, ∂t
- DTC - Total water depth in test cell
- DUDT - Temporal acceleration (zonal component), $\partial U / \partial t$
- DVDT - Temporal acceleration (meridional component), $\partial V / \partial t$
- DW - Total depth of water at U-point west of test cell
- DX - Zonal finite difference grid size
- DY - Meridional finite difference grid size
- D1 - Total water depth at I or J on a ∂ -point
- D2 - Total water depth at I+1 or J+1 on a ∂ -point
- E - Tidal elevation
- EN - New value of E
- EDDYX - Zonal component of eddy viscosity
- EDDYY - Meridional component of eddy viscosity
- ELEVE - Average depth along the eastern edge of cell
- ELEVN - Average depth along the northern edge of cell
- ELEVS - Average depth along the southern edge of cell
- ELEVW - Average depth along the western edge of cell
- EMEAN - Mean value of elevations surrounding cell
- E1 - Tidal elevation at I or J
- E2 - Tidal elevation at I+1 or J+1
- F - Coriolis parameter
- FDL - Counter for output routines
- FP6 - Counter for every 6th value of ψ
- FP10 - Counter for every 10th value of ψ
- FRICX - Zonal frictional component
- FRICY - Meridional frictional component
- GDEDX - Slope term in the east-west direction
- GDEDY - Slope term in the north-south direction
- H - Depth of sea bed at h-point
- HE - Depth of sea bed at ζ -point

HEAST - Depth of sea bed at U-point east of cell
 HED - Horizontal eddy diffusion
 HEDD - Horizontal eddy diffusion as a function of depth
 HN - Depth of sea bed at V-point north of cell
 HS - Depth of sea bed at V-point south of cell
 HW - Depth of sea bed at U-point west of cell
 H1 - Depth of sea bed at I or J on a ∂ -point
 H2 - Depth of sea bed at I+1 or J+1 on a ∂ -point
 I - North to south coordinate
 I - Counter in DO loops
 IPSI - Integer value of ψ
 IP6 - Every 6th value of ψ
 IP10 - Every 10th value of ψ
 ITC - Number of tidal cycle
 ITCA - Number of tidal cycle for beginning of analysis
 ITCR - Tidal cycle in which shoal is raised
 ITS - Number of time step
 J - East to west coordinate
 KEY - Switch to indicate instability
 KHE - Counter to specify depths or to read from file
 KIE - Counter for specifying elevations or to read from file
 KIS - Counter for 'cold' or 'hot' start
 KN - Switch to indicate dry cell
 KOP - Switch for output to file
 KWET - Switch to indicate wetted cell
 K4 - Switch to locate a maximum of four surrounding wet cells
 NDAL - Counter for choice of drying algorithm
 NOC - Output channel to mainframe file space
 NRUN - Run number
 OPSI - Counter for screen dump every 36th value of ψ
 P - Tidal phase
 PSI - Tidal time angle, ψ°
 PSIN - New value of ψ
 PSIR - Tidal time angle in radians
 PSI8 - Double precision value of PSI
 PSI36 - Every 36 $^\circ$ of ψ
 RATEX - Stream rate at U-point
 RATEY - Stream rate at V-point
 RR - Key for flat or Gaussian bathymetry
 R2 - Value of I (coordinate) used to create shoal
 U - Zonal depth averaged velocity
 UATVP - Zonal velocity component at V-point
 UDUDX - Advective term
 UDVDX - Advective term
 UN - New value of U
 UV - U or V value
 V - Meridional depth averaged velocity
 VATUP - Meridional velocity at U-point
 VDUDY - Advective term

VDVDY - Advective term

VN - New value of V

WIND - Value for 'winding up'

10

```

C-----
C-----
C-----
C----- *****
C----- * 2-D MODEL USING HYDRODYNAMIC EQUATIONS *
C----- *
C----- * UTILIZING 4 DIFFERENT 'DRYING' METHODS *
C----- *****
C-----
C-----
C----- BY
C-----
C----- MR. S STRIPLING
C-----
C----- UNIVERSITY OF PLYMOUTH
C-----
C-----
C-----
C-----

```

program model

```

parameter (mpti=40,mptj=40)
dimension u(mpti,mptj),v(mpti,mptj),un(mpti,mptj),vn(mpti,mptj)
&,kwet(mpti,mptj),e(mpti,mptj),en(mpti,mptj),he(mpti,mptj)
&,deepp(mpti,mptj),h(mpti,mptj),kn(mpti,mptj)
dimension dudt(mpti,mptj),corx(mpti,mptj),gdedx(mpti,mptj)
&,fricx(mpti,mptj),dvdt(mpti,mptj),cory(mpti,mptj)
&,gdedy(mpti,mptj),fricy(mpti,mptj)
dimension a(mpti,mptj),p(mpti,mptj),dec(mpti,mptj)
&,hs(mpti,mptj),em(mpti,mptj),um(mpti,mptj),vm(mpti,mptj)
common /lim/ ny,nx
common /coord/ if,jf,dx,dy
common /time/ itc,psi,its,dt,hour,psin
common /grid/ ngs,nsbc,ndal
common /numb/ pi,rad
common /stab/ cd,cv,key
common /cons/ fdl,hed,cdrag,f
common /start/ kie,kis,nrun,rr

```

```

integer hour
character wash*1
real etime, dtime, tim(2)

```

```

psi8 = 0.d0

```

```

c---- To force the grid-size

```

```

ngs = 3

```

```

c---- To set switch for output

```

```

kop = 1

```

```

c---- To specify the number of the run

```

```

write(*,*) '
write(*,*) '
write(*,*) ' Input the run-number'
write(*,*) '
write(*,*) '
read(*,1)nrun
1 format(i5)

```

```

c nrun = 115

```

c----- To specify counter for 'full' boundary levels at the start

kic = 0

c----- To gather information on the run

```
write(*,*) '
write(*,*) 'Do you wish to run the Wash model ? (y/n)'
write(*,*) '
read(*, '(a1)')wash
write(*,*) '
write(*,*) 'Is this to be (1) a hot run, or (2) a cold run ?'
write(*,*) '
read(*,*)kis
```

c----- To determine the dimensions of the grid

ny = 40
nx = 40

if(wash.eq.'y')then

ny = 60
nx = 65

endif

c----- To set stability limits

cv = 9.9
cd = 6.0

rr = -1.0

c----- To specify constants

rad = 0.0174532925
pi = 3.141592654
f = 2.0*7.29e-05*sin(50.*rad)
hed = 10.0
cdrag = 0.0025
fdl = 0.1
hour = 0
if = 18
jf = 21

if(wash.eq.'y')then

dy = 741.3
dx = 741.3
dt = 62.1

else

```
write(*,*) 'This model may be run with a grid size of:'
write(*,*) '
write(*,*) '(1) 5000m or (2) 1000m'
write(*,*) '
write(*,*) 'Which would you prefer, (1) or (2) ? '
write(*,*) '
read(*,*)ngs
```

if(ngs.eq.1)then

dy = 5000.
dx = 5000.

```
dt      = . 124.2
```

```
else
```

```
dy      = 1000.
```

```
dx      = 1000.
```

```
dt      = 62.1
```

```
endif
```

```
endif
```

```
c-----
```

```
Opening files
```

```
open(25,file='knout')
```

```
open(54,file='fintop')
```

```
open(56,file='newstore')
```

```
open(22,file='ddl')
```

```
open(23,file='ddf')
```

```
open(24,file='ddo')
```

```
open(99,file='bathys')
```

```
open(13,file='slp-depths')
```

```
open(50,file='hhestore')
```

```
open(11,file='wasdep')
```

```
open(43,file='washhe')
```

```
open(63,file='dds')
```

```
open(64,file='ddse')
```

```
open(30,file='magn00')
```

```
open(70,file='dir00')
```

```
open(31,file='magn01')
```

```
open(71,file='dir01')
```

```
open(32,file='magn02')
```

```
open(72,file='dir02')
```

```
open(33,file='magn03')
```

```
open(73,file='dir03')
```

```
open(34,file='magn04')
```

```
open(74,file='dir04')
```

```
open(35,file='magn05')
```

```
open(75,file='dir05')
```

```
open(36,file='magn06')
```

```
open(76,file='dir06')
```

```
open(37,file='magn07')
```

```
open(77,file='dir07')
```

```
open(38,file='magn08')
```

```
open(78,file='dir08')
```

```
open(39,file='magn09')
```

```
open(79,file='dir09')
```

```
open(40,file='magn10')
```

```
open(80,file='dir10')
```

```
open(41,file='magn11')
```

```
open(81,file='dir11')
```

```
c-----
```

```
Specifying bathymetry
```

```
if(wash.eq.'y')then
```

```
nsbc    = 3
```

```
if(kis.eq.2)call batwas(i,j,h,he)
```

```
if(kis.eq.1)call washhe(h,he)
```

```
else
```

```
write(*,*) 'You may choose a sea-bed configuration of:'
```

```
write(*,*) ' '
```

```
write(*,*) ' '
```

```
write(*,*) ' (1) A basin with a sloping beach'
```



```

write(*,*) ' '
write(*,*) ' or'
write(*,*) ' '
write(*,*) '(2) A basin with a Gaussian Island.'
write(*,*) ' '
read(*,*)nsbc

```

```

if(kis.eq.1)call sethhe(he,h)

```

```

if(kis.eq.2)then

```

```

    if(nsbc.eq.1)call bathys(he,h)
    if(nsbc.eq.2)call depths(h,he,kwet)

```

```

endif

```

```

endif

```

```

c-----      Setting initial conditions

```

```

if(wash.eq.'y')then

```

```

    call wasic(un,vn,en,e,u,v,a,p)

```

```

else

```

```

    call setic(un,vn,en,e,u,v,h,he)

```

```

endif

```

```

if(kis.eq.1)then

```

```

    itc      =  5

```

```

else

```

```

    itc      =  0

```

```

endif

```

```

its      =  0

```

```

if(ngs.eq.3)then

```

```

    itca     =  4

```

```

else

```

```

    itca     =  5

```

```

endif

```

```

c-----      To select a drying algorithm

```

```

write(*,*) 'Would you like to run the model using:'

```

```

write(*,*) ' '

```

```

write(*,*) '1: Flather & Heaps (1975). drying algorithm'

```

```

write(*,*) ' or'

```

```

write(*,*) '2: Leendertses (1970) drying algorithm'

```

```

write(*,*) ' or'

```

```

write(*,*) '3: Owens (1984) drying algorithm'

```

```

write(*,*) ' or'

```

```

write(*,*) '4: George & Stripling (1994) drying system ?'

```

```

write(*,*) ' '

```

```

read(*,*)ndal

```

```

print *, 'elapsed:', etime, ' user:', tim(1), ', sys:', tim(2)

if(ndal.eq.1) call setwet(kn)

c-----
c-----      Solution of the hydrodynamic equations:
c-----

100 continue

  if(ndal.eq.4) then

    call dpoint(h, deepp, he)
    call calcus(dudt, corx, gdedx, fricx, un, he, e, h, v,
&              u, dudt1, corx1, gdedx1, fricx1)
    call calcvs(dvdt, cory, gdedy, fricy, vn, he, e, h, u,
&              v, dvdt1, cory1, gdedy1, fricy1)

  else

    call calcu(dudt, corx, gdedx, fricx, kwet, e, he, un, v,
&             u, dudt1, corx1, gdedx1, fricx1, h, kn)
    call calcv(vn, dvdt, cory, gdedy, fricy, kwet, e, he, u,
&             v, dvdt1, cory1, gdedy1, fricy1, h, kn)

  endif

  call expluv(un, vn)
  call smooth(un, vn)

  if(ngs.eq.1) psin = real(psi8) + 1.
  if(ngs.eq.2) psin = real(psi8) + 0.25
  if(ngs.eq.3) psin = real(psi8) + 0.5

  ip10 = int(psin/10.)
  fp10 = (psin/10.) - ip10

  if(ngs.eq.3) then

    call wasen(e, a, p)

  else

    call seten(en)

  endif

  if(ndal.eq.4) then

    call calces(he, un, vn, en, e, deepp, h,
&              u, v, dudt, corx, gdedx, fricx, dvdt, cory,
&              gdedy, fricy, dec)

  else

    call calce(en, e, he, h, kn, un, vn, dudt, corx,
&             gdedx, fricx, dvdt, cory, gdedy, fricy, u, v,
&             kwet)

  endif

c-----      To check for stability

c      call chstab(en, un, vn)
c      if(key.eq.1) go to 90

```

```

c-----
c-----      Output Options
c-----
c-----      To call subroutine quiver for output

      psi      =  real(psi8)

      if(itc.eq.6)then

          p10    =  psi - 10.
          p30    =  int((psi - 10.)/30.)

          if(p30.ge.0)then

              op    =  ((psi - 10.)/30.) - p30
              ip    =  int(psi)

              if(abs(op).lt.1.0e-06)then

                  call quiver(u,un,v,vn,e,he)
                  hour  =  hour + 1

              endif

          endif

      endif

c-----      To output information into fintops

      ip6    =  int(psi/6.)
      fp6    =  (psi/6.) - ip6
      if(abs(fp6).lt.1.0e-06)call intop(e,u,un,v,vn,
&                                     em,um,vm)

c-----      To store e,u,v,h,he at a set time

      if((itc.eq.4).and.(psi.ge.359.9))then

          call store(he,e,u,v,hs)
          call stohhe(he,h)

      endif

c      if(itc.eq.itcr)call raise(h,he,deepp)
      if(itc.eq.itca+2)go to 90

c-----      Up-dating

      if(ngs.eq.1)psi8    =  psi8 + 1.0d0
      if(ngs.eq.2)psi8    =  psi8 + 0.25d0
      if(ngs.eq.3)psi8    =  psi8 + 0.5d0

      if(psi8.gt.360.d0)then

          itc    =  itc + 1
          psi8    =  psi8 - 360.d0

      endif

      its    =  its + 1

      do 300 i = 1,ny

```



```

do 300 j = 1,nx
    u(i,j) = un(i,j)
    v(i,j) = vn(i,j)
300 e(i,j) = en(i,j)

go to 100

90 call intop(e,u,un,v,vn,em,um,vm)

etime = dtime(tim)
print *, 'elapsed:', etime, ' user:', tim(1), ' sys:', tim(2)

stop
end

```

```

subroutine areaf(ec, hc, hne, hnw, hse, hsw, af)
c-----
c-----      To establish the wetness of a cell by areal factors
c-----

```

```

dimension hk(4)

hk(1) = hne
hk(2) = hnw
hk(3) = hse
hk(4) = hsw
z4 = -99.

do 2 k = 1,4
    if(hk(k).gt.z4)then

        z4 = hk(k)
        k4 = k

    endif

2 continue

z1 = 99.

do 3 k = 1,4
    if(hk(k).lt.z1)then

        z1 = hk(k)
        k1 = k

    endif

3 continue

if(ec.ge.hne.and.ec.ge.hnw.and.ec.ge.hse.and.ec.ge.hsw)then
    af = 1.
    return
elseif(ec.le.hne.and.ec.le.hnw.and.ec.le.hse.and.ec.le.hsw)then
    af = 0.
    return
endif

```



```

do 4 k = 1,4
    if(k.eq.k1.or.k.eq.k4)then
        go to 4
    else
        k2 = k
        go to 5
    endif
4 continue
5 do 6 k = 1,4
    if(k.eq.k1.or.k.eq.k2.or.k.eq.k4)then
        go to 6
    else
        k3 = k
        go to 7
    endif
6 continue
7 if(hk(k3).le.hk(k2))then
    kt = k2
    k2 = k3
    k3 = kt
else
    continue
endif

c----- to evaluate areal factor for case (i)
if(ec.lt.hk(k2))then
    af = 0.5*(ec - hk(k1))*2/((hk(k2) - hk(k1))*(hk(k3)
&      - hk(k1)))
    return
endif

c----- to evaluate areal factor for case (ii)
if(ec.lt.hk(k3))then
    y2 = (hk(k3) - ec)/(hk(k3) - hk(k1))
    x3 = (hk(k3) - ec)/(hk(k3) - hk(k2))
    y3 = x3
    call heron(0.,0.,0.,y2,x3,y3,at1)

    y2 = (ec - hk(k2))/(hk(k4) - hk(k2))
    x3 = (ec - hk(k2))/(hk(k3) - hk(k2))
    y3 = x3
    call heron(0.,0.,0.,y2,x3,y3,at2)

```

```

af = 0.5 - at1 + at2
return

```

```

else

```

```

c----- to evaluate areal factor for case (iii)

```

```

    afl = 0.5*(hk(k4) - ec)**2/((hk(k4) - hk(k2))*(hk(k4)
&      - hk(k3)))
    af = 1.0 - afl
    return

```

```

endif

```

```

end

```

```

subroutine bathys(he,h)

```

```

c-----
c----- To input a sloping bathymetry
c-----

```

```

dimension he(ny,nx),h(ny,nx)
common /lim/ ny,nx

```

```

do 200 i = 1,ny
do 200 j = 1,nx

```

```

    he(i,j) = 5.0
    he(i,j) = he(i,j) - (i-1) + (drand() - 0.5)

```

```

    if(i.gt.25)then

```

```

        he(i,j) = -50. + (drand() - 0.5)

```

```

    elseif(j.lt.11.or.j.gt.29)then

```

```

        he(i,j) = 5.0

```

```

    endif

```

```

200 continue

```

```

do 400 i = 1,ny-1
do 400 j = 1,nx-1

```

```

    h(i,j) = 5.0
    h(i,j) = h(i,j) - (i-0.5) + (drand() - 0.5)

```

```

    if(i.ge.25)then

```

```

        h(i,j) = -50. + (drand() - 0.5)

```

```

    elseif(j.lt.10.or.j.gt.29)then

```

```

        h(i,j) = 5.0

```

```

    endif

```

```

400 continue

```

```

do 600 i = 1,ny

```

```

    write(99,5) (he(i,j),j = 1,nx)

```

```

600    write(99,5) (h(i,j),j = 1,nx)

```



```

5      format(10f8.2)

      return
      end

      subroutine batwas(i,j,h,he)
c-----
c-----      To read bathymetry for the Wash from wasdep
c-----      and to evaluate he(i,j).
c-----

      dimension h(ny,nx), he(ny,nx)
      common /lim/ ny,nx

      do 200 i = 1,ny
          read(11,75) (h(i,j),j = 1,nx)

          do 300 j = 1,nx
              h(i,j) = h(i,j)*0.1 - 3.4

300      continue

200 continue

      do 1 j = 1,nx
          he(1,j) = h(1,j)
          he(ny,j) = 200.

1      continue

      do 2 i = 1,ny
          he(i,1) = h(i,1)
          he(i,nx) = h(i,nx)

2      continue

      do 3 i = 2,ny
          do 4 j = 2,nx
              he(i,j) = 0.25*(h(i,j) + h(i-1,j) + h(i-1,j-1)
&                  + h(i,j-1))

4      continue
3      continue

      open(43,file='washhe')

      do 5 i = 1,ny
          write(43,100) (h(i,j),j = 1,nx)

5      continue

      do 6 i = 1,ny
          write(43,100) (he(i,j),j = 1,nx)

6      continue

75 format(65f5.0)
100 format(65f5.1)

```

```
return  
end
```

```
subroutine calce(en,e,he,h,kn,un,vn,dudt,corx,  
& gdedx,fricx,dvdt,cory,gdedy,fricy,u,v,  
& kwet)
```

```
c-----  
c-----      To calculate the elevation at a grid-point using  
c-----      the conservation of mass equation.  
c-----
```

```
dimension u(ny,nx), v(ny,nx), un(ny,nx), vn(ny,nx)  
dimension e(ny,nx), en(ny,nx), he(ny,nx), h(ny,nx)  
dimension dudt(ny,nx), corx(ny,nx), gdedx(ny,nx),  
& fricx(ny,nx), dvdt(ny,nx), cory(ny,nx),  
& gdedy(ny,nx), fricy(ny,nx), kwet(ny,nx), kn(ny,nx)  
common /lim/ ny,nx  
common /time/ itc,psi,its,dt,hour,psin  
common /coord/ if,jf,dx,dy  
common /grid/ ngs,nsbc,ndal  
common /start/ kie,kis,nrun,rr
```

```
do 20 i = 2,ny-1  
do 20 j = 2,nx-1
```

```
    en(i,j) = 0.
```

```
c-----      Depths at e-points for plotting purposes:
```

```
    dtc    = e(i,j) - he(i,j)  
    dee    = e(i,j+1) - he(i,j+1)  
    dew    = e(i,j-1) - he(i,j-1)  
    den    = e(i-1,j) - he(i-1,j)  
    des    = e(i+1,j) - he(i+1,j)
```

```
c-----      Depths at gates for calculation purposes:
```

```
    de     = 0.5*(e(i,j) + e(i,j+1) - h(i-1,j) - h(i,j))  
    dw     = 0.5*(e(i,j) + e(i,j-1) - h(i,j-1) - h(i-1,j-1))  
    dn     = 0.5*(e(i,j) + e(i-1,j) - h(i-1,j-1) - h(i-1,j))  
    ds     = 0.5*(e(i,j) + e(i+1,j) - h(i,j-1) - h(i,j))
```

```
c-----      To calculate e using Flather & Heaps' method:
```

```
    if(ndal.eq.1)then  
        if(kn(i,j).eq.0.and.he(i,j).gt.-6.)then  
            en(i,j) = he(i,j)  
            go to 10  
        endif
```

```
c-----      To calculate e using Leendertse's method:
```

```
    elseif(ndal.eq.2)then  
        if(kwet(i,j).eq.0)then  
            call wetest(i,j,kwet,e,he,dn,ds,de,dw)  
            if(kwet(i,j).eq.0)then  
                en(i,j) = he(i,j)  
                go to 10
```

```

endif

elseif(de.le.0..or.dw.le.0..or.dn.le.0..or.ds.le.0.)
&      then

      kwet(i,j) = 0
      en(i,j)   = he(i,j)
      go to 10

endif

c----- To calculate e using Owen's method:
elseif(ndal.eq.3)then

      hmax = h(i,j)
      if(h(i,j-1).lt.hmax)hmax = h(i,j-1)
      if(h(i-1,j-1).lt.hmax)hmax = h(i-1,j-1)
      if(h(i-1,j).lt.hmax)hmax = h(i-1,j)
      dc = e(i,j) - hmax

c----- N.B. The value dc may seem a bit odd, but it is
c----- merely a representation of the volume of a cell,
c----- not it's depth.

      if(kwet(i,j).eq.0)then

          call wetowe(i,j,kwet,e,he,dn,ds,de,dw)
          if(kwet(i,j).eq.0)then

              en(i,j) = he(i,j)
              go to 10

          endif

      elseif(dc.le.0.)then

          kwet(i,j) = 0
          en(i,j)   = he(i,j)
          go to 10

      endif

endif

ddx = (de*un(i,j) - dw*un(i,j-1))/dx
ddy = (dn*vn(i-1,j) - ds*vn(i,j))/dy
dedt = -ddx-ddy
en(i,j) = dedt*dt + e(i,j)

if(en(i,j).le.he(i,j))then

    if(ndal.eq.1)then

        en(i,j) = he(i,j)

    elseif(ndal.eq.2.or.ndal.eq.3)then

        kwet(i,j) = 0
        en(i,j)   = he(i,j)

    endif

elseif(ndal.eq.2)then

    call leen3(i,j,kwet,h,en,he)

```

```

elseif (ndal.eq.3) then

    call owen3(i,j,h,en,he,kwet)

endif

10  if(i.eq.if.and.j.eq.jf) then

    if(ndal.eq.1) then

        call focus(23,dee,dew,den,des,dtc,e(i,j+1),e(i,j-1),
&                e(i-1,j),e(i+1,j),e(i,j),un(i,j),dudt(i,j),
&                corx(i,j),gdedx(i,j),fricx(i,j),vn(i,j),
&                dvdt(i,j),cory(i,j),gdedy(i,j),fricy(i,j),
&                he(if,jf),he(if,jf+1),he(if,jf-1),
&                he(if-1,jf),he(if+1,jf))

        elseif(ndal.eq.2) then

            call focus(22,dee,dew,den,des,dtc,e(i,j+1),e(i,j-1),
&                e(i-1,j),e(i+1,j),e(i,j),un(i,j),dudt(i,j),
&                corx(i,j),gdedx(i,j),fricx(i,j),vn(i,j),
&                dvdt(i,j),cory(i,j),gdedy(i,j),fricy(i,j),
&                he(if,jf),he(if,jf+1),he(if,jf-1),
&                he(if-1,jf),he(if+1,jf))

            elseif(ndal.eq.3) then

                call focus(24,dee,dew,den,des,dtc,e(i,j+1),e(i,j-1),
&                e(i-1,j),e(i+1,j),e(i,j),un(i,j),dudt(i,j),
&                corx(i,j),gdedx(i,j),fricx(i,j),vn(i,j),
&                dvdt(i,j),cory(i,j),gdedy(i,j),fricy(i,j),
&                he(if,jf),he(if,jf+1),he(if,jf-1),
&                he(if-1,jf),he(if+1,jf))

            endif

        endif

20  continue
200 format(f6.2)
    return
end

```

```

subroutine calces(he,un,vn,en,e,deepp,h,
&                u,v,dudt,corx,gdedx,fricx,dvdt,cory,
&                gdedy,fricy,dec)

```

```

c-----
c-----    To calculate the elevation of a grid-point using the
c-----    momentum equation, and Stripling & George's drying
c-----    algorithm
c-----

```

```

dimension u(ny,nx), v(ny,nx), un(ny,nx),vn(ny,nx), dec(ny,nx),
&          en(ny,nx), he(ny,nx), deepp(ny,nx), e(ny,nx),
&          h(ny,nx), dudt(ny,nx), corx(ny,nx),
&          gdedx(ny,nx), fricx(ny,nx), dvdt(ny,nx),
&          cory(ny,nx), gdedy(ny,nx), fricy(ny,nx)
common /lim/ ny,nx
common /time/ itc,psi,its,dt,hour,psin
common /coord/ if,jf,dx,dy
common /grid/ ngs,nsbc,ndal
common /start/ kie,kis,nrun,rr

```

```

do 20 i = 2,ny-1
do 20 j = 2,nx-1

kslp = 1
if(he(i,j).lt.-6.)kslp = 0
if((he(i,j).gt.5..and.ngs.lt.3).or.(he(i,j).ge.20..and.
&   ngs.eq.3))then

    un(i,j) = 0.
    vn(i,j) = 0.
    en(i,j) = 0.
    go to 20

endif

c-----      To calculate surrounding elevations for plotting purposes

dtc          = e(i,j) - deepp(i,j)
dec(i,j)     = e(i,j) - he(i,j)
if(dec(i,j).le.0.)dec(i,j) = 0.
dee          = e(i,j+1) - he(i,j+1)
if(dee.le.0.)dee = 0.
dew          = e(i,j-1) - he(i,j-1)
if(dew.le.0.)dew = 0.
den          = e(i-1,j) - he(i-1,j)
if(den.le.0.)den = 0.
des          = e(i+1,j) - he(i+1,j)
if(des.le.0.)des = 0.

c-----      To evaluate water depths at the edges of the cell:

if(kslp.eq.0)then

c-----      without sloping facets;

    de = 0.5*(e(i,j) + e(i,j+1) - h(i-1,j) - h(i,j))
    dw = 0.5*(e(i,j) + e(i,j-1) - h(i,j-1) - h(i-1,j-1))
    dn = 0.5*(e(i,j) + e(i-1,j) - h(i-1,j-1) - h(i-1,j))
    ds = 0.5*(e(i,j) + e(i+1,j) - h(i,j-1) - h(i,j))

else

c-----      with sloping facets;

    eeg = 0.5*(e(i,j) + e(i,j+1))
    ewg = 0.5*(e(i,j) + e(i,j-1))
    eng = 0.5*(e(i,j) + e(i-1,j))
    esg = 0.5*(e(i,j) + e(i+1,j))

    call dedgec(eeg,h(i-1,j),h(i,j),de)
    call dedgec(ewg,h(i,j-1),h(i-1,j-1),dw)
    call dedgec(eng,h(i-1,j-1),h(i-1,j),dn)
    call dedgec(esg,h(i,j-1),h(i,j),ds)

endif

ddx          = (de*un(i,j) - dw*un(i,j-1))/dx
ddy          = (dn*vn(i-1,j) - ds*vn(i,j))/dy
af           = 1.

if(kslp.eq.1)then

    call areaf(e(i,j),he(i,j),h(i-1,j),h(i-1,j-1),
&             h(i,j),h(i,j-1),af)

    if(af.lt.0.01)af = 0.01

```

endif

dedt = (-ddx-ddy)*af
en(i,j) = dedt*dt + e(i,j)

if(en(i,j).le.deepp(i,j).and.kslp.eq.1)en(i,j) = deepp(i,j)

if(i.eq.if.and.j.eq.jf)then

call focus(63,dee,dew,den,des,dec,e(i,j+1),e(i,j-1),
& e(i-1,j),e(i+1,j),e(i,j),un(i,j),dudt(i,j),
& corx(i,j),gdedx(i,j),fricx(i,j),vn(i,j),
& dvdt(i,j),cory(i,j),gdedy(i,j),fricy(i,j),
& he(if,jf),he(if,jf+1),he(if,jf-1),
& he(if-1,jf),he(if+1,jf))

endif

20 continue

return
end

subroutine calcu(dudt,corx,gdedx,fricx,kwet,e,he,un,v,
& u,dudt1,corx1,gdedx1,fricx1,h,kn)

c-----
c----- To calculate the u-component of the depth mean velocity
c----- using the easterly direction equation for the continuity
c----- of momentum.
c-----

dimension u(ny,nx), v(ny,nx), un(ny,nx),
& kwet(ny,nx), e(ny,nx), he(ny,nx),
& h(ny,nx), dudt(ny,nx), corx(ny,nx),
& gdedx(ny,nx), fricx(ny,nx), kn(ny,nx)

common /lim/ ny,nx
common /time/ itc,psi,its,dt,hour,psin
common /coord/ if,jf,dx,dy
common /grid/ ngs,nsbc,ndal
common /cons/ fdl,hed,cdrag,f

do 50 i = 1,ny-1
do 50 j = 1,nx-1

un(i,j) = 0.
eddyx = 0.
ududx = 0.
vdudy = 0.
dudt(i,j) = 0.
corx(i,j) = 0.
gdedx(i,j) = 0.
fricx(i,j) = 0.

if(kwet(i,j).eq.0.and.ndal.ne.1)go to 30
if(i.eq.1)go to 50

depthx = 0.5*(-h(i,j+1) - h(i,j) + e(i,j) + e(i,j+1))
if(depthx.le.0.)then

if(ndal.eq.1)kn(i,j) = 0
go to 30

endif

```

      if (ndal.eq.1) then
        call wdtest(i,j,e(i,j),he(i,j),e(i,j+1),he(i,j+1),kn(i,j)
&          ,un(i,j))
        if (kn(i,j).eq.0.and.he(i,j).gt.-6.) go to 30
      endif

c      if (e(i,j).le.he(i,j)) go to 30
      if (depthx.lt.fdl) depthx = fdl

c----- Coriolis

      vatup      = (v(i-1,j) + v(i-1,j+1) + v(i,j) + v(i,j+1))*0.25
      corx(i,j)  = f*vatup

c----- Pressure Gradient

      gdedx(i,j) = 9.81*(e(i,j+1) - e(i,j))/dx

c----- Eddy viscosity

      if (i.gt.(ny-1)) go to 10
      if (j.eq.1.or.j.gt.(nx-2)) go to 10

      hedd      = hed*depthx
      call ceddyx(i,j,u,hedd,eddyx)
      call cududx(i,j,u,ududx)
      call cvdudy(i,j,u,vdudy,vatup)

c----- Friction

      10      ratex      = sqrt(u(i,j)*u(i,j) + vatup*vatup)
      fricx(i,j) = cdrag*u(i,j)*ratex/depthx

c----- Temporal

      dudt(i,j) = - gdedx(i,j) - fricx(i,j) + eddyx - ududx - vdudy
&          + corx(i,j)

c----- New value of u

      un(i,j) = u(i,j) + dt*dudt(i,j)

      30      dudt1      = dudt(if,jf)
      corx1      = corx(if,jf)
      gdedx1     = gdedx(if,jf)
      fricx1     = fricx(if,jf)

      50 continue

      return
      end

      subroutine calcus(dudt,corx,gdedx,fricx,un,he,e,h,v,
&          u,dudt1,corx1,gdedx1,fricx1)

c-----
c----- As for subroutine calcu but in case of sloping facets.
c-----

      dimension u(ny,nx), v(ny,nx), un(ny,nx), e(ny,nx),
&          he(ny,nx), h(ny,nx), dudt(ny,nx),
&          corx(ny,nx), gdedx(ny,nx), fricx(ny,nx)
      common /lim/ ny,nx
      common /time/ itc,psi,its,dt,hour,psin

```

```

common /coord/ if,jf,dx,dy
common /grid/ ngs,nsbc,ndal
common /cons/ fdl,hed,cdrag,f

```

```

do 50 i = 1,ny-1
do 50 j = 1,nx-1

```

```

    eddyx      = 0.
    ududx      = 0.
    vdudy      = 0.
    dudt(i,j)  = 0.
    corx(i,j)  = 0.
    gdedx(i,j) = 0.
    fricx(i,j) = 0.
    un(i,j)    = 0.

```

```

    if (he(i,j).ge.5..or.he(i,j+1).ge.5..and.nsbc.ne.3)go to 50
    if (he(i,j).ge.20..or.he(i,j+1).ge.20.)go to 50
    if (i.eq.1)go to 50

```

```

    kslp      = 1
    if (he(i,j).lt.-6..and.he(i,j+1).lt.-6.)kslp = 0

```

```

    if (kslp.eq.0)then

```

```

        dg = 0.5*(e(i,j) + e(i,j+1) - h(i-1,j) - h(i,j))

```

```

    else

```

```

        eg = 0.5*(e(i,j) + e(i,j+1))
        call dedgec(eg,h(i-1,j),h(i,j),dg)
        if (dg.lt.fdl)dg = fdl

```

```

    endif

```

```

    if (dg.le.0.)go to 30

```

```

c----- Coriolis

```

```

    vatup      = (v(i-1,j) + v(i-1,j+1) + v(i,j) + v(i,j+1))*0.25
    corx(i,j)  = f*vatup

```

```

c----- Pressure Gradient

```

```

    gdedx(i,j) = 9.81*(e(i,j+1) - e(i,j))/dx

```

```

c----- Eddy viscosity

```

```

    if (i.gt.(ny-1))go to 10
    if (j.eq.1.or.j.gt.(nx-2))go to 10

```

```

    hedd      = hed*dg
    call ceddyx(i,j,u,hedd,eddyx)
    call cududx(i,j,u,ududx)
    call cvdudy(i,j,u,vdudy,vatup)

```

```

c----- Friction

```

```

10    ratex      = sqrt(u(i,j)*u(i,j) + vatup*vatup)
    fricx(i,j)  = cdrag*u(i,j)*ratex/dg

```

```

c----- Temporal

```

```

    dudt(i,j)  = - gdedx(i,j) - fricx(i,j) + eddyx - ududx - vdudy
&              + corx(i,j)

```



```

c-----      New value of u

      un(i,j)      =  u(i,j) + dt*dudt(i,j)

30      dudt1      =  dudt(if,jf)
      corx1       =  corx(if,jf)
      gdedx1      =  gdedx(i,j)
      fricx1      =  fricx(i,j)

50 continue

      return
      end

      subroutine calcv(vn,dvdt,cory,gdedy,fricy,kwet,e,he,u,
&      v,dvdt1,cory1,gdedy1,fricy1,h,kn)
c-----
c-----      To calculate the v-component of the depth mean velocity
c-----      using the continuity of momentum equation (depth averaged)
c-----      in the northerly direction.
c-----

      dimension u(ny,nx), v(ny,nx), vn(ny,nx),
&      kwet(ny,nx), e(ny,nx), he(ny,nx),
&      h(ny,nx), dvdt(ny,nx), cory(ny,nx),
&      gdedy(ny,nx), fricy(ny,nx), kn(ny,nx)
      common /lim/ ny,nx
      common /time/ itc,psi,its,dt,hour,psin
      common /coord/ if,jf,dx,dy
      common /grid/ ngs,nsbc,ndal
      common /cons/ fdl,hed,cdrag,f

      do 50 i = 1,ny-1
      do 50 j = 1,nx-1

          vn(i,j)      =  0.
          eddyy        =  0.
          vdvdy        =  0.
          udvdx        =  0.
          dvdt(i,j)    =  0.
          cory(i,j)    =  0.
          gdedy(i,j)   =  0.
          fricy(i,j)   =  0.

          if(kwet(i,j).eq.0.and.ndal.gt.1)go to 30
          if(j.eq.1)go to 50

c      kn(i,j)          =  0.

          depthy = 0.5*(e(i,j) + e(i+1,j) - h(i+1,j) - h(i,j))
          if(depthy.le.0.)then

              if(ndal.eq.1)kn(i,j) = 0.
              go to 30

          endif

          if(ndal.eq.1)then

              call wdtest(i,j,e(i,j),he(i,j),e(i+1,j),he(i+1,j),kn(i,j)
&              ,vn(i,j))
              if(kn(i,j).eq.0.and.he(i,j).gt.-6.)go to 30

          endif

```



```

c      if(e(i,j).le.he(i,j))go to 30
      if(depthy.lt.fdl)depthy = fdl

c-----      Coriolis

      uatvp      = (u(i,j-1) + u(i+1,j-1) + u(i+1,j) + u(i,j))*0.25
      cory(i,j)  = f*uatvp

c-----      Pressure Gradient

      gdedy(i,j) = 9.81*(e(i,j) - e(i+1,j))/dy

c-----      Eddy Viscosity

      if(i.lt.2.or.i.gt.(ny-2).or.j.gt.(nx-1))go to 10
      hedd      = hed*depthy
      call ceddy(i,j,v,hedd,eddy)
      call cvdvy(i,j,v,vdvy)
      call cudvx(i,j,v,udvx,uatvp)

c-----      Friction

10     ratey      = sqrt(uatvp*uatvp + v(i,j)*v(i,j))
      fricy(i,j)  = cdrag*v(i,j)*ratey/depthy

c-----      Temporal

      dvdt(i,j)  = - gdedy(i,j) - fricy(i,j) + eddy - udvx
&          - vdvy - cory(i,j)

c-----      New value of v

      vn(i,j)    = v(i,j) + dt*dvdt(i,j)

30     dvdt1     = dvdt(if,jf)
      cory1      = cory(if,jf)
      gdedy1     = gdedy(if,jf)
      fricy1     = fricy(if,jf)

50     continue

      return
      end

      subroutine calcvs(dvdt,cory,gdedy,fricy,vn,he,e,h,u,
&          v,dvdt1,cory1,gdedy1,fricy1)

c-----
c-----      As for calcv but in case of sloping facets
c-----

      dimension u(ny,nx), v(ny,nx), vn(ny,nx), e(ny,nx),
&          he(ny,nx), h(ny,nx), dvdt(ny,nx),
&          cory(ny,nx), gdedy(ny,nx), fricy(ny,nx)
      common /lim/ ny,nx
      common /time/ itc,psi,its,dt,hour,psin
      common /coord/ if,jf,dx,dy
      common /grid/ ngs,nsbc,ndal
      common /cons/ fdl,hed,cdrag,f

      do 50 i = 1,ny-1
      do 50 j = 1,nx-1

          eddyx      = 0.
          udvx       = 0.
          vdvy       = 0.

```



```

dvdt(i,j) = 0.
cory(i,j) = 0.
gdedy(i,j) = 0.
fricy(i,j) = 0.
vn(i,j) = 0.

if (he(i,j).ge.5..or.he(i+1,j).ge.5..and.nsbclt.3)go to 50
if (he(i,j).ge.20..or.he(i+1,j).ge.20.)go to 50

if(j.eq.1)go to 50

kslp = 1
if (he(i,j).lt.-6..and.he(i+1,j).lt.-6.)kslp = 0

if(kslp.eq.0)then
    dg = 0.5*(e(i,j) + e(i+1,j) - h(i,j-1) - h(i,j))
else
    eg = 0.5*(e(i,j) + e(i+1,j))
    call dedgec(eg,h(i,j),h(i,j-1),dg)
    if (dg.lt.fdl)dg = fdl
endif

if(dg.le.0.)go to 30

c----- Coriolis

uatvp = (u(i,j-1) + u(i+1,j-1) + u(i+1,j) + u(i,j))*0.25
cory(i,j) = f*uatvp

c----- Pressure Gradient

gdedy(i,j) = 9.81*(e(i,j) - e(i+1,j))/dy

c----- Eddy Viscosity

if(i.lt.2.or.i.gt.(ny-2).or.j.gt.(nx-1))go to 10
hedd = hed*dg
call ceddy(i,j,v,hedd,eddy)
call cvdvy(i,j,v,vdvy)
call cudvdx(i,j,v,udvdx,uatvp)

c----- Friction

10 ratey = sqrt(uatvp*uatvp + v(i,j)*v(i,j))
fricy(i,j) = cdrag*v(i,j)*ratey/dg

c----- Temporal

dvdt(i,j) = - gdedy(i,j) - fricy(i,j) + eddy - udvdx
&          - vdvy - cory(i,j)

c----- New value of v

vn(i,j) = v(i,j) + dt*dvdt(i,j)

30 dvdt1 = dvdt(if,jf)
cory1 = cory(if,jf)
gdedy1 = gdedy(if,jf)
fricy1 = fricy(if,jf)

50 continue

```

```
return
end
```

```
subroutine ceddyx(i,j,u,hedd,eddyx)
```

```
c-----
c-----      To calculate eddy viscosity in the x-direction
c-----
```

```
dimension u(ny,nx)
common /lim/ ny,nx
common /coord/ if,jf,dx,dy

d2udx2 = (u(i,j-1) + u(i,j+1) - 2.*u(i,j))/(dx*dx)
d2udy2 = (u(i-1,j) + u(i+1,j) - 2.*u(i,j))/(dy*dy)

eddyx = hedd*(d2udx2 + d2udy2)

return
end
```

```
subroutine ceddy(y,i,j,v,hedd,eddyy)
```

```
c-----
c-----      To calculate eddy viscosity in the y-direction
c-----
```

```
dimension v(ny,nx)
common /lim/ ny,nx
common /coord/ if,jf,dx,dy

d2vdx2 = (v(i,j+1) + v(i,j-1) - 2.*v(i,j))/(dx*dx)
d2vdy2 = (v(i-1,j) + v(i+1,j) - 2.*v(i,j))/(dy*dy)

eddyy = hedd*(d2vdx2 + d2vdy2)

return
end
```

```
subroutine chstab(en,un,vn)
```

```
c-----
c-----      To check the stability of the model
c-----
```

```
dimension en(ny,nx), un(ny,nx), vn(ny,nx)
common /lim/ ny,nx
common /time/ itc,psi,its,dt,hour,psin
common /stab/ cd,cv,key

key = 0

do 1 i = 1,ny
do 1 j = 1,nx

  if(en(i,j).lt.-cd.or.en(i,j).gt.cd.or.un(i,j).lt.-cv.
&    or.un(i,j).gt.cv.or.vn(i,j).lt.-cv.or.vn(i,j).gt.cv
&    )then

    key = 1

    write(*,20)i,j
    write(*,25)un(i,j),vn(i,j),en(i,j),psi

return
```

endif

1 continue

20 format('/' Incipient Instability at i =',i3,', j =',i3)
25 format('/'un=',f9.3,' vn=',f9.3,' en =',f7.3,' psi=',f5.0)

return
end

subroutine cududx(i,j,u,ududx)

c-----
c-----
c-----

To calculate ududx

dimension u(ny,nx)
common /lim/ ny,nx
common /coord/ if,jf,dx,dy

small = 1.0e-06

if(abs(u(i,j-1)).lt.small.and.abs(u(i,j+1)).lt.small)then

ududx = 0.
return

elseif(abs(u(i,j-1)).lt.small)then

c-----
c-----
c-----

To evaluate ududx near to an east-facing coastline

if(u(i,j).gt.0.)then

ududx = 0.
return

else

c-----

central and eastern point

ududx = u(i,j)*(u(i,j+1) - u(i,j))/dx
return

endif

elseif(abs(u(i,j+1)).lt.small)then

c-----
c-----
c-----

To evaluate ududx near to a west-facing coastline

if(u(i,j).lt.0.)then

ududx = 0.
return

else

c-----

central and western point

ududx = u(i,j)*(u(i,j) - u(i,j-1))/dx
return

endif

else

```
    ududx = u(i,j)*(u(i,j+1) - u(i,j-1))/(2.*dx)
    return
```

endif

end

subroutine cudvdx(i,j,v,udvdx,uatvp)

c-----
c-----
c-----

To calculate udvdx

```
dimension v(ny,nx)
common /lim/ ny,nx
common /coord/ if,jf,dx,dy
```

small = 1.0e-06

if(abs(v(i,j-1)).lt.small.and.abs(v(i,j+1)).lt.small)then

c-----
c-----
c-----

If the flow is through a channel then udvdx is zero.

```
    udvdx = 0.
    return
```

elseif(abs(v(i,j-1)).lt.small)then

c-----
c-----
c-----

To evaluate udv/dx for an east-facing coastline.

```
    udvdx = uatvp*(v(i,j+1) - v(i,j))/dx
    return
```

elseif(abs(v(i,j+1)).lt.small)then

c-----
c-----
c-----

To evaluate udv/dx for a west-facing coastline.

```
    udvdx = uatvp*(v(i,j) - v(i,j-1))/dx
    return
```

else

```
    udvdx = uatvp*(v(i,j+1) - v(i,j-1))/(2.*dx)
```

endif

end

subroutine cvdudy(i,j,u,vdudy,vatup)

c-----
c-----
c-----

To calculate vdudy

```
dimension u(ny,nx)
common /lim/ ny,nx
common /coord/ if,jf,dx,dy
```

```

small = 1.0e-06

if(abs(u(i-1,j)).lt.small.and.abs(u(i+1,j)).lt.small)then
c-----
c-----      If the flow is through a channel then vdudy is zero
c-----

      vdudy = 0.
      return

elseif(abs(u(i+1,j)).lt.small)then

c-----
c-----      To evaluate vdu/dy for a north-facing coastline
c-----

      vdudy = vatup*(u(i-1,j) - u(i,j))/dy
      return

elseif(abs(u(i-1,j)).lt.small)then

c-----
c-----      To evaluate vdu/dy for a south-facing coastline
c-----

      vdudy = vatup*(u(i,j) - u(i+1,j))/dy
      return

else

      vdudy = vatup*(u(i-1,j) - u(i+1,j))/(2.*dy)
      return

endif

end

subroutine cvdvdvdy(i,j,v,vdvdvdy)
c-----
c-----      To calculate vdvdvdy
c-----

dimension v(ny,nx)
common /lim/ ny,nx
common /coord/ if,jf,dx,dy

small = 1.0e-06

if(abs(v(i-1,j)).lt.small.and.abs(v(i+1,j)).lt.small)then

      vdvdvdy = 0.
      return

elseif(abs(v(i-1,j)).lt.small)then

c-----
c-----      To evaluate vdvdvdy for a south-facing coastline
c-----

      if(v(i,j).lt.0.)then

          vdvdvdy = 0.
          return

```

```

else
c-----      central and southern points
      vdvdy = v(i,j)*(v(i,j) - v(i+1,j))/dy
      return

endif

elseif(abs(v(i+1,j)).lt.small)then

c-----
c-----      To evaluate vdvdy for a north-facing coastline
c-----

      if(v(i,j).gt.0.)then
            vdvdy = 0.
            return
      else
c-----      central and northern points
            vdvdy = v(i,j)*(v(i-1,j) - v(i,j))/dy
            return

      endif

else
      vdvdy = v(i,j)*(v(i-1,j) - v(i+1,j))/(2.*dy)
      return

endif

end

subroutine dedgec(eg,h1,h2,dg)
c-----
c-----      To evaluate the depth along the edge of a cell
c-----

      if(eg.gt.h1.and.eg.gt.h2)then
            dg = eg - 0.5*(h1 + h2)
            return
      elseif(eg.le.h1.and.eg.le.h2)then
            dg = 0.
            return
      elseif(h1.gt.h2)then
            dg = (eg - h2)*(eg - h2)*0.5/(h1 - h2)
            return
      else
            dg = (eg - h1)*(eg - h1)*0.5/(h2 - h1)
            return
      endif

```

end

subroutine depths(h,he,kwet)

c-----
c-----
c-----

To specify depths

dimension he(ny,nx), h(ny,nx), kwet(ny,nx)

common /lim/ ny,nx

common /start/kie,kis,nrun,rr

if(rr.gt.0)then

c----- To create a flat sea-bed, with slight random variation

do 50 i = 1,ny

do 50 j = 1,nx

h(i,j) = 0.

he(i,j) = -50. + (drand() - 0.5)*rr

50 h(i,j) = 0.25*(he(i,j) + he(i,j+1) + he(i+1,j)
& + he(i+1,j+1))

else

c----- To create a Gaussian shoal

do 60 i = 1,ny

do 60 j = 1,nx

r2he = (real(i-19.5))**2 + (real(j-19.5))**2

he(i,j) = -50.*(1 - exp(-r2he*0.01))

r2h = (real((i+0.5) - 19.5))**2

& + (real((j+0.5) - 19.5))**2

h(i,j) = -50.*(1 - exp(-r2h*0.01))

if(he(i,j).lt.0.)then

kwet(i,j) = 1

else

kwet(i,j) = 0

endif

60 continue

endif

do 70 i = 15,25

70 write(*,20) (h(i,j), j = 15,25)

do 80 i = 1,ny

write(13,30) (h(i,j), j = 1,nx)

80 write(13,30) (he(i,j), j = 1,nx)

20 format(11f7.2)

30 format(10f8.2)

return

end

subroutine dpoint(h,deepp,he)

c-----
c-----
c-----
c-----

To establish the deepest point of a cell.
(Based around the elevation point).

```
dimension he(ny,nx), deepp(ny,nx), h(ny,nx)
common /lim/ ny,nx
common /coord/ if,jf,dx,dy
common /time/ itc,psi,its,dt,hour,psin
common /grid/ ngs,nsbc,ndal
```

```
do 50 i = 2,ny-1
do 50 j = 2,nx-1
```

```
deepp(i,1) = he(i,1)
deepp(i,nx) = h(i,nx)
deepp(1,j) = h(1,j)
deepp(ny,j) = h(ny,j)
deepp(1,1) = he(1,1)
deepp(1,nx) = h(1,nx)
deepp(ny,nx) = h(ny,nx)
deepp(ny,1) = h(ny,1)
```

```
if(nsbc.eq.1)deepp(ny,1) = 5.0
```

```
if(h(i,j).ge.5..and.nsbc.lt.3)then
```

```
    deepp(i,j) = h(i,j)
```

```
elseif(h(i,j).ge.20..and.nsbc.eq.3)then
```

```
    deepp(i,j) = h(i,j)
```

```
else
```

```
    deepp(i,j) = h(i,j)
```

```
    if(h(i-1,j).lt.deepp(i,j))deepp(i,j) = h(i-1,j)
    if(h(i-1,j-1).lt.deepp(i,j))deepp(i,j) = h(i-1,j-1)
    if(h(i,j-1).lt.deepp(i,j))deepp(i,j) = h(i,j-1)
```

```
endif
```

```
50 continue
```

c----- To display depths of cells taken for analysis

```
if(its.eq.0)write(*,200)h(if,jf),he(if,jf)
200 format(' h(if,jf) = ',f6.2,'m',9x,' he(if,jf) = ',f6.2,'m.')
```

```
if(its.eq.0)then
```

```
    write(*,*)
    write(*,*)
    write(*,*)'          Deepest Points'
    write(*,*)
    write(*,*)
```

```
do 15 i = 15,25
```

```
    write(*,16)(deepp(i,j),j = 15,25)
```

```
15 continue
```

```
write(*,*)
```

```

write(*,*)
write(*,*)'      H-values'
write(*,*)
write(*,*)

```

```

do 17 i = 15,25

```

```

    write(*,16) (h(i,j),j = 15,25)

```

```

17    continue

```

```

16    format(11f7.2)

```

```

endif

```

```

return

```

```

end

```

```

subroutine expluv(un,vn)

```

```

c-----

```

```

c-----      To extrapolate u and v on the boundaries

```

```

c-----

```

```

dimension un(ny,nx), vn(ny,nx)

```

```

common /lim/ ny,nx

```

```

do 1 j = 2,nx-2

```

```

    un(1,j)      = 2.*un(2,j) - un(3,j)

```

```

    un(ny,j)     = 2.*un(ny-1,j) - un(ny-2,j)

```

```

1 continue

```

```

do 2 i = 2,ny-2

```

```

    vn(i,1)      = 2.*vn(i,2) - vn(i,3)

```

```

    vn(i,nx)     = 2.*vn(i,nx-1) - vn(i,nx-2)

```

```

2 continue

```

```

c-----      at the corners:

```

```

un(1,1)         = 2.*un(2,2) - un(3,3)

```

```

vn(1,1)         = 2.*vn(2,2) - vn(3,3)

```

```

un(ny,1)        = 2.*un(ny-1,2) - un(ny-2,3)

```

```

vn(ny-1,1)      = 2.*vn(ny-2,2) - vn(ny-3,3)

```

```

un(1,nx)        = 2.*un(2,nx-2) - un(3,nx-3)

```

```

vn(1,nx)        = 2.*vn(2,nx-1) - vn(3,nx-2)

```

```

un(ny,nx-1)     = 2.*un(ny-1,nx-2) - un(ny-2,nx-3)

```

```

vn(ny-1,nx)     = 2.*vn(ny-2,nx-1) - vn(ny-3,nx-2)

```

```

return

```

```

end

```

```

subroutine focus(nc,t1,t2,t3,t4,t5,t6,t7,t8,t9,t10,t11,t12,

```

```

&          t13,t14,t15,t16,t17,t18,t19,t20,

```

```

&          hx,he1,he2,he3,he4)

```

```

c-----

```

```

c-----      To focus on values in and surrounding the test cell.

```

```

c-----

```

```

common /grid/ ngs,nsbc,ndal

```

```

common /start/kie,kis,nrun,rr

```

```

ta = t1*100.

```

```

tb = t2*100.
tc = t3*100.
td = t4*100.
te = t5*100.
tf = t6*100.
tg = t7*100.
th = t8*100.
ti = t9*100.
tj = t10*100.
tk = t11*100.
tl = t12*1.0e+05
tm = t13*1.0e+05
tn = t14*1.0e+05
to = t15*1.0e+05
tp = t16*100
tq = t17*1.0e+05
tr = t18*1.0e+05
ts = t19*1.0e+05
tt = t20*1.0e+05

```

```

if(ndal.eq.4)then

```

```

    if(t10.le.hx)then

```

```

        ta = 0.
        tb = 0.
        tc = 0.
        td = 0.
        te = 0.
        tj = hx*100.
        tk = 0.
        tl = 0.
        tm = 0.
        tn = 0.
        to = 0.
        tp = 0.
        tq = 0.
        tr = 0.
        ts = 0.
        tt = 0.

```

```

    endif

```

```

    if(t6.le.he1)tf = he1*100.
    if(t7.le.he2)tg = he2*100.
    if(t8.le.he3)th = he3*100.
    if(t9.le.he4)ti = he4*100.

```

```

endif

```

```

write(nc,10)ta,tb,tc,td,te,tf,tg,th,ti,tj,tk,tl,tm,tn,to,tp,tq,
&          tr,ts,tt,nrun
10 format(11f7.1,2f7.2,2(f8.3,1x),f7.1,1x,2f7.2,2(f8.3,1x),i5)

```

```

return
end

```

```

subroutine heron(x1,y1,x2,y2,x3,y3,area)

```

```

c-----
c-----
c-----

```

```

    To find the area of a triangle using Heron's formula

```

```

a = sqrt((x2 - x1)**2 + (y2 - y1)**2)
b = sqrt((x3 - x2)**2 + (y3 - y2)**2)
c = sqrt((x1 - x3)**2 + (y1 - y3)**2)

```



```

s = 0.5*(a + b + c)
d = s*(s - a)*(s - b)*(s - c)

if(d.le.0.)then

    area = 0.
    return

else

    area = sqrt(d)
    return

endif

end

subroutine intop(e,u,un,v,vn,em,um,vm)
c-----
c-----      Tp provide an interim output at the time horizon for e
c-----

dimension u(ny,nx), v(ny,nx), un(ny,nx),
&          vn(ny,nx), e(ny,nx)
integer um(ny,nx), vm(ny,nx), em(ny,nx)
common /lim/ ny,nx
common /time/ itc,psi,its,dt,hour,psin
common /start/ kie,kis,nrun,rr

do 1 i = 1,ny
do 1 j = 1,nx

    em(i,j) = int(100.*e(i,j))
    um(i,j) = int(50.*(u(i,j) + un(i,j)))
    vm(i,j) = int(50.*(v(i,j) + vn(i,j)))

1 continue

jff = 40
jfi = jff - 6

do 2 k = 1,1

    write(54,20)nrun,itc,psi
    write(54,21)(j,j,j = jfi,jff)

do 2 i = 34,40

    write(54,22)i,(em(i,j),um(i,j),j = jfi,jff)
    write(54,23)i,(vm(i,j),j = jfi,jff)

2 continue

20 format(1h1,' run no. ',i3,9x,'Tidal Cycle no. ',i2,9x,
&'psi = ',f6.2//)
21 format(5x,22i5/)
22 format(i3,2x,22i5)
23 format(i3,2x,11(i5,5x))

return
end

```



```

subroutine leen3(i,j,kwet,h,en,he)
c-----
c----- to execute Leendertses' (1970) 3rd drying test
c-----

dimension en(ny,nx), he(ny,nx), h(ny,nx), kwet(ny,nx)
common /lim/ ny,nx

if(kwet(i,j).eq.0)then

    return

else

    kwet(i,j) = 1
    hn        = 0.5*(h(i-1,j-1) + h(i-1,j))
    hmin       = hn
    hs         = 0.5*(h(i,j-1) + h(i,j))

    if(hs.gt.hmin) hmin = hs

    heast      = 0.5*(h(i-1,j) + h(i,j))

    if(heast.gt.hmin) hmin = heast

    hw         = 0.5*(h(i-1,j-1) + h(i,j-1))

    if(hw.gt.hmin) hmin = hw

    ecrit      = 0.02 + hmin

    if(en(i,j).lt.ecrit)then

        kwet(i,j) = 0
        en(i,j)   = he(i,j)

    endif

endif

return
end

```

```

subroutine owen3(i,j,h,en,he,kwet)
c-----
c----- to execute Owens' (1984) 3rd drying test
c-----

dimension en(ny,nx), he(ny,nx), h(ny,nx),
&      kwet(ny,nx)
common /lim/ ny,nx

if(kwet(i,j).eq.0)then

    return

else

    kwet(i,j) = 1
    hn        = 0.5*(h(i-1,j-1) + h(i-1,j))
    hmax       = hn
    hs         = 0.5*(h(i,j-1) + h(i,j))

    if(hs.lt.hmax) hmax = hs

```



```

heast      = 0.5*(h(i-1,j) + h(i,j))

if(heast.lt.hmax) hmax = heast

hw         = 0.5*(h(i-1,j-1) + h(i,j-1))

if(hw.lt.hmax)  hmax = hw

ecrit      = 0.1 + hmax

if(en(i,j).lt.ecrit)then

    en(i,j) = he(i,j)
    kwet(i,j) = 0.

endif

```

```
endif
```

```
return
end
```

```
subroutine quiver(u,un,v,vn,e,he)
```

```

c-----
c-----      To determine the magnitude and direction of the current
c-----      vector for production of quivers

```

```

dimension u(ny,nx), v(ny,nx), un(ny,nx),
&          vn(ny,nx), e(ny,nx), he(ny,nx)
common /lim/ ny,nx
common /time/ itc,psi,its,dt,hour,psin
common /numb/ pi,rad

return
end

```

```
subroutine raise(h,he,deepp)
```

```

c-----
c-----      To raise the sea-bed by 0.05m per time-step
c-----

```

```

dimension he(ny,nx), deepp(ny,nx), h(ny,nx)
common /lim/ ny,nx
common /time/ itc,psi,its,dt,hour,psin

```

```
if(psi.lt.270..or.psi.ge.350.)then
```

```
    return
```

```
else
```

```

do 1 i = 1,ny
do 1 j = 1,nx

```

```

    h(i,j) = h(i,j) + 0.05
    he(i,j) = he(i,j) + 0.05

```

```
1    continue
```

```

do 2 i = 1,ny-1
do 2 j = 1,nx-1

```

```
    deepp(i,j) = deepp(i,j) + 0.05
```

2 continue

return

endif

end

subroutine seten(en)

c-----
c-----
c-----

To set en on the boundaries

dimension en(ny,nx)
common /lim/ ny,nx
common /time/ itc,psi,its,dt,hour,psin
common /grid/ ngs,nsbc,ndal
common /numb/ pi,rad

psir = psin*rad
wind = 1.
if(itc.eq.0)wind = psin/360.

if(ngs.eq.2)then

c-----
c-----
c-----

North and South boundaries (1000m)

p0 = 0.
do 1 j = 1,nx

dp = (real(j) - 20.5)*0.005
if(nsbc.eq.2)en(1,j) = 2.8*cos(psir - p0 - dp)*wind
en(ny,j) = 3.2*cos(psir - p0 - dp)*wind

1 continue

c-----
c-----
c-----

East and West boundaries (1000m)

if(nsbc.eq.1)then

do 2 i = 20,40

a = 3.+real(i-20)*0.01
en(i,nx) = a*cos(psir - p0 - 0.1)*wind

2 continue

return

else

do 3 i = 2,ny-1

a = 3.+(real(i) - 20.5)*0.01
if(nsbc.eq.2)en(i,1) = a*cos(psir - p0 + 0.1)*wind
en(i,nx) = a*cos(psir - p0 - 0.1)*wind

3 continue

return

endif

else

c-----
c-----
c-----

North and South boundaries (5000m)

p0 = 0.

do 4 j = 1,nx

dp = (real(j) - 20.5)*0.025

if(nsbc.eq.2)en(1,j) = 2.0*cos(psir - p0 -dp)*wind

en(ny,j) = 4.0*cos(psir - p0 -dp)*wind

4 continue

c-----
c-----
c-----

East and West boundaries (5000m)

if(nsbc.eq.1)then

do 5 i = 10,40

a = 3.+real(i-20)*0.05

en(i,nx) = a*cos(psir - p0 - 0.5)*wind

5 continue

return

else

do 6 i = 2,ny

a = 3.+(real(i) - 20.5)*0.05

en(i,1) = a*cos(psir - p0 + 0.5)*wind

en(i,nx) = a*cos(psir - p0 - 0.5)*wind

6 continue

return

endif

endif

end

subroutine sethhe(he,h)

c-----
c-----
c-----

To set h and he in case of hot-start

dimension he(ny,nx), h(ny,nx)

common /lim/ ny,nx

common /grid/ ngs,nsbc,ndal

if(nsbc.eq.1)then

do 100 i = 1,ny

100 read(99,20) (he(i,j), j = 1,nx)

do 200 i = 1,ny

200 read(99,20) (h(i,j), j = 1,nx)

```

else
    do 500 i = 1,ny
500      read(50,20) (he(i,j), j = 1,nx)
    do 600 i = 1,ny
600      read(50,20) (h(i,j), j = 1,nx)
    endif
    20 format(5e16.5)
    return
end

subroutine setic(un,vn,en,e,u,v,h,he)
c-----
c-----      To set initial conditions
c-----

    dimension u(ny,nx), v(ny,nx), un(ny,nx),
&            vn(ny,nx), e(ny,nx), en(ny,nx),
&            he(ny,nx), h(ny,nx)
    common /lim/ ny,nx
    common /grid/ ngs,nsbc,ndal
    common /start/kie,kis,nrun,rr

    do 50 i = 1,ny
    do 50 j = 1,nx

        en(i,j) = 0.
        un(i,j) = 0.
        vn(i,j) = 0.

50 continue

    if(kis.eq.1)then
c-----      Hot-start; e,u and v fields read from euvstore
c-----      and modified for dry cells.

        do 60 i = 1,ny
            read(56,65) (e(i,j), j = 1,nx)

            do 60 j = 1,nx
                if(e(i,j).lt.he(i,j))e(i,j) = he(i,j)

60          continue

            do 70 i = 1,ny
                read(56,65) (u(i,j), j = 1,nx)

                do 70 j = 1,nx-1
                    if((e(i,j) - he(i,j)).lt.1.0e-06)u(i,j) = 0.
                    if((e(i,j+1) - he(i,j+1)).lt.1.0e-06)u(i,j) = 0.

70          continue

```



```

do 80 i = 1,ny-1
    read(56,65) (v(i,j), j = 1,nx)
do 80 j = 1,nx
    if((e(i,j) - he(i,j)).lt.1.0e-06)v(i,j) = 0.
    if((e(i+1,j) - he(i+1,j)).lt.1.0e-06)v(i,j) = 0.

80    continue
else
c-----    Cold-start; e = u = v = 0 everywhere.

do 150 i = 1,ny
do 150 j = 1,nx

    e(i,j) = 0.
    u(i,j) = 0.
    v(i,j) = 0.

150    continue

    if(kie.eq.0) return

    call setice(e)
    if(h(i,j).gt.5..or.he(i,j).gt.5.)then

        do 160 i = 1,ny
        do 160 j = 1,nx

            e(i,j) = 0.
            u(i,j) = 0.
            v(i,j) = 0.

160        continue

        endif

    endif

65 format(5e16.5)

return
end

subroutine setice(e)
c-----
c-----    To set the initial conditions on the boundaries.
c-----

dimension e(ny,nx)
common /lim/ ny,nx
common /time/ itc,psi,its,dt,hour,psin
common /grid/ ngs,nsbc,ndal
common /numb/ pi,rad

psir = psi*rad

do 100 i = 1,ny

    if(ngs.eq.1)da = real(i-20.5)*0.05
    if(ngs.eq.2)da = real(i-20.5)*0.01

```

```

      a = 3. + da
do 100 j = 1,nx
      if(ngs.eq.1)dp = real(j-20.5)*0.025
      if(ngs.eq.2)dp = real(j-20.5)*0.005
      p = (180.*rad) + dp
      e(i,j) = a*cos(psir - p)
100 continue

      return
      end

      subroutine setwet(kn)
c-----
c-----      To set everywhere wet
c-----

      dimension kn(ny,nx)
      common /lim/ ny,nx

      do 100 i = 1,ny
      do 100 j = 1,nx

          kn(i,j) = 1

100 continue

      return
      end

      subroutine smool(x,is,js,iif,jjf)
c-----
c-----      To smooth a line of values
c-----

      dimension x(ny,nx), ws(70)
      common /lim/ ny,nx

      small = 1.0e-06

      if(js.eq.jjf)then
c-----      Meridional smoothing

          ws(is) = x(is,jjf)
          ws(is+1) = 0.25*(x(is,jjf) + 2.*x(is+1,jjf) + x(is+2,jjf))
          ws(iif-1) = 0.25*(x(iif-2,jjf) + 2.*x(iif-1,jjf) +
&              x(iif,jjf))
          ws(iif) = x(iif,jjf)

          do 8 i = is+2,iif-2
          do 6 ii = i-2,i+2

              if(x(ii,jjf).gt.20..or.abs(x(ii,jjf)).lt.small)go to 7

6          continue

          ws(i) = (6.*x(i,jjf) + 4.*(x(i-1,jjf) + x(i+1,jjf)) +

```

```

&          x(i-2,jjf) + x(i+2,jjf))/16.

      go to 8

7      ws(i) = x(i,jjf)
8      continue

      do 9 i = is,iif

          x(i,jjf) = ws(i)

9      continue

      return

else

c-----      Zonal smoothing

      if(is.ne.iif)return

      ws(js) = x(is,js)
      ws(js+1) = 0.25*(x(is,js) + 2.*x(is,js+1) + x(is,js+2))
      ws(jjf-1) = 0.25*(x(is,jjf-2) + 2.*x(is,jjf-1) + x(is,jjf))
      ws(jjf) = x(is,jjf)

      do 3 j = js+2,jjf-2
      do 1 jj = j-2,j+2

          if(x(is,jj).gt.20..or.abs(x(is,jj)).lt.small)go to 2

1      continue

          ws(j) = (6.*x(is,j) + 4.*(x(is,j-1) + x(is,j+1))
&              + x(is,j-2) + x(is,j+2))/16.
          go to 3

2      ws(j) = x(is,j)

3      continue

      do 4 j = js,jjf

          x(is,j) = ws(j)

4      continue

      return

endif

end

subroutine smooth(un,vn)
c-----
c-----      To smooth values of un and vn on the boundaries
c-----

      dimension un(ny,nx), vn(ny,nx)
      common /lim/ ny,nx

      call smool(un,1,1,1,nx-1)
      call smool(un,ny,1,ny,nx-1)
      call smool(un,1,nx-1,ny,nx-1)
      call smool(un,1,1,ny,1)

```

```

call smool(vn,1,1,1,nx)
call smool(vn,ny-1,1,ny-1,nx)
call smool(vn,1,nx,ny-1,nx)
call smool(vn,1,1,ny-1,1)

```

```

return
end

```

```

subroutine stohhe(he,h)

```

```

c-----
c-----      To store he and h at the end of the nth cycle
c-----

```

```

dimension he(ny,nx), h(ny,nx)
common /lim/ ny,nx

```

```

rewind 50

```

```

do 100 i = 1,ny

```

```

    write(50,200) (he(i,j), j = 1,nx)

```

```

100 continue

```

```

do 150 i = 1,ny

```

```

    write(50,200) (h(i,j), j = 1,nx)

```

```

150 continue

```

```

200 format(5e16.5)

```

```

return
end

```

```

subroutine store(he,e,u,v,hs)

```

```

c-----
c-----      To store e, u, v at the end of the nth cycle
c-----

```

```

dimension e(ny,nx), he(ny,nx), u(ny,nx),
&          v(ny,nx), hs(ny,nx)
common /lim/ ny,nx

```

```

rewind 56

```

```

do 10 i = 1,ny

```

```

do 10 j = 1,nx

```

```

    hs(i,j) = 0.

```

```

10 continue

```

```

do 60 i = 1,ny

```

```

    write(56,65) (e(i,j), j = 1,nx)

```

```

60 continue

```

```

do 61 i = 1,ny

```

```

    write(56,65) (u(i,j), j = 1,nx)

```

```

61 continue

```

```

do 62 i = 1,ny
    write(56,65) (v(i,j),j = 1,nx)
62 continue

do 63 i = 1,ny
    write(56,65) (hs(i,j),j = 1,nx)
63 continue

write(*,20)
20 format('Data have been stored in file newstore')
65 format(5e16.5)

return
end

subroutine wasen(e,a,p)
c-----
c-----    To specify e on the boundaries
c-----

dimension e(ny,nx), a(ny,nx), p(ny,nx)
common /lim/ ny,nx
common /time/ itc,psi,its,dt,hour,psin
common /numb/ pi,rad

wind = 1.
wm2 = 28.98410422
t = 12.42*psin/360..

if(itc.eq.0)wind = psin/360.

do 1 j = 40,nx
    e(1,j) = a(1,j)*cos((wm2*t - p(i,j))*rad)*wind
1 continue

do 2 i = 2,24
    e(i,nx) = a(i,nx)*cos((wm2*t - p(i,65))*rad)*wind
2 continue

return
end

subroutine washhe(h,he)
c-----
c-----    To read h and he from washhe in case of
c-----    a hot start.
c-----

dimension h(ny,nx), he(ny,nx)
common /lim/ ny,nx

open(43,file='washhe')

do 100 i = 1,ny

```

1000

```
      read(43,75) (h(i,j), j = 1,nx)
```

```
100 continue
```

```
      do 200 i = 1,ny
```

```
          read(43,75) (he(i,j), j = 1,nx)
```

```
200 continue
```

```
75 format(65f5.1)
```

```
      return
```

```
      end
```

```
      subroutine wasic(un,vn,en,e,u,v,a,p)
```

```
c-----  
c-----      To set the initial conditions for the Wash.  
c-----
```

```
      dimension un(ny,nx), vn(ny,nx), en(ny,nx),
```

```
&              e(ny,nx), u(ny,nx), v(ny,nx),
```

```
&              a(ny,nx), p(ny,nx)
```

```
      common /lim/ ny,nx
```

```
      common /numb/ pi,rad
```

```
      do 100 i = 1,nx
```

```
      do 100 j = 1,ny
```

```
          un(i,j) = 0.
```

```
          vn(i,j) = 0.
```

```
          u(i,j) = 0.
```

```
          v(i,j) = 0.
```

```
          e(i,j) = 0.
```

```
100 continue
```

```
      call wasice(i,j,e,a,p)
```

```
      return
```

```
      end
```

```
      subroutine wasice(i,j,e,a,p)
```

```
c-----  
c-----      To read the boundary values of a(i,j) and p(i,j)  
c-----      for the Wash model.  
c-----
```

```
      dimension e(ny,nx), a(ny,nx), p(ny,nx)
```

```
      real amp,phase
```

```
      common /lim/ ny,nx
```

```
      open(10,file='was-bcez')
```

```
      do 50 m = 1,49
```

```
          read(10,111) i,j,amp
```

```
          a(i,j) = amp*0.001
```

```
50 continue
```

```
      rewind 10
```



```

do 100 m = 1,49

    read(10,112) i,j,phase
    p(i,j) = phase*0.1

100 continue

111 format(3x,i2,3x,i2,31x,f5.0)
112 format(3x,i2,3x,i2,36x,f5.0)

return
end

subroutine wdtest(i,j,e1,h1,e2,h2,kn,uv)
c-----
c-----      Wet or dry test using:
c-----      Flather & Heaps' (1975) drying algorithm
c-----

dimension kn(ny,nx)
common /lim/ ny,nx
kn(i,j) = 0
uv      = 0.

c      go to 1000

if(e2.gt.20..or.e1.gt.20.)then
    kn(i,j) = 0
    return

else

    d1 = e1 - h1
    d2 = e2 - h2

endif

if(d1.le.0..and.d2.le.0.)then
    kn(i,j) = 0
    return

elseif(d1.le.0.)then

    if((e2 - e1).le.0.1)then
        kn(i,j) = 0
        return

    else

        kn(i,j) = 1
        return

    endif

elseif(d2.le.0.)then

    if((e1 - e2).le.0.1)then
        kn(i,j) = 0
        return

    else

        kn(i,j) = 1
        return

    endif

```

```

        endif

else

    kn(i,j) = 1
    return

endif

return

1000 if((e2.gt.20..or.e1.gt.20.))return

d1 = e1 - h1
d2 = e2 - h2
if((d1.le.0..and.d2.le.0.))return
if(d1.le.0.)go to 2
if(d2.le.0.)go to 3
go to 5
2 if((e2 - e1).le.0.1)return
go to 5
3 if((e1 - e2).le.0.1)return
5 kn(i,j) = 1
return
end

subroutine wetest(i,j,kwet,e,he,dn,ds,de,dw)
c-----
c----- to test whether a dry cell has become wet (Leendertse 1970)
c-----

dimension e(ny,nx), he(ny,nx), kwet(ny,nx)
common /lim/ ny,nx

kwet(i,j) = 0
k4 = 0
emean = 0.

if(e(i-1,j).gt.he(i-1,j).or.dn.gt.0.)then

    k4 = k4 + 1
    emean = emean + e(i-1,j)

endif

if(e(i+1,j).gt.he(i+1,j).or.ds.gt.0.)then

    k4 = k4 + 1
    emean = emean + e(i+1,j)

endif

if(e(i,j+1).gt.he(i,j+1).or.de.gt.0.)then

    k4 = k4 + 1
    emean = emean + e(i,j+1)

endif

if(e(i,j-1).gt.he(i,j-1).or.dw.gt.0.)then

    k4 = k4 + 1
    emean = emean + e(i,j-1)

endif

```

```
if(k4.ne.0)then
```

```
    emean = emean/real(k4)  
    if(emean.ge.e(i,j))kwet(i,j) = 1
```

```
endif
```

```
return  
end
```

```
subroutine wetowe(i,j,kwet,e,he,dn,ds,de,dw)
```

```
c-----  
c-----      To test for a flooding cell using Owewns' (1984)  
c-----      improved method  
c-----
```

```
dimension e(ny,nx), he(ny,nx), kwet(ny,nx)  
common /lim/ ny,nx
```

```
kwet(i,j) = 0  
kx        = 0  
emean     = 0.
```

```
if(e(i-1,j).gt.he(i-1,j).or.dn.gt.0..or.(-he(i-1,j) + e(i-1,j)).gt  
&  .(-he(i,j) + e(i,j)))then
```

```
    kx      = kx + 1  
    emean   = emean + e(i-1,j)
```

```
endif
```

```
if(e(i+1,j).gt.he(i+1,j).or.ds.gt.0..or.(-he(i+1,j) + e(i+1,j)).gt  
&  .(-he(i,j) + e(i,j)))then
```

```
    kx      = kx + 1  
    emean   = emean + e(i+1,j)
```

```
endif
```

```
if(e(i,j+1).gt.he(i,j+1).or.de.gt.0..or.(-he(i,j+1) + e(i,j+1)).gt  
&  .(-he(i,j) + e(i,j)))then
```

```
    kx      = kx + 1  
    emean   = emean + e(i,j+1)
```

```
endif
```

```
if(e(i,j-1).gt.he(i,j-1).or.dw.gt.0..or.(-he(i,j-1) + e(i,j-1)).gt  
&  .(-he(i,j) + e(i,j)))then
```

```
    kx      = kx + 1  
    emean   = emean + e(i,j-1)
```

```
endif
```

```
if(kx.ne.0)then
```

```
    emean = emean/real(kx)  
    if(emean.gt.e(i,j))kwet(i,j) = 1
```

```
endif
```

```
return  
end
```

APPENDIX 2

PROGRAM GPLOT

C-----
C-----
C-----

To plot terms using GINOGRAPH routines.

```

DIMENSION TX(360,21),KQ(5),TE(360,11)
CHARACTER FLOW*1
CALL GINO
CALL PLOTTR
CALL DEVPAP(400.,300.,0)
CALL SHIFT2(0.,50.)
CALL PA4F
NDAL=4
PRINT *, '
PRINT *, 'Would you like to analyse the flow'
PRINT *, '
PRINT *, '        around an E-point ? (Y/N) '
PRINT *, '
READ(*,'(A1)')FLOW
IF(FLOW.EQ.'Y')GO TO 1000
PRINT *, 'Would you like a plot of terms obtained from:'
PRINT *
PRINT *, '1: Flather & Heaps (1975) method,'
PRINT *
PRINT *, '2: Leendertses (1970) method, '
PRINT *
PRINT *, '3: Owens (1984) improved method '
PRINT *
PRINT *, '        or '
PRINT *
PRINT *, '4: George & Striplings (1993) much improved method ?'
PRINT *
READ *,NDAL
IF(NDAL.EQ.1)GO TO 900
IF(NDAL.EQ.2)GO TO 500
IF(NDAL.EQ.3)GO TO 159
OPEN(63,FILE='DDS')
DO 100 I=1,360
  READ(63,10) (TX(I,J),J=1,10)
10  FORMAT(10F7.1)
  DO 100 J=1,10
100  TX(I,J)=TX(I,J)/100.
  READ(63,150)NRUN
150  FORMAT(148X,I6)
  CALL MOVTO2(100.,180.)
  CALL CHASIZ(3.,3.)
  CALL MOVBY2(10.,0.)
  CALL MOVTO2(70.,185.)
  CALL CHAINT(NRUN,3)
  CALL MOVTO2(90.,185.)
  CALL CHAHOL(30HGEORGE & STRIPLING'S (1993) *.)
  CALL CHAHOL(18H DRYING ALGORITHM*.)
  REWIND 63
  DO 200 I=1,360
    READ(63,11) (TX(I,J),J=11,15)
11  FORMAT(70X,F7.1,2F7.2,F8.3,F9.3)
    TX(I,11)=TX(I,11)/100.
    IF(TX(I,5).LE.0.)TX(I,11)=0.
    TX(I,12)=TX(I,12)*10.
    IF(TX(I,5).LE.0.)TX(I,12)=0.
    TX(I,13)=TX(I,13)*10.
    IF(TX(I,5).LE.0.)TX(I,13)=0.
    TX(I,14)=TX(I,14)*10.
    IF(TX(I,5).LE.0.)TX(I,14)=0.
    TX(I,15)=TX(I,15)*10.
    IF(TX(I,5).LE.0.)TX(I,15)=0.
200  CONTINUE

```

```

REWIND 63
DO 300 I=1,360
  READ(63,12) (TX(I,J),J=16,20),NRUN
12  FORMAT(108X,F8.1,F8.2,F7.2,F8.3,F9.3,I6)
  TX(I,16)=TX(I,16)/100.
  IF (TX(I,5).LE.0.)TX(I,16)=0.
  TX(I,17)=TX(I,17)*10.
  IF (TX(I,5).LE.0.)TX(I,17)=0.
  TX(I,18)=TX(I,18)*10.
  IF (TX(I,5).LE.0.)TX(I,18)=0.
  TX(I,19)=TX(I,19)*10.
  IF (TX(I,5).LE.0.)TX(I,19)=0.
  TX(I,20)=TX(I,20)*10.
  IF (TX(I,5).LE.0.)TX(I,20)=0.
300  CONTINUE
C----- TO CALCULATE A BASIC TIDE-CURVE FOR NO SHOAL PRESENT
DO 301 I=1,360
  A=REAL(I-1)
301  TX(I,21)=2.*COS((A-180.)*0.0174532925)
  CALL SCREEN(KQ,KHE,KUV,KAC)
  CALL AXISTT
  CALL AXISHE(KHE)
  CALL AXISUV(KUV,NDAL)
  CALL AXISAC(KAC)
  CALL SHIFT2(90.,100.)
  CALL DRA5L(TX,KQ,NDAL)
  GO TO 90
500  OPEN(62,FILE='DDL5')
  DO 501 I=1,360
  A=REAL(I-1)
501  TX(I,21)=2.*COS((A-180.)*0.0174532925)
  DO 600 I=1,360
  READ(62,16) (TX(I,J),J=1,10)
  16  FORMAT(10F7.1)
  DO 600 J=1,10
  600  TX(I,J)=TX(I,J)/100.
  READ(62,650)NRUN
650  FORMAT(148X,I6)
  CALL MOVTO2(100.,180.)
  CALL CHASIZ(3.,3.)
  CALL MOVBY2(10.,0.)
  CALL MOVTO2(70.,185.)
  CALL CHAINT(NRUN,3)
  CALL MOVTO2(90.,185.)
  CALL CHAHOL(20HLEENDERTSES' 1970 *.)
  CALL CHAHOL(18H DRYING ALGORITHM*.)
  REWIND 62
  DO 700 I=1,360
  READ(62,18) (TX(I,J),J=11,15)
  18  FORMAT(70X,F7.1,2F7.2,F8.3,F9.3)
  TX(I,11)=TX(I,11)/100.
  TX(I,12)=TX(I,12)*10.
  TX(I,13)=TX(I,13)*10.
  TX(I,14)=TX(I,14)*10.
  TX(I,15)=TX(I,15)*10.
700  CONTINUE
  REWIND 62
  DO 800 I=1,360
  READ(62,19) (TX(I,J),J=16,20),NRUN
  19  FORMAT(108X,F8.1,F8.2,F7.2,F8.3,F9.3,I6)
  TX(I,16)=TX(I,16)/100.
  TX(I,17)=TX(I,17)*10.
  TX(I,18)=TX(I,18)*10.
  TX(I,19)=TX(I,19)*10.
  TX(I,20)=TX(I,20)*10.
800  CONTINUE

```

```

CALL SCREEN(KQ,KHE,KUV,KAC)
CALL AXISTT
CALL AXISHE(KHE)
CALL AXISUV(KUV,NDAL)
CALL AXISAC(KAC)
CALL SHIFT2(90.,100.)
CALL DRA5L(TX,KQ,NDAL)
GO TO 90
C----- To plot terms from Owens (1984) algorithm.
159 OPEN(64,FILE='DDOS')
DO 156 I=1,360
A=REAL(I-1)
156 TX(I,21)=2.*COS((A-180.)*0.0174532925)
DO 160 I=1,360
READ(64,161)(TX(I,J),J=1,10)
161 FORMAT(10F7.1)
DO 160 J=1,10
160 TX(I,J)=TX(I,J)/100.
READ(64,162)NRUN
162 FORMAT(148X,I6)
CALL MOVTO2(100.,180.)
CALL CHASIZ(3.,3.)
CALL MOVBY2(10.,0.)
CALL MOVTO2(70.,185.)
CALL CHAINT(NRUN,3)
CALL MOVTO2(90.,185.)
CALL CHAHOL(23HOWENS' 1984 IMPROVED *.)
CALL CHAHOL(18HSDRYING ALGORITHM*. )
REWIND 64
DO 163 I=1,360
READ(64,164)(TX(I,J),J=11,15)
164 FORMAT(70X,F7.1,2F7.2,F8.3,F9.3)
TX(I,11)=TX(I,11)/100.
TX(I,12)=TX(I,12)*10.
TX(I,13)=TX(I,13)*10.
TX(I,14)=TX(I,14)*10.
TX(I,15)=TX(I,15)*10.
163 CONTINUE
REWIND 64
DO 165 I=1,360
READ(64,166)(TX(I,J),J=16,20),NRUN
166 FORMAT(108X,F8.1,F8.2,F7.2,F8.3,F9.3,I6)
TX(I,16)=TX(I,16)/100.
TX(I,17)=TX(I,17)*10.
TX(I,18)=TX(I,18)*10.
TX(I,19)=TX(I,19)*10.
TX(I,20)=TX(I,20)*10.
165 CONTINUE
CALL SCREEN(KQ,KHE,KUV,KAC)
CALL AXISTT
CALL AXISHE(KHE)
CALL AXISUV(KUV,NDAL)
CALL AXISAC(KAC)
CALL SHIFT2(90.,100.)
CALL DRA5L(TX,KQ,NDAL)
900 OPEN(23,FILE='DDF')
DO 904 I=1,360
READ(23,902)(TX(I,J),J=1,10)
902 FORMAT(10F7.1)
DO 904 J=1,10
904 TX(I,J)=TX(I,J)/100.
READ(23,950)NRUN
950 FORMAT(148X,I6)
CALL MOVTO2(100.,180.)
CALL CHASIZ(3.,3.)
CALL MOVBY2(10.,0.)

```



```

CALL MOVTO2(70.,185.)
CALL CHAINT(NRUN,3)
CALL MOVTO2(90.,185.)
CALL CHAHOL(24HFLATHER & HEAPS' 1975 *.)
CALL CHAHOL(18H DRYING ALGORITHM*.)
REWIND 23
DO 908 I=1,360
  READ(23,910) (TX(I,J),J=11,15)
910  FORMAT(70X,F7.1,2F7.2,F8.3,F9.3)
  TX(I,11)=TX(I,11)/100.
  TX(I,12)=TX(I,12)*10.
  TX(I,13)=TX(I,13)*10.
  TX(I,14)=TX(I,14)*10.
  TX(I,15)=TX(I,15)*10.
908  CONTINUE
  REWIND 23
  DO 915 I=1,360
  READ(23,912) (TX(I,J),J=16,20),NRUN
912  FORMAT(108X,F8.1,F8.2,F7.2,F8.3,F9.3,I6)
  TX(I,16)=TX(I,16)/100.
  TX(I,17)=TX(I,17)*10.
  TX(I,18)=TX(I,18)*10.
  TX(I,19)=TX(I,19)*10.
  TX(I,20)=TX(I,20)*10.
915  CONTINUE
C----- TO CALCULATE A BASIC TIDE-CURVE FOR NO SHOAL PRESENT
DO 920 I=1,360
  A=REAL(I-1)
920  TX(I,21)=2.*COS((A-180.)*0.0174532925)
  CALL SCREEN(KQ,KHE,KUV,KAC)
  CALL AXISTT
  CALL AXISHE(KHE)
  CALL AXISUV(KUV,NDAL)
  CALL AXISAC(KAC)
  CALL SHIFT2(90.,100.)
  CALL DRA5L(TX,KQ,NDAL)
1000  OPEN(64,FILE='DDSE')
  DO 1010 I=1,360
1010  READ(64,1020) (TE(I,J),J=1,10)
1020  FORMAT(10F6.1,F5.2)
  REWIND 64
  READ(64,1030)NRUN
1030  FORMAT(65X,I5)
  CALL MOVTO2(100.,180.)
  CALL CHASIZ(3.,3.)
  CALL MOVBY2(10.,0.)
  CALL MOVTO2(70.,185.)
  CALL CHAINT(NRUN,3)
  CALL MOVTO2(90.,185.)
  CALL CHAHOL(24HFLOW AROUND 'E' POINT *.)
C  CALL CHAINT(IF,3)
C  CALL CHAINT(JF,2)
  CALL SCRNE(KQ,KHE,KUV)
  CALL AXISTT
  CALL AXISHE(KHE)
  CALL AXISUV(KUV,NDAL)
  CALL SHIFT2(90.,100.)
  CALL DRA5LE(TE,KQ)
90  CALL GINEND
  STOP
  END

SUBROUTINE PA4F
C----- to draw an A4 frame horizontally.
  CALL MOVTO2(0.,0.)
  CALL LINBY2(297.,0.)

```

1000
1000
1000

1

1

1

1

1000

```

CALL LINBY2(0.,210.)
CALL LINBY2(-297.,0.)
CALL LINBY2(0.,-210.)
RETURN
END

```

```

SUBROUTINE SCREEN(KQ,KHE,KUV,KAC)
C---- to choose terms from the SCREEN.
DIMENSION KQ(5)
KHE=0
KUV=0
KAC=0
WRITE(1,20)
20 FORMAT(/'The terms available are as follows:      ,0 = no curve')
PRINT *
PRINT *, '1: Depth east of the test-cell'
PRINT *, '2: Depth west of the test-cell'
PRINT *, '3: Depth north of the test-cell'
PRINT *, '4: Depth south of the test-cell'
PRINT *, '5: Depth of the test-cell'
PRINT *, '6: Elevation east of the test-cell'
PRINT *, '7: Elevation west of the test-cell'
PRINT *, '8: Elevation north of the test-cell'
PRINT *, '9: Elevation south of the test-cell'
PRINT *, '10: Elevation in the test-cell'
PRINT *, '11: Eastward velocity component'
PRINT *, '12: Eastward temporal acceleration'
PRINT *, '13: Eastward Coriolis acceleration'
PRINT *, '14: Eastward pressure force/mass'
PRINT *, '15: Eastward frictional force/mass'
PRINT *, '16: Northward velocity component'
PRINT *, '17: Northward temporal acceleration'
PRINT *, '18: Northward Coriolis acceleration'
PRINT *, '19: Northward pressure force/mass'
PRINT *, '20: Northward frictional force/mass'
PRINT *, '21: Base curve for elevations'
WRITE(1,10)
10 FORMAT(/' Type the code numbers for 5 variables')
READ(1,*)KQ
DO 1 K=1,5
IF (KQ(K).EQ.0)GO TO 1
IF (KQ(K).LE.10)KHE=1
IF ((KQ(K).EQ.11).OR.(KQ(K).EQ.16))KUV=1
IF ((KQ(K).GE.12).AND.(KQ(K).LE.15))KAC=1
IF ((KQ(K).GE.17).AND.(KQ(K).LE.20))KAC=1
1 CONTINUE
RETURN
END

```

```

SUBROUTINE AXISTT
C---- to plot axis for Tidal Time (degrees)
CALL SHIFT2(90.,100.)
CALL AXIPOS(1,0.,0.,180.,1)
CALL AXISCA(2,36,0.,360.,1)
CALL AXIDRA(1,1,1)
CALL AXNSTR('TIDAL TIME ANGLE (degrees)',-90.,1,0)
CALL SHIFT2(-90.,-100.)
RETURN
END

```

```

SUBROUTINE AXISAC(KAC)
C---- to plot AXIS for ACcelerations
IF (KAC.EQ.0)RETURN
CALL SHIFT2(30.,100.)
CALL AXIPOS(1,0.,-75.,150.,2)
CALL AXISCA(2,6,-0.003,0.003,2)

```

```

CALL AXIDRA(-2,-1,2)
CALL AXNSTR('ACCELERATION (m/s***2)',-15.,-2,0)
CALL SHIFT2(-30.,-100.)
KAC=0
RETURN
END

```

```

SUBROUTINE AXISHE(KHE)
C---- to plot AXIS for water depth
IF (KHE.EQ.0) RETURN
CALL SHIFT2(90.,100.)
CALL AXIPOS(1,0.,-75.,150.,2)
CALL AXISCA(2,8,-4.0,4.0,2)
CALL AXIDRA(-2,-1,2)
CALL AXNSTR('WATER DEPTH, (m)',-15.,-2,0)
CALL SHIFT2(-90.,-100.)
KHE=0
RETURN
END

```

```

SUBROUTINE AXISUV(KUV,NDAL)
C---- to plot AXIS for plot of velocity
IF (KUV.EQ.0) RETURN
CALL SHIFT2(60.,100.)
CALL AXIPOS(1,0.,-75.,150.,2)
IF (NDAL.EQ.1) CALL AXISCA(2,20,-1.0,1.0,2)
IF ((NDAL.EQ.2).OR.(NDAL.EQ.3)) CALL AXISCA(2,20,-2.0,2.0,2)
CALL AXIDRA(-2,-1,2)
CALL AXNSTR('VELOCITY, (m/s)',-15.,-2,0)
CALL SHIFT2(-60.,-100.)
KUV=0
RETURN
END

```

```

SUBROUTINE DRA5L(TX,KQ,NDAL)
C---- to Draw up to 5 Lines
DIMENSION TX(360,21),KQ(5),Q(360),MCO(30)
CHARACTER*50 TITEL(30)
DATA MCO/6,5,7,2,9,6,5,7,2,9,2,2,4,5,6,7,9,1,0,0,2,2,4,5,6,7,9,0,
+0,0/
DO 1 L=1,30
1 TITEL(L)='
TITEL(1)='Depth east of the test-cell
TITEL(2)='Depth west of the test-cell
TITEL(3)='Depth north of the test-cell
TITEL(4)='Depth south of the test-cell
TITEL(5)='Depth of the test-cell
TITEL(6)='Elevation east of the test-cell
TITEL(7)='Elevation west of the test-cell
TITEL(8)='Elevation north of the test-cell
TITEL(9)='Elevation south of the test-cell
TITEL(10)='Elevation in the test-cell
TITEL(11)='Eastward velocity component
TITEL(12)='Eastward temporal acceleration
TITEL(13)='Eastward Coriolis acceleration
TITEL(14)='Eastward pressure force/mass
TITEL(15)='Eastward frictional force/mass
TITEL(16)='Northward velocity component
TITEL(17)='Northward temporal acceleration
TITEL(18)='Northward Coriolis acceleration
TITEL(19)='Northward pressure force/mass
TITEL(20)='Northward frictional force/mass
TITEL(21)='Base curve for elevations
DO 2 K=1,5
LQ=KQ(K)
IF (LQ.EQ.0) GO TO 2

```

```

DO 3 I=1,360
3 Q(I)=TX(I,LQ)
F=19.5
IF(LQ.GT.10)F=0.125
IF((LQ.EQ.11).OR.(LQ.EQ.16))F=75.
IF(LQ.EQ.21)F=19.5
CALL DELLIN(Q,F,MCOL(LQ))
Y=-60.-REAL(K-1)*6.
CALL MOVTO2(10.,Y)
CALL LINBY2(15.,0.)
CALL MOVTO2(30.,Y)
CALL CHASIZ(2.,2.)
CALL CHASTR(TITEL(LQ))
2 CONTINUE
RETURN
END

```

```

SUBROUTINE DELLIN(Q,F,NCOL)
DIMENSION Q(360)
CALL LINCOL(NCOL)
DO 2 I=1,360
Y=Q(I)*F
X=REAL(I-1)*0.5
IF(I.GT.1)GO TO 1
CALL MOVTO2(X,Y)
GO TO 2
1 CALL LINTO2(X,Y)
2 CONTINUE
RETURN
END

```

```

SUBROUTINE SCRNE(KQ,KHE,KUV)
C----- to choose terms from the SCREEN.
DIMENSION KQ(5)
KHE=0
KUV=0
KAC=0
WRITE(1,20)
20 FORMAT(/'The terms available are as follows:      ,0 = no curve')
PRINT *
PRINT *, '1: U(i,j)'
PRINT *, '2: U(i,j-1)'
PRINT *, '3: V(i,j)'
PRINT *, '4: V(i-1,j)'
PRINT *, '5: Depth at the U-point east of the E-point'
PRINT *, '6: Depth at the V-point south of the E-point'
PRINT *, '7: Depth at the U-point west of the E-point'
PRINT *, '8: Depth at the V-point north of the E-point'
PRINT *, '9: Depth at the E-point'
PRINT *, '10: Computational depth of the cell'
WRITE(1,10)
10 FORMAT(/' Type the code numbers for up to 5 variables')
READ(1,*)KQ
DO 1 K=1,5
IF(KQ(K).EQ.0)GO TO 1
IF(KQ(K).LT.5)KUV=1
IF(KQ(K).GT.4)KHE=1
1 CONTINUE
RETURN
END

```

```

SUBROUTINE DRA5LE(TE,KQ)
C----- to DRAW up to 5 Lines
DIMENSION TE(360,11),KQ(5),Q(360),MCOL(30)
CHARACTER*50 TITEL(30)
DATA MCOL/6,5,7,2,9,6,5,7,2,9,2,2,4,5,6,7,9,1,0,0,2,2,4,5,6,7,9,0,

```

```

+0,0/
DO 1 L=1,15
1 TITEL(L)='
  TITEL(1)='U(i,j)
  TITEL(2)='U(i,j-1)
  TITEL(3)='V(i,j)
  TITEL(4)='V(i-1,j)
  TITEL(5)='Depth at the U-point east of the E-point
  TITEL(6)='Depth at the V-point south of the E-point
  TITEL(7)='Depth at the U-point west of the E-point
  TITEL(8)='Depth at the V-point north of the E-point
  TITEL(9)='Depth at the E-point
  TITEL(10)='Computational depth of the cell
DO 2 K=1,5
LQ=KQ(K)
IF (LQ.EQ.0) GO TO 2
DO 3 I=1,360
3 Q(I)=TE(I,LQ)
F=0.195
IF ((LQ.GE.1).AND.(LQ.LT.5)) F=0.75
CALL DELLIN(Q,F,MCOL(LQ))
Y=-60.-REAL(K-1)*6.
CALL MOVTO2(10.,Y)
CALL LINBY2(15.,0.)
CALL MOVTO2(30.,Y)
CALL CHASIZ(2.,2.)
CALL CHASTR(TITEL(LQ))
2 CONTINUE
RETURN
END

```

APPENDIX 3

TIME	DEPTH	VEL.
------	-------	------

Station 0		24.6.93
-----------	--	---------

8.65	0.92	0.047
8.67	0.95	0.065
8.7	1.06	0.093
8.72	1.11	0.112
8.75	1.14	0.102
8.78	1.19	0.064
8.8	1.22	0.072
8.82	1.25	0.07
8.83	1.27	0.071
8.87	1.3	0.057
8.88	1.32	0.058
8.93	1.36	0.054
8.95	1.39	0.054
8.97		0.052
9	1.48	0.058
9.25	1.6	0.06
9.5	1.7	0.081
9.75	1.8	0.075
10	1.8	0.064
10.25	1.6	0.06
10.5	1.54	0.053
10.75	1.25	0.022
10.97	1.24	0.047
11.02	1.16	0.047
11.05	1.12	0.063
11.1	1.08	0.088
11.12	1.06	0.081
11.13	1.05	0.082
11.15	1.03	0.105
11.17	1.02	0.085
11.18	1	0.088
11.19	0.97	0.151
11.21	0.96	0.135
11.24	0.94	0.197
11.26	0.93	0.125
11.28	0.92	0.125
11.29	0.91	0.117
11.31	0.9	0.128
11.33	0.89	0.124

11.34 0.85 0.102

STAT 1 21.6.93

TIME DEPTH VEL.

6.67	1.2	0.192
6.75	1.25	0.113
7	1.5	0.071
7.25	1.6	0.082
7.5	1.8	0.07
7.75	1.8	0.063
8	1.7	0.057
8.25	1.6	0.05
8.5	1.4	0.05
8.75	1.2	0.082
9	1.15	0.147
9.25	1.1	0.18

STAT 3(b) 23.6.93

TIME DEPTH VEL. SET

20.05	0.86	0.311	
20.07	0.9	0.417	
20.1	1	0.247	
20.13	1.05	0.196	
20.15	1.1	0.146	
20.17	1.13	0.149	
20.18	1.2	0.182	
20.22	1.25	0.157	
20.23	1.27	0.173	
20.25	1.34	0.166	
20.5	1.6	0.154	350
20.75	1.9	0.155	
21	2.1	0.122	340
21.25	2.3	0.069	
21.5	2.4	0.071	10
21.75	2.4	0.06	
22	2.3	0.058	30
22.25	2.2	0.041	

22.5	2.17	0.047	40
22.75	1.9	0.047	
23	1.6	0.075	50
23.25	1.4	0.122	
23.5	1.25	0.167	90
23.58	1.15	0.149	
23.6	1.1	0.134	
23.62	1.06	0.13	
23.63	1.05	0.13	
23.65	1	0.142	
23.68	0.95	0.158	
23.7	0.93	0.116	70
23.72	0.9	0.098	

STAT 4 19.6.93

TIME	DEPTH	VEL.	SET
17.25	1.1	0.135	
17.5	1.5	0.115	
17.75	1.8	0.146	310
18	2	0.144	340
18.25	2.1	0.19	
18.5	2.15	0.155	330
18.75	2.2	0.229	
19	2.1	0.076	10
19.25	2	0.044	
19.5	1.9	0.078	40
19.75	1.7	0.102	
20	1.5	0.108	60
20.25	1.3	0.044	

STAT 5a 21.6.93

TIME	DEPTH	VEL.
18.43	0.88	0.162
18.45	0.93	0.351
18.47	0.98	0.256
18.48	1.02	0.275
18.53	1.08	0.273

1000

1000

1000

18.57	1.12	0.177
18.58	1.15	0.138
18.67	1.29	0.145
18.92	1.6	0.168
19.25	2.05	0.149
19.5	2.3	0.159
19.75	2.35	0.147
20	2.45	0.177
20.25	2.48	0.175
20.5	2.37	0.127
20.75	2.33	0.095
21	2.15	0.09
21.25	1.95	0.091
21.5	1.75	0.123
21.75	1.5	0.126
22	1.28	0.123
22.12	1.1	0.118
22.13	1.08	0.104
22.15	1.05	0.107
22.17	1.03	0.115
22.18	1.01	0.11
22.2	0.99	0.114
22.22	0.97	0.101
22.23	0.95	0.114
22.25	0.93	0.154
22.26	0.91	0.119
22.28	0.9	0.154
22.3	0.88	0.079
22.32	0.86	0.173
22.33	0.84	0.088

STAT 5b 19.6.93

TIME	DEPTH	VEL.
------	-------	------

4.75	1	0.14
5	1.4	0.153
5.25	1.6	0.136
5.5	1.9	0.172
5.75	2	0.16
6	2.1	0.19
6.25	2.2	0.183

6.5	2.2	0.113
6.75	2.1	0.117
7	2	0.104
7.25	1.8	0.101
7.5	1.7	0.1
7.75	1.5	0.094
8	1.3	0.091

STAT 6 22.6.93

TIME DEPTH VEL.

18.8	0.82	0.298	
18.82	0.87	0.318	
18.83	0.96	0.315	
18.85	0.97	0.438	
18.87	1.03	0.432	
18.88	1.05	0.399	
18.9	1.09	0.444	
18.92	1.16	0.424	
18.93	1.22		
18.95	1.29		
18.98	1.31		
19	1.37	0.399	
19.08	1.41	0.373	
19.17	1.57	0.35	
19.25	1.8	0.345	
19.33	1.97	0.323	310
19.42	2.05	0.298	
19.5	2.2	0.275	
19.75	2.65	0.198	300
20	2.8	0.163	
20.25	3.2	0.126	10
20.5	3.3	0.116	
20.75	3.35	0.168	40
21	3.38	0.179	
21.25	3.3	0.189	60
21.5	3.25	0.163	
21.75	3.05	0.136	60
22	2.9		
22.33	2.7	0.123	80
22.5	2.55	0.103	

22.75	2.28	0.122	50
23	2.02	0.149	90
23.25	1.64	0.208	
23.5	1.35	0.229	80
23.67	1.13	0.203	
23.75	0.99	0.163	
23.8	0.93		
23.83	0.91		
23.85	0.89		
23.87	0.87		
23.88	0.84		

APPENDIX 4

L

L

L

00.

70

70

70
2000
00

00.

00-

00-

00-

00-

00-00

00-

00-

L

L

-200														
-200														
-200														
0.4 52 48.00 00 00. Holbeach										L				
0.4 53 12. 00 12. SKEGNESS														
-200-200-200-200-200-200-200-200-200-200-200-200-200-200-200 -27 39 40 46 49														
-200-200-200-200-200-200-200-200-200-200-200-200-200-200-200 -26 34 39 43 49														
-200-200-200-200-200-200-200-200-200-200-200-200-200-200-200 -25 06 40 50 46														
-200-200-200-200-200-200-200-200-200-200-200-200-200-200-200 -24 20 40 50 52														
-200-200-200-200-200-200-200-200-200-200-200-200-200-200-200 -10 37 36 42 49														
-200-200-200-200-200-200-200-200-200-200-200-200-200-200-200 -10 32 33 42 45														
-200-200-200-200-200-200-200-200-200-200-200-200-200-200-200 -10 33 35 42 47														
-200-200-200-200-200-200-200-200-200-200-200-200-200-200-200 -13 14 36 39 48														
-200-200-200-200-200-200-200-200-200-200-200-200-200-200-200 -13 23 31 42 51														
-200-200-200-200-200-200-200-200-200-200-200-200-200-200-200 -23 02 21 45 50														
-200-200-200-200-200-200-200-200-200-200-200-200-200-200-200 -28 06 10 24 57 62														
-200-200-200-200-200-200-200-200-200-200-200-200-200-200-200 -29 02 26 25 47 54														
-200-200-200-200-200-200-200-200-200-200-200-200-200-200-200 -31 08 42 36 25 07														
-200-200-200-200-200-200-200-200-200-200-200-200-200-200-200 -30 35 32 20 22 59														
-200-200-200-200-200-200-200-200-200-200-200-200-200-200-200 -16 -03 31 03 04 00 60														
0.4 53 06.00 00 12. Friskney Flats														
-200-200-200-200-200-200-200-200-200-200 -37-037-037 -35-034 008 14 02 00 07 72														
-200-200-200-200-200-200-200-200 -40 -37-037-037-037-032-012 017 21 17 38 28 61														
-200-200-200-200-200-200 -46-043-041-036-035-033-027 030 002 30 40 13 60 43														
-200-200-200-200-200 -53-050-047-046-043-038-035-016 021 040 45 21 45 38 58														
-200-200-200-200 -55-052-048-047-045-050-042-039-001 035 060 60 41 19 18 53														
-200-200-200 -57-053-050-047-045-044-040-041-037 000 065 056 30 -04 -36 02 66														
-200-200 -60-056-051-050-045-042-040-037-036-029 030 094 067 09 -31 -50 08 96														
-76 -77-059-055-051-046-040-038-038-034-026-020 047 106 048 -12 -23 -23 31 120														
-075-069-057-053-050-045-039-035-030-025-020 001 088 090 019 -23 -25 06 113 92														
-059-062-055-050-046-042-038-029-024-001 030 099 104 045-005 -10 24 77 65 113														
-054-055-050-048-041-039-039-023 029 081 101 100 077 029 032 15 27 29 27 178														
-046-039-040-040-030-020-004 036 084 070 077 044 013-019-023 00 -05 07 115 274														
-038-038-032-027-008 030 063 055 073 098 041-006-020-023-025 -19 -01 114 260 327														
-029-029-023 011 015 071 104 098 039 005-010-013-017 000 019 70 134 262 333 330														
-040-041-026-006 050 091 117 050-010-020-019-019-006 015 060 120 210 260 320 330														
0.4 53 00. 0 12. Roaring Middle														
-013 013 058 088 100 099 020-025-026-014-014-004 026 080 120 200 270 260 270 240														
057 075 099 063 037-020-019-024-015-008 023 058 100 150 190 230 280 210 250 160														
086 058 018-022-010-015-008 011 032 050 080 100 140 180 210 220 230 210 200 180														
054 020-005-010 004 010 018 028 049 060 120 150 200 220 190 150 200 200 180 150														
-025-008 037 027 017 021 030 047 069 100 160 210 220 120 090 150 160 150 140 150														
-027-032-016 019 031 030 046 060 070 120 190 190 150 100 100 140 150 150 110 150														
-029-022-011-009-001 015 042 070 150 180 170 140 100 080 100 130 130 120 100 140														
-012-010-019-011 009 037 051 060 160 160 120 140 080 060 140 140 110 90 110 100														
-002 000-019-006 008 032 071 110 130 110 100 070 070 090 130 120 80 70 80 110														
093 052 023 036 049 070 110 130 120 010 070 045 060 110 110 70 60 60 60 90														
-020 006 036 034 030 060 100 100 080 080 070 032 080 110 070 60 50 49 149 70														
-028-010 004 005 037 070 100 080 070 090 043 061 095 081 051 44 41 26 25 55														
-006-012-002 017 039 080 060 050 090 050 028 075 072 062 040 25 22 06 26 37														
019-016 007 022 058 045 037 060 085 027 057 055 058 030 019 10 41 02 21 32														
-012 015 020 033 046 028 050 090 048 050 041 051 037 007 006 08 30 00 12 13														
0.4 52 54. 0 12. (north of Breast Sand)														
-020-010 008 020 030 009 065 073 022 030 033 041 004-007-010 28 05 -08 22 04														
-019-016-006 041 013 015 099 059 023 011 030 002-021-020-022 28 -16 -20 14 00														
-028-011 045-002 003 033 063 062-005 000 039-010-039-032-045 23 -15 19 -25 14														
-025-019 027-005 000 057 035 050-024-029 038-027-037-041-041 06 -03 16 -13 10														
-027-022 023-013-009 052-002 038 004-018 027-028-040-041-027 -10 11 -10 -05 -14														
-031-022 010-010-003 025 022 009 009-017 020-040-039-040-028 -08 -08 07 -14 -15														
-033-022-008 005-022-018 022 000-003-010 011-037-036-035-023 -09 -26 -12 -14 -19														
-044-010-010-013-022-033-008 010-016 000 012-026-034-034-025 -14 -20 -17 -38 -45														
-053-015-022-023-018-031-032-018-020-030-001-011-012-028-027 -24 -21 -28 -30 -46														
-077-028-031-035-030-031-032-033-025-031-027-014-007-007-028 -14 -16 -33 -43 -51														
-063-044-039-042-037-037-040-031-016-034-034-030-033-018-037 -14 -29 -38 -52 -56														
-64-063-049-047-047-046-042-041-037-046-042-037-040-040-023 -20 -37 -50 -58 -66														
-200-056-061-057-058-050-056-049-048-061-060-047-051-025-032 -15 -45 -55 -64 -65														

1

2

3

Bulldog Channel

[illegible]

L

Docking Shoal

90	150	200	200	210	220	200	100	60	55	60	65	70	64	70	94	122	155	150	160
110	186	200	200	210	210	150	55	55	55	58	60	75	70	75	90	95	113	124	145
104	186	200	210	210	200	140	55	54	40	50	65	81	70	50	72	58	49	61	100
130	200	200	210	210	200	100	55	57	60	72	50	45	56	60	44	52	60	72	94
153	205	210	200	200	110	42	36	40	45	50	45	50	37	40	41	57	72	85	127
194	210	170	164	150	100	42	45	42	40	39	42	50	54	54	54	56	60	80	110
195	210	120	100	91	54	51	50	50	54	55	60	55	52	51	56	54	62	72	100
200	167	060	91	148	110	51	55	63	65	60	60	55	54	55	57	49	47	45	78
164	110	60	90	100	110	118	100	63	65	66	60	65	70	60	54	40	58	68	84
130	50	60	70	90	110	110	105	80	65	72	72	75	75	50	49	50	60	70	75
60	51	60	70	84	90	95	107	105	103	110	110	84	75	75	75	52	63	69	69
17	33	50	54	70	70	70	60	70	75	100	110	80	75	72	74	84	84	70	59
23	35	40	50	60	63	65	65	65	69	60	65	70	75	74	74	78	72	60	51
14	30	42	42	42	63	65	65	70	75	70	55	70	75	76	78	80	65	54	52
15	20	27	30	45	50	63	65	78	80	81	60	51	50	55	60	84	80	62	54

Burnham Flats

16	23	25	27	48	50	56	60	60	70	70	65	65	55	44	51	71	80	73	75
20	23	23	31	29	50	47	60	60	63	63	65	67	72	50	54	63	70	84	70
39	35	33	36	36	40	42	50	57	57	48	50	70	75	60	51	60	60	75	92
30	33	33	33	31	33	36	39	40	40	50	42	42	50	52	54	57	63	70	94
20	23	30	25	20	28	25	23	36	36	45	35	30	35	50	50	54	68	65	78
15	20	25	20	20	23	20	20	27	30	36	36	32	37	25	34	50	55	60	62
09	13	14	22	20	20	20	20	27	25	23	30	36	39	45	35	41	33	34	36
07	11	14	20	17	20	20	20	27	25	20	23	30	40	50	60	63	64	63	52
10	12	20	20	14	20	20	36	30	30	31	33	37	42	50	52	62	78	70	65
33	33	26	17	30	24	21	28	30	30	32	40	50	58	64	69	68	66	74	78
23	22	20	20	24	27	24	23	30	30	50	55	60	72	64	70	42	40	41	35
14	16	12	14	20	27	24	23	24	24	55	66	38	35	30	27	24	20	23	23
24	23	20	20	18	18	23	23	20	23	31	34	20	20	20	36	34	36	40	42
33	38	28	23	41	34	50	45	45	50	27	28	17	20	05	20	24	32	45	57
20	30	45	39	45	45	63	63	60	57	60	49	35	19	11	16	21	27	36	36

Scolt Head

[illegible]

I

0.4 52 48. 0 36: (land)

I

APPENDIX 5

File HWC-BCEZ

i	j	lat.	long.	H of M ₂ (mm)	g of M ₂ (1/10°)
03	06 8	54 08	0-03.	1780	1230
03	07 8	54 08.	0 00.	1760	1235
03	08 8			1740	1240
03	09 8			1720	1245
03	10 8			1700	1250
03	11 8			1680	1255
03	12 8	54 08.	+0 15.	1660	1260
03	13 8			1640	1265
03	14 8			1620	1270
03	15 8			1600	1275
03	16 8			1580	1280
03	17 8	54 08.	+0 30.	1560	1285
03	18 8			1540	1290
03	19 8			1520	1295
03	20 8			1500	1300
03	21 8			1480	1305
03	22 8	54 08.	+0 45.	1460	1310
03	23 8			1440	1315
03	24 8			1420	1320
03	25 8			1400	1325
03	26 8			1380	1330
03	27 1	54 08.	+1 00.	1360	1335
04	27 2	54 06.	+1 00.	1368	1350
05	27 2	54 04.	+1 00.	1376	1365
06	27 2	54 02.	+1 00.	1384	1380
07	27 2	54 00.	+1 00.	1392	1395
08	27 2			1400	1410
09	27 2			1408	1425
10	27 2			1416	1440
11	27 2			1424	1455
12	27 2	53 50.	+1 00.	1432	1470
13	27 2			1440	1485
14	27 2			1448	1500
15	27 2			1456	1515
16	27 2			1464	1530
17	27 2	53 40.	+1 00.	1472	1545
18	27 2			1480	1560
19	27 2			1488	1575
20	27 2			1496	1590
21	27 2			1504	1605
22	27 2	53 30.	+1 00.	1512	1620

23	27 2			1520 1635
24	27 2			1528 1650
25	27 2			1536 1665
26	27 2			1544 1680
27	27 2	53 20.	+1 00.	1552 1695
28	27 2			1560 1710
29	27 2			1568 1725
30	27 2			1576 1740
31	27 2			1584 1755
32	27 2	53 10.	+1 00.	1592 1770
33	27 2			1600 1785
34	27 2			1608 1800
35	27 2			1616 1815
36	27 2			1624 1830
37	27 2	53 00.	+1 00.	1632 1845
38	27 2	52 58.	+1 00.	1640 1860

File HWC-BCE2

i	j	lat.	long.	H of S ₂	g of S ₂	H of N ₂	g of N ₂
03	06 8	54 08	0-03.	668 1730	356 1030		
03	07 8	54 08.	0 00.	660 1735	352 1035		
03	08 8			652 1740	348 1040		
03	09 8			645 1745	344 1045		
03	10 8			638 1750	340 1050		
03	11 8			630 1755	336 1055		
03	12 8	54 08.	+0 15.	622 1760	332 1060		
03	13 8			615 1765	328 1065		
03	14 8			608 1770	324 1070		
03	15 8			600 1775	320 1075		
03	16 8			592 1780	316 1080		
03	17 8	54 08.	+0 30.	585 1785	312 1085		
03	18 8			578 1790	308 1090		
03	19 8			570 1795	304 1095		
03	20 8			562 1800	300 1100		
03	21 8			555 1805	296 1105		
03	22 8	54 08.	+0 45.	548 1810	292 1110		
03	23 8			540 1815	288 1115		
03	24 8			532 1820	284 1120		
03	25 8			525 1825	280 1125		
03	26 8			518 1830	276 1130		
03	27 1	54 08.	+1 00.	510 1835	272 1135		
04	27 2	54 06.	+1 00.	513 1850	274 1150		
05	27 2	54 04.	+1 00.	516 1865	275 1165		
06	27 2	54 02.	+1 00.	519 1880	277 1180		

07	27 2	54 00.	+1 00.	522 1895	278 1195
08	27 2			525 1910	280 1210
09	27 2			528 1925	282 1225
10	27 2			531 1940	283 1240
11	27 2			534 1955	285 1255
12	27 2	53 50.	+1 00.	537 1970	286 1270
13	27 2			540 1985	288 1285
14	27 2			543 2000	290 1300
15	27 2			546 2015	291 1315
16	27 2			549 2030	293 1330
17	27 2	53 40.	+1 00.	552 2045	294 1345
18	27 2			555 2060	296 1360
19	27 2			558 2075	298 1375
20	27 2			561 2090	299 1390
21	27 2			564 2105	301 1405
22	27 2	53 30.	+1 00.	567 2120	302 1420
23	27 2			570 2135	304 1435
24	27 2			573 2150	306 1450
25	27 2			576 2165	307 1465
26	27 2			579 2180	308 1480
27	27 2	53 20.	+1 00.	582 2195	310 1495
28	27 2			585 2210	312 1510
29	27 2			588 2225	314 1525
30	27 2			591 2240	315 1540
31	27 2			594 2255	317 1555
32	27 2	53 10.	+1 00.	597 2270	318 1570
33	27 2			600 2285	320 1585
34	27 2			603 2300	322 1600
35	27 2			606 2315	323 1615
36	27 2			609 2330	325 1630
37	27 2	53 00.	+1 00.	612 2345	326 1645
38	27 2	52 58.	+1 00.	615 2360	328 1660

APPENDIX 6

MODEL PREDICTIONS FOR 1993 6 19

All times are in G.M.T.

52 56 N 0 06 E

DATE AND TIME	HEIGHT	SET	RATE
(m)	(degT)	(m/s)	
1993/06/19 00:00	-1.13	0.	.00
1993/06/19 00:30	-1.13	0.	.00
1993/06/19 01:00	-1.13	0.	.00
1993/06/19 01:30	-1.13	0.	.00
1993/06/19 02:00	-1.13	0.	.00
1993/06/19 02:30	-.51	305.	.45
1993/06/19 03:00	.33	229.	.46
1993/06/19 03:30	1.02	239.	.36
1993/06/19 04:00	1.68	237.	.26
1993/06/19 04:30	2.15	233.	.18
1993/06/19 05:00	2.42	227.	.14
1993/06/19 05:30	2.60	225.	.11
1993/06/19 06:00	2.70	212.	.03
1993/06/19 06:30	2.58	57.	.10
1993/06/19 07:00	2.26	56.	.15
1993/06/19 07:30	1.91	58.	.18
1993/06/19 08:00	1.45	57.	.25
1993/06/19 08:30	.92	56.	.32
1993/06/19 09:00	.36	57.	.38
1993/06/19 09:30	-.19	53.	.39
1993/06/19 10:00	-.71	45.	.43
1993/06/19 10:30	-1.13	0.	.00
1993/06/19 11:00	-1.13	0.	.00
1993/06/19 11:30	-1.13	0.	.00
1993/06/19 12:00	-1.13	0.	.00
1993/06/19 12:30	-1.13	0.	.00
1993/06/19 13:00	-1.13	0.	.00
1993/06/19 13:30	-1.13	0.	.00
1993/06/19 14:00	-1.13	0.	.00
1993/06/19 14:30	-1.13	0.	.00
1993/06/19 15:00	-.31	298.	.44
1993/06/19 15:30	.55	228.	.48
1993/06/19 16:00	1.28	240.	.34
1993/06/19 16:30	1.94	238.	.25
1993/06/19 17:00	2.37	230.	.18
1993/06/19 17:30	2.63	227.	.14
1993/06/19 18:00	2.81	228.	.09

1993/06/19 18:30	2.86	75.	.02
1993/06/19 19:00	2.64	59.	.13
1993/06/19 19:30	2.29	56.	.15
1993/06/19 20:00	1.88	59.	.21
1993/06/19 20:30	1.36	57.	.28
1993/06/19 21:00	.80	55.	.35
1993/06/19 21:30	.21	56.	.40
1993/06/19 22:00	-.34	51.	.42
1993/06/19 22:30	-.86	44.	.46
1993/06/19 23:00	-1.13	0.	.00
1993/06/19 23:30	-1.13	0.	.00

MODEL PREDICTIONS FOR 1993 6 20

All times are in G.M.T.

52 56 N 0 06 E

DATE AND TIME	HEIGHT	SET	RATE
(m)	(degT)	(m/s)	
1993/06/20 00:00	-1.13	0.	.00
1993/06/20 00:30	-1.13	0.	.00
1993/06/20 01:00	-1.13	0.	.00
1993/06/20 01:30	-1.13	0.	.00
1993/06/20 02:00	-1.13	0.	.00
1993/06/20 02:30	-1.13	0.	.00
1993/06/20 03:00	-1.13	0.	.00
1993/06/20 03:30	-.06	283.	.41
1993/06/20 04:00	.79	231.	.46
1993/06/20 04:30	1.56	240.	.32
1993/06/20 05:00	2.20	236.	.23
1993/06/20 05:30	2.58	230.	.18
1993/06/20 06:00	2.83	227.	.14
1993/06/20 06:30	3.01	231.	.06
1993/06/20 07:00	2.96	58.	.08
1993/06/20 07:30	2.65	58.	.14
1993/06/20 08:00	2.29	58.	.17
1993/06/20 08:30	1.80	58.	.24
1993/06/20 09:00	1.24	57.	.32
1993/06/20 09:30	.66	56.	.38
1993/06/20 10:00	.06	55.	.41
1993/06/20 10:30	-.50	49.	.45
1993/06/20 11:00	-1.02	43.	.48
1993/06/20 11:30	-1.13	0.	.00
1993/06/20 12:00	-1.13	0.	.00

1993/06/20 12:30	-1.13	0.	.00
1993/06/20 13:00	-1.13	0.	.00
1993/06/20 13:30	-1.13	0.	.00
1993/06/20 14:00	-1.13	0.	.00
1993/06/20 14:30	-1.13	0.	.00
1993/06/20 15:00	-1.13	0.	.00
1993/06/20 15:30	-.89	310.	.61
1993/06/20 16:00	.22	256.	.42
1993/06/20 16:30	1.05	235.	.43
1993/06/20 17:00	1.83	240.	.30
1993/06/20 17:30	2.43	232.	.21
1993/06/20 18:00	2.78	227.	.18
1993/06/20 18:30	3.03	228.	.13
1993/06/20 19:00	3.17	217.	.02
1993/06/20 19:30	3.00	58.	.11
1993/06/20 20:00	2.63	57.	.15
1993/06/20 20:30	2.23	60.	.19
1993/06/20 21:00	1.69	58.	.27
1993/06/20 21:30	1.09	56.	.34
1993/06/20 22:00	.50	56.	.40
1993/06/20 22:30	-.11	54.	.43
1993/06/20 23:00	-.67	48.	.47
1993/06/20 23:30	-1.17	43.	.50

MODEL PREDICTIONS FOR 1993 6 21

All times are in G.M.T.

52 56 N 0 06 E

DATE AND TIME	HEIGHT	SET	RATE
(m)	(degT)	(m/s)	
1993/06/21 00:00	-1.13	0.	.00
1993/06/21 00:30	-1.13	0.	.00
1993/06/21 01:00	-1.13	0.	.00
1993/06/21 01:30	-1.13	0.	.00
1993/06/21 02:00	-1.13	0.	.00
1993/06/21 02:30	-1.13	0.	.00
1993/06/21 03:00	-1.13	0.	.00
1993/06/21 03:30	-1.13	0.	.00
1993/06/21 04:00	-.59	307.	.59
1993/06/21 04:30	.51	236.	.50
1993/06/21 05:00	1.33	238.	.39
1993/06/21 05:30	2.12	240.	.28
1993/06/21 06:00	2.63	232.	.20

1993/06/21 06:30	2.96	227.	.17
1993/06/21 07:00	3.21	230.	.10
1993/06/21 07:30	3.26	64.	.04
1993/06/21 08:00	2.99	59.	.14
1993/06/21 08:30	2.61	56.	.16
1993/06/21 09:00	2.13	60.	.22
1993/06/21 09:30	1.55	58.	.30
1993/06/21 10:00	.93	55.	.37
1993/06/21 10:30	.32	56.	.43
1993/06/21 11:00	-.28	52.	.45
1993/06/21 11:30	-.84	46.	.49
1993/06/21 12:00	-1.13	0.	.00
1993/06/21 12:30	-1.13	0.	.00
1993/06/21 13:00	-1.13	0.	.00
1993/06/21 13:30	-1.13	0.	.00
1993/06/21 14:00	-1.13	0.	.00
1993/06/21 14:30	-1.13	0.	.00
1993/06/21 15:00	-1.13	0.	.00
1993/06/21 15:30	-1.13	0.	.00
1993/06/21 16:00	-1.13	0.	.00
1993/06/21 16:30	-.26	299.	.53
1993/06/21 17:00	.79	231.	.52
1993/06/21 17:30	1.61	240.	.36
1993/06/21 18:00	2.38	236.	.25
1993/06/21 18:30	2.83	230.	.20
1993/06/21 19:00	3.13	228.	.16
1993/06/21 19:30	3.36	235.	.06
1993/06/21 20:00	3.28	59.	.09
1993/06/21 20:30	2.93	59.	.14
1993/06/21 21:00	2.54	60.	.18
1993/06/21 21:30	2.00	58.	.25
1993/06/21 22:00	1.38	57.	.33
1993/06/21 22:30	.77	55.	.39
1993/06/21 23:00	.14	56.	.44
1993/06/21 23:30	-.45	51.	.47

MODEL PREDICTIONS FOR 1993 6 22

All times are in G.M.T.

52 56 N 0 06 E

DATE AND TIME	HEIGHT	SET	RATE
(m)	(degT)	(m/s)	
1993/06/22 00:00	-.99	45.	.50

1993/06/22 00:30	-1.13	0.	.00
1993/06/22 01:00	-1.13	0.	.00
1993/06/22 01:30	-1.13	0.	.00
1993/06/22 02:00	-1.13	0.	.00
1993/06/22 02:30	-1.13	0.	.00
1993/06/22 03:00	-1.13	0.	.00
1993/06/22 03:30	-1.13	0.	.00
1993/06/22 04:00	-1.13	0.	.00
1993/06/22 04:30	-1.13	0.	.00
1993/06/22 05:00	.09	279.	.46
1993/06/22 05:30	1.06	232.	.48
1993/06/22 06:00	1.89	242.	.33
1993/06/22 06:30	2.58	232.	.23
1993/06/22 07:00	2.99	227.	.20
1993/06/22 07:30	3.28	229.	.14
1993/06/22 08:00	3.45	215.	.01
1993/06/22 08:30	3.25	57.	.12
1993/06/22 09:00	2.86	57.	.15
1993/06/22 09:30	2.42	61.	.20
1993/06/22 10:00	1.84	58.	.28
1993/06/22 10:30	1.20	56.	.35
1993/06/22 11:00	.59	56.	.41
1993/06/22 11:30	-.04	54.	.45
1993/06/22 12:00	-.63	49.	.49
1993/06/22 12:30	-1.13	0.	.00
1993/06/22 13:00	-1.13	0.	.00
1993/06/22 13:30	-1.13	0.	.00
1993/06/22 14:00	-1.13	0.	.00
1993/06/22 14:30	-1.13	0.	.00
1993/06/22 15:00	-1.13	0.	.00
1993/06/22 15:30	-1.13	0.	.00
1993/06/22 16:00	-1.13	0.	.00
1993/06/22 16:30	-1.13	0.	.00
1993/06/22 17:00	-.81	308.	.65
1993/06/22 17:30	.43	248.	.47
1993/06/22 18:00	1.32	235.	.43
1993/06/22 18:30	2.16	242.	.30
1993/06/22 19:00	2.74	233.	.22
1993/06/22 19:30	3.11	227.	.19
1993/06/22 20:00	3.39	231.	.11
1993/06/22 20:30	3.46	63.	.05
1993/06/22 21:00	3.16	59.	.14
1993/06/22 21:30	2.77	57.	.16
1993/06/22 22:00	2.27	60.	.23
1993/06/22 22:30	1.66	58.	.31
1993/06/22 23:00	1.02	55.	.37

1993/06/22 23:30 .40 56. .43

MODEL PREDICTIONS FOR 1993 6 23

All times are in G.M.T.

52 56 N 0 06 E

DATE AND TIME	HEIGHT (m)	SET (degT)	RATE (m/s)
1993/06/23 00:00	-.22	53.	.46
1993/06/23 00:30	-.79	47.	.50
1993/06/23 01:00	-1.13	0.	.00
1993/06/23 01:30	-1.13	0.	.00
1993/06/23 02:00	-1.13	0.	.00
1993/06/23 02:30	-1.13	0.	.00
1993/06/23 03:00	-1.13	0.	.00
1993/06/23 03:30	-1.13	0.	.00
1993/06/23 04:00	-1.13	0.	.00
1993/06/23 04:30	-1.13	0.	.00
1993/06/23 05:00	-1.13	0.	.00
1993/06/23 05:30	-.43	303.	.59
1993/06/23 06:00	.72	233.	.53
1993/06/23 06:30	1.57	238.	.38
1993/06/23 07:00	2.39	237.	.27
1993/06/23 07:30	2.88	231.	.21
1993/06/23 08:00	3.21	228.	.18
1993/06/23 08:30	3.46	235.	.07
1993/06/23 09:00	3.40	60.	.09
1993/06/23 09:30	3.05	60.	.14
1993/06/23 10:00	2.65	60.	.17
1993/06/23 10:30	2.10	59.	.25
1993/06/23 11:00	1.47	57.	.33
1993/06/23 11:30	.84	55.	.39
1993/06/23 12:00	.22	56.	.44
1993/06/23 12:30	-.39	51.	.47
1993/06/23 13:00	-.95	45.	.51
1993/06/23 13:30	-1.13	0.	.00
1993/06/23 14:00	-1.13	0.	.00
1993/06/23 14:30	-1.13	0.	.00
1993/06/23 15:00	-1.13	0.	.00
1993/06/23 15:30	-1.13	0.	.00
1993/06/23 16:00	-1.13	0.	.00
1993/06/23 16:30	-1.13	0.	.00
1993/06/23 17:00	-1.13	0.	.00

1993/06/23 17:30	-1.13	0.	.00
1993/06/23 18:00	-.05	290.	.50
1993/06/23 18:30	.97	231.	.50
1993/06/23 19:00	1.81	241.	.34
1993/06/23 19:30	2.54	233.	.24
1993/06/23 20:00	2.97	228.	.21
1993/06/23 20:30	3.27	229.	.15
1993/06/23 21:00	3.47	234.	.03
1993/06/23 21:30	3.29	57.	.11
1993/06/23 22:00	2.91	58.	.14
1993/06/23 22:30	2.49	61.	.19
1993/06/23 23:00	1.92	58.	.27
1993/06/23 23:30	1.28	56.	.34

MODEL PREDICTIONS FOR 1993 6 24

All times are in G.M.T.

52 56 N 0 06 E

DATE AND TIME	HEIGHT (m)	SET (degT)	RATE (m/s)
1993/06/24 00:00	.66	55.	.41
1993/06/24 00:30	.04	55.	.44
1993/06/24 01:00	-.55	49.	.48
1993/06/24 01:30	-1.08	0.	.00
1993/06/24 02:00	-1.13	0.	.00
1993/06/24 02:30	-1.13	0.	.00
1993/06/24 03:00	-1.13	0.	.00
1993/06/24 03:30	-1.13	0.	.00
1993/06/24 04:00	-1.13	0.	.00
1993/06/24 04:30	-1.13	0.	.00
1993/06/24 05:00	-1.13	0.	.00
1993/06/24 05:30	-1.13	0.	.00
1993/06/24 06:00	-.98	309.	.67
1993/06/24 06:30	.28	261.	.45
1993/06/24 07:00	1.19	234.	.45
1993/06/24 07:30	2.02	242.	.31
1993/06/24 08:00	2.63	232.	.22
1993/06/24 08:30	3.01	226.	.19
1993/06/24 09:00	3.28	229.	.12
1993/06/24 09:30	3.41	70.	.02
1993/06/24 10:00	3.16	58.	.13
1993/06/24 10:30	2.77	56.	.15
1993/06/24 11:00	2.31	61.	.21

1993/06/24 11:30	1.73	58.	.29
1993/06/24 12:00	1.10	56.	.36
1993/06/24 12:30	.49	56.	.42
1993/06/24 13:00	-.13	54.	.45
1993/06/24 13:30	-.71	48.	.49
1993/06/24 14:00	-1.13	0.	.00
1993/06/24 14:30	-1.13	0.	.00
1993/06/24 15:00	-1.13	0.	.00
1993/06/24 15:30	-1.13	0.	.00
1993/06/24 16:00	-1.13	0.	.00
1993/06/24 16:30	-1.13	0.	.00
1993/06/24 17:00	-1.13	0.	.00
1993/06/24 17:30	-1.13	0.	.00
1993/06/24 18:00	-1.13	0.	.00
1993/06/24 18:30	-.59	307.	.61
1993/06/24 19:00	.55	236.	.50
1993/06/24 19:30	1.38	237.	.39
1993/06/24 20:00	2.18	240.	.28
1993/06/24 20:30	2.69	232.	.20
1993/06/24 21:00	3.01	227.	.17
1993/06/24 21:30	3.25	231.	.10
1993/06/24 22:00	3.29	63.	.06
1993/06/24 22:30	2.99	59.	.14
1993/06/24 23:00	2.62	57.	.16
1993/06/24 23:30	2.13	59.	.23